Targeting the Ser/Thr protein kinase RSK to reduce breast cancer metastasis

by

Roman Michal Mrozowski

Dissertation
Submitted to the Faculty of the
Graduate School of Vanderbilt University
in partial fulfillment of the requirements
for the degree of
DOCTOR OF PHILOSOPHY
in
Pathology

August 2015

Nashville, Tennessee

Approved:

Alissa M. Weaver, M.D. Ph.D.

Deborah A. Lannigan, Ph.D.

Ian G. Macara, Ph.D.

Vito Quaranta, M.D.

David H. Wasserman, Ph.D.

Andries Zijlstra, Ph.D.

Abstract

RSK is a family of four Ser/Thr protein kinases activated by ERK1/2 signaling. RSK has been found to be misregulated in a variety of cancers, including breast and prostate. More recently, RSK1 and RSK2 have been shown to promote metastasis in vivo. Currently, no targeted therapies to inhibit metastasis are available. Our laboratory has described the first potent and selective small molecule of RSK, SL0101. We found that this compound is not suitable for in vivo studies, therefore we set out to develop and validate new analogues based on the SL0101 pharmacophore. Here, we report a series of modifications improving the in vivo properties of SL0101.

We characterize the mode of inhibition of RSK by SL0101. We find that this molecule acts as an allosteric non-competitive inhibitor of RSK. We postulate that this unusual mode of inhibition of RSK accounts for a remarkable selectivity of SL0101 for this kinase. We identify a number of modifications to the parent molecule that increase its in vitro affinity and stability in cell-based assays. We characterize new analogues that maintain the selectivity of the inhibitor for RSK. In addition, we discover that SL0101 is an isoform-selective inhibitor of RSK1/2 and not RSK3/4. The importance of these findings is highlighted by the fact that RSK1/2 serve tumor-promoting functions, while RSK3/4 are thought to be tumor suppressors. Therefore, SL0101 displays a desired isoform-selectivity as a potential novel therapeutic strategy to treat cancers.

Isoform-specific functions of RSK are not very well understood. Here, we describe development of a biotin labeling-mediated proteomic screen to identify novel RSK1 interacting partners. We find that a portion of RSK1 interacts with intracellular membranes, while RSK2 does not. We identify potential novel RSK1-binding partners

among the proteins of the endoplasmic reticulum and mitochondrial membranes. Therefore, we postulate that RSK1 may be involved in regulation of protein synthesis and energy homeostasis.

Finally, we uncover a novel function of RSK1/2 in stimulating mitochondrial oxidative phosphorylation in breast cancer cells. We find that this function of RSK1/2 is specific to transformed cells. Therefore, we postulate that RSK1 can be involved in the metabolic transformation of breast cancer cells. Blocking this function by means of small molecules we develop could constitute a novel therapeutic strategy to target alterations in metabolism of cancer cells.

Given the emerging roles of RSK1/2 in promoting metastasis, we envision that RSK inhibitors could constitute a novel class of drugs targeting this aspect of cancers. Our studies open new avenues of investigation of RSK-mediated cellular processes and their role in various disease states.

Dedication

This thesis is dedicated to my partner, Josh Escue- who created a home away from home for me, to my parents Anna and Janusz Mrozowscy, who have always encouraged me to chase my dreams, to my grandparents Krystyna Mrozowska and Alicja and Tadeusz Starosta, for being my patrons on every step of my education and introducing me to the world of science, and to my best friend Katarzyna Ludwik, for embarking on that journey with me.

Acknowledgements

I would like to thank those people who contributed to my training as a scientist and to my graduate experience at Vanderbilt University. I would like to express my deepest appreciation to my mentor Deborah A. Lannigan PhD, for guiding me on the path to a future career. I would also like to thank my thesis committee chair, Alissa Weaver MD PhD for her support and guidance. I am grateful to my thesis committee members, Ian G. Macara PhD, Vito Quaranta MD, David Wasserman PhD and Andries Zijlstra PhD for all their help and invaluable suggestions. I would like to thank my Director of Graduate Studies, W. Gray Jerome PhD for all his support and advice.

I would like to acknowledge my collaborators, George O'Doherty PhD, Michael Hilinski PhD, Donald F. Hunt PhD, Lissa Anderson PhD and Jeffrey Shabanowitz PhD, as well as Kyle Hoehn PhD. I was an honor and privilege to work with them. I am grateful for the support and assistance form the administrative staff of the Department of Pathology, Microbiology and Immunology, Kristi Hargrove and Whit Adams.

Finally, I would like to thank the current and past members of the Lannigan Laboratory, for their kindness, friendship and patience. Working with them has been a wonderful experience. In particular, I would like to thank Katarzyna Ludwik, Lejla Pasic, Miranda Sowder, Preston James Campbell PhD, Zachary Sandusky and Allison Isabelli, as well as David Clark and Karin Eisinger-Mathason.

Table of contents

List of figures and tables

List of abbreviations

4E-BP1	eukaryotic translation initiation factor 4E-binding protein 1
Abl	Abelson murine leukemia
ACO2	mitochondrial aconitase 2
AF1	activation-function 1
AGC	protein A, protein G and protein C
Akt	protein kinase B
AMP-PNP	adenylylimidodiphosphate
AMPK	AMP-activated protein kinase
ANT	adenine nucleotide translocase
APC	anaphase-promoting complex
AS160	Akt substrate 160 kDa
ATF4	activating transcription factor 4
ATP	adenosine triphosphate
AUC	area under the curve
Bad	BCL2-associated agonist of cell death
Bcl-xL	BCL2-like 1

Bcl2	B-cell CLL/lymphoma 2
BCR-Abl	breakpoint cluster region- Abelson murine leukemia
BH3	Bcl-2 homology-3
BHK	baby hamster kidney
BMDC	bone marrow derived dendritic cells
BRAF	v-raf murine sarcoma viral oncogene homolog B
BSA	bovine serum albumin
c-Myc	v-myc avian myelocytomatosis viral oncogene homolog
C/EBPβ	CCAAT/enhancer binding protein beta
CAD	collisionally activated dissociation
CaMK	calcium/calmodulin dependent protein kinase
cAMP	cyclic adenosine monophosphate
CBP	CREB-binding protein
CCA	alpha-cyano-4-hydroxycinnamic acid
Cdc25C	cell division cycle 25C
CDK2	cyclin-dependent kinase 2
CHIP	STIP1 homology and U-box containing protein 1, E3 ubiquitin protein ligase

CHK1	Checkpoint kinase 1
CK1	casein kinase 1
CLK1/2	CDC-like kinases 1 and 2
CLL	chronic lymphocytic leukemia
CLN6	ceroid-lipofuscinosis, neuronal 6, late infantile, variant
CLS	Coffin-Lowry syndrome
cmk	chloromethyl ketone
CML	chronic myelogenous leukemia
CREB	cAMP response-element-binding protein
CTKD	C-terminal kinase domain
DAPK	death associated protein kinase
DBA	dibenzylideneacetone
DC	dendtitic cells
DDQ	2,3-dichloro-5,6-dicyano-1,4-benzoquinone
DDX54	DEAD (Asp-Glu-Ala-Asp) box polypeptide 54
DMAP	4-dimethylaminopyridine
DMEM	Dulbecco's modified Eagle's medium
DMSO	dimethyl sulfoxide

DTT	dithiotreitol
DYRK1a	dual-specificity tyrosine-(Y)-phosphorylation regulated kinase 1A
EDTA	ethylene diamine tetraacetic acid
EEA1	early endosome antigen-1
eEF2	eukaryotic translation elongation factor
eEF2K	eukaryotic translation elongation factor-2 kinase
EGF	epidermal growth factor
EGFR	epidermal growth factor receptor
eIF2B	eukaryotic translation initiation factor 4E
eIF3	eukaryotic translation initiation factor-3
eIF4B	eukaryotic translation initiation factor-4B
eIF4E	eukaryotic translation initiation factor 2B
Elk1	ETS-like gene 1
ER	endoplasmic reticulum
ER81	ETS translocation variant 1
ERα	estrogen receptor alpha
ERE	estrogen response element
ERK1/2	extracellular signal regulated kinases 1 and 2

ERK5	extracellular signal regulated kinase 5
ETC	electron transport chain
ETD	electron transfer dissociation
ETS	E26 transformation-specific
FAK	focal adhesion kinase
FBS	fetal bovine serum
FCCP	carbonyl cyanide-p-trifluoromethoxyphenylhydrazone
FGFR3	fibroblast growth factor receptor 3
FLT3	fms-related tyrosine kinase 3
fmk	fluoromethyl ketone
FRA1	Fos-related antigen 1
FT	Fourier transform
GAP	GTPase activating protein
GLUT4	glucose translocator 4
GSK3	glycogen synthase kinase 3
GST	glutathione S-transferase
HBD	hormone-binding domain
HEK	human embryonic kidney

HEPES	4-(2-hydroxyethyl)-1-piperazineethanesulfonic acid
HER2	human epidermal growth factor receptor 2
HIP1-3	huntingtin interacting proteins 1-3
HK1	hexokinase 1
HKDC1	hexokinase domain containing 1
HNSCC	head and neck squamous cell carcinoma
HPLC	high pressure liquid chromatography
HRP	horseradish peroxidase
hTERT	human telomerase reverse transcriptase
i.p.	intraperitoneal
i.v.	intravenous
IC50	half-inhibitory response
ICER	inducible cAMP repressor
IGF-1R	insulin-like growth factor-1 receptor
IκB	inhibitor of kappa B
Il8	interleukin-8
IR	infrared
IRAK	interleukin-1 receptor-associated kinase 4

IRS-1	insulin receptor substrate 1
KIT	Mast/stem cell growth factor receptor
LC/MS	liquid chromatography mass spectrometry
Lck	lymphocyte-specific protein tyrosine kinase
Lkb1	liver kinase B1
LRRK2	leucine-rich repeat kinase 2
Mad1	mitotic arrest defficient protein 1
MALDI-TOF	matrix-assisted laser desorption ionization time-of-flight
MAP3K1	MAPK kinase kinase 1
MAPK	mitogen activated protein kinase
MAPKAP-K2	MAPK-activated protein kinase 2
Max	MYC associated factor X
Mcl1	myeloid cell leukemia 1
MCU	mitochondrial calcium uniporter
MCUR1	mitochondrial calcium uniporter regulator 1
MDCK	Madin-Darby canine kidney
MEK	Mitogen-activated protein kinase kinase
MEK5	MAPK kinase 5

MELK	maternal embryonic leucine zipper kinase
MICU1	mitochondrial calcium uptake 1
MK2/3	mitogen-activated protein kinase-activated protein kinases 2 and 3
MOI	multiplicity of infection
MSK1/2	mitogen and stress-regulated kinases 1 and 2
MST2	serine/threonine kinase 3
MTCO2	mitochondrially encoded cytochrome C oxidase II
mTOR	mammalian target of rapamycin
Myt1	myelin transcription factor 1
NADH	nicotinamide adenine dinucleotide
NF-κB	nuclear factor kappa B
NHE1	sodium proton exchanger 1
NLS	nuclear localization signal
NMO	N-methylmorpholine
NMR	nuclear magnetic resonance
NOP56	nucleolar protein 56
NTKD	N-terminal kinase domain
OCR	oxygen consumption rate

OMSSA	open mass spectrometry search algorithm
PABP1	poly(A)-binding protein 1
PBS	phosphate-buffered saline
PDCD4	programmed cell death protein 4
PDGFR	Platelet-derived growth factor receptor
PDK1	3-phosphoinositide-dependent protein kinase
PDZ	post synaptic density protein (PSD95), Drosophila disc large tumor suppressor (Dlg1), and zonula occludens-1 protein (zo-1)
PKA	protein kinase A
PKC	protein kinase C
PLK1	Polo-like kinase 1
PMA	phorbol myristate acetate
PMB	phenylmagnesium bromide
PRKD1-3	protein kinases D1, D2 and D3
RabGAP	Rab-GTPase-activating protein
Ran	Ras-related nuclear protein
Raptor	regulatory-associated protein of mTOR
RAS	Rat sarcoma protein

RelA	v-rel avian reticuloendotheliosis viral oncogene homolog A
Rheb	Ras homolog enriched in brain
RhoA	ras homolog family member A
RIPK2	receptor-interacting serine-threonine kinase 2
ROCK1	Rho-associated, coiled-coil containing protein kinase 1
RSK	ribosomal S6-kinase
RSL1D1	ribosomal L1-domain-containing protein 1
S6K1/2	p70 S6 kinases 1 and 2
SAR	structure-activity relationship
SD	standard deviation
SDS	sodium dodecyl sulfate
SH3BP1	RasGAP SH3-domain-binding protein 1
SLC	solute carrier protein
SRF	serum response factor
STIP1	stress-induced phosphoprotein 1
STK10	serine/threonine kinase 10
STK11	serine/threonine kinase 11
STK16	serine/threonine kinase 16

STK4	serine/threonine kinase 4
SV40	simian vacuolating virus 40
t1/2	half-life
TCA	tricarboxylic acid
THF	tetrahydrofuran
TIA1	T-cell restricted intracellular antigen-1
TLC	thin layer chromatography
TMRM	tetramethylrhodamine methyl ester
TPA	tetradecanoyl phorbol acetate
TSC2	tuberous sclerosis complex 2
UCP	uncoupling protein
UQCRH	ubiquinol-cytochrome C reductase hinge protein
UV	ultraviolet
VDAC1	voltage-dependent anion channel-1
WT	wild-type
YB-1	Y-box protein 1

Chapter 1

Introduction: Overview of RSK inhibitors

1.1. Kinases as drug targets

Protein kinases represent one of the most important classes of molecular targets used in treatment of human diseases. The therapeutic potential of targeting kinases is based on three main observations. First, with the human kinome comprising approximately 520 kinases, almost every cellular process is controlled through a mechanism involving transduction of the phosphorylation signal (Manning et al., 2002, Zhang et al., 2009). Therefore, kinase inhibition can allow for a modulation of diverse processes. Second, even though kinases share a high degree of similarity in the mechanism of ATP binding and phosphotransfer, highly selective small molecules with desired biological properties can be developed (Bain et al., 2007, Davies et al., 2000). Third, biological studies have revealed that selective kinase inhibitors against specific targets involved in the disease can often be well tolerated by normal cells, providing a potential window for the therapeutic intervention (Zhang et al., 2009). In recent decades, 29 small-molecule kinase inhibitors have been approved for clinical use, the majority of them in oncological disorders (Fabbro, 2015). Approximately 130 further kinase inhibitors are reported to currently be in phase I-III clinical trials (Fabbro, 2015). Some of the approved molecules have proven very successful in therapy. An excellent example of such success is imatinib, an inhibitor of the oncogenic fusion kinase Bcr-Abl in the treatment of chronic myelogenous leukemia (CML) (O'Brien et al., 2003, Druker et al.,

2006). In addition to cancer, kinase inhibitors have found use in diverse disorders, including immunological, neurological, metabolic and infectious diseases (Zhang et al., 2009). Even beyond the novel therapeutic potential, selective small molecule kinase inhibitors remain an invaluable tool for studying basic biological processes regulated by kinases. Therefore, there is an ongoing effort to develop new molecules against known kinase targets, as well as to identify novel kinases amenable for therapeutic intervention.

1.2. Kinase domain structure

Several decades of extensive research in the area of structural biology have allowed us to understand the basic structure and mechanism of action of protein kinases (Cowan-Jacob et al., 2014). Protein kinases can be divided into two major groups, depending on the selectivity for the substrate amino acid. Kinases can phosphorylate Ser and Thr residue within their target, or a Tyr residue (Manning et al., 2002). Despite differences in certain regulatory motifs between these two classes of enzymes, they share the same overall domain structure. A kinase domain consists of a small N-lobe formed mostly from β-sheets, and a larger C-lobe comprising mostly α-helices (fig. 1). The two lobes are connected via a short hinge region. The groove formed between the two lobes of the kinase forms the binding site for the ATP molecule, which is the source of the phosphate group. The ATP molecule binds to the kinase through the hydrogen bonds between the adenine ring of ATP and amino acid residues within the hinge region of the kinase. The N-lobe contains a glycine-rich loop, which is involved in the proper positioning of the γ-phosphate for the phosphotransfer. Another part of the N-lobe interacting with the phosphates is the C-helix, which contains a Glu

residue that forms a salt-bridge with the Lys residue of the active site. The C-helix is a dynamic regulatory element of the kinase, and is often referred to as the signal integration motif (Johnson et al., 2001). The distance between the C-helix and the activation loop in the C-lobe is an essential determinant of the ability of the kinase to catalyze phosphotransfer, and therefore it defines the open and closed conformations of the enzyme (Narayana et al., 1997).

The C-lobe of the kinase contains the activation loop that is linked via a salt bridge to the aforementioned C-helix. The activation loop can undergo substantial conformational changes, which regulates the activity of the kinase. There is a wide diversity of conformations found among inactive states of kinases, and in some inactive kinases the activation loop is disordered. However, upon activation, almost all kinases attain a very highly conserved structure of the activation loop (Kornev et al., 2006). This activation is triggered by the phosphorylation of a regulatory Thr of Ser residue within the loop. The activation loop starts with a conserved sequence of three amino acids, Asp-Phe-Gly, hence it is referred to as the DFG motif. This motif coordinates the Mg2+ ion positioned close to the phosphate section of ATP, and this metal ion is essential for the cleavage of the phosphate bond. In many kinases in the inactive conformation the Phe residue within the DFG motif is occluding the site typically occupied by the ATP molecule, a conformation referred to as “DFG-out”. In these kinases, phosphorylation of the activation loop causes a rearrangement of this segment that switches the orientation of Phe residue, moving it away from the ATP site. Therefore, it now becomes the “DFG-in” conformation. In some kinases, however, as in the case of Src and CDK2,

Figure 1. Protein kinase domain structure.

A) Linear representation of the protein kinase secondary structures. Blue arrows represent β-strands, green cylinders represent α-helices, and red lines represent functionally relevant loops. The N-lobe consists mostly of β-strands and includes the glycine-rich loop and an αC-helix. The C-lobe is mostly composed of α-helices and includes the catalytic loop and the activation loop segment. The catalytic loop includes the catalytically active amino acid triad, HRD. The activation segment starts with the DFG amino acid triad and ends with the APE amino acid triad.

B) Tertiary structure of ATP bound to the active conformation of the kinase. Blue blocks represent core domains of the N- and C-lobe. Teal circle represents αC-helix within the N-lobe. Orange line represents activation loop, and within it red amino acid residues represent the DFG motif. Green line represents the catalytic loop and within it green amino acids represent the HRD motif. Dark blue line represents the hinge region between the two lobes. Gray loop represents the kinase substrate peptide. Lys residue within the αC-helix forms a salt bridge with Glu residue within the core of the N-lobe, and coordinates the triphosphate chain of ATP. Phe residue in the DFG motif moves away from the ATP-site to allow ATP binding. Phosphorylated residue in the activation loop interacts electrostatically with Arg residue within the HRD motif. His residue from the HRD motif catalyses γ-phosphate bond cleavage in the ATP molecule.

Figure 1

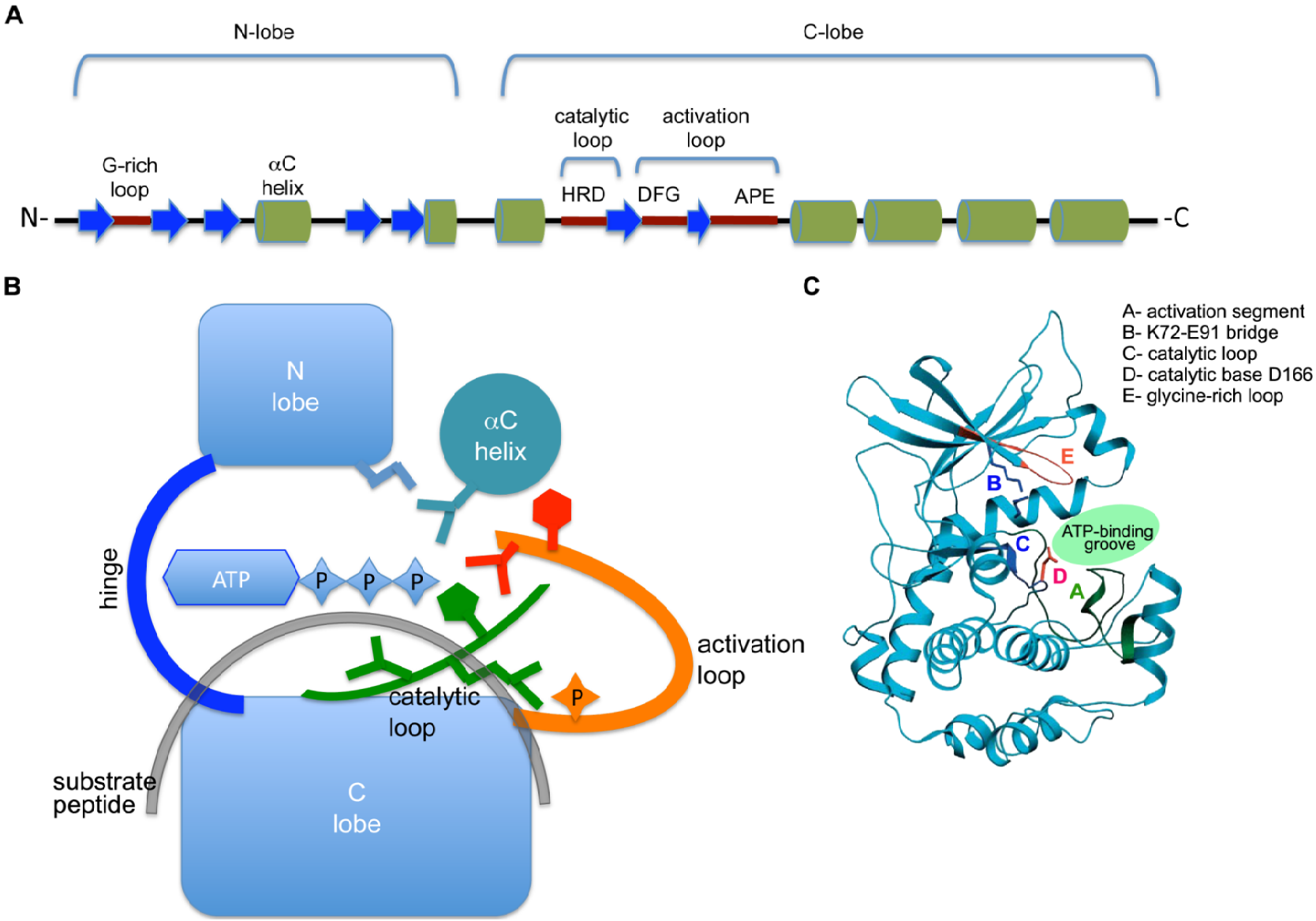
A
N-lobe
C-lobe
catalytic loop
activation loop
G-rich loop
αC helix
HRD
DFG
APE
N-
-C
B
N lobe
αC helix
ATP
P
P
P
hinge
activation loop
catalytic loop
P
substrate peptide
C lobe
C
A- activation segment
B- K72-E91 bridge
C- catalytic loop
D- catalytic base D166
E- glycine-rich loop
E
B
ATP-binding groove
C
D
A

the inactive conformation of the kinase still represents the DFG-out arrangement, and the activation of the kinase is mostly driven by the changes in the C-helix position. Whereas the DFG-in conformation will always indicate inactive kinase, the DFG-out conformation is not the only determinant of the activation state.

The activation loop ends with another triad of conserved residues, the APE motif. This motif is thought to assist in substrate recognition of the kinase. The binding of the substrate is performed by the P+1 loop, which binds the amino acid directly downstream from the phosphorylated residue of the substrate, hence the P+1 name. The phosphotransfer reaction is catalyzed by the residues contained in the catalytic loop of the C-lobe. The catalytic core of this segment is a sequence of three amino acid residues, the HRD motif. Within this motif, the Asp residue is a base acceptor for the proton transfer. The arginine residue coordinates with the phoshorylated residue in the activation loop to stabilize the active conformation. The presence of phosphorylated Ser/Thr residue is conserved among all kinases, however the exact interactions between this residue and the HRD motif differ between Ser/Thr and Tyr kinases (Krupa et al., 2004).

1.3. Modes of kinase inhibition

All kinases share a very conserved active site responsible for ATP binding and phosphotransfer. Therefore, small molecule inhibitors designed to bind to this site are likely to be able to inhibit a very wide range of kinases. In an effort to overcome this issue, early studies aimed at identifying sequence-specific features of the ATP-binding sites that could confer ligand binding specificity.

Figure 2. Structural diversity of kinase inhibitors

A) Mode of binding of the ATP molecule to the hinge region of the kinase. R indicates the position of the gatekeeper residue. Dashed lines represent hydrogen bonds.
B) Mode of binding of a type 1 inhibitor. A represents hydrogen bond acceptor and D represents hydrogen bond donor in the inhibitor molecule. HYD represents the hydrophobic core of the molecule. Type 1 inhibitor utilizes similar hydrogen bonds as ATP in binding to the hinge region of the kinase.
C) Mode of binding of a type 1.5 inhibitor. A represents hydrogen bond acceptor and D represents hydrogen bond donor in the inhibitor molecule. HYD represents the hydrophobic core of the molecule. Type 1.5 inhibitor utilizes similar hydrogen bonds as ATP in binding to the hinge region of the kinase, but also interacts with the peptide bond within the DFG motif in “DFG-in” conformation and a conserved Glu residue.
D) Mode of binding of a type 2 inhibitor. A represents hydrogen bond acceptor and D represents hydrogen bond donor in the inhibitor molecule. HYD represents the hydrophobic parts of the molecule. Type 2 inhibitor binds to the kinase in the “DFG-out” conformation, which exposes new hydrophobic pocket behind the DFG motif.

Figure 2

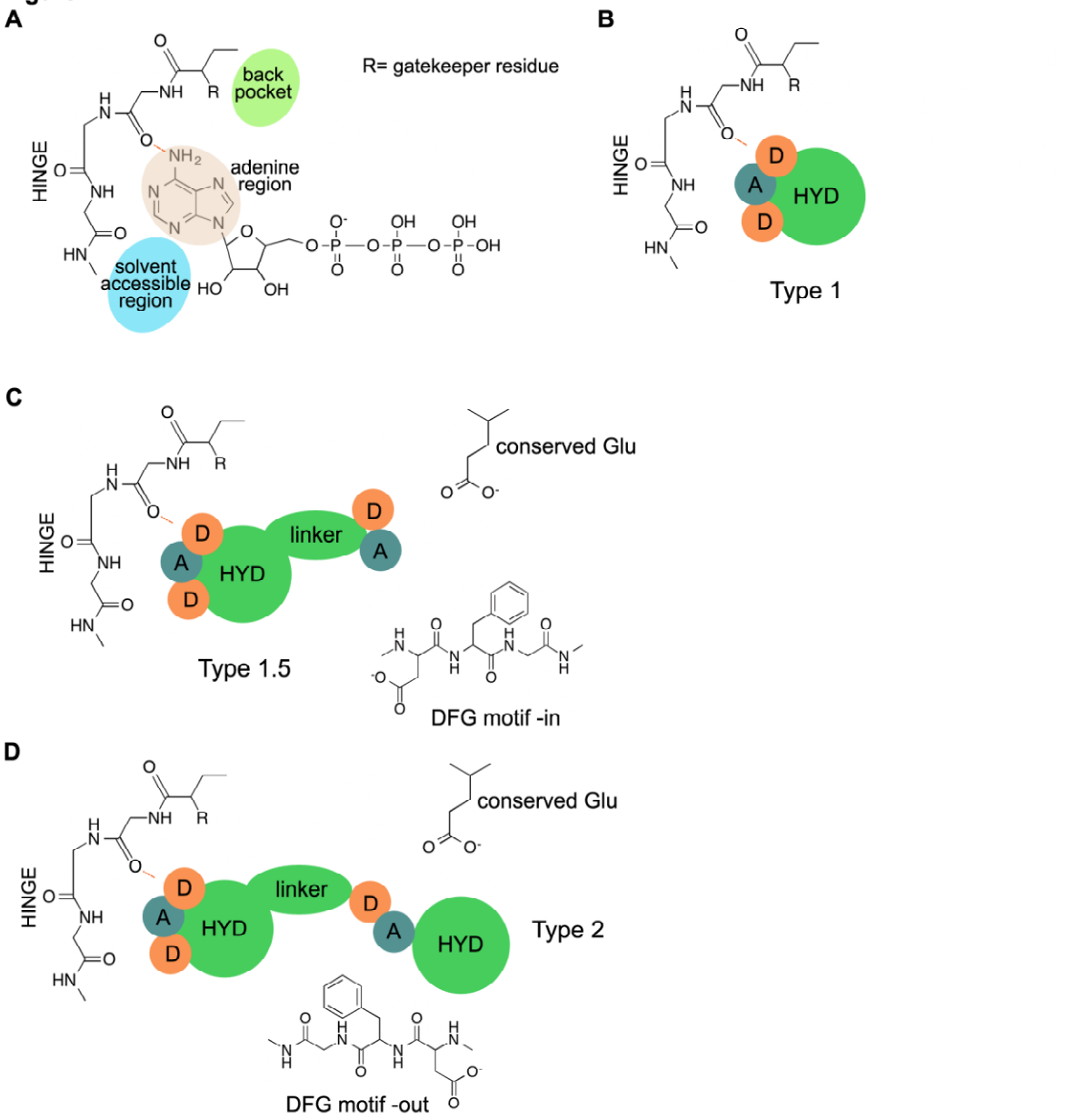
A
back pocket
R= gatekeeper residue
HINGE
adenine region
solvent accessible region
B
HINGE
D
A
HYD
D
Type 1
C
conserved Glu
HINGE
D
A
D
HYD
linker
D
A
Type 1.5
DFG motif -in
D
conserved Glu
HINGE
D
A
D
HYD
linker
D
A
HYD
Type 2
DFG motif -out

Through these studies the gatekeeper residue was identified (constituent “R” in fig. 2A). This amino acid side chain is typically located in the vicinity of the adenine-binding site and regulates the access of the small molecule to a hydrophobic pocket extending away from the hinge region of the kinase (Liu et al., 1999). It has been observed that 77% of all kinases in human kinome have a relatively large gatekeeper residue, such as leucine, methionine and phenylalanine, which effectively block the access of small molecules to the hydrophobic pocket (Taylor and Kornev, 2011). However, in 21% of all kinases, the gatekeeper residue is a small amino acid such as threonine and valine, which allows design of small molecules that would engage the hydrophobic pocket. The small gatekeeper is most frequently found in the tyrosine kinases and was first utilized in developing the Src kinase inhibitors (Liu et al., 1999). The selectivity of Gleevec, the inhibitor oncogenic kinase BCR-Abl, also relies on the presence of the threonine gatekeeper residue in the Abl kinase domain (Buchdunger et al., 2000). The rationale behind utilizing the gatekeeper residue for the drug design relies on creating a small molecule that would only fit in the hydrophobic pocket of the target kinase. Therefore, even though the ATP binding pocket of all kinases are very similar, the presence of both the gatekeeper and the hydrophobic pocket allow to rationalize highly specific small molecule inhibitors of kinases.

Based on the mode of inhibitor binding to the kinase, the small molecules can be classified into three general categories. Type I inhibitors will bind to the same site as the ATP molecule, acting as ATP mimetics (fig. 2B). A common feature of all type I inhibitors is the fact that they bind to the “DFG-in” conformation of the kinase. In the majority of cases this arrangement represents the active form of the kinase.

This bias can be explained by the fact that in most *in vitro* studies to identify new kinase inhibitors, the kinase molecules are fully activated. Therefore, such studies favor identification of molecules that will strongly interact with the active kinase conformation. In addition, many kinase inhibitors have been designed to mimic the size and shape of the ATP molecule. Such inhibitors will typically consist of a heterocyclic ring system occupying the adenine-binding site in the kinase groove (Zhang et al., 2009). As mentioned above, the selectivity of type I inhibitors often relies on the properties of the gatekeeper residue and the size and shape of the hydrophobic back pocket. Classic examples of type I inhibitors include gefitnib and erlotinib, the inhibitors of the epidermal growth factor receptor (EGFR) (Fabbro, 2015). In addition to the hydrophobic back pocket, selective type I inhibitors can employ more distant surfaces of the kinase for binding, such as the peptide-binding site. Examples of such molecules are bivalent/bitopic inhibitors (Hill et al., 2012) and macrocycles (Tao et al., 2007).

As mentioned above, in some kinases the DFG-in conformation is not sufficient to determine the activation state of the kinase. The inhibitors that utilize this property are classified as type 1.5 (fig. 2C). An example of such inhibitor is another inhibitor of EGFR, lapatinib. In the case of lapatinib, the molecule binds to a conformation in which the C-helix is pushed away from the activation loop (Wood et al., 2004). Therefore, even though the kinase is in the DFG-in fold, it is not active.

The second general class of inhibitors binds to the inactive DFG-out conformation of the kinase. Since these inhibitors are still binding to the same site as the ATP molecule, they still act as ATP-competitive inhibitors. The switch between the active DFG-in and inactive DFG-out conformation exposes an additional hydrophobic

pocket adjacent to the ATP site, which becomes engaged by the inhibitor molecule (fig. 2D). This interaction stabilizes the kinase in the inactive conformation (Cowan-Jacob et al., 2014). The examples of type 2 inhibitors include the inhibitors of PDGFR, KIT and Abl, imatinib and nilotinib (Fabbro, 2015).

The third main class of inhibitors represents those molecules that do not bind to the hinge region of the kinase. Since these compounds do not bind to the same site as ATP, in general they do not act as ATP-competitive inhibitors. Instead, binding of ATP can occur even when the inhibitor is bound to the kinase. Such inhibitors will therefore be classified as non-competitive inhibitors. The binding surface for the inhibitor is called the allosteric site, therefore type 3 inhibitors can also be referred to as allosteric inhibitors. This type of inhibitors tends to exhibit the highest degree of selectivity, because they rely on a very specific feature of the target kinase that does not have to be conserved in other enzymes. The modes of binding of allosteric inhibitors vary greatly between the representatives of this class of molecules, each exhibiting a unique set of properties. The best-characterized example of an allosteric kinase inhibitor is CI-1040, an inhibitor of MEK1/2. This compound occupies a site adjacent to the ATP-binding groove of MEK, but the surfaces involved in binding of the two molecules do not overlap (Ohren et al., 2004). Special cases of type 3 inhibitors are those that bind to an allosteric site, but the binding induces the DFG-out conformation of the kinase. In such case the Phe residue of the DFG motif forms a steric hindrance to the binding of ATP. Therefore, such inhibitors will act as functional ATP-competitors. The examples of such compounds include the inhibitors of insulin-like growth factor-1 receptor (IGF-1R) (Heinrich et al., 2010), FAK (Tomita et al., 2013) and p38 (Over et al., 2013). Allosteric

inhibition can also occur through the interactions of the molecule with the substrate-binding surface of the kinase, like in the case of thioqinazolinones, the CHK1 inhibitors (Converso et al., 2009). Finally, allosteric inhibitors can bind to regulatory sites of the kinase that are far removed from the ATP binding site, like in the case of Abl inhibitors binding to the myristate pocket of the kinase (Adrian et al., 2006).

1.4. MAPK pathway as a drug target

RAS-MAPK pathway has long been recognized as a very important pro-survival and pro-growth pathway that is often activated in cancer (Sebolt-Leopold and Herrera, 2004). More than 30% of all human cancers harbor mutations within this pathway, mostly leading to gain of function and hyperactivation of the pathway (Hoshino et al., 1999). In addition, RAS-MAPK has also been investigated in the context of inflammatory diseases, cardiac hypertrophy and pain (Stanton et al., 2003, Hofman, 2004, Ji, 2004). Therefore, there has been a lot of interest in developing means of targeting this pathway, both in basic research and in clinical studies (Zhang et al., 2009). However, early studies revealed that inhibiting RAS/MAPK pathway could prove too toxic to normal proliferating cells, such as the gut and skin epithelia (Sebolt-Leopold and Herrera, 2004). Additional caveat to targeting the RAS-MAPK pathway lies in the number of feedback loops regulating the activity of the pathway that could overcome the inhibition. Therefore, targeting the downstream effectors of the RAS-MAPK pathway has emerged as a potential new way of blocking the pro-proliferative and pro-survival signaling of the RAS-MAPK axis. Since each downstream effector of the RAS-MAPK pathway regulates only a subset of all MAPK-regulated proteins, targeting these individual effectors would in principle decrease the likelihood of engaging the feedback

loops (Eisinger-Mathason et al., 2010). RSK is one of these downstream effectors that have been proposed as a target for RAS-MAPK signaling intervention.

1.5. RSK family of kinases

RSK is a family of four Ser/Thr protein kinases activated by the ERK1/2 pathway in response to growth factors, cytokines and neurotransmitters (Bonni et al., 1999, Bhatt and Ferrell, 1999). The four isoforms share very high degree of sequence similarity and are expressed as products of separate genes (Anjum and Blenis, 2008). RSK is unusual among other kinases in that it possesses two fully functional kinase domains (Fisher and Blenis, 1996) (fig. 3A). The only other dual kinases are two close relatives of RSK, the mitogen and stress regulated kinases 1 and 2 (MSK1/2). Despite very similar structures, MSK kinases appear to have very different biological functions (Arthur, 2008). MSK is predominantly activated by p38 MAPK family of kinases, and to a much lesser extent by ERK1 (Pierrat et al., 1998). The C-terminal kinase domain (CTKD) of RSK belongs to the calcium/calmodulin dependent protein kinase superfamily (CaMK), while the N-terminal kinase domain (NTKD) is a member of the superfamily encompassing protein kinases A, G and C (AGC). The sequences of the kinase domains of RSK are >80% conserved between the isoforms, while the N- and C-terminal extension and the linker between the kinase domains share less homology (Romeo et al., 2012). The linker region contains multiple regulatory sequences that are important for RSK interaction with other proteins, and activation of the protein. It is unclear why RSK and MSK evolved to have two functional kinase domains within one protein. It is thought that the complexity of RSK protein structure allows it to integrate signaling downstream of ERK1/2 with high fidelity in response to additional stimuli from

other pathways (Romeo et al., 2012). This notion is based on complex mode of activation of RSK kinases.

1.5.1. RSK activation cascade

The C-terminal tail of RSK contains an ERK1/2 docking site (Smith et al., 1999). Interaction of RSK with ERK1/2 through that motif is required for the activation of the kinase in response to mitogens. In the inactive state, ERK and RSK form a complex (Roux et al., 2003). When ERK1/2 is activated, it phosphorylates Thr577 residue within the CTKD of RSK, as well as two residues within the linker region, Thr365 and Ser369. Active ERK then dissociates from RSK and does not form a complex until is inactivated again. The mechanism of dissociation of the RSK-ERK complex involves RSK autophosphorylation of Ser737 in a close proximity of the ERK-binding site. Therefore, the re-assembly of the complex between the inactive kinases requires phosphatase action, however the identity of this phosphatase remains elusive. Phosphorylation of Thr577 mediated by ERK allows for the activation of the CTKD of RSK. The only known function of the CTKD is to autophosphorylate Ser386 residue in a hydrophobic motif within the linker of RSK (Frodin et al., 2000). This phosphorylation provides a docking site for PDK1, which phosphorylates Ser227 within the activation loop of the NTKD (fig. 3A) (Jensen et al., 1999). It has been suggested that in certain cellular contexts, additional kinases can phosphorylate Ser386, allowing for the activation of the NTKD in the absence of the CTKD-mediated stimulus. However, this alternative activation of the NTKD has only been reported in the context of dendritic cells (DC) and macrophages (Cohen et al., 2007, Zaru et al., 2007). In these cells, Toll-like receptor signaling triggered by lipopolysaccharide (LPS) signals through p38 to activate kinases MK2/3

that will phosphorylate Ser386 (Zaru et al., 2015). It is unknown whether the CTKD-independent activation of RSK is unique to the immune cells, or whether it can occur in other cell types, and what stimuli could activate this alternative pathway. It is important to note that Toll-like receptors are expressed by multiple cell types, including fibroblasts and epithelial and endothelial cells (Broz and Monack, 2013).

Regardless of the pathway leading to the phosphorylation of Ser386 in the linker region of RSK, the signal is always further propagated by PDK1, as there is no evidence of any other kinases phosphorylating Ser227 of RSK (Frodin et al., 2000). Therefore, it appears that even though there could be several pathways activating the Ser386, this signal requires PDK1 involvement in transferring the stimulus leading to the activation of the NTKD. Consistently, massive overexpression of PDK1 is sufficient to activate RSK in the absence of ERK activation (Jensen et al., 1999). PDK1 is also involved in the activation of Akt downstream of the PI3 kinase, and this activation requires PDK1 and Akt to colocalize at the plasma membrane (Alessi et al., 1997, Stokoe et al., 1997). However, unlike Akt, RSK is activated by PDK1 independent of the ability of PDK1 to interact with the cell membrane (McManus et al., 2004). Consistent with this notion, inhibition of the PI3 kinase does not reduce the activation of RSK, but completely blocks Akt activation (Moritz et al., 2010, Degen et al., 2013, De Mesquita et al., 2001). Therefore, although PDK1 is involved in the regulation of both RSK and Akt, it does not serve as a node integrating the ERK and PI3K pathway signals to stimulate RSK.

It is important to note, however, that although PDK1 is required for full activation of RSK1-3, RSK4 appears to have high basal activity that is independent of PDK1 (Dummler et al., 2005). That constitutive activity of RSK4 is associated with its

phosphorylation at conserved residues analogous to other members of RSK family, including the PDK1 docking site, but even in the complete absence of PDK1 Ser227 within the NTKD of RSK4 is still phosphorylated. The kinase phosphorylating Ser227 of RSK4 in the absence of PDK1 has never been identified, and it was proposed to be performed by RSK4 CTKD itself (Dummler et al., 2005). The phosphorylation of Ser227 induces changes in the conformation of the activation loop. These changes involve stabilization of the αC-helix in the ATP-binding pocket of the kinase, allowing for the optimal positioning of the amino acid residues involved in the phosphotransfer (Taylor and Kornev, 2011, Hauge et al., 2007). Interestingly, phosphorylation of Ser227 itself was found to account for only 10% of the maximal activity of the kinase (Frodin et al., 2002). The remaining 90% of activity is accomplished by the interactions of phosphorylated hydrophobic motif in the linker with the phosphate-binding site within the ATP-binding groove of the NTKD (Biondi et al., 2001). Therefore, Ser386 is responsible for both recruiting PDK1 to phosphorylate Ser227, and for increasing the activity of the NTKD through conformational change.

1.5.2. RSK knockout studies

Mutations in the RSK2 gene were shown to be associated with the Coffin-Lowry Syndrome (CLS), a form of X-linked mental retardation and dysmorphism (Temtamy et al., 1975, Jacquot et al., 1998). A wide spectrum of mutations in the RSK2 gene was observed in patients with CLS, but a common feature of all these alterations was a loss of RSK2 kinase activity (Pereira et al., 2010). Patients with CLS display short body stature, delayed bone age, delayed closure of fontanelles, osteopenia and digital dysmorphism. The skeletal abnormalities observed in CLS are also recapitulated in the

genetic RSK2 knockout mouse model. In addition to phenocopying the symptoms of CLS, RSK2 knockout mice display a number of other abnormalities, including insulin resistance, lipodystrophy and increased glycogen synthesis (El-Haschimi et al., 2003, Dufresne et al., 2001). RSK1/2/3 triple knockout animal has also been characterized to reproduce the cranioskeletal abnormalities observed in the RSK2 single knockout mice (Laugel-Haushalter et al., 2014). In addition to RSK2 knockout mice, loss of RSK2 has also been reported to cause skeletal abnormalities and cardiac hypertrophy in the zebra fish model (Lara et al., 2013). However, the knockout models of the three remaining isoforms individually have never been described. Therefore, the functions of individual members of the RSK family in development are still not very well understood.

1.5.3. RSK expression patterns

RSK1-3 appear to be ubiquitously expressed in all human tissues, although the relative expression levels of each isoform vary between cell types (Zeniou et al., 2002, Moller et al., 1994, Wu et al., 2009). On the mRNA level, RSK1 appears to be more abundant in the lung, kidney, pancreas, bone marrow and T cells, whereas RSK2 seems to be more highly expressed in T cells, skeletal muscle, heart, pancreas, lymph nodes and the prostate, compared to other tissues. RSK3 mRNA is most highly expressed in the lung, brain, skeletal muscle, heart, pancreas, spinal cord and retina. RSK4 mRNA is found at much lower levels compared to the other 3 RSK isoforms, and its levels seem to vary much less between the tissues (Kohn et al., 2003, Dummler et al., 2005, Wu et al., 2009). However, RSK4 was found to produce multiple splice variants of highly variable lengths, complicating our understanding of the expression patterns of this protein (Sun et al., 2013).

Figure 3. Complex biology of the RSK family of kinases.

A) RSK displays a modular structure with two fully functional kinase domains, as well as a linker and the C- and N-terminal extensions. In basal state ERK1/2 remains bound to the C-terminus of RSK. Upon ERK1/2 activation, this kinase phosphorylates residue Thr577 in the activation loop of the C-terminal kinase domain (CTKD), as well as two residues in the linker, Thr365 and Ser369. Activated CTKD phosphorylates Ser386 in the hydrophobic motif o the linker, which recruits the kinase PDK1. PDK1 phosphorylates Ser227 in the activation loop of the N-terminal kinase domain (NTKD), which leads to activation of the kinase. NTKD phosphorylates downstream targets of RSK.

B) RSK1 and RSK2 phosphorylate diverse groups of substrates to reglate protein synthesis and gene expression programs.

C) RSK kinases have been implicated in a variety of mechanisms regulating cellular nutrient uptake and energy homeostasis.

Figure 3

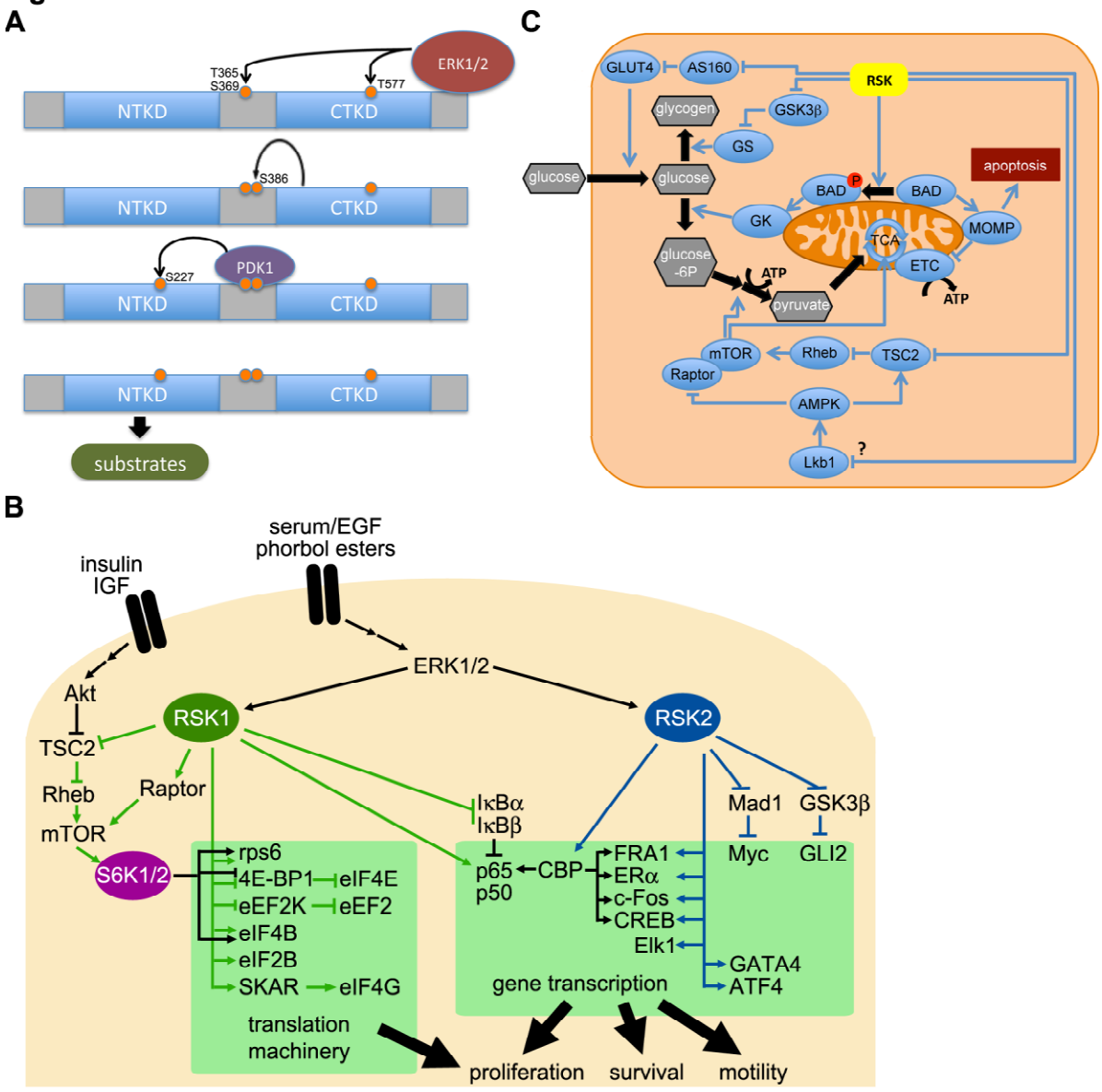
A
ERK1/2
T365
S369
T577
NTKD
CTKD
S386
PDK1
S227
substrates
C
GLUT4
AS160
RSK
glycogen
GSK3β
GS
glucose
BAD
P
apoptosis
GK
MOMP
TCA
glucose -6P
ATP
ETC
pyruvate
mTOR
Rheb
TSC2
Raptor
AMPK
Lkb1
?
B
insulin
IGF
serum/EGF
phorbol esters
ERK1/2
Akt
RSK1
RSK2
TSC2
Rheb
Raptor
mTOR
S6K1/2
IκBα
IκBβ
p65
p50
CBP
Mad1
GSK3β
Myc
GLI2
rps6
4E-BP1
eIF4E
eEF2K
eEF2
eIF4B
eIF2B
SKAR
eIF4G
FRA1
ERα
c-Fos
CREB
Elk1
GATA4
ATF4
gene transcription
translation
machinery
proliferation
survival
motility

Variable expression patterns and co-expression of multiple isoforms of RSK in tissues have long been proposed as the evidence of isoform-specific functions of RSK (Lara et al., 2013). However, teasing apart these isoform-specific functions has proven notoriously difficult. Many of the studies that reported the functions of RSK in specific cellular contexts have not investigated which isoform was responsible for the observed phenotypes. In many cases it is also unclear if the specified isoform is the only RSK that can perform a given function and what is the degree of redundancy between the isoforms. Despite all these limitations, with the history of over 20 years of studies, we can begin to observe common themes and tendencies of certain isoforms to be more likely to perform a specific function. In the following sections, such common themes will be proposed.

1.5.4. RSK substrate recognition

To better understand what are the potential phosphorylation targets of the RSK family of kinases, the consensus phosphorylation motif of these proteins has been characterized by several groups. It was found that RSK preferentially phosphorylates *in vitro* Ser and Thr residues contained within a consensus motif RxRxx(S/T) or RRx(S/T), where Arg can also be Lys (Leighton et al., 1995, Galan et al., 2014, Stokoe et al., 1993). Interestingly, the same consensus motif has also been found to be phosphorylated by other kinases of the AGC superfamily, including Akt and S6K1 (Leighton et al., 1995, Stokoe et al., 1993). All these studies used *in vitro* phosphorylation of peptide libraries to map the phosphorylation sites, and the kinase used in these studies was either RSK1 or it was not specified which isoform was used. However, since S6K1 kinase domain shares 56% identity with RSK1 NTKD, and all four

RSK isoforms are >90% identical in their NTKD sequence, it is very likely that all these isoforms will phosphorylate the same consensus motif. Indeed, an analysis of all RSK substrates reported to date has confirmed that these substrates share the RxRxxS or RRxS motifs (Smadja-Lamere et al., 2013). Intriguingly, only 3 out of 47 reported RSK substrates are phosphorylated on Thr residue, but the basis for such selectivity remains unknown.

Since multiple AGC kinases can potentially phosphorylate the same motif, additional levels of regulation are required for the appropriate substrate choice. In case of RSK, substrate selectivity has been proposed to be achieved by specific interactions of substrates with the PDZ-binding motif in the extreme C-terminus of RSK (Romeo et al., 2012). This motif has been shown to be important in the regulation of RSK2-dependent synaptic functions in the rat brain (Thomas et al., 2005). However, the PDZ ligand sequence of RSK is not conserved in *Drosophila* and in *Caenorhabditis elegans.* In addition, all four isoforms of RSK possess this PDZ ligand motif in their sequences. Finally, many of known RSK substrates do not contain the PDZ motif. These observations suggest that the PDZ ligand motif is responsible for regulating phosphorylation of a small subset of RSK2-substrates, and it is not the only factor regulating substrate specificity of RSK.

A potential mechanism contributing to the substrate-specificity of RSK isoforms could involve differential localization of these proteins to various cellular compartments. When inactive, all 4 RSK isoforms were found to predominantly localize to the cytoplasm (Chen et al., 1992, Zhao et al., 1995, Eisinger-Mathason et al., 2008). However, several pieces of evidence suggest that upon activation, RSK isoforms can

change their sub-cellular distribution. First, Active RSK1 was suggested to transiently localize to the plasma membrane, and then translocate to the nucleus (Richards et al., 2001). However, the study used an overexpression of avian RSK1, and the localization of the endogenous RSK1 still remains controversial. One study using RSK1-specific antibody in immunohistochemistry found that in brain tissue sections RSK1 localizes to the perinuclear region in cells and is not found in the nuclei (Heffron and Mandell, 2005). The authors of this study suggested that the perinuclear region enriched in RSK1 staining could represent the Golgi apparatus. However, multiple other sub-cellular compartments, including mitochondria, endosomes and lysosomes are also known to accumulate in the perinuclear region in multiple cell types.

RSK1 and RSK2 have also been suggested to associate in the cytoplasm with polysomes, the actively translating ribosomes (Angenstein et al., 1998). Inactive RSK2 was found to be cytoplasmic and to translocate into the nucleus upon mitogen activation (Eisinger-Mathason et al., 2008). In addition, this study found that RSK2 localized to cytoplasmic protein-mRNA aggregates called stress granules. Nuclear localization of RSK seems to require its phosphorylation and activation, however the lack of isoform-specific antibodies of phospho-RSK has impeded the identification of specific isoforms capable of nuclear localization.

Of all the isoforms, only RSK3 has a putative nuclear accumulation signal (NLS), and was found to localize to the nucleus using RSK3-specific antibody (Zhao et al., 2003). Nuclear localization of RSK3 is supported by the staining pattern observed in the immunohistochemistry of multiple tissues reported in the Human Protein Atlas (Uhlen et al., 2015). Sub-cellular distribution of RSK4 was only investigated once, and in this

study it was found to be predominantly cytoplamic (Romeo et al., 2012, Dummler et al., 2005). The authors of this study also found RSK4 to be consitutively active, suggesting that activation of this protein does not lead to its nuclear accumulation.

Taken these observations together, differential sub-cellular localization of RSK isoforms remains a potential factor contributing to the substrate specificity of RSK family members. However futher studies are required to elucidate the exact distribution of isoforms, as well as the underlying mechanisms of targeting RSK proteins to different cellular compartments.

The fact that several kinases share the same substrate recognition motif further supports the hypothesis that additional, yet undiscovered factors, regulate the substrate specificity of RSK. Furthermore, the same phophorylation sites could be modified by other kinases in addition to RSK. Indeed, the studies of small-molecule inhibitors of MEK and PI3K, the upstream activators of RSK and Akt, respectively, showed a significant overlap between the phosphorylation targets of these kinases in the context of gastric and lung cancer cell lines (Moritz et al., 2010). Excellent examples of such overlapping targets are CREB, TSC2 and ribosomal S6 protein (rps6). These observations further complicate the understanding of the exact signals mediated by RSK. With these caveats in mind, the following sections of this chapter will summarize the current state of knowledge on the functions of RSK in various cellular processes.

1.5.5. RSK regulation of translation

RSK was originally discovered to phosphorylate rps6 *in vitro* (Erikson and Maller, 1986). However, later studies indicated that in somatic cells this phosphorylation was

predominantly mediated by p70 S6 kinases (S6K1 and S6K2) (Blenis et al., 1991). In addition, inhibition of S6K1/2 signaling by blocking its upstream activator, mTOR, using rapamycin, showed complete loss of insulin-stimulated rps6 phosphorylation, further suggesting major role of S6K1/2 in phosphorylating S6 protein (Chung et al., 1992). Finally, cells derived form S6K1/2 double knockout mice showed almost complete loss of rps6 phosphorylation (Pende et al., 2004). However, the same S6K1/2 double knockout cells still displayed very low levels of phosphorylation of rps6 that were still dependent on MAPK activation, suggesting residual role of RSK in phosphorylating this target *in vivo*. That role of RSK in phosphorylating rps6 in addition to S6K1/2 was further supported by studies using silencing of RSK1/2 in serum-stimulated HEK293 and HeLa cells (Roux et al., 2007). This study revealed that out of four phosphorylation sites within rps6, two were exclusively phosphorylated by S6K1 (Ser240 and Ser244), while the other two sites were phosphorylated by both RSK1/2 and S6K1 (Ser235/236). Ser235/236 phosphorylation enables rps6 protein interaction with the 7-methylguanosine cap complex, which promotes cap-dependent translation and polysome assembly (Roux et al., 2007). Therefore, RSK1/2 appears to regulate global protein translation in response to mitogenic stimulation, and it does so in cooperation with S6K1 through co-regulation of rps6. This notion is supported by the finding that both RSK1 and RSK2 associate with actively translating ribosomes (Angenstein et al., 1998).

In addition to phosphorylating rps6, RSK has been reported to regulate multiple other proteins involved in controlling global protein translation. For example, RSK1 was shown to phosphorylate kinase eEF2K (Wang et al., 2001b, Das et al., 2010). The only

known substrate of this kinase is eukaryotic elongation factor-2 (eEF2) (Kaul et al., 2011). RSK1-mediated phosphorylation of eEF2K inactivates this kinase, which leads to a decrease in the phosphorylation of eEF2. De-phosphorylation of eEF2 enables it to promote the elongation step of translation. Therefore, active RSK1 stimulates protein translation through maintaining the de-phosphorylated state of eEF2. Both studies of the role of RSK in regulating eEF2 phosphorylation have used the dominant negative (DN) mutant of RSK1 to show that loss of RSK1 activity is sufficient to block eEF2K function. These results suggested that it is RSK1, and not other RSK isoforms, that phosphorylates eEF2K. It is possible that the DN mutant of RSK1 would interfere with the activities of other RSK isoforms, and the two studies did not assess changes in pS380 or pS227 of RSK upon DN-RSK1 expression. Therefore, it remains a theoretical possibility that one of the other RSK isoforms of RSK is also involved in the regulation of eEF2.

RSK1 has also been reported to phosphorylate the eukaryotic translation initiation factor-4B (eIF4B) in three independent studies (Shahbazian et al., 2006, Degen et al., 2013, Kroczynska et al., 2009, Kuang et al., 2011). These studies used silencing and knock-down of RSK1, as well as expression of DN-RSK1 mutant, to show that loss of the activity of this kinase was sufficient to abrogate eIF4B phosphorylation. RSK1-mediated phosphorylation of this protein was shown to increases eIF4B interaction with the eukaryotic translation initiation factor 3 (eIF3), which stimulated cap-dependent translation. While several studies showed the ability of RSK1 to phosphorylate eIF4B, RSK2 knock-down did not change the phospho-eIF4B levels,

suggesting that eIF4B is a specific target of RSK1, and not of other RSK family members (Kroczynska et al., 2009).

The connection between RSK activity and eIF4B has also been reported in the context of the lytic replication of the Kaposi Sarcoma-associated Herpesvirus (KHSV). The authors of the study reported that RSK activation in the Kaposi sarcoma cell line was triggered by the expression of the KHSV-derived protein ORF45, which led to an increase in the phospho-eIF4B levels (Kuang et al., 2011). This increase in eIF4B could be reversed by silencing of both RSK1 and RSK2 simultaneously, and was increased by over-expression of both wild-type and consitutively-active RSK2, but not by an over-expression of the kinase-dead version of RSK2. However, it was not determined whether silencing of individual isoforms alone was sufficient to block the phosphorylation of eIF4B. In addition, the effects of the ectopic expression of RSK2 on the activity of RSK1, were not assessed. Therefore, it remains unknown if RSK2 can phosphorylate eIF4B. Despite these shortcomings, it is important to note that this study provided additional evidence for the role of RSK in regulating eIF4B phosphorylation in various cellular contexts. It also implicated RSK in stimulating the replicative potential of the KHSV virus, suggesting that RSK could also play a role in viral infections.

Finally, another mechanism by which RSK was shown to regulate cap-dependent translation is through the phosphorylation of 4E-BP1 (Kroczynska et al., 2011). 4E-BP1 can be phosphorylated by S6K1 in response to insulin stimulation, and this phosphorylation is completely rapamycin-sensitive (Wang et al., 2005). However, stimulation of a human adenocarcinoma cell line, as well as a retinal pigment epithelial cell line and immortalized mouse embryonic fibroblasts, with interferon-lambda (IFN-λ)

was shown to induce phosphorylation of 4E-BP1 that was partially inhibited by both rapamycin and the MEK inhibitor UO126 (Kroczynska et al., 2011). In these cells, inactive RSK1 was associated with a repressive complex of 4E-BP1 and eIF4E, and IFN-λ–triggered activation of this kinase caused both phosphorylation of 4E-BP1 and release of eIF4E. Although rapamycin treatment partially reduced the phosphorylation of 4E-BP1, it was not sufficient to dissociate RSK1 from 4E-BP1 and release the inhibition of eIF4E. Therefore, in the context of IFN-λ in both normal epithelial and cancer cell lines, RSK1 was shown to integrate the ERK1/2 input with signals downstream of mTOR to ultimately stimulate the cap-dependent translation through 4E-BP1/eIF4E complex. It is also worth mentioning that this manuscript corroborated the previous findings that eIF4B was a target of RSK1 (Kroczynska et al., 2009, Kroczynska et al., 2011). Interestingly, IFN-λ is an important cytokine produced by multiple cell types in response to viral infections (Kotenko et al., 2003). Therefore, the studies of RSK1 in the context of eIF4B and 4E-BP1 have also suggested its involvement in viral infection. Consistent with this hypothesis, a recent study has demonstrated that RSK1 phosphorylates SKAR in response to another cytokine, interferon-alpha (INF-α) (Kroczynska et al., 2014). This phosphorylation facilitates interaction of SKAR with eIF4G, resulting in an increase in cap-dependent translation.

Early studies have also implicated RSK in phosphorylation of the glycogen synthase kinase-3β (GSK3β) both *in vitro* in cell-based assays (Sutherland et al., 1993, Stambolic and Woodgett, 1994, Torres et al., 1999, Eldar-Finkelman et al., 1995). GSK3β phosphorylates and thereby inactivates the eukaryotic translation initiation factor-2B (eIF2B) (Wang et al., 2002). Therefore, active RSK could increase the activity

of eIF2B to drive translation. As these studies were performed before the complexity of RSK family became appreciated, it is very difficult to determine which isoforms were investigated in this context. For example, one report by the Cohen group mentions using RSK2 *in vitro* (Sutherland et al., 1993), while the same group later states that RSK1 was used in this study (Stambolic and Woodgett, 1994). The sequences of used contructs were not included in the manuscripts, making it impossible to independently identify the isoforms. It is important to note, that GSK3β is regulated by multiple other kinases, including PKA, Akt and S6K1/2 (Cross et al., 1995, Fang et al., 2000). As a result, it is still unknown to what extent RSK contributes to the regulation of protein translation by GSK3β. The regulation of GSK3β by RSK could heavily depend on the cell type and the activating stimulus, just like in the case of 4E-BP1. For example, in rat cerebellar granule neurons potassium triggers phosphorylation of GSK3β that is completely independent of MEK-ERK-RSK activation (Song et al., 2010).

As mentioned above, multiple examples demonstrated that RSK can share its substrates with the elements of the mTOR pathway. This pathway itself has been extensively studied in the context of global protein synthesis (Mayer and Grummt, 2006). For example, mTOR activates transcription of RNA polymerases I and III, which are responsible for the synthesis of ribosomal RNA. In addition, mTOR drives expression of RNA polymerase II, which is responsible for the expression of ribosomal proteins. Finally, mTOR activates S6K1/2, which cooperates with RSK1 to phosphoylate and activate rps6, eIF4B and 4E-BP1. Adding to the complexity of the regulation of protein translation by both mTOR through S6K1/2 and ERK1/2 through RSK, a crosstalk between these two pathways has also been discovered. RSK1 was revealed to be the

protein mediating this crosstalk, and it was shown to perform this function through at least two meachinsms. First, it was shown to phosphorylate the protein protein tuberous sclerosis complex-2 (TSC2) (Roux et al., 2004). This phosphorylation leads to a release of TSC2-mediated inhibition of the upstream activator of mTOR, Rheb (Inoki et al., 2003). Second, RSK has been shown to phosphorylate another component of the mTOR pathway, the mTORC1 component Raptor (Carriere et al., 2008a). In the case of Raptor, RSK1 was shown to phosphorylate it *in vitro*, but in cell based assays a dual silencing of RSK1/2 and inhibition of all 4 isoforms of RSK was used. As a result, it is still not clear which isoform of RSK phosphorylates Raptor in intact cells. Taken these observations together, RSK1, and potentially other RSK isoforms as well, could regulate global protein translation through promoting mTOR-mediated ribosome biogenesis and cap-dependent translation.

In addition to functions in stimulating ribosome biogenesis and translational activity, RSK was shown to participate in stabilizing mRNA molecules. Under certain stress conditions that reduce or block protein translation cells will sequester nascent mRNA molecules into cytoplasmic RNA-protein aggregates called stress granules (Kedersha et al., 2002, Kedersha et al., 2005). The function of stress granules is to protect mRNA molecules from degradation such that when the block in translation is alleviated cells can rapidly restore synthesis of necessary proteins. In addition to mRNA, stress granules contain multiple proteins, including the T-cell restricted intracellular antigen-1 (TIA1), poly(A)-binding protein-1 (PABP1), RasGAP SH3-domain-binding protein-1 (SH3BP1), elongation factors 2 and 3 (eIF2, eIF3) and 40S ribosomal components (Kedersha et al., 1999, Kedersha et al., 2000, Kedersha et al., 2005,

Kedersha et al., 2002, Tourriere et al., 2003). Intriguingly, RSK2 was found to regulate formation and be recruited to newly formed stress granules upon induction of oxidative stress in breast epithelial cells (Eisinger-Mathason et al., 2008). RSK2 was found to regulate stress granule formation through its interactions with TIA1. This ability to stimulate stress granule assembly was dependent on RSK2 kinase activity, as both RSK small-molecule inhibition and RSK2 kinase-dead mutant prevented stress granule formation. This study also found that RSK2-dependent assembly of stress granules promotes cell survival in response to oxidative stress. Finally, while silencing RSK2 prevented formation of the stress granules, loss of RSK1 expression did not have the same effect.

In summary, RSK has been shown to activate protein translation through a variety of mechanisms (fig. 3B). In the majority of studies RSK1 was suggested as a predominant isoform responsible for the effects. Some of the downstream targets of RSK1 in this context are shared by S6K1/2 and mTOR. These two kinases themselves can be regulated by RSK1 through the inhibitory phosphorylation of TSC2. Therefore, RSK appears to stimulate translation in partial co-operation with the mTOR pathway. The role of RSK in this context could be to serve as an integrator of Ras-MAPK and PI3K-mTOR inputs leading to changes of protein translation. Regulation of global protein translation by RSK highlights the importance of this family of kinases in promoting cell growth and prolifertation. Interestingly, global protein translation has been proposed to act as a potential driver of transformation and drug resistance in various tumor types (Larsson et al., 2007, Lim et al., 2013b, Meric-Bernstam et al., 2012, Pervin et al., 2008). Consistent with the potential role of RSK1-dependent

translation in the context of cancer, a recent report has demonstrated that over-expression of RSK1 conferred resistance of MCF-7 breast cancer cell line to the inhibition of the PI3 kinase pathway (Serra et al., 2013). This aquired resistance was associated with a rescue in a phosphorylation of rps6. Furthermore, blocking RSK activity sensitized multiple cell lines to the inhibitors of the PI3K-Akt pathway. Intriguingly, an overexpression screen of kinases conferring resistance to PI3K inhibitors performed in this study also identified RSK3 and RSK4 as potential proteins involved in the resistance to PI3K inhibitors. Over-expression of each of these two kinases was sufficient to partially rescue both phospho-rps6 and phospho-eIF4B levels in cells treated with PI3K inhibitors, suggesting that RSK3/4 could also regulate protein translation (Serra et al., 2013). Since the study did not assess the effects of RSK3/4 expression on S6K1/2 phosphostatus, it remains unclear whether these two isoforms of RSK act to directly phosphorylate the components of the cap-dependent translation, or to re-activate S6K1/2 kinases, for example through the RSK-TSC2-mTOR crosstalk. It also remains unclear whether the role of RSK3 and RSK4 in regulating protein translation is limited to breast cencer cell lines and what is their contribution to this process relative to RSK1.

1.5.6. RSK regulation of transcription

Among the plethora of cellular functions regulated by ERK1/2, changes in gene expression have long been of great interest. Since RSK is almost excusively activated by ERK1/2 in most cell types and is thought to be a major downstream effector of this pathway, this family of kinases has also been studied in the context of transcriptional regulation. Indeed, one study performed in MDCK cell line demonsrated a critical role of

RSK as a downstream mediator of ERK1/2-dependent gene transcription (Doehn et al., 2009). The study revealed that out of 1089 ERK-regulated genes, 288 were under the control of RSK. This regulation of a range of targets involved several mechanisms, and 53 of the 288 RSK-mediated effects appeared to involve the transcription factor FRA1. FRA1 was shown to be regulated by RSK, either through mRNA expression or on a post-transcriptional level, depending on the cell type. Interestingly, ~25% of the genes regulated by RSK are involved in motility and invasiveness, suggesting the role of RSK in regulating this cellular property. It is important to note that the study used a small-molecule inhibitor RSK1,2,4 for gene expression analysis, therefore it did not determine which isoform was responsible for the observed changes in transcription. In trems of genes associated with motility, silencing of RSK1 and RSK2 individually caused non-overlapping changes in some, but not all targets identified through gene expression analysis, suggesting that multiple RSK isoforms play roles in regulating pro-motile and pro-invasive phenotypes downstream of ERK1/2.

A close relative of the transcription factor FRA1, c-Fos, has also been proposed to be regulated by RSK. RSK was shown to directly phosphorylate c-Fos, which leads to both protein stabilization and activation of its transcriptional activity (Chen et al., 1993, Chen et al., 1996). These studies did not specify which RSK isoform was responsible for the observed effects. In addition, RSK was proposed to be involved in the regulation of mitogen-stimulated expression of c-Fos. One potential mechanism of c-Fos regulation by RSK is through phosphorylation and activation of the Elk1/SRF (serum response factor) complex (Bruning et al., 2000, Rivera et al., 1993). This study was perfomed in embryonic fibroblast lines derived from RSK2 knock-out mice, suggesting

that this particular isoform was responsible for the observed effects on c-Fos expression. Another mechanism of c-Fos regulation by RSK was proposed to involve the cAMP-response-element-binding protein (CREB) (Ginty et al., 1994),(Xing et al., 1996). CREB phosphorylation and c-fos transcription were found to be severely decreased in a fibroblast cell line drived from a Coffin-Lowry syndrome patient with a frameshift mutation in the RPS6KA3 gene resulting in expression of a RSK2 mutant lacking the entire C-terminal half of the protein (De Cesare et al., 1998). Importantly, this loss in CREB phosphorylation and c-Fos expression was observed only in cells stimulated with EGF, but not in cells treated with full serum or UV radiation, suggesting that other kinases can also phosphorylate and activate CREB. Indeed, MSK1/2 was also shown to phosphorylate CREB in mouse embryonic fibroblasts, resulting in changes in c-Fos expression, in the context of UV irradiation and serum stimulation, but in the case of EGF treatment (Wiggin et al., 2002). Therefore, c-Fos expression through CREB appears to be regulated by RSK2 and MSK1/2 in the stimulus-dependent manner. In summary, RSK2 has been shown to regulate c-Fos through several mechanisms, both directly and indirectly through Elk1/SRF and CREB. The physiological significance of this regulation is highlighted by the fact that in RSK2-knock-out mice c-Fos overexpression failed to induce ostesarcomas (David et al., 2005).

RSK has been studied in the context of another CREB family member, activating transcription factor-4 (ATF4). RSK2 was found to physically interact with in the nucleus and directly phosphorylate ATF4, which leads to an increase in the transcriptional activity of ATF4 (Yang et al., 2004). The function of ATF4 is to promote osteoblast

differentiation and function, which is essential for the maintenance of proper bone density. RSK2 knockout and ATF4 knockout mice share the same defects in bone morphology, supporting the role of this interaction between RSK2 and ATF4. The function of RSK2 in regulating this important transcription factor in osteoblast differentiation could help explain skeletal abnormalities in patients with Coffin-Lowry syndrome (Temtamy et al., 1975).

RSK has also been shown to phosphorylate Ser167 within the activation function-1 (AF1) domain of the estrogen receptor-α (ERα) (Joel et al., 1998, Yamnik and Holz, 2010). This phosporylation leads to mitogen-dependent activation of transcription of ERα target genes independently of the stimulation by the receptor ligand, estrogen. Joel et al used in-gel kinase assay of the N-terminal part of ERα to find that RSK1 was capable of phosphorylating this protein. However, the other RSK isoforms were not evaluated in this study. Yamnik et al silenced RSK1 and RSK2 simultaneously to reduce ERα phosphorylation on Ser167 in response to potent mitogen phorbol myristate acetate (PMA), but not in response to insulin. Therefore, these two studies together suggested that RSK1 and/or RSK2 can phosphorylate ERα, but it remains unknown which isoform performs this function in intact cells and *in vivo*. Interestingly, RSK2 was also shown to regulate transcriptional activity of ERα through the allsoteric modulation of the hormone-binding domain (HBD) (Clarkl et al., 2001). This regulation was shown to be mediated by RSK2 binding to the HBD of the receptor, which induced a conformational change leading to the activation of the transcriptional activity. This effect could be blocked by anti-estrogens, like 4-hydroxytamoxifen, which disrupted this interaction and prevented allosteric activation of ERα by RSK2. Potential

role of RSK-mediated phosphorylation of ERα-Ser167 was supported by the observations that in breast cancer tissue samples this phosphorylation was strongly correlated with active RSK, and the presence of ERα-phosphoSer167 predicted better responses of patients to anti-estrogen therapy (Jiang et al., 2007).

RSK has been proposed to regulate another important transcription factor, c-Myc. For example, inhibition of RSK1-4 has been shown to decrease Myc levels in squamous cell carcinoma cell lines (Degen et al., 2013). Additionally, RSK has been shown to phosphorylate a negative regulator of c-Myc, mitotic arrest-deficient protein 1 (Mad1) (Zhu et al., 2008). The function of Mad1 is to compete with an essential transcriptional co-activator of Myc, Max (Rottmann and Luscher, 2006). When phosphorylated by RSK, Mad1 was sent to proteosomal degradation, which enabled Myc-Max interaction (Zhu et al., 2008). The study used RSK1 to demonstrate Mad1 phosphorylation *in vitro*, and silencing of both RSK1 and RSK2 in cell-based assays, therefore it remains unknown which isoform was responsible for the effects.

Recent studies have also indicated the role of RSK in regulating the stability of the GLI2 transcription factor (Liu et al., 2014). This transcription factor is constitutively cleaved by the proteasome in a phosphorylation-dependent manner, which blocks its ability to stimulate transcription of target genes (Pan et al., 2009, Bhatia et al., 2006). Activation of the Hedgehog (HH) signaling pathway represses phosphorylation of GLI2 and allows for its stabilization and transcriptional activation. Among the kinases that phosphorylate GLI2 to stimulate its proteasomal processing is GSK3β (Jia et al., 2005). RSK2 has been fond to stabilize GLI2 by repressing GSK activity, leading to an increase in the expression of GLI2 target genes, including anti-apoptotic protein BCL2,

the constitutively active HH transcription factor GLI1 and pro-tumorigenic cell-cycle control protein cyclin D1 (Liu et al., 2014). The implications of the study are two-fold. First, it provided further evidence that in certain cellular contexts GSK3β is a physiologically relevant substrate of RSK. Second, RSK was shown to cooperate with the HH signals to stimulate activity of transcription factors with critical functions in regulating development and normal tissue homeostasis in multiple organs, including breast epithelium (Lee et al., 2013, Vokes et al., 2007, Vokes et al., 2008, Lee et al., 2010, Chandramouli et al., 2013). Interestingly, RSK activity has been shown to participate in cell fate determination in mammary epithelial cells, which is consistent with its potential role in modulating the HH signaling network (Pasic et al., 2011). In addition, RSK2 was also shown to drive cyclin D1 expression in transformed mammary epithelial cells (Eisinger-Mathason et al., 2008). Deregulation of the HH pathway has been observed in various pathological processes, including cellular transformation (Harrison et al., 2014, Wellbrock et al., 2015, Schnidar et al., 2009, Thiyagarajan et al., 2007), suggesting that RSK activation could contribute to tumorigenesis through its ability to stabilize and activete GLI transcription factors.

Another transcription factor important in development that was found to be under the control of RSK is GATA4 (Li et al., 2012b). This transcription factor is a critical regulator of heart development and homeostasis, and its overactivation is associated with cardiac hypertrophy (Yamak et al., 2014, Stefanovic et al., 2014, Molkentin and Olson, 1997, Molkentin et al., 1997, Liang et al., 2001a). RSK2 overexpression was found to increase phosphorylation of GATA4, which stimulated its ability to bind to target gene promoters and drive their transcription (Li et al., 2012b). The authors of this study

also showed that this mechanism was responsible for the cardiac hypertrophy induced by phenylephrine, as the effects of this α1-adrenergic receptor agonist could be completely blocked by small-molecule inhibition of RSK. Interestingly, GATA4 has also been shown to be modified by other kinases as well, including those downstream of the PI3K-Akt pathway (Yanazume et al., 2002, Chandrasekar et al., 2005, Morisco et al., 2001, Liang et al., 2001b), suggesting that RSK could function as a fidelity factor contributing to the integration of multiple upstream signals to drive specific gene expression program in the heart.

As mentioned before, RSK has been shown to be activated by immune cytokines, suggesting its potential role in the inflammatory response. Therefore, this family of kinases has also been investigated in the context of the transcriptional program associated with inflammation. Indeed, RSK1 was shown to phosphorylate endogenous inhibitors of the transcription factor NF-κB, IκBα and IkBβ (Schouten et al., 1997, Xu et al., 2006). This phosporylation led to the degradation of the two proteins, releasing NF-κB from inhibition (Ghoda et al., 1997). In addition to sending inhibitors of NF-κB for degradation, RSK1 has also been shown to directly phosphorylate NF-κB component p65 (RelA) (Zhang et al., 2005, Bohuslav et al., 2004). This RSK1-mediated phosphorylation disrupted the interaction of p65 with its negative regulators, allowing its activation independent of the presence of IκB. Interestingly, in this study RSK activation leading to phosphorylation of p65 was due to p53-mediated activation of the upstream activator of ERK, MEK1. Therefore, activation of p65 by RSK did not occur in response to mitogens, however it still involved the classical upstream activator of RSK, ERK. The ability of p53 to activate MEK1 independent of growth factors has previously been

reported (Ryan et al., 2000). It highlights the possibility that RSK can be activated by other pathways than the growth factors, such as DNA damage that will activate p53, as long as ERK becomes activated in the process.

It has been noted that many of the nuclear proteins that are phosphorylated and regulated by RSK have been shown to interact with the transcriptional co-activator CREB-binding protein (CBP). The proteins interacting and being regulated by CBP include CREB, c-Fos, ERα and NF-κB (Kwok et al., 1994, Chrivia et al., 1993, Bannister and Kouzarides, 1995, Papoutsopoulou and Janknecht, 2000, Goel and Janknecht, 2004, Chakravarti et al., 1996, Hanstein et al., 1996, Huang et al., 2007). Based on its ability to interact with these proteins, CBP was proposed to be a transcriptional co-regulator of two major groups of targets: those activated by cAMP through CREB and those activated by mitogen signaling (Arias et al., 1994, Cardinaux et al., 2000). Growth factors such as insulin were shown to inhibit activation of cAMP-responsive genes, presumably through interfering with CBP interaction with CREB (Quinn, 1994). Interestingly, activated RSK has been found to interact with CBP in the nucleus, and this interaction led to an increase in C/EBP ability to drive expression of mitogen-stimulated genes (Nakajima et al., 1996). In addition, the formation of the CBP-RSK complex suppressed the ability of CBP to stimulate expression of cAMP-responsive genes. Therefore, it appears that RSK is a factor responsible for mediating the mitogen-dependent suppression of CREB-CBP function (Wang et al., 2003). As a result, RSK can help fine-tune the global gene expression program in response to growth factors. Interestingly, the ability of RSK to regulate CBP function appeared to be independent of the phosphotransferase activity of RSK, as the kinase-dead mutant of RSK still

interacted with CBP and had the same effects on CBP function as the wild-type RSK (Wang et al., 2003). All these studies investigating the connection between RSK and CBP used avian RSK1 over-expression, or RSK1-specific antibody in nuclear extracts. Therefore, it is unclear whether RSK1 is the only isoform interacting with CBP. In addition, while RSK2 localization to the nucleus has previously been described in multiple cell types, the ability of RSK1 to translocate to the nucleus is much less supported in the literature. Finally, CBP was proposed to help RSK mediate its effects on various transcription factors, but the majority of these effects were observed in the context of RSK2, and not RSK1. As a result, the true identity of the RSK isoform interacting with CBP in the nucleus is still debatable. Despite this caveat, CBP remains an important target of RSK that offers the potential explanation of how this kinase can regulate a wide array of transcription factors.

In summary, multiple transpription factors and transcriptional co-regulators have been found to be the substrates of RSK kinases (fig. 3B). Although the distinction between RSK isoform-specific functions in the context of gene expression is less clean-cut than in the case of global protein synthesis, the emerging trend suggests a more prominent role of RSK2. This general observation is particularily evident when resident nuclear proteins, such as ERα, c-Fos, ATF4 and GATA4, are concerned. Consistent with such compartmentalization of RSK functions, the inhibitors of NF-kB transcription factor, which exert their effects in the cytoplasm, were found to be regulated by RSK1. Compared to RSK1/2, the functions of the remaining two RSK isoforms are almost completely unknown. It is surprising, given the proposed nuclear locaization of RSK3.

Several proteins that are phosphorylated by RSK have also been shown to be controlled by other kinases, in particular those in the PI3K-Akt pathway. These observations suggest that, while being an important downstream mediator of the Ras-MAPK pathway, it exerts many of its functions in cooperation with other signaling pathways. It is conceivable that such collaboration between different networks allows for integration of the signals and the choice of an appropriate biological effect in the context of the entire signaling landscape. Therefore, even though RSK is almost exclusively activated by ERK1/2, the physiological outcome of RSK signaling will be impacted by other signaling pathways as well. The common theme among all the transctiptional responses stimulated by RSK signaling is to promote survival, proliferation and differentiation of various cell types.

1.5.7. RSK and cell cycle

As summarized in pervious sections, RSK functions in transcription and translation are often associated with accelerated cellular proliferation (fig. 3B). Additional factors, such as direct influence of RSK on the cell cyce machinery, could contribute to the observed increases in proliferation. Indeed, several studies have demonstrated that RSK could participate in the regulation of cell cycle progression, through a variety of mechanisms. One very important cell cycle protein under the control of RSK is cyclin D1 (Eisinger-Mathason et al., 2008). Cyclin D1 expression was shown to be regulated on the transcriptional level by RSK2, but not RSK1. Although the exact mechanism of this regulation was not determined, it was suggested to be independent of CREB and c-Fos. Instead, the proposed pathway involved ERα, as the promoter of cyclin D1 is known to contain estrogen-response elements (EREs) and its expression

has been shown to be stimulated by estrogen (Basu and Rowan, 2005). Therefore, cyclin D1 appears to be transcriptionally regulated by ERα. As mentioned above, RSK has been shown to interact with ERα, which leads to its activation, both in phosphorylation-dependent and independent manner (Joel et al., 1998, Clarkl et al., 2001). Furthermore, in addition to ERa, cyclin D1 levels could be regulated by RSK2 through its ability to stabilize and transcriptionally activate the transcription factor GLI2 (Liu et al., 2014).

Another cell-cycle regulator under the control of RSK is the inhibitor of the cyclin-dependent kinase-2 (CDK2), $p27^{kip1}$ (Fujita et al., 2003, Larreaa et al., 2009). $p27^{kip1}$ is regulated by RSK through two mechanisms. This protein is phosphorylated by RSK1, which creates a recognition site for 14-3-3 protein binding to $p27^{kip1}$ (Fujita et al., 2003). 14-3-3 protein sequesters $p27^{kip1}$ to the cytoplasm, away from the CDK2-cyclin E complex, which is localized to the nucleus. $p27^{kip1}$ localization to the cytoplasm releases CDK2-cyclin E from inhibition and allows cell entry into S phase. RSK1 by itself also forms a complex with p27kip1 in the cytoplasm, further contributing to cytoplasmic localization of $p27^{kip1}$ (Larreaa et al., 2009). Interestingly, RSK1-mediated phosphorylation of p27 plays an additional role in regulating $p27^{kip1}$ function as a regulator of cell motility and cytoskeleton organization. When phosphorylated by RSK1 and localized to the cytoplasm, $p27^{kip}$ interacts with RhoA (Larreaa et al., 2009). $p27^{kip1}$ binding to this GTPase leads to inhibition of RhoA activation of ROCK1, and a subsequent increase in cell motility (Besson et al., 2004). Therefore, interactions of RSK1 with p27kip result in both increase in cell entry to S phase and an increase in motility.

RSK2 has been proposed to regulate the spindle assembly checkpoint at the onset of mitosis. It has been observed that inhibition of RSK leads to a loss of localization of Mad1 and Mad2 at the kinetochore (Vigneron et al., 2010). Interestingly, Mad1 has also been shown to be regulated by RSK in the context of Myc activity in the G1/S phase of the cell cycle (Zhu et al., 2008). In addition to the regulation of mitosis, RSK1 has been shown to regulate activation of meiosis in *Xenopus* (Schmitt and Nebreda, 2002). RSK1 phosphorylates the kinase myelin transcription factor-1 (Myt1), which is a negative regulator of $p34^{cdc2}$ (Palmer et al., 1998). Inactivation of Myt1 by RSK-mediated phosphorylation leads to a release of the inhibition of $p34^{cdc2}$ and allows cell entry into M phase. In addition to Myt1, RSK phosphorylates and activates another regulator of $p34^{cdc2}$, Cdc25C (Wang et al., 2010, Wu et al., 2014). Interestingly, RSK1 seems to be a negative regulator of oocyte maturation, through activation of the metaphase II arrest. RSK1 phosphorylates two regulators of anaphase-promoting complex (APC), kinase Bub1 and early mitotic inhibitor-2 (Emi2) (Schwab et al., 2001, Nishiyama et al., 2007). When phosphorylated by RSK1, these two proteins inactivate APC, leading to a block in cell cycle progression. Despite being well characterized in frog oocytes, however, RSK does not seem to play a role in regulating meiosis in mouse oocytes (Dumont et al., 2005). Therefore, RSK function in regulation of meiosis in other organisms than frog remains controversial.

Increased proliferation rates induced by mitogenic signaling exert a significant stress on the DNA, which promotes DNA damage and replication checkpoints (Bartkova et al., 2005, Gorgoulis et al., 2005). One of the proteins involved in cell cycle regulation in this context is Chek1 (Zhao and Piwnica-Worms, 2001). RSK has been shown to

phosphorylate Chek1 in response to serum stimulation in hTERT-immortalized retinal pigment epithelial cells, as well as HeLa and U2OS cancer cell lines, as well as mediate constitutive Chek1 phosphorylation in Raf-mutant melanoma cell lines (Li et al., 2012a, Ray-David et al., 2013). Overexpression of each RSK isoform was could induce Chk1 phosphorylation in HEK293, HeLa and U2OS cell lines, but RSK1 had the strongest effect (Ray-David et al., 2013). In addition, silencing of RSK1 alone was sufficient to reduce Chk1 phosphorylation to the same extent as RSK1/2 double silencing, and RSK inhibition with both SL0101 and BI-D1870. Although both studies found the same effects of RSK on Chk1 phosphorylation upon serum stimulation, they demonstrated the opposite effects on G2/M block. Therefore, it remained unclear whether the function of RSK was to induce the block in cell cycle following DNA damage, or to promote bypassing this checkpoint.

The possibility that RSK acts to promote the G2/M checkpoint was supported by the observations that RSK2 knock-out mouse embryonic fibroblasts and fibroblasts derived from CLS patients failed to arrest in G2/M phase in response to genotoxic stress (Lim et al., 2013a). Re-introduction of RSK2 in theses cells was sufficient to restore ATM and p53 phosphorylation, and proper activation of the DNA-damage checkpoint.

The hypothesis that RSK promoted bypassing of the G2/M checkpoint was supported by a study in which RSK inhibition and silencing of RSK1/2 in prostate cancer cell lines, PC3 and LnCaP, caused stalling in the G2/M transition (Chen et al., 2013). However, the authors of this study did not investigate the changes in Chk1 phosphorylation. Instead, a new mechanism was proposed, in which RSK

phosphorylated the protein meiotic recombination-11 (Mre11), which resulted in suppressed ability of ATM to bind to damaged DNA and activate damage response. Furthermore, RSK was shown to drive entry into mitosis in PC3 cells through direct phosphorylation of Cdc25 (Wu et al., 2014). In the context of Chk1 phosphorylation, previous studies have showed that this modification caused re-distribution of Chk1 into the cytoplasm and failure to activate the G2/M checkpoint (Puc et al., 2005, King et al., 2004). Therefore, it appeared that both opposing models of RSK regulation of DNA-damage checkpoint are supported by experimental evidence. This conflict could be reconciled by the fact that inhibition of RSK caused G2/M block in cells with high basal activity of ERK and constitutive phosphorylation of Chk1, while loss of RSK activity resulted in the block in G2/M phase transition in cells with basal low ERK activity that becomes induced by genotoxic stress or serum stimulation. Such observations suggest an interesting model in which a function of RSK in normal homeostasis is to promote DNA-damage checkpoint to allow cells to repair the lesions, while in the state of chronic ERK activation RSK allows cells to proliferate despite DNA damage.

Taken all this information together, RSK can drive cell cycle progression by phosphorylating specific cell cycle regulators, in addition to the transcriptionally regulated processes. Such ability to post-translationally impact cell cycle machinery would enable RSK to elicit its effects in a more acute way, in addition to a long-term alterations of cellular phenotype. Therefore, RSK could represent a signaling component allowing for rapid adaptation of the cell cycle to the changes in cellular environment, in particular in the context of mitogenic stimulation. The functions of RSK in cell cycle regulation seem to involve both RSK1 and RSK2, and could potentially

include RSK3 and RSK4 as well. However, it appears that all isoforms may contribute to cell cycle regulation in non-overlapping ways, as loss of individual RSK proteins is sufficient to induce changes in cell cycle progression. Therefore, RSK family could act in coordination, rather than in redundancy in the context of cell cycle regulation.

1.5.8. RSK and apoptosis

RSK has been found to inhibit apoptosis through phosphorylation of specific targets. For example, in hepatic stellate cells treated with transforming growth factor-alpha (TGFα), or a hepatotoxin CCl_4, RSK phosphorylates the protein CCAAT/enhancer binding protein β (C/EBPβ) (Buck et al., 1999, Buck et al., 2001). The phosphorylation of this protein enables it to interact with caspases 1 and 8. This interaction prevents activation of these caspases and blocks the propagation of the death signal. Interestingly, C/EBPβ-RSK1 interplay has also been recently reported in lung epithelium (Lin et al., 2014). In this study thrombin induced phosphorylation of C/EBPβ by RSK1, which led to association of C/EBPβ with the promoter region of interleukin-8 (IL8) and an increase in expression and secretion of this chemokine by lung epithelium. IL8 has been shown to stimulate pro-survival and pro-proliferation signaling in multiple cancers (Waugh and Wilson, 2008). Therefore, the function of RSK1 in phopshorylating C/EBPβ is not limited to the inhibition of apoptotic cascade through caspases 1 and 8, but can also stimulate cell survival through changes in cellular microenvironment.

RSK has been shown to phosphorylate Bad, the pro-apoptotic BH3-only protein found in the outer mitochondrial membrane (Bonni et al., 1999, Shimamura et al., 2000). Phosphorylation of Bad enhances its interaction with the cytosolic 14-3-3 proteins,

which sequesters Bad away from the mitochondrial membrane and prevents incorporation of Bad into the mitochondrial permeability transition pore. As a result, sequestering Bad into the cytoplasm prevents opening of the pore and release of cytochrome C from the intramembrane space. This prevents cytochrome C-mediated activation of the apoptotic cascade. The studies of BAD phosphorylation by RSK used overexpression to show that both isoforms were capable of modifying this protein, however it remains to be determined which RSK is a physiological kinase for BAD.

Another pro-apoptotic protein that has been found to be negatively regulated by RSK is the protein Bcl-2 interacting mediator of cell death (Bim) (Dehan et al., 2009). Endogenous RSK1 was demonstrated to interact with and phosphorylate Bim, and inhibition of RSK as well as silencing of RSK1/2 prevented this phosphorylation. The function of this post-translational modification was to induce proteasomal degradation of Bim, thereby decreasing the cellular levels of this strong inducer of apoptosis. RSK was also shown to phosphorylate and thereby inactivate the pro-apoptotic death associated protein kinase (DAPK) (Anjum et al., 2005). Similarily to BAD, in this study both RSK1 and RSK2 were shown to increase phosphorylation of DAPK when over-expressed, and silencing of RSK1/2 decreased this modification of DAPK. Finally, another mechanism through which RSK could inhibit apoptosis is through phosphorylation of Apaf-1. This modification was shown to facilitate Apaf-1 binding to 14-3-3ε and decrease Apaf-1 interactions with cytochrome c, which prevented apoptosome formation (Kim et al., 2012). As in previous cases, the study used consitutively active RSK1 and RSK2 overexpression, as well as RSK1/2 double silencing in the experiments, therefore it

remains unknown which isoform is physiologically responsible for Apaf-1 phosphorylation.

In summary, RSK has been shown to phosphorylate and thereby regulate several proteins involved in the induction of apoptosis. The function of RSK in this context is to inhibit cell death. While both RSK1 and RSk2 were suggested to mediate the anti-apoptotic signals downstream of ERK1/2, the relative contributions of these two isoforms remain unknown. Furthermore, the role of RSK3/4 in the context of apoptosis remains almost completely unexplored.

1.5.9. RSK and cell migration and adhesion

The ability of RSK to regulate cell motility was first proposed based on the observation that RSK could phosphorylate the actin-cytoskeleton associated protein filamin-A (Woo et al., 2004). RSK-mediated phosphorylation of filamin A resulted in an increase in membrane ruffling, which is a hallmark of a migratory cell phenotype (Vadlamudi et al., 2002b, Vadlamudi et al., 2002a). Silencing of RSK1 and RSK2 individually had similar effects on filamin A phosphorylation, suggesting that both isoforms are involved. Another piece of evidence showing the ability of RSK to promote cell motility comes from the observations that RSK1 could phosphorylate Src homology-3 domain containing protein-2 (SH3P2) (Tanimura et al., 2011). This protein was identified through a cDNA overexpression screen of novel regulators of motility and was proposed to act as a negative regulator of motility. RSK1 was shown to phosphorylate and thereby inactivate SH3P2, leading to an increase in migration and invasion of multiple cancer cell lines. Silencing of RSK1 alone was sufficient to reduce cell invasion,

while silencing of RSK2 had no effect on invasiveness in these studies, suggesting a predominant role of RSK1 in stimulating motility. The mechanism of SH3P2 action as a suppressor of motility was not elucidated in this report.

In addition to phosphorylating and regulating specific regulators of motility, RSK has also been found to control pro-migratory gene expression programs. The role of RSK as an important regulator of cell motility was further supported by the study mentioned in section 1.5.6. In this study both RSK1 and RSK2 were found to promote a broad pro-migratory gene expression program in both normal and transformed cells. This ability of RSK to promote pro-migratory phenotype was found in a wide range of cell types, including kidney, colon, breast, prostate and thyroid (Doehn et al., 2009). The gene program triggered by RSK encompassed a variety of targets, including integrins and matrix remodeling enzymes, and was at least in part mediated through the FRA1 transcription factor. Interestingly, FRA1 has independently been shown to be an important regulator of motility in multiple cell types (Kustikova et al., 1998, Sayan et al., 2012).

Another high-throughput study screened genes whose knockdown promoted motility and invasiveness in non-transformed breast epithelial cell line MCF10A. As a result of this screen, 31 genes were identified. Interestingly, knocking down each of these genes was associated with an activation of (Smolen et al., 2010). The pro-migratory phenotype induced by knocking down each of the 31 genes could be blocked by small molecule inhibition of RSK and by silencing RSK1. Interestingly, loss of RSK1 was not as effective in blocking cell migration as pharmacological inhibition, suggesting that other isoforms of RSK can also be involved in regulating the pro-migratory

phenotype of these cells. These observations are consistent with the findings that RSK2 can also promote invasiveness of multiple cell types (Doehn et al., 2009).

While the majority of studies have suggested both RSK1 and RSK2 to promote migration and invasion, a high-throughput siRNA screen done in non-small cell lung cancer (NSCLC) cell line A549 identified RSK1 as a negative regulator of invasion, while RSK2 and RSK4 promoted motility in these cells (Lara et al., 2011). These observations suggest that the function of RSK in promoting motility could depend on cell type. Finally, this study highlighted the necessity to further investigate the functions of RSK3 and RSK4 in the context of migration.

1.5.10. RSK and cellular energy homeostasis

In addition to cellular functions summarized above, the phenotypes observed in RSK2 knockout mice have suggested that RSK family of kinases could also play a role in regulating energy homeostasis. Indeed, some of the proteins described in the sections above are known to also be involved in these cellular processes. For example, GSK3β has been extensively studied in the context of glucose and glycogen metabolism (McCubrey et al., 2014). mTOR is known to be involved in amino acid sensing (Jewell and Guan, 2013, Jewell et al., 2013), as well as regulation of glycolysis through its role as a modulator of the hypoxia inducible factor-1 alpha (HIF-1α) (Sun et al., 2011, Duvel et al., 2010). Finally, RSK is known to regulate Bad, which resides in the mitochondrial membrane (Shimamura et al., 2000, Bonni et al., 1999). In addition to promoting apoptosis, Bad has been suggested to regulate mitochondrial energy production through various mechanisms (Danial, 2008, Gimenez-Cassina and Danial,

2015). Therefore, RSK could regulate cellular energy metabolism through its interactions with many proteins with known functions in energy homeostasis (fig. 3C).

In addition to the substrates mentioned above, RSK1 has been proposed to regulate the liver kinase-B1 (Lkb1), also known as serine/threonine kinase-11 (STK11), by phosphorylating it on residue Ser341 (Sapkota et al., 2001). Lkb1 phosphorylates AMPK, which is a master sensor of the cellular energetic state (Shackelford and Shaw, 2009). Therefore, Lkb1 participates in regulating a broad range of cellular processes involved in nutrient signaling. Interestingly, while the study mentioned above showed that in addition to RSK1, the same site on Lkb1 was phosphorylated by PKA, the individual kinases mediated the phosphorylation of Lkb1 in response to different stimuli. The activator of adenylate cyclase, forskolin, induced Lkb1 phosphorylation through PKA, but not through RSK. In EGF-stimulated cells RSK was the only kinase mediating the phosphorylation of Lkb1, as inhibition of mTOR or PKA, or knock-down of MSK1/2, did not affect the ability of this growth factor to induce Lkb1 phosphorylation. However, the study did not evaluate whether phosphorylation of Lkb1 was associated with any changes in cellular metabolism. The only identified function of this phosphorylation was to prevent the anti-proliferative effect of Lkb1 overexpression in a cancer cell line that does not normally express Lkb1. Other studies have shown that phosphorylation of Lkb1 on Ser341 does not alter its ability to associate with the plasma membrane or phosphorylate AMPK (Fogarty and Hardie, 2009, Houde et al., 2014). Therefore, it remains unknown whether RSK1-mediated phosphorylation of Lkb1 results in changes in cellular metabolism.

RSK1 has been found to phosphorylate the protein Akt substrate of 160 kDa (AS160) (Geraghty et al., 2007). AS160 is Rab GTPase-activating protein (RabGAP) whose role is to inhibit membrane localization of the glucose transporter GLUT4 (Kane et al., 2002). Upon stimulation with various growth factors, including insulin and EGF, the GAP activity of AS160 is reduced, leading to GLUT4 translocation to the plasma membrane and a subsequent increase in cellular glucose uptake. Phosphorylation of AS160 by RSK1 was shown to promote the association of AS160 with the cytoplasmic 14-3-3 protein, which interferes with AS160 GAP activity. Therefore, RSK1 was shown to be the kinase mediating the growth factor-induced signal leading to inactivation of AS160. As a result, RSK1 was shown to potentiate glucose uptake in cells stimulated with insulin and EGF. It is important to note, however, that many cell types express multiple glucose transporters, and of those GLUT1-3 are constitutively localized to the plasma membrane. Therefore, insulin-stimulated GLUT4 translocation to the plasma membrane is not the only mechanism by which cells regulate glucose uptake. The role of RSK1 in changing the glucose uptake into cells will therefore depend on the activities of insulin-independent glucose transporters.

Taken all these observations together, both RSK1 and RSK2 were implicated in regulation of cellular energy and nutrient metabolism in a variety of cell types (fig. 3C). However, the exact involvement of RSK in promoting energy production in cells remains poorly understood. It is also unclear whether the proposed mechanisms of RSK regulation of cellular energy production and nutrient utilization are unique to the investigated cell types, or can be extended to other biological contexts. Given the increasing numbers of reported RSK phosphorylation targets with known functions in

cellular energy homeostasis, and the expanding literature implicating known RSK-dependent pathways in this new context, futher studies of RSK involvement in the cellular energy production are warranted.

1.5.11. RSK substrates in the heart and brain

RSK has been extensively studied in the context of cardiac and neuronal biology. Interestingly, whereas in a majority of studies RSK mediates pro-survival and pro-proliferation signals, in heart and neuronal injury RSK activity is associated with cell death. RSK activity could promote cell death in these tissues through several potential mechanisms. For example, RSK was identified as a potential regulator of the sodium-proton exchanger NHE1 (Takahashi et al., 1999, Cuello et al., 2007, Roberts et al., 2005). NHE1 was shown to be activated upon cardiac and neuronal ischemia reperfusion injury, which leads to cellular sodium accumulation (Karmazyn, 1988, Kintner et al., 2004, Luo et al., 2005). Increased sodium triggers calcium influx into the cell, which is a signal for apoptosis. Phosphorylation of NHE1 by RSK was also shown to activate this channel, which contributes to the cellular ion imbalance following ischemia-reperfusion (Takahashi et al., 1999). Blocking RSK activity following ischemia-reperfusion increased survival of cardiomyocytes and neurons, suggesting a protective potential of RSK inhibition following myocardial and cerebral ischemic insult (Maekawa et al., 2006, Manhas et al., 2010). It remains unclear whether the function of RSK in regulating cellular pH and ion homeostasis is limited to cardiomyocytes and neurons, and which RSK isoform is responsible for these effects. It is important to note, however, that NHE1 is ubiquitously expressed and seems to be a major channel for

sodium/proton exchange in multiple cell types (Fuster and Alexander, 2014). Therefore, the role of RSK in regulating cellular pH could extend to other cell types.

In addition to NHE1, the kinase ERK5 was proposed to be a target of RSK in the heart (Le et al., 2012). The study was conducted in the context of a diabetic mouse model. The authors of the study show that following myocardial infarction RSK binds to and phosphorylates ERK5. This interaction prevents ERK5 from binding to the ubiquitin ligase CHIP. As a result, the ubiquitin ligase activity of CHIP is decreased. The function of CHIP is to mediate the proteosomal degradation of the inducible cAMP repressor (ICER). Following myocardial infarction ICER acts to increase expression of pro-apoptotic proteins. As a result, RSK interaction with ERK5 leads to the stabilization of ICER, and an increase in apoptosis. The ERK5-RSK interaction and phosphorylation of NHE1 by RSK together provide evidence for RSK involvement in ischemia-reperfusion injury. In this context, RSK activity increases apoptosis of cardiac tissue following ischemic insult. Therefore, RSK inhibition has been proposed to constitute a potential therapeutic strategy to limit tissue damage following cardiac infarction (Avkiran et al., 2008).

1.5.12. RSK in the context of cancer

As described above, RSK has been shown to mediate a variety of pro-growth and pro-survival signals downstream of the Ras-MAPK pathway. Therefore, there has been a lot of interest in studying the role of RSK in promoting tumorigenesis. Ectopic expression of RSK2 was shown to increase proliferation and anchorage-independent

transformation in epidermal growth factor (EGF) and phorbol ester (TPA) stimulated mouse embryonic fibroblasts (Cho et al., 2007). RSK1 and RSK2 have also been shown to be overexpressed in a portion of breast and prostate cancer patients (Smith et al., 2005, Clark et al., 2005). RSK2 is thought to mediate the FGFR3-dependent transformation of haematopoietic cells (Kang et al., 2007b, Kang et al., 2007a). RSK inhibition has been recently shown to block proliferation and induce apoptosis in both multiple myeloma cell lines and patient-derived myeloma cell cultures (Shimura et al., 2012). Another study found that FGFR1-transformed mammary epithelial cells rely on RSK activity for survival and anchorage-independent growth (Xian et al., 2009). Knock-down of RSK1 and RSK2 together was shown to reduce tumor growth in BRAF-mutant melanomas (Romeo et al., 2013). RSK2 knock-down inhibited osteosarcoma development, and this effect was mediated through the regulation of ATF4 transcription factor (David et al., 2005). Taken these results together, RSK has been shown to promote survival and proliferation in multiple types of cancer.

In a phosphoproteomic study designed to identify novel substrates in melanomas RSK has been recently found to phosphorylate the putative tumor suppressor programmed cell death protein-4 (PDCD4) (Galan et al., 2014). Phosphorylation of PDCD4 promoted its binding to 14-3-3 protein, leading to the proteasomal degradation of PDCD4. The role of PDCD4 as a tumor suppressor is not limited to melanoma, as this protein has also been implicated in inhibiting tumorigenesis in multiple other tumor types, including lung, colon and breast cancer and glioma (Lankat-Buttgereit and Goke, 2009). Therefore, RSK could regulate tumorigenesis through PDCD4 in other tumor types as well. In addition, in the cells of hematopoietic origin, but not in the mouse

embryonic fibroblasts, PDCD4 has been reported to be a substrate of RSK1 (Kroczynska et al., 2012). The analysis of the putative RSK phosphorylation site done by the Galan et al revealed a similarity between this motif and the reported 14-3-3 binding peptide (Gardino and Yaffe, 2011). Therefore, the authors used a separate screen to identify proteins binding to 14-3-3. Interestingly, out of 274 potential 14-3-3-interacting partners, 54 were also identified as potential RSK phosphorylation targets (Galan et al., 2014). These observations suggested that phosphorylation-induced binding of the target protein to 14-3-3 could be a common mechanism of regulation of this protein activity by RSK. Importantly, this 14-3-3 mediated modulation of RSK targets has been demonstrated before, in such proteins as AS160, $p27^{kip}$ and Bad (Geraghty et al., 2007, Fujita et al., 2003, Bonni et al., 1999).

RSK has been shown to regulate an important transcription factor in breast cancer, Y-box protein-1 (YB-1) (Stratford et al., 2008). Phosphorylation of YB-1 by RSK1/2 stimulates its nuclear localization and subsequent transcriptional activity, which drives expression of a variety of genes involved in transformation, including EGFR, HER2 and c-Myc (Sakura et al., 1988, Kolluri and Kinniburgh, 1991, Stratford et al., 2007). Therefore, blocking RSK1/2 activity could reduce breast cancer proliferation and survival through the inhibition of YB-1 activity. This observation was confirmed in a subsequent study, highlighting the role of RSK in tumor maintenance and proliferation in aggressive breast cancer (Stratford et al., 2012). Although these studies were performed in the context of an aggressive subtype of breast cancer, YB-1 has also been implicated in the transformation in other tumor types, including prostate, lung and colon cancers, as well as in osteocarcinomas, sarcomas and glioblastomas (Wu et al., 2006,

Gimenez-Bonafe et al., 2004, Oda et al., 1998, Gu et al., 2001, Shibahara et al., 2001, Shibao et al., 1999, Oda et al., 2003, Faury et al., 2007). Therefore, regulation of YB-1 by RSK could prove relevant in multiple tumor types beyond breast cancer.

Consistent with multiple studies implicating RSK in regulation of cell motility, RSK2 was found to promote metastasis in head and neck squamous cell carcinoma (HNSCC) (Kang et al., 2010). In patients with HNSCC high expression of RSK2 correlated with increased metastasis, and RSK2 knock-down in a mouse xenograft of human HNSCC reduced metastatic potential. Interestingly, RSK1 did not play a role in HNSCC metastasis. These results provide further evidence for isoform specific actions of RSK1 and RSK2 in regulating cell motility and invasiveness in various cell types.

Whereas RSK1 and RSK2 have been shown to mediate pro-survival and pro-proliferation signaling in the context of multiple cancers, non-transformed cells appear to not rely on RSK signaling for their survival. For example, the proliferation of the breast cancer cell line MCF7 is reduced by RSK inhibition, while the non-transformed breast epithelial cell line MCF10A is not sensitive to RSK inhibition (Clark et al., 2005), chapters 3-6 and 8). In addition, RSK2 is dispensable for normal haematopoiesis (Lin et al., 2008), but essential for survival and proliferation in a subtype of myeloid leukemias (Elf et al., 2011). Therefore, targeting RSK1 and RSK2 in cancer therapy could potentially lead to less side-effects than therapies affecting normal cell function.

The functions of RSK3 and RSK4 in the context of cancer are much less understood. Recent studies have suggested that RSK3 and RSK4 may act as putative tumor suppressors. RSK3 was found to be down-regulated in ovarian cancer, and re-

expression of RSK3 in ovarian cancer cell lines was shown to induce cell cycle arrest and apoptosis (Bignone et al., 2007). However, the mechanism of tumor suppression induced by RSK3 in ovarian cancer remains unknown. RSK4 expression was found to be reduced in colon and renal tumors (Richards et al., 2001). In addition, low expression of RSK4 in colorectal tumors was found to be correlated with poor outcome (Cai et al., 2014). Overexpression of RSK4 in breast cancer cells was shown to induce growth arrest and apoptosis (Thakur et al., 2008). As with RSK3, the mechanism of tumors suppression by RSK4 remains elusive, but was suggested to involve p53-mediated growth arrest and induction of senescence (Lopez-Vicente et al., 2009). In contrast to these suggested functions of RSK3 and RSK4 as putative tumor suppressors, these two kinases have also been recently identified as potential promoters of resistance to PI3K inhibitors in breast cancer (Serra et al., 2013). These findings highlight the importance of further studies of RSK3/4 functions.

In order to better understand the biology of RSK, as well as explore the possibility of targeting this family of kinases in therapy, there has been an ongoing effort to identify novel small molecule inhibitors. The following section will summarize the advances in this field.

1.6. RSK inhibitors

As discussed in section 1.5., RSK proteins consist of two fully functional kinase domains. Therefore, each molecule of RSK possesses two ATP-binding grooves that could potentially be targeted by kinase inhibitors. The inhibitors of both the NTKD and CTKD of RSK have been characterized.

1.6.1. Inhibitors of the N-terminal kinase domain

1.6.1.1. SL0101

The first small-molecule inhibitor of RSK was discovered by our laboratory by screening the collection of botanical extracts of plants of rare genera (Clark et al., 2005). The screen was performed *in vitro* against the full-length active RSK2 kinase. The read-out of the screen was the ability to inhibit phosphorylation of a peptide containing the estrogen receptor-alpha (ERα) Ser167 sequence, which is a physiological target of RSK (Joel et al., 1998).

Figure 4. Structural diversity of the inhibitors of RSK NTKD

A) Chemical structure of the RSK inhibitor SL0101. SL0101 is a glycosylated flavonoid, in which the rhamnose sugar residue is acetylated at two positions.

B) Chemical structure of the RSK inhibitor BI-D1870.

C) Chemical structure of the RSK inhibitor BIX 02565. BIX 02565 was developed in a series of indole inhibitors of RSK.

D) Chemical structure of the RSK inhibitor compound 15. Compound 15 was generated as a derivative of BIX 02565 with decreased ability to interfere with adrenergic receptors.

E) Chemical structure of the RSK inhibitor LJH685.

F) Chemical structure of the RSK inhibitor LJI308. Compounds LJH685 and LJI308 belong to the same family of compounds and display very similar biological and chemical properties.

G) Summary table of the *in vitro* and cell-based efficacies of the RSK inhibitors.

Figure 4

A

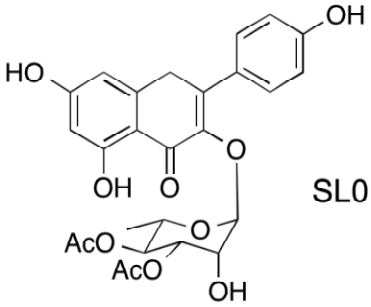

SL0101

B

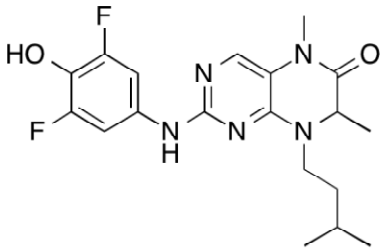

BI-D1870

C

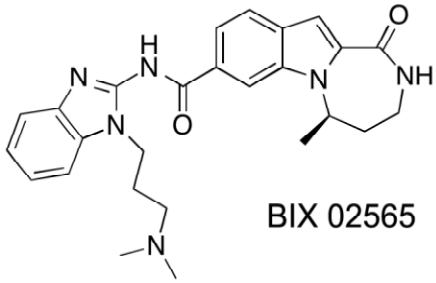

BIX 02565

D

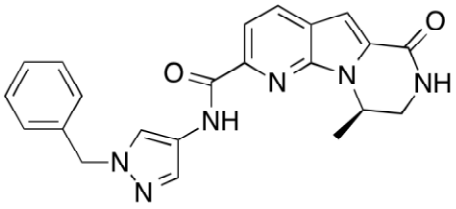

compound 15

E

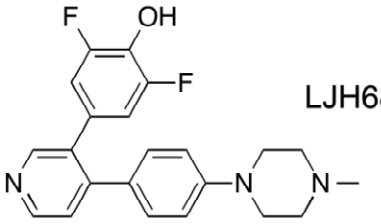

LJH685

F

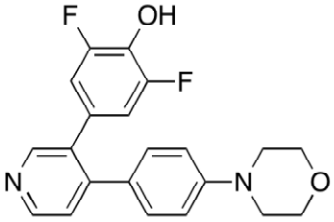

LJI308

G

compound name	RSK1 *in vitro* IC_{50} [μM]	RSK2 *in vitro* IC_{50} [μM]	RSK3 *in vitro* IC_{50} [μM]	RSK4 *in vitro* IC_{50} [μM]	cell-based IC_{50} [μM]
SL0101	0.144	0.127	>30	>30	60
BI-D1870	0.031	0.024	0.018	0.015	1
BIX 02565	N.T.	0.001	N.T.	N.T.	0.02
Compound 15	N.T.	0.0002	N.T.	N.T.	0.00032
LJH685	0.006	0.005	0.004	N.T.	0.2-0.3
LJI308	0.006	0.004	0.013	N.T.	0.2-0.3

Remarkably, out of ~10,000 extractstested only one showed the ability to inhibit RSK2 *in vitro*. This extract was derived from *Forsteronia refracta*, a tropical forest plant with no known medicinal properties. On further investigation the extract was found to contain three compounds of very similar chemical structure that showed efficacy against RSK2 *in vitro* (Xu et al., 2006). The compounds represented the same chemical backbone, consisting of a kaempferol flavonoid part linked via the glycosydic bond to an unusual deoxyhexose sugar, L-rhamnose. The difference between the three compounds lay in the acetylation state of the hydroxyl groups of the sugar moiety. The most active of the three compounds, possessing acetate residues in positions 3" and 4" of rhamnose, showed the *in vitro* IC50 of 89 nM, and was subsequently chosen for further studies. This compound was called SL0101 (fig. 4A).

SL0101 has been shown to inhibit RSK1 and RSK2, with a trend towards a higher efficacy against RSK1 (Bain et al., 2007, Smith et al., 2005). However, the efficacy of SL0101 against RSK3 and RSK4 has not been investigated. We have recently found that, unexpectedly, this inhibitor does not affect the *in vitro* activity of RSK3 and RSK4 (chapter 2). This result was unanticipated as there is no clear indication within the amino acid sequences of RSK isoforms that would suggest the differential ability of SL0101 to bind to and inhibit these kinases. SL0101 has been consistently found to be remarkably specific for RSK (Bain et al., 2007, Doehn et al., 2009). Out of ~80 kinases tested, the only off-target kinases significantly inhibited by SL0101 were Aurora B, PIM1 and PIM3 (Bain et al., 2007). Importantly, SL0101 did not inhibit the most closely related kinases to RSK, MSK1/2 and p70S6K (Smith et al., 2005).

The original report on SL0101 properties described the inhibitor to act as an ATP competitor (Smith et al., 2005). The ATP-binding site of RSK NTKD represents a typical sequence found in all members of the AGC kinase superfamily, which suggests that if SL0101 utilized typical features of this binding site, it would also inhibit other kinases as well, as in the case of relatively non-selective kinase inhibitors staurosporin and H89 (Tamaoki et al., 1986, Ikuta et al., 2007, Davies et al., 2000, Bain et al., 2003, Lochner and Moolman, 2006). In contrast to these two non-specific kinase inhibitors, however, SL0101 is remarkably specific for RSK1/2. Therefore, a more detailed study of SL0101 interaction with RSK NTKD was warranted. The crystal structure of RSK NTKD bound to SL0101 showed the inhibitor bound at a site partially overlapping with the ATP-binding groove between the two lobes of the kinase domain (Utepbergenov et al., 2012). Surprisingly, however, the binding of the inhibitor was associated with a dramatic rearrangement of the entire N-lobe of the kinase. Due to the steric hindrances between individual secondary structures of RSK, this structural rearrangement was very unlikely to occur via a simple rotation of one lobe with respect to the rest of the kinase domain. Instead, it would require a partial unfolding and re-folding of the kinase domain. Therefore, the analysis of the crystal structure of RSK2 NTKD bound to SL0101 strongly suggests that this compound is an allosteric inhibitor of RSK. We have explored this possibility by performing an enzyme inhibition kinetics study and provide evidence in support of the function of SL0101 as an allosteric inhibitor of RSK (chapter 2). Allosteric regulation of RSK activity by SL0101 could explain the remarkable selectivity of this inhibitor for RSK and highlights the potential for further development of this small molecule. We have published a number of studies exploring the properties of SL0101

pharmacophore and demonstrate a promising platform amenable to chemical modifications (chapters 3-6).

The initial study of the effects of SL0101 on proliferation of breast cancer and normal breast epithelial cell lines revealed an ability of this compound to specifically inhibit the proliferation of cancer cells, without affecting the non-transformed cells (Smith et al., 2005). This differential ability to inhibit transformed breast epithelial cells was found to correlate well with the selectivity of small molecules towards RSK, highlighting the role of these kinases in promoting growth and survival of breast cancer cells (Smith et al., 2005; chapters 3-6). The concentrations of SL0101 required to elicit growth inhibition and decreases in downstream markers of RSK activity in cell lines are several-fold higher than the IC50 of SL0101 against RSK2 *in vitro*. These observations could suggest a limited permeability of the inhibitor. In addition, other proteins present in the cells could affect the ability of the kinase to bind to SL0101, effectively increasing the IC50 value in cell-based assays. SL0101 could be decomposed in the cell-based assays, decreasing the apparent concentration of the inhibitor. Importantly, removal of two acetates in the sugar moiety of the inhibitor drastically increases the *in vitro* IC50 of SL0101, but this compound can still inhibit RSK *in vitro* (Smith et al., 2005). Another potential product of decomposition of SL0101, kaempferol, is also known to be a relatively weak inhibitor of multiple kinases (Calderon-Montano et al., 2011). Consistent with the possibility that SL0101 can be decomposed by cellular enzymes, SL0101 has a very short half-life *in vivo* (chapter 3). The sub-optimal properties of SL0101 in biological systems have led to limited applicability of this compound in studies of RSK functions. However, we have shown that SL0101 is amenable to modifications that can improve

on these properties (chapters 3-5 and appendix). Therefore, we continue to develop analogs of SL0101 with improved cell-based and *in vivo* properties.

1.6.1.2. BI-D1870

A distinct pharmacophore that was shown to inhibit RSK was identified through a kinase selectivity screen of the derivatives of the Src family inhibitor PD180970 (Kraker et al., 2000). The compound was named BI-D1870 (fig. 4B) (Sapkota et al., 2007). Interestingly, various modifications to the initial Src inhibitor have produced selective inhibitors of diverse kinases (Zhang et al., 2009), including PD173074, an inhibitor of FGFR1, FGFR3 and FGFR4 (Mohammadi et al., 1998), and BI-2356, an inhibitor of Polo-like kinases (Lenart et al., 2007). The initial study of BI-D1870 demonstrated the compound to inhibit all four isoforms of RSK in the low nanomolar range, from RSK4 IC50 of 15 nM to RSK1 IC50 of 30 nM at 100 μM ATP. The ability of BI-D1870 to inhibit RSK1/2 *in vitro* depended on the ATP concentration, which the authors of the study used as the evidence of this compound being an ATP-competitive inhibitor, however this possibility was not formally tested. It is possible that inhibition involves both ATP-competitive and non-competitive modes. To fully understand how the inhibitor binds to its target, enzyme kinetic analysis in the presence of various ATP and inhibitor concentrations should be performed (Cornish-Bowden, 1974, Dixon, 1953). When used in the HEK 293 cell line, BI-D1870 could inhibit RSK-mediated activation of GSK with an IC50 of 1 μM, demonstrating that this compound is a very potent RSK inhibitor both *in vitro* and in cell-based assays.

Although being relatively selective inhibitor of RSK1-4, BI-D1870 was shown to inhibit a number of off-target kinases (Sapkota et al., 2007, Bain et al., 2007). These off-target kinases include PLK1, Aurora B, DYRK1a, CDK2-A, Lck, CK1, GSK3β, MELK, PIM3 and MST2. Importantly, the efficacies of BI-D1870 against RSK2 and off-target kinases PLK1 and Aurora B are very similar (Aronchik et al., 2014). In addition to *in vitro* kinase inhibition, BI-D1870 selectivity was also tested in cell-based assays using nucleotide acyl phosphate labeling (Edgar et al., 2014). In this method cells are incubated with the ATP analogue modified with a biotin group. This analogue will bind to the ATP sites of kinases and use a conserved Lys residue within this site to covalently attach the biotin tag to the kinase (Patricelli et al., 2007). The inhibitor will compete with the ATP-biotin label and decrease tagging of the kinase it binds to. As a result, comparing abundances of biotin-labeled kinases from cells treated with and without the inhibitor allows identification of those kinases that the inhibitor binds to (Patricelli et al., 2007). When tested in bone marrow-derived dendritic cells (BMDC), BI-D1870 significantly inhibited IRAK4, Slk, STK10 and STK4 kinases, in addition to RSK1-3 and PLK1 (Edgar et al., 2014). These kinases were not included in the *in vitro* inhibitor selectivity screens performed before. Interestingly, Slk, STK10 and STK4 are all members of the STE-20 like kinase family (Manning et al., 2002). Therefore, BI-D1870 exhibits a considerable amount of off-target effects, and the results using this inhibitor should be interpreted with caution.

Thanks to a very high potency *in vitro* and in cell-based assays, BI-D1870 has been extensively used as a tool compound in the studies of RSK functions. For example, BI-D1870 was used in a study of the role of RSK1 as a negative regulator of

IRS-1 in myocytes and hepatocytes (Smadja-Lamere et al., 2013). This compound was also employed in a study investigating the cross-talk between RAS-MAPK and mTOR signaling induced by the mitogen PMA in multiple cell lines (Fonseca et al., 2011). BI-D1870 was also used to validate the results of an RNAi screen that identified RSK as a critical regulator of epithelial cell migration and invasiveness (Smolen et al., 2010). Finally, BI-D1870 was used in a phosphoproteomics study to identify novel downstream targets of RSK in the context of melanoma (Galan et al., 2014). To our knowledge, however, BI-D1870 has never been used in animal studies, and its pharmacokinetic properties have never been assessed.

1.6.1.3. BIX 02565 and other indole inhibitors

A third class of selective RSK inhibitors was identified through a high-throughput screen against RSK2 NTKD and is based on an indole pharmacophore (fig. 4C) (Boyer et al., 2012). Interestingly, some indole derivatives have previously been identified as inhibitors of MAPKAP-K2 (Goldberg et al., 2008). The design and testing of indole inhibitors or RSK described in the original study was assisted by the proprietary X-ray crystallography structures of RSK2 NTKD and by homology modeling to the structures of RSK1 and RSK3. Selected indole inhibitors were then tested for selectivity *in vitro* against a panel of 20 kinases and, in some cases, 227 kinases, based on the highest degree of cross-reactivity of the early analogs in the indole series (Kirrane et al., 2012). The study identified compound BIX 02565 that had very high affinity for RSK (IC50 of 1 nM) and maintained relatively high selectivity, with *in vitro* IC50 below 1 μM found in 10 other kinases: LRRK2, PRKD1, PRKD2, PRKD3, RET, CLK1, CLK2, FGFR2, PDGFRα and FLT3. Even though these ten kinases were also inhibited by BIX 02565 with IC50

value below 1 μM, the difference in potency of the compound against RSK and off-target kinases was between 16- and 1000-fold.

The properties of BIX 02565 in cell-based assays have not been very well investigated. The initial report only tested its ability to inhibit CREB phosphorylation, as the readout of RSK inhibition in cells. The IC50 of BIX 02565 was determined to be 20 nM in this cell-based assay (Kirrane et al., 2012). Subsequently, BIX 02565 selectivity in cells was assessed in the study using nucleotide phosphate acyl labeling. This study compared cell-based selectivity of BIX 02565 in BMDC cells to that of BI-D1870. BIX 02565 demonstrated almost complete specificity for RSK1-3 in the BMDC cells, IRAK4 being the only other protein significantly affected by the inhibitor treatment (Edgar et al., 2014). Additionally, BIX 02565 was shown to significantly reduce phosphorylation of RSK downstream targets BAD and filamin A in BMDC cells at concentrations above 1 μM. Therefore, BIX 02565 appears to be a potent and selective inhibitor of RSK in cell-based assays. The described study is the only example in the literature of the use of BIX 02656 in cell-based assays.

BIX 02565 was developed as an indirect way of targeting the NHE1 activation in the treatment of cardiac ischemia-reperfusion injury (Boyer et al., 2012). Therefore, it was tested *in vivo* to assess potential cardiotoxicity (Fryer et al., 2012). This study was the only instance of the use of BIX 02565 in vivo. Interestingly, the inhibitor was found to induce a rapid and strong drop in both mean arterial pressure and heart rate when injected intravenously into rats. Of all the other RSK inhibitors, only SL0101 and fmk, the inhibitor of the C-terminal kinase domain of RSK, were also used *in vivo* (chapter 3;(Li et al., 2013). Acute cardiotoxicity was not observed upon RSK inhibition in either of

these two studies. Therefore, BIX 02565-induced decrease in heart function was due to its off-target effects. BIX 02565 was found to inhibit multiple α- and β- adrenergic receptors as well as the imidazoline I_2 receptor, with IC50 values between 0.052 and 1.820 μM. The authors of the study concluded that BIX 02565 exhibits intolerable cardiotoxicity *in vivo* that is independent of its kinase selectivity. Subsequently, 31 novel analogues of BIX 02565 were screened for their ability to inhibit RSK2 *in vitro* and in a cell-based assay, without significantly inhibiting α1A- and α2A- adrenergic receptor ligand binding *in vitro* (Fryer et al., 2012). As a result, an extremely potent inhibitor of RSK2, compound 15, was identified (fig. 4D). The RSK2 *in vitro* IC50 of compound 15 is 0.2 nM, and the cell-based IC50 is 0.32 nM. Interestingly, among all 31 analogs, there was no correlation between RSK2 efficacy and the ability to inhibit adrenergic receptors, suggesting that distinct parts of the pharmacophore are responsible for affinities towards RSK and adrenergic receptors. The selectivity of compound 15 towards other kinases was not assessed. Since initial characterization, the use of compound 15 has not been reported in any other studies and its applicability for cell-based and *in vivo* studies of RSK remain to be determined.

1.6.1.4. LJH685 and LJI308

A final class of RSK NTKD inhibitors has very recently been characterized (Aronchik et al., 2014). The series is based on the difluorophenyl pyridine pharmacophore, with the two representatives of this series being LJH685 and LJI308 (fig. 4E-F). The two inhibitors have the *in vitro* IC50 of 4-13 nM against RSK1-3. These two compounds were not tested in an *in vitro* kinase assay against RSK4. However, KinomeScan kinase binding assay showed that LJH685 and LJI308 bound to all 4

isoforms of RSK. When interrogated against a panel of 442 kinases, in addition to RSK compounds LJH685 and LJI308 only bound to MEK4, S6K1 and HIP1-3. However, this assay was performed at 10 μM inhibitor. When tested *in vitro* against S6K1, LJI308 displayed IC50 of 0.8 μM, which is 200-fold higher than that of RSK2. In addition, MEK4 was inhibited by less than 50% at 10 μM LJI308 and HIP1 activity was reduced by less than 50% by 1 μM LJI308. Cell-based assays in COS-7 cell line showed that both LJH685 and LCI308 reduced phosphorylation of the downstream targets of RSK, YB-1 and BAD, with the IC50 of 0.2-0.3 μM. Therefore, both LJH685 and LJI308 appear to be very potent and selective inhibitors of all four RSK isoforms *in vitro* and in cell-based assays. When analyzed by X-ray crystallography, RSK2 NTKD (aa 53-359) bound to LJH685 showed an unusual conformation with Phe212 residue from the DFG motif bent outwards and away from the ATP-binding cleft, reminiscent of the DFG-out conformation of a kinase. The authors of this study hypothesized that this unusual conformation was responsible for the selectivity of LJH685.

The authors of the study describing the two difluorophenyl pyridine inhibitors have made a number of very interesting observations concerning the anti-proliferative effects of RSK inhibition. Multiple cancer cell lines with activating mutations in RAS-MAPK pathway were relatively resistant to RSK inhibitors LJH685 and LJI308 in a 2D monolayer culture, despite robust decrease in the markers of RSK activity (Aronchik et al., 2014). However, the same cells grown in soft agar became extremely sensitive to RSK inhibition. For example, proliferation of aggressive breast cancer cell line MDA-MB-231 was inhibited by 50% at 48 μM compound when grown in attachment, but the IC50 of the compound dropped to 0.73 μM in soft agar. Similarly, the IC50 of LJH685 in

the lung cancer cell line NCI-H358 was reduced from 66 μM to 0.79 μM by changing the growth conditions from attachment to soft agar. Therefore, cancer cell lines with activating mutations in the RAS-MAPK pathway rely very heavily on RSK activity for the survival and proliferation in 3D cultures, whereas RSK signaling is dispensable for the survival of these cell lines in monolayer. These results are consistent with the observations that upon transforming with FGFR1, the non-transformed breast epithelial cell line MCF10A, becomes sensitive to RSK inhibition for survival and proliferation (Xian et al., 2009). The study of LJH685 and LJI308 highlighted the unique role of RSK in regulating anchorage-independent growth of cancer cells that has not previously been appreciated.

1.6.1.5. Summary of the NTKD-specific RSK inhibitors

Several diverse classes of RSK inhibitors have been described to date. The inhibitors vary in their *in vitro* affinity and cell-based efficacy against RSK isoforms (fig. 4G). Compounds BI-D1870 and SL0101 have been most extensively used in cell-based studies of RSK signaling. Although BI-D1870 is a more potent inhibitor of RSK2 *in vitro*, it is less selective for RSK than SL0101. On the other hand, SL0101 appears to be less potent in cell-based assays than BI-D1870, presumably due to limited cell permeability of the compound. SL0101 is very unstable *in vivo*, and therefore it was never used in animal studies, beyond the initial pharmacokinetic characterization (chapter 3). There are no reports of the use of BI-D1870 *in vivo*, but in the case of this inhibitor cell-based and in vivo stability have never been reported. Of all the other RSK inhibitors, only the indole RSK inhibitors were tested in vivo, and of those BIX 02565 caused acute cardiotoxicity. BIX 02565 was used in one more study, whereas all the

other RSK NTKD inhibitors were never used beyond the studies describing initial report of discovery.

Of all the RSK NTKD inhibitors described to date, the majority appears to be ATP-competitive. SL0101 constitutes a notable exception, the kinetic data strongly suggesting that this compound is an allosteric inhibitor of RSK. In addition, SL0101 is the only isoform-specific inhibitor of RSK1/2 described to date, all the other inhibitors being equally potent against all four isoforms of RSK. Neither the kinetics nor the structural biology data for the majority of the other RSK inhibitors has been reported. The only other published structure of RSK NTKD bound to a selective inhibitor is that of the difluorophenyl pyridine LJH685. This structure showed an unusual conformation of RSK resembling the inactive DFG-out fold. However, the kinetic data for LJH685 is not available, therefore there is no clear evidence that this compound is an allosteric inhibitor of RSK.

1.6.2. Inhibitors of the C-terminal kinase domain.

As discussed in section 1.3., the presence of a gatekeeper residue in the vicinity of the ATP-binding site of kinases is an important determinant of the selectivity of the kinase inhibitors. Small gatekeeper residue, like Thr or Val, enables design of inhibitors that would interact with the hydrophobic back pocket of the ATP groove. Interestingly, three out of four isoforms of RSK have a Thr gatekeeper residue in their CTKDs (Cohen et al., 2005). These isoforms are RSK1, RSK2 and RSK4 (fig. 5A). Therefore, the C-terminal kinase domain of RSK was identified as a very promising candidate for the design of selective small molecule inhibitors (Cohen et al., 2005).

Figure 5. Covalent inhibitors of the C-terminal kinase domain of RSK.

A) Sequence alignment of the hinge region of kinases with a reactive Cys residue, and the gatekeeper residue of these kinases. RSK1, RSK2 and RSK4 have a small gatekeeper residue, while RSK3 and two close relatives of RSK, MSK1 and MSK2, have a large gatekeeper residue.

B) Chemical structure of the irreversible covalent inhibitors of RSK CTKD, fmk and cmk. The X atom in fmk is fluorine, while in cmk it is chlorine.

C) Chemical structure of the reversible covalent inhibitor of the RSK CTKD, CN-NHiP.

Figure 5

A

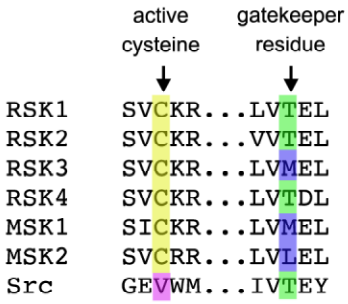
active
cysteine
gatekeeper
residue
RSK1 SVCKR...LVTEL
RSK2 SVCKR...VVTEL
RSK3 SVCKR...LVMEL
RSK4 SVCKR...LVTDL
MSK1 SICKR...LVMEL
MSK2 SVCRR...LVLEL
Src GEVWM...IVTEY

B

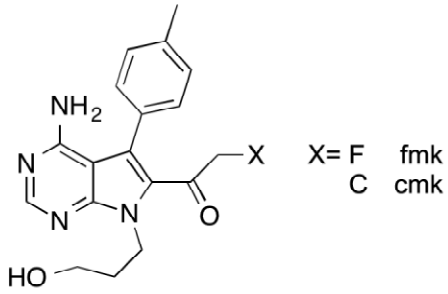
NH2
N
N
N
X
O
HO
X= F fmk
C cmk

C

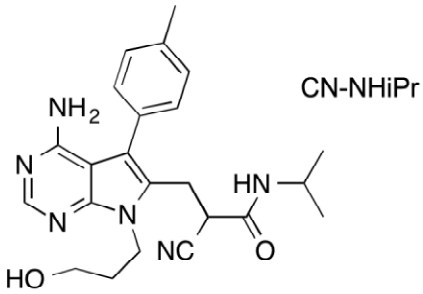
CN-NHiPr
NH2
N
N
N
HN
NC
O
HO

Among all 20 amino acids, cysteine has unique chemical properties that allow this residue to form covalent bonds with electrophilic molecules. This property has led to proposing that cysteine residues in the vicinity of the ATP-binding site could allow for a generation of an irreversible covalent kinase inhibitor (Cohen et al., 2005). This rationale was first tested in the design of covalent EGFR inhibitors (Fry et al., 1998). However, cysteine by itself does not confer the specificity of the kinase inhibitor, it only allows for a covalent bond formation. Rational kinase inhibitor design efforts have therefore focused on combining the cysteine reactivity with a method to confer the inhibitor specificity, such as the presence of a Thr gatekeeper. Interestingly, among all 491 human kinases investigated, only RSK1, RSK2 and RSK4 have both the Thr gatekeeper residue and a Cys residue within a flexible glycine-rich loop (fig. 5A). Therefore, RSK has been identified as a very promising target for covalent inhibitor design (Cohen et al., 2005). The first study to employ this property has yielded identification of the first specific inhibitors of the RSK CTKD, called fmk and cmk (Cohen et al., 2005).

1.6.2.1. Fmk and cmk

Fmk and cmk were designed based on the adenine scaffold. p-tolyl residue was added to employ the hydrophobic pocket behind the Thr gatekeeper. Chloromethylketone (fmk) and fluoromethylketone (cmk) represented the electrophilic component that was intended to react with the cysteine residue (fig.5B). This design approach resulted in the identification of remarkably specific and potent inhibitors, and due to a higher chemical stability fmk was further studied. This compound was shown to inhibit RSK2 with an IC50 of 15 nM at 100 μM ATP, and this inhibitory activity was

completely dependent on the presence of the Cys residue in the kinase and chloromethylketone residue in the inhibitor. It is important to note, however, that the conventional *in vitro* IC50 measurements are of limited value in the case of covalent inhibitors (Singh et al., 2011). In a typical measurement of IC50, the binding of inhibitor to its target is determined at equilibrium. Unlike the non-covalent inhibitors, however, the binding reaction of the covalent inhibitor to its target continues until completion, and not equilibrium. Fmk inhibited the phosphorylation of Ser386 of RSK2, the only known substrate for the RSK CTKD, with an IC50 of 200 nM in cell-based assays (Vik and Ryder, 1997, Dalby et al., 1998). MSK1 has a Cys residue in the same position as RSK1/2, but the gatekeeper residue in MSK1 is Met. As a result, fmk does not inhibit MSK1 at all. However, mutating this gatekeeper to Thr is sufficient for MSK1 to become equally sensitive to fmk as RSK2. These results together prove evidence for the predicted mechanism for fmk potency and selectivity. Since fmk covalently binds to RSK, it was relatively easy to assess its ability to react with other proteins. When biotinylated fmk was incubated with cell lysate, only two proteins reacted with this compound and were subsequently affinity purified using streptavidin column. These two proteins were RSK1 and RSK2. The authors of the study did not provide explanation to the fact that even though RSK4 also possesses both the reactive Cys residue and the Thr gatekeeper residue, it was not identified in the screen of fmk-bound proteins. This experiment was performed in HEK 293T cells, which do express RSK4, albeit at very low levels (Uhlen et al., 2015, Sun et al., 2013). Fmk specificity has also been tested *in vitro* against a panel of ~80 kinases and was proven to be remarkably specific (Bain et al., 2007). This inhibitor only showed activity at 3 μM concentration against Src, Lck

and to a lesser extent against S6K1. However, at a concentration that fully inhibited RSK2 in cell lines, fmk did not reverse the phenotypes induced by v-Src (Cohen et al., 2005), further supporting the selectivity of fmk in cell-based systems.

1.6.2.2. CN-NHiPr

Following the success of rational design of fmk, the unusual features of the RSK CTKD ATP-binding site were used in further studies of novel covalent inhibitors of RSK CTKD (Serafimova et al., 2012, Miller et al., 2013, London et al., 2014). CN-NHiPr, an fmk derivative intended to be a reversible covalent inhibitor (fig. 5C), maintained remarkable specificity for RSK1 *in vitro*, and in addition was proven to inhibit RSK4 (Serafimova et al., 2012). Of the 442 kinases tested *in vitro*, CN-NHiPr at 1 μM significantly inhibited 6 proteins, including MAP3K1, RIPK2, MEK5, STK16, RET and PDGFRB. This molecule was not tested against RSK2. Despite being a reversible inhibitor *in vitro*, however, this compound showed the same persistence of RSK inhibition in cell-based assays as fmk, suggesting that its half-life is longer than the turnover rate of the protein. The other two series of covalent inhibitors of RSK CTKD were designed using fragment-based screening design (Miller et al., 2013, London et al., 2014). In both cases however, the developed inhibitors were equally potent against MSK1/2 as RSK1/2.

Figure 6. Alternative mode of activation of the NTKD of RSK in the absence of CTKD activity.

CTKD inhibitors fmk and cmk block CTKD-mediated autophosphorylation of the hydrophobic motif in the linker region of RSK. Alternative kinases, like MK2/3 in immune cells, can phosphorylate this residue, bypassing the CTKD inhibition. Phoshorylated hydrophobic motif recruits PDK1, which phosphorylates and activates NTKD of RSK.

Figure 6

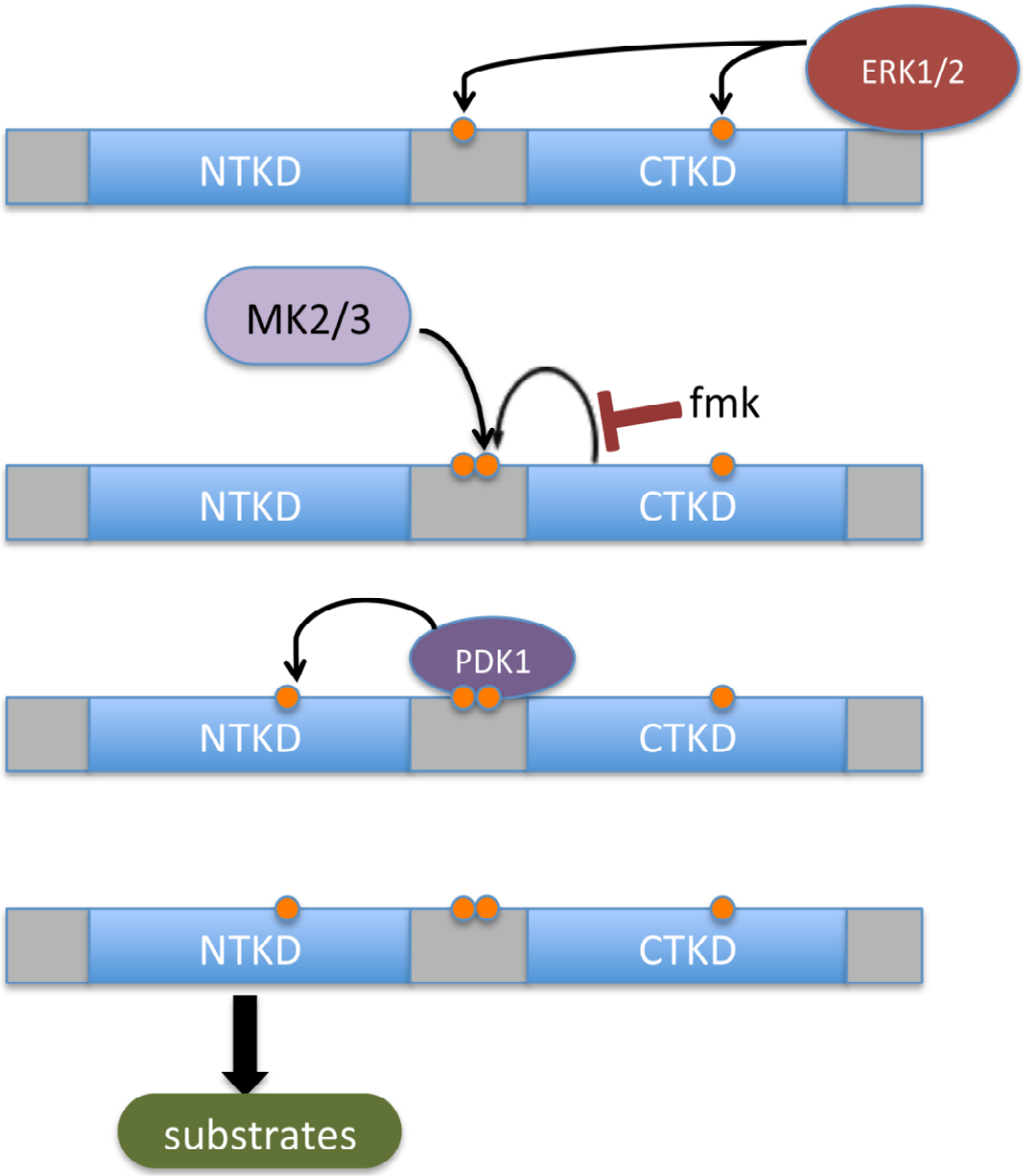
ERK1/2
NTKD
CTKD
MK2/3
fmk
NTKD
CTKD
PDK1
NTKD
CTKD
NTKD
CTKD
substrates

1.6.2.3. Biological significance of the inhibitors of RSK CTKD

The use of CTKD-specific inhibitors of RSK allowed for exploring the role of the autophosphorylation of Ser386, which is essential for the full activation of the NTKD. It has been observed that this residue could be phosphorylated in the absence of CTKD activity, but the identity of the kinase mediating this modification was unknown (Frodin et al., 2000, Chrestensen and Sturgill, 2002). The authors of one the study used a more cell-permeable propargylamine derivative of fmk (fmk-pa), which inhibited mitogen-induced Ser386 phosphorylation in intact bone marrow-derived macrophages with an IC50 of 30 nM (Cohen et al., 2007). In the same cells stimulated with lipopolysaccharide (LPS), 1 μM fmk-pa did not affect the phosphorylation levels of Ser386 at all. However, this effect seemed to be cell-type specific, as LPS did not rescue Ser386 phosphorylation in fmk-pa-treated MA-MB-231 cell line. Consistent with the results of this study, RSK was later shown to be phosphorylated on Ser386 by MK2 and MK3 downstream of p38 in dendritic cells (Zaru et al., 2007). One would expect RSK NTKD-specific inhibitors to block RSK downstream signaling irrespective of the mode of the Ser386 activation. Therefore, these studies suggested that in certain cellular contexts CTKD-specific inhibitors could yield different results than inhibiting RSK using NTKD-specific compounds.

The usefulness of fmk in inhibiting RSK downstream signaling has been proven by a number of studies. For example, fmk was used to demonstrate the role of RSK2 in mediating the transformation potential of FGFR3 in human myeloma cells (Kang et al., 2007b). Fmk was also used to prove that RSK phosphorylates and activates the sarcolemmal sodium-proton exchanger NHE1 in response to alpha-1-adrenergic

stimulation in adult myocardium (Cuello et al., 2007). Finally, consistent with an emerging role of RSK in promoting metastasis, fmk was used in mouse xenograft studies of aggressive head and neck squamous cell carcinoma (HNSCC) (Li et al., 2013). In these studies RSK inhibition by fmk caused a reduction in lymph node metastasis of the NHSCC cells, without affecting the size of the primary tumor. Therefore, RSK was shown to be an attractive therapeutic target for specifically inhibiting metastasis in HNSCC.

CTKD-specific inhibitors of RSK act to block the autophosphorylation-mediated activation of RSK (fig. 6). Therefore, these inhibitors will be the most effective when the basal activation status of the kinase is low. If RSK is active when CTKD inhibitor is introduced, the phosphorylation of Ser386 has to be removed, either by a phosphatase, or by turning over the whole protein. In contrast, the NTKD-specific inhibitors will block phosphorylation of the downstream targets of RSK even when the protein is fully activated. As a result, the temporal differences in the response to these two different classes of RSK inhibitors could be expected. In addition, as mentioned above, in certain cell contexts Ser386 of RSK can be phosphorylated by other kinases, which would bypass the effects of the CTKD-specific RSK inhibitor (fig. 6).

1.7. Summary

Two decades of studies of the RSK family of kinases have allowed us to appreciate the complex biology of these proteins. RSK has emerged as a multifunctional downstream effector of the mitogenic signaling that is responsible for mediating a major fraction of all ERK1/2 functions. The processes regulated by RSK

ultimately aim at supporting cellular proliferation and survival. This goal is achieved by coordinated modulation of gene expression, protein synthesis, cell cycle and apoptosis. Multiple targets of RSK also receive inputs from the PI3K-Akt pathway, and the cooperation between these signals ultimately determines the biological outcome.

With the increasing number of studies investigating specific mechanisms regulated by the RSK family of kinases, we are now beginning to understand that these proteins could perform non-overlapping functions that appear to be isoform- and cell type-specific. The emerging patterns suggest that RSK2 functions could preferentially partition into the nucleus, while RSK1 could perform the majority of its roles in the cytoplasm. As a result, the former isoform would have a heavier impact on gene transcription, while the latter would support protein translation. Compared to RSK1/2, much less is known about the remaining two isoforms, therefore such predictions are very difficult to formulate with respect to RSK3/4. These differences in the involvement of RSK isoforms in already discovered mechanisms highlight the importance of developing methods to investigate the functions of individual RSK family members. In this context, RSK isoform-selective small molecule inhibitors could constitute an invaluable tool for future mechanistic studies of RSK isoform-specific biological functions.

The full understanding of the biological functions of RSK has also been limited by the paucity of in vivo studies using genetically engineered mouse models. In fact the only mouse models reported so far were a RSK2 knock-out and a RSK1/2/3 triple knock-out. As a consequence, the vast majority of the mechanistic data concerning the functions of RSK kinases were derived from studies performed in cell lines. It remains to

be determined whether these observations can be translated to meaningful biological effects in vivo. Small molecule inhibitors of the RSK kinases could offer a possibility to investigate the in vivo functions of RSK kinases in the absence of the genetically engineered models.

Being involved in critical processes regulating cellular proliferation and survival, RSK has been shown to play a role in various pathologies, including cancer. Therefore, it has been proposed to constitute a promising target for therapeutic intervention. To this end, several small molecule inhibitors of RSK have been discovered, however they display limited applicability *in vivo*. As a result, the therapeutic potential of RSK inhibition as a novel strategy to treat cancer *in vivo* remains almost completely unexplored. Therefore, there is a need to further develop inhibitors of RSK in order to identify clinically relevant lead compounds.

Taken all these factors together, there has been an ongoing effort to develop the small molecule inhibitors of RSK that could be used in vivo, as well as isoform-selective inhibitors of RSK. Here, we describe the properties of SL0101 as a very promising platform for further development of such clinically relevant RSK inhibitors. We demonstrate the complex interactions of this compound with its target, which contribute to our understanding of the basis for its efficacy and selectivity as a kinase inhibitor. We explore the biological space available to SL0101 derivatives and identify chemical modifications to the parent molecule that confer increased affinity for RSK *in vitro*, as well as its stability in cell-based systems. Finally, we identify a previously overlooked property of SL0101 as an isoform-selective inhibitor of RSK1/2 and not RSK3/4. These observations further highlight the usefulness of developing the analogs of this inhibitor,

both as tool compounds for the mechanistic studies of RSK1/2 isoforms, and as novel agents for investigating the therapeutic potential of inhibiting RSK in the treatment of various pathologies, including cancer.

We expand our studies beyond developing new RSK inhibitors to deepen our understanding of the biology of this family of kinases. We develop high-throughput proteomics approach to studying specific functions of RSK1 in intact cells and identify potential roles of this protein at an intersection of cellular energy homeostasis and protein synthesis. These results add to an increasing body of evidence in support of the potential role of RSK as a regulator of cellular energy and nutrient homeostasis (section 1.5.10). Since this emerging novel function of the RSK family of kinases is still relatively understudied, we set out to further pursue this biological function of RSK. Our results show for the first time that inhibition of RSK1/2 does alter cellular energy and nutrient homeostasis, specifically through the suppression of mitochondrial oxidative phosphorylation downstream of multiple nutrients. Intriguingly, we discover a preferential dependency of transformed cell lines on RSK1/2 for maintaining their mitochondrial function. These observations add another element to an expanding repertoire of RSK functions in supporting cellular proliferation and survival, particularly in the context of cellular transformation. Finally, our novel findings highlighting the unique role of RSK1/2 in stimulating oxidative phosphorylation in transformed cells point to the potential of RSK inhibition as a novel strategy to specifically target energy homeostasis in cancer cells.

Chapter 2

SL0101 is an allosteric inhibitor of RSK1 and RSK2.

Summary

A family of Ser/Thr protein kinases RSK has been shown to play important roles in regulation proliferation and motility in a variety of cancers. Therefore, RSK has been proposed as a potential novel therapeutic target in various malignancies. Of the four isoforms, RSK1 and RSK2 were shown to promote tumor growth and metastasis, while RSK3 and RSK4 are thought to be tumor suppressors. As a result, there is a need to develop isoform-specific inhibitors of RSK. SL0101 is a small-molecule inhibitor of RSK that was identified though a high-throughput screen of natural plant extracts. Previous studies have shown that this compound exhibits remarkable kinase selectivity. The analysis of the crystal structure the N-terminal kinase domain of RSK with SL0101 revealed a unique conformation of the kinase bound to the inhibitor, suggesting that SL0101 is an allosteric inhibitor of RSK. Here, we provide evidence that SL0101 is a non-competitive inhibitor of RSK, and the binding of SL0101 induces a conformational change of the kinase. In addition, we show that SL0101 is a selective inhibitor of RSK1/2 and not RSK3/4. Therefore, this compound represents the first isoform-selective, allosteric inhibitor of RSK1/2.

2.1. Introduction

Kinases represent the most promising class of potential targets for therapeutic intervention in a variety of disease states, including cancer (Fabbro, 2015). Among signaling cascades that have been most extensively pursued in cancer research is the mitogen-activated protein kinase (MAPK) cascade (Sebolt-Leopold and Herrera, 2004). MAPK pathway is reported to be deregulated in up to 30% of all cancers (Hoshino et al., 1999). However, inhibition of the MAPK pathway could prove too toxic for normal proliferating cells (Sebolt-Leopold and Herrera, 2004). In addition, the pathway is involved in a number of feedback loops, which complicates the ability to predict cellular responses to its inhibition (Eisinger-Mathason et al., 2010). Therefore, we propose that downstream effectors of MAPK constitute potential drug targets for the inhibition of the MAPK pathway. One major downstream target of MAPK that has been extensively studied in the context of normal cell homeostasis and tumorigenesis is the family of p90 ribosomal S6 kinases (RSK) ((Anjum and Blenis, 2008).

RSK is a family of four Ser/Thr protein kinases that are highly similar in terms of protein sequence, but appear to perform distinct functions in mammalian cells (Lara et al., 2013). RSK is unusual among other kinases in that it possesses two fully functional kinase domains within one polypeptide sequence (Anjum and Blenis, 2008). The C-terminal kinase domain (CTKD) is involved in the autophosphorylation and activation cascade of the kinase, while the N-terminal kinase domain (NTKD) phosphorylates downstream targets of RSK (Bjorbaek et al., 1995). The NTKD belongs to the AGC (protein A, protein G and protein C) superfamily, while the CTKD is the member of the calcium-calmodulin dependent protein kinase (CaMK) superfamily (Anjum and Blenis,

2008). RSK is classically activated by ERK1/2 in response to various stimuli, including growth factors, hormones and neurotransmitters, and regulates various cellular processes promoting cell survival and proliferation (Anjum and Blenis, 2008). RSK1 and RSK2 were shown to be over-expressed in a variety of tumors, including breast and prostate (Smith et al., 2005, Clark et al., 2005), and appear to serve a variety of pro-tumorigenic functions (Cho et al., 2007, Eisinger-Mathason et al., 2010, Kang et al., 2007a, Romeo et al., 2013). RSK1/2 has been characterized as a major mediator of ERK1/2 signaling in promoting motility and invasiveness in melanoma (Doehn et al., 2009). The study estimated that 20% of all ERK1/2 targets were co-regulated by RSK1/2, highlighting the central role of RSK as a downstream effector of the MAPK pathway in melanoma. In addition, blocking RSK by means of a covalent inhibitor was demonstrated to significantly inhibit the metastatic potential of the human head and neck squamous cell carcinoma in mouse xenografts (Li et al., 2013). Therefore, RSK emerges as a potential major therapeutic target for blocking both primary tumor growth and metastasis (Sulzmaier and Ramos, 2013).

The exact functions of individual RSK isoforms are not very well understood (Lara et al., 2013). Recent studies has suggested that, as opposed to established pro-tumorigenic and pro-metastatic functions of RSK1/2, the remaining two isoforms act as putative tumor suppressors (Thakur et al., 2008, Cai et al., 2014, Bignone et al., 2007). Therefore, there is an ongoing effort to identify isoform-selective inhibitors of RSK for both biological and clinical studies (Nguyen, 2008). An ideal therapeutic agent would inhibit exclusively RSK1 or RSK2, or both these isoforms, without affecting the activities

of RSK3 and RSK4. Such inhibitor has not been characterized yet. However, not all reported RSK inhibitors were tested for their ability to inhibit all four isoforms of RSK.

SL0101 is an inhibitor of RSK that was derived from the plant extract of a tropical plant, *Forsteronia refracta* (Smith et al., 2005). Since initial discovery, it has been used as a tool compound in a number of studies of the functions of RSK (Nguyen, 2008). A major advantage of SL0101 over other RSK inhibitors is a remarkable selectivity of the compound for RSK (Bain et al., 2007). Of all kinases tested, only Aurora B, PIM1 and PIM3 appear to be potential off-target kinases inhibited by SL0101. However, the applicability of SL0101 in cell-based and *in vivo* studies has been limited by poor cell permeability and stability of the compound in biological systems (Smith et al., 2005; chapter 3). SL0101 has proven amenable to chemical modifications that improve on those properties, and it is continued to be developed as a potential novel RSK inhibitor *in vivo* (chapters 3-5 and appendix).

The selectivity of SL0101 is surprising, considering a relatively common structure of the molecule. SL0101 is a glycosylated flavonoid consisting of a kaempferol ring system and an unusual sugar, L-rhamnose (Smith et al., 2005). Kaempferol and many of its derivatives are non-selective inhibitors of kinases with relatively low affinity for multiple targets (Calderon-Montano et al., 2011). Interestingly, the X-ray diffraction crystal structure of SL0101 bound to the N-terminal kinase domain of RSK2 has recently been reported (Utepbergenov et al., 2012). This structure displayed a very unusual fold of the kinase bound to the inhibitor, opening a possibility that SL0101 is an allosteric inhibitor of RSK.

Given the potential for developing novel kinase-selective inhibitors of RSK based on the SL0101 pharmacophore, and recent findings that SL0101 could owe its remarkable selectivity for RSK to its unusual mode of binding, we set out to better characterize the properties of this compound as a RSK inhibitor. We found that SL0101 inhibits RSK through a non-competitive mode, and this inhibition involves a change in the conformation of the kinase. In addition, we find that SL0101 is a selective inhibitor of RSK1/2, and not RSK3/4.

2.2. Materials and methods

Reagents

SL0101 was synthesized by collaborators: George O'Doherty (Northeastern University, Boston MA), Michael Hilinski (University of Virginia, Charlottesville VA) or David Maloney (National Institutes of Health, Bethesda MD), according to a previously described synthetic route (Maloney and Hecht, 2005). BI-D1870 was purchased from Enzo Life Sciences (Farmingdale NY). Recombinant active RSK2, RSK3 and RSK4 were purchased from Invitrogen (Carlsbad CA). Profection Calcium Phosphate Transfection kit was purchased from Promega (Madison WI). Primary antibodies used were mouse monoclonal anti-RSK2 (E-1), rabbit anti-RSK1 (C-21) and goat anti-RSK3 (C-20) from Santa Cruz Biotechnology (Santa Cruz CA), mouse monoclonal anti-HA (Lymphocyte Culture Center, University of Virginia, Charlottesville VA) and rabbit anti-ERα-pSer167 (Smith et al., 2005). Secondary antibodies conjugated to horseradish peroxidase (HRP) were donkey anti-goat, donkey anti-rabbit and goat anti-mouse from Jackson Immunoresearch (West Grove PA).

Cell culture and treatment

BHK-21 cells were cultured as directed by American Type Culture Collection (ATCC). For protein expression, pKH3 plasmids containing RSK1-4 cDNA were transfected into cells using calcium phosphate method as described previously (Poteet-Smith et al., 1999). 42 hours post-transfection cells were stimulated with 200 ng/mL EGF in fresh serum-containing medium for 15 min, followed by lysis on the plate using ice-cold lysis buffer (50 mM Tris, pH 8, at 4 °C, 150 mM NaCl, 1% Nonidet P-40, 0.5% Triton X-100, 1.5 mM $MgCl_2$, 1 mM EDTA, 1 mM EGTA, 1X Protease Inhibitor Cocktail, 1 mM phenylmethylsulfonyl fluoride, 200 µM Na_3VO_4, 1 µM microcystin LR). The lysate was sheared by passing thrice through a 27G needle and snap-frozen in liquid nitrogen.

Immunoprecipitation

Anti-HA antibody-conjugated magnetic beads were used for the immunoprecipitation of HA-tagged RSK proteins from BHK cell lysates. Briefly, 50 µL of bead slurry for 15 cm confluent plate of BHK cells was washed twice with lysis buffer and incubated at 4°C for 1 hour on a rotator. The beads were then washed 2 times with lysis buffer and 3 times with kinase assay buffer (5 mM β-glycerophosphate, pH 7.4, 25 mM HEPES, pH 7.4, 1.5 mM DTT, 30 mM $MgCl_2$, 0.15 M NaCl). Immunoprecipitated protein was eluted with 250 mM HA peptide in kinase assay buffer by incubating overnight in a thermomixer at 4°C. The protein amount in the elution was determined by Western Blotting against a loading control of recombinant RSK protein.

In vitro kinase activity assays

The assays of RSK activity were performed as described previously (Smith et al., 2005). Briefly, 50 μL of 5 nM kinase in kinase assay buffer with 1% bovine serum albumin (BSA)(Roche, France) was loaded into each well of a 96-well Maxisorp-treated polystyrene plate (Nunc, Denmark) coated with 1 μg of the GST-ERαSer167 peptide, sequence RRLASTND. 25 μL of inhibitor at indicated concentration, or DMSO vehicle, was added to each well and incubated for 15 min or 120 min at room temperature. The reaction was initiated by addition of ATP in kinase assay buffer with 1% BSA at indicated concentrations. The reaction was allowed to proceed for 20 min, which is within the linear range of the assay (Smith et al., 2005). As a background control, 75 μL of 500 mM EDTA pH 8.0 in water was added to the well before ATP. The reactions were terminated by addition of 500 mM EDTA pH 8.0 in water. After extensive washes of wells, rabbit antibody against phosphorylated Ser167 of ERα was incubated for 30 min. Following extensive washes, the secondary donkey anti-rabbit antibody conjugated to horseradish peroxidase (HRP) was incubated for 30 min. The secondary antibody was removed, the plate was washed and Enhanced Luminescence Reagent (Perkin-Elmer, Boston MA) was used to measure HRP activity, according to manufacturer's protocol. Half-inhibitory concentration of the compound (IC50) was calculated using non-linear regression analysis of the data (GraphPad Prism).

Figure 7. SL0101 is an isoform-selective inhibitor of RSK1/2.

A) Immunoprecipitated RSK1-4 isoforms are enzymatically active. pSer signal in an *in vitro* kinase assay for each kinase was normalized to the signal of the negative control. combined N≥2 in triplicate, Bars mean ±SD.

B) SL0101 inhibits *in vitro* kinase activity of immunoprecipitated RSK1 and RSK2, but does not inhibit the activities of immunoprecipitated RSK3 and RSK4. The bars represent kinase activity, normalized to DMSO-control treated kinase for each kinase separately, combined N≥2 in triplicate, ±SD, asterisk indicates $p<0.01$ compared to respective control.

C) BI-D1870 inhibits all three purified RSK isoforms tested, with similar potencies. Combined normalized activity of the kinase in a range of inhibitor concentrations, N=2 in triplicate, ±SD.

D) SL0101 inhibits purified RSK2, but not purified RSK3 and RSK4 tested. Combined normalized activity of the kinase in a range of inhibitor concentrations, N=2 in triplicate, ±SD.

Figure 7

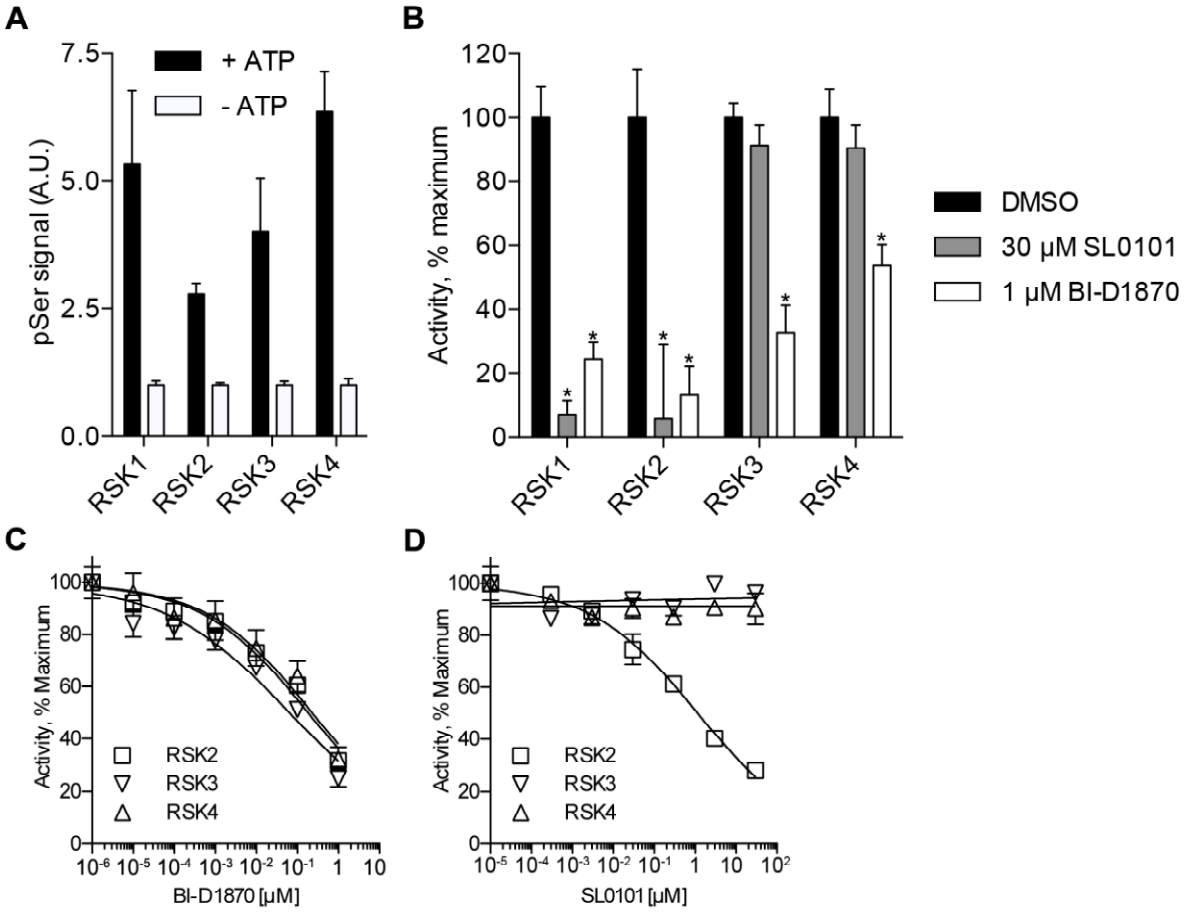
A
7.5
5.0
2.5
0.0
pSer signal (A.U.)
+ ATP
- ATP
RSK1
RSK2
RSK3
RSK4
B
120
100
80
60
40
20
0
Activity, % maximum
DMSO
30 μM SL0101
1 μM BI-D1870
C
Activity, % Maximum
RSK2
RSK3
RSK4
BI-D1870 [μM]
D
Activity, % Maximum
SL0101 [μM]

2.3. Results

The two most widely used small molecule inhibitors of RSK are BI-D1870 and SL0101 (Sapkota et al., 2007, Smith et al., 2005). BI-D1870 has been shown to inhibit all four isoforms of RSK with similar efficacies *in vitro* (Bain et al., 2007). However, SL0101 has only been confirmed to inhibit RSK1 and RSK2, and its ability to inhibit RSK3 and RSK4 is not known (Smith et al., 2005). To better understand the properties of SL0101 and its analogs as a potential novel therapeutic agents in cancer treatment we set out to characterize the isoform-selectivity of SL0101. Initially, we tested BI-D1870 and SL0101 at concentrations ~100-fold higher than the reported *in vitro* IC50 of these compounds against RSK isoforms. Both inhibitors were used against the wild-type full-length isoforms of RSK that were immunoprecipitated from EGF-stimulated BHK cells. All immunoprecipitated kinases were active (fig. 7A). Consistently with the previous reports, BI-D1870 significantly inhibited all four isoforms of RSK at 1 μM (fig. 7B). SL0101 inhibited RSK1 and RSK2, which is in agreement with the reported activity of this inhibitor against these two isoforms (Smith et al., 2005, Bain et al., 2007). However, RSK3 and RSK4 isoforms were not inhibited by 30 μM SL0101. These results suggested that SL0101 is an isoform-specific inhibitor of RSK1/2.

To further support the hypothesis that SL0101 is an isoform-specific inhibitor of RSK, we performed *in vitro* kinase assays using commercially available purified RSK proteins (Invitrogen, CA). Consistent with the previous findings, BI-D1870 inhibited all 3 tested isoforms with similar potencies (fig. 1C). However, while SL0101 efficiently inhibited RSK2, the activities of RSK3 and RSK4 were not decreased (fig. 1D). Therefore, we conclude that SL0101 is an isoform-specific inhibitor of RSK1/2, and not

RSK3/4, and this ability differentiates it from another well-characterized inhibitor of RSK, BI-D1870.

Given very high similarity in the protein sequence of the four kinases, the specificity of SL0101 against RSK1/2 was very surprising. Therefore, we decided to further investigate the mechanism of RSK1/2 inhibition by RSK. The X-ray crystal structures of this inhibitor bound to the N-terminal kinase domain (NTKD) of RSK2, as well as the structure of RSK2 NTKD bound to the non-cleavable ATP analog, AMP-PNP, have been previously reported (Utepbergenov et al., 2012, Malakhova et al., 2009). These structures revealed a very unusual conformation of the kinase bound to the inhibitor, compared to AMP-PNP. The protein displayed extensive rearrangement of the N-lobe of the kinase with respect to the C-lobe, resulting in a formation of a new binding site for the inhibitor that was adjacent to the ATP-binding site in the groove between the two lobes. This structural rearrangement involved transitions of the secondary features of the kinase that appeared to be very energetically unfavorable and involved partial unfolding and re-folding of the kinase. Therefore, we hypothesized that the conformational change induced by SL0101 binding could occur only when the kinase is allowed to incubate with the inhibitor for extended period of time. In order to test this hypothesis, we performed *in vitro* kinase assays with SL0101 pre-incubated with full-length RSK2 protein for 15 min and 120 min, before adding the substrate (ATP). We first tested this hypothesis using the RSK2 Y707A mutant, which has an elevated basal activity (Poteet-Smith et al., 1999). The mutation is within the auto-inhibitory loop of the C-terminal kinase domain of RSK, which causes an increase in basal activity of the CTKD. When tested *in vitro* against RSK2Y707A, SL0101 displayed

a significant difference in the ability to inhibit the kinase in 15 min vs. 120 min. pre-incubation, with a ~14-fold higher IC50 at the shorter incubation time (fig. 8A,F). This inhibitor was much more potent against RSK2 when pre-incubated for extended period of time, suggesting that a conformational change of the kinase occurs between 15 min and 120 min of pre-incubation. When wild-type full length RSK2 was tested *in vitro*, it also displayed the change in IC50 of SL0101 between 15 min and 120 min (fig. 8B,F). The difference in the *in vitro* IC50 of SL0101 between 15 min and 120 min pre-incubation was ~6-fold in the WT-RSK2, compared to ~14-fold in RSK2Y707A. Both variants of the protein displayed a very similar IC50 at 120 min pre-incubation, indicating equal sensitivity for the inhibitor. However, the IC50 of RSK2Y707A at 15 min pre-incubation was >4-fold higher. These results suggest that the mutationally activated CTKD of RSK interferes with the ability of its NTKD to undergo the conformational change upon SL0101 binding.

In order to test the hypothesis that the C-terminal part of RSK influences the ability of the NTKD to undergo the conformational change following SL0101 binding we tested *in vitro* a truncation mutant of RSK2 (RSK2(1-389)). This mutant contains the N-terminus and the entire NTKD, as well as the majority of the linker region, including the PDK1-docking site that is required for the activation of the RSK2 NTKD (Frodin et al., 2000, Frodin et al., 2002). The *in vitro* IC50 of SL0101 for the truncation mutant at 120 min pre-incubation was consistent with that of both full-length RSK2 constructs, suggesting that all 3 variants of RSK2 were inhibited in a similar fashion by SL0101 in these conditions (fig. 8C,F). However, when pre-incubated for 15 min, RSK2(1-389) was equally sensitive to SL0101 as when pre-incubated for 120 min, suggesting that in both

pre-incubation conditions SL0101 is equally capable of forming the unusual complex with RSK2 NTKD (fig. 8C,F). These results further support the role of the CTKD of RSK2 in regulating the conformation of the NTKD. These results together indicate that SL0101 binding to RSK at extended periods of time allows for a formation of the unusual conformation of the kinase that is more efficiently inhibited by SL0101, and that the existence of this new conformation in solution is impeded by the CTKD of RSK2.

As mentioned above, we and others have shown that RSK1 is also inhibited by SL0101. Therefore, we investigated the ability of SL0101 to differentially inhibit RSK1 in 15 min vs. 120 min pre-incubation. When tested *in vitro*, WT-RSK1 was more effectively inhibited by SL0101 at longer pre-incubation, compared to a 15 min pre-incubation (fig. 8D,F). However, the difference in IC50 between two pre-incubation times was only 2.5-fold, compared to 6-fold difference in the case of RSK2. The IC50 of SL0101 against RSK1 as measured at 120 min pre-incubation with the kinase was consistent with the IC50 of both WT-RSK2 and RSK2Y707A at longer pre-incubation condition. These results indicate that full-length wild-type RSK1 and RSK2 are equally sensitive to SL0101 at 120 min pre-incubation.

To further evaluate the role of the CTKD of RSK in regulating the affinity of SL0101 for the NTKD, we generated a chimeric protein, in which the C-terminal portion of RSK2 was replaced with the corresponding sequence of RSK1. The chimeric protein displayed the same ability to be differentially inhibited by SL0101 in long vs. short pre-incubation conditions as the wild-type RSK2, as the IC50 of SL0101 for either condition was consistent with that found for the full-length wild-type RSK2 (fig. 8E,F).

These results suggest that the C-terminus of RSK1 can perform the same function as the C-terminus of RSK2 in regulating SL0101 affinity for the NTKD. Therefore, these results provide evidence for a common mechanism of the CTKD involvement on the binding of SL0101.

The IC50 of a compound is related to its affinity to the target protein, which is defined as the inhibition constant K_i (Cheng and Prusoff, 1973, Brandt et al., 1987). Therefore, we hypothesized that the inhibition constant of SL0101 for RSK was changing between the 15 min vs. 120 min pre-incubation. A change in inhibition constant can only occur as a result of an alteration in the conformation of the inhibitor-molecule complex (Knight and Shokat, 2005). Therefore, variations in inhibition constant would provide direct evidence of the hypothesized switch in the conformation of the kinase. In order to measure the inhibition constant of SL0101 at 15 min and 120 min pre-incubation, the *in vitro* activity assays were performed at varying concentrations of inhibitor and ATP. Plotting the reciprocal of the reaction rate against the inhibitor concentration for each ATP concentration allows the identification the inhibition constant of the enzyme-substrate complex (Dixon, 1953). The abscissa of the intersection point of the lines for each ATP concentration defines the $-K_i$ value. At 120 min pre-incubation, the K_i value of SL0101 was 7.81 μM (fig. 9A,E). However, at 15 min pre-incubation the lines representing varying ATP concentrations were parallel, indicating no binding of the inhibitor to free enzyme in this condition (fig. 9B). Therefore, we observed a dramatic change in the ability of the inhibitor to bind to the enzyme between 15 min and 120 min pre-incubation times.

Figure 8. C-terminal kinase domain of RSK1/2 regulates potency of SL0101 against the N-terminal kinase domain of RSK.

A) SL0101 is a 14-fold more potent inhibitor of purified recombinant RSK2Y707A when allowed to pre-incubate with the kinase for 120 min. Combined normalized kinase activity, N=3 in quadruplicate, ±SD.

B) SL0101 is a 6-fold more potent inhibitor of immunoprecipitated RSK2 when allowed to pre-incubate with the kinase for 120 min. Combined normalized kinase activity, N=3 in triplicate, ±SD.

C) SL0101 is equally potent against the RSK2(1-389) truncation mutant containing full NTKD and linker region of the kinase in both pre-incubation conditions. Combined normalized kinase activity, N=2 in triplicate, ±SD.

D) SL0101 is a 2.5-fold more potent inhibitor of purified recombinant RSK2Y707A when allowed to pre-incubate with the kinase for 120 min. Combined normalized kinase activity, N=2 in quadruplicate, ±SD.

E) SL0101 is a 4.5-fold more potent inhibitor of immunoprecipitated RSK2/1 chimeric protein when pre-incubated with the kinase for 120 min. Combined normalized kinase activity, N=3 in triplicate, ±SD.

F) Summary table of the inhibitor concentration required for a 50% reduction in kinase activity (IC50) for given constructs at 120 min and 15 min pre-incubation times. IC50 was calculated for each repeat of the experiment separately using the non-linear regression analysis of the data, values represent mean IC50 ±SD for N≥2 in triplicate or quadruplicate. p value, Student t-test of IC50 at 120 min vs. 15 min.

Figure 8

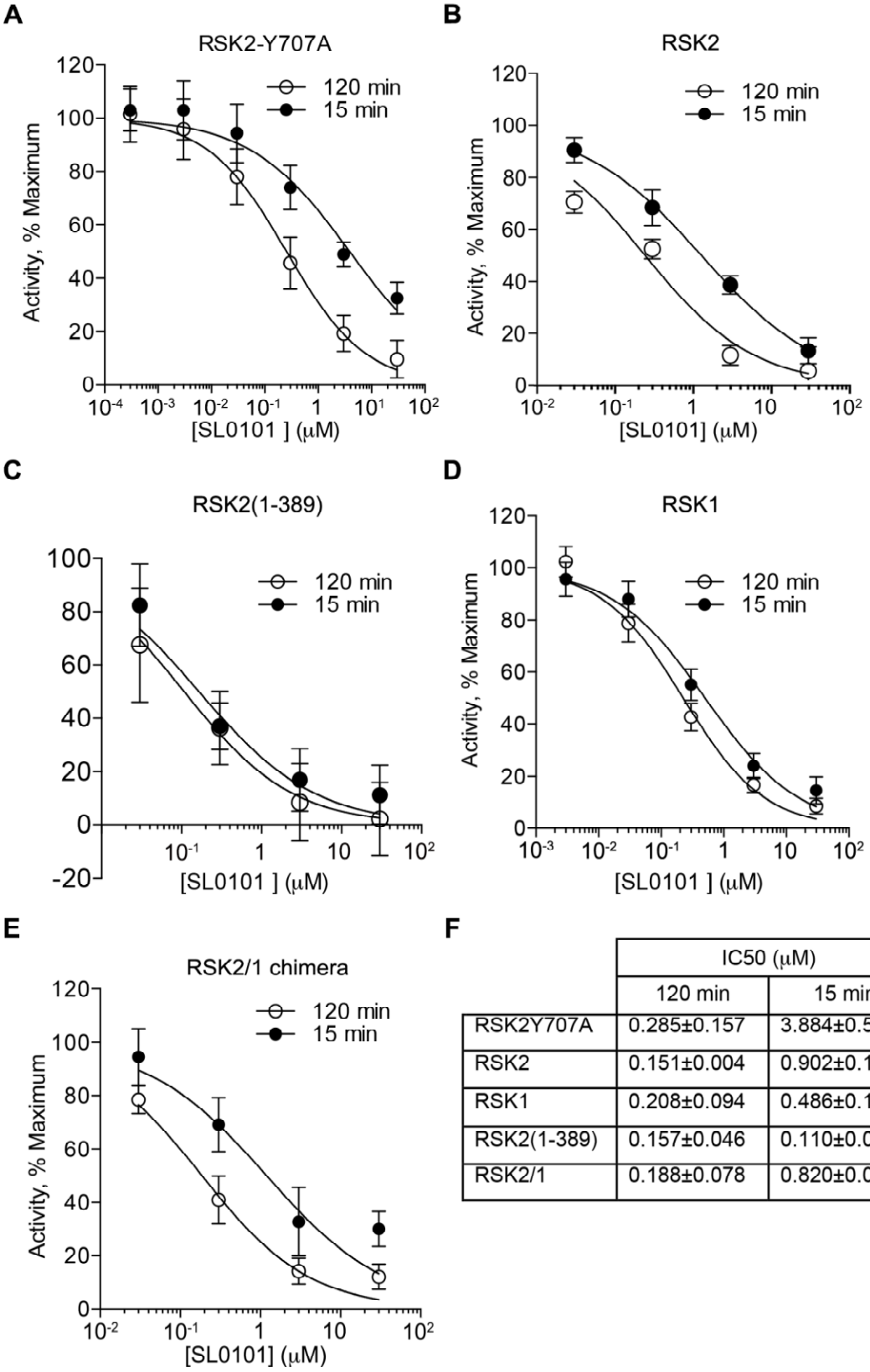

F

	IC50 (μM)		*p* value
	120 min	15 min	
RSK2Y707A	0.285±0.157	3.884±0.5915	<0.001
RSK2	0.151±0.004	0.902±0.134	<0.001
RSK1	0.208±0.094	0.486±0.125	0.001
RSK2(1-389)	0.157±0.046	0.110±0.011	>0.01
RSK2/1	0.188±0.078	0.820±0.087	<0.001

Figure 9. Conformation of RSK2 incubated with SL0101 changes between 120 min and 15 min incubation with the inhibitor.

A) SL0101 binds to free RSK2 protein at 120 min with an inhibition constant of K_i of 7.81±3.22 μM. Representative Dixon plot of one experiment done in quadruplicate, mean ±SD, N=4.

B) SL0101 does not bind to free RSK2 protein at 15 min. Representative Dixon plot of one experiment done in quadruplicate, mean ±SD, N=3.

C) SL0101 binds to RSK-ATP complex at 120 min with an inhibition constant K_i' of 11.5 ±6.69 μM. Representative Cornish-Bowden plot of one experiment done in quadruplicate, mean ±SD, N=4.

D) SL0101 binds to RSK-ATP complex at 15 min with an inhibition constant K_i' of 12.52 ±4.77 μM. Representative Cornish-Bowden plot of one experiment done in quadruplicate, mean ±SD, N=3.

E) SL0101 is a non-competitive inhibitor of RSK2 when incubated for 120 min, while at 15 min pre-incubation it acts as an uncompetitive inhibitor. The abscissa of the intersection point of all lines in Dixon and Cornish-Bowden plots was calculated for each experiment separately, K_i and K_i' values represent mean ±SD of ≥3 experiments in quadruplicate.

Figure 9

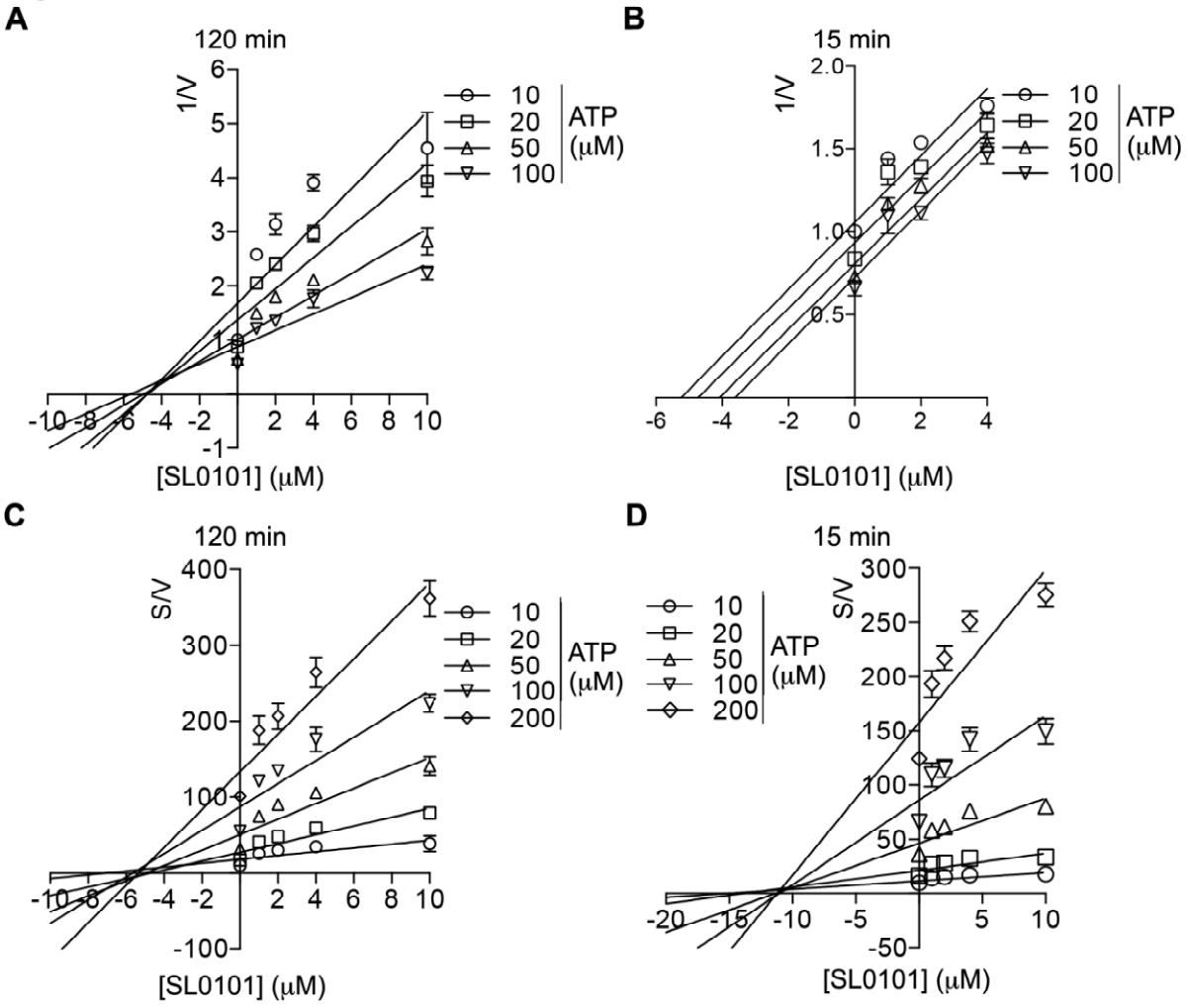

E

	120 min	15 min
K_i	7.81±3.22	---
K_i'	11.57±6.69	12.52±4.77

Figure 10. SL0101 analogs display the same ability to induce conformational change of RSK2 as the parent compound.

A) Compound 216, the C6''-n-propyl cyclitol analog of SL0101, is a more potent inhibitor of RSK2Y707A *in vitro* when allowed to bind to the kinase for 120 min. The schematic represents the chemical structure of this SL0101 analog. Combined normalized activity of N=2 in quadruplicate, mean ±SD. Data was fit using the non-linear regression analysis.

B) Compound 249, the C6''-n-propyl- 3,4''-bicarbamate cyclitol analog of SL0101, is a more potent inhibitor of RSK2Y707A *in vitro* when allowed to bind to the kinase for 120 min. The schematic represents the chemical structure of this SL0101 analog. Combined normalized activity of N=2 in quadruplicate, mean ±SD. Data was fit using the non-linear regression analysis.

Figure 10

A

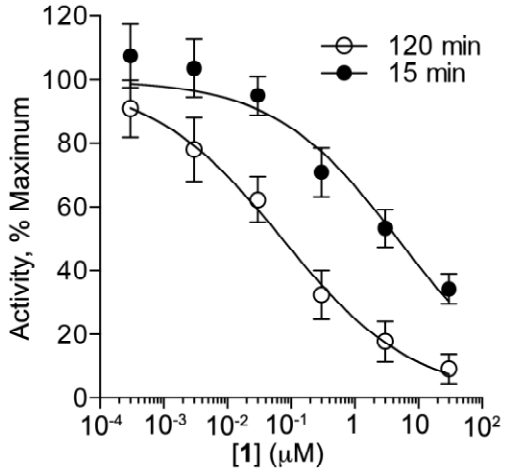
120 min
15 min
Activity, % Maximum
[1] (μM)

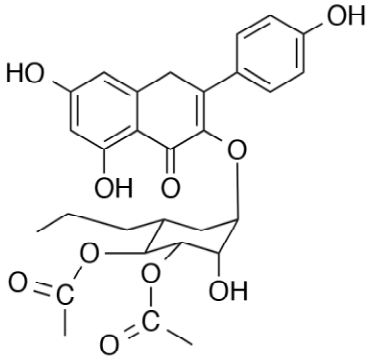
HO
OH
OH
O
O
O
O
O
OH
O

B

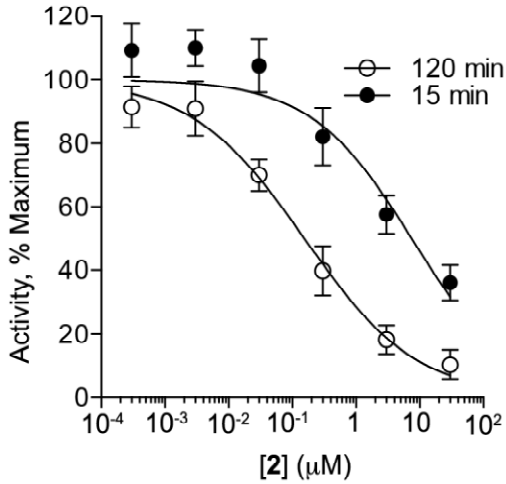
120 min
15 min
Activity, % Maximum
[2] (μM)

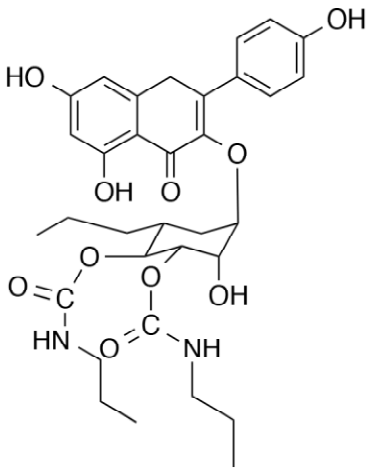
HO
OH
OH
O
O
O
O
O
OH
HN
NH
O

In addition to binding to the free enzyme, an inhibitor can act through binding to the enzyme-substrate complex. The inhibition constant of the enzyme-substrate complex is designated as K_i' (Schlamowitz et al., 1969). K_i' can be calculated by plotting the product of substrate concentration and the reciprocal of the reaction rate (S/V) against inhibitor concentration (Cornish-Bowden, 1974). The abscissa of the intersecting point of the lines representing different ATP concentration defines the $-K_i$' value. We measured the ability of SL0101 to bind to the enzyme-substrate complex using this method at 15 min vs. 120 min pre-incubation. Interestingly, in both pre-incubation conditions the lines intersected at a point with a similar X values suggesting a similar affinity of SL0101 for the enzyme-substrate complex in both conditions (fig. 9C-E). Taken together, the values of K_i and K_i' indicate that SL0101 displays different modes of inhibition between 15 min and 120 min pre-incubation times. At 15 min, SL0101 is unable to bind to the free enzyme and only binds to enzyme-substrate complex, therefore it acts as an uncompetitive inhibitor (Cornish-Bowden, 1974). At 120 min, however, SL0101 binds to both free enzyme and the enzyme substrate complex, therefore it acts as a mixed inhibitor.

A special case of a mixed inhibitor is a compound that has equal affinities for the free enzyme and the enzyme-substrate complex. In such case the values of K_i and K_i' for the inhibitor are equal (Cornish-Bowden, 1974). Another indication of a non-competitive inhibitor is the intersection point of the both reciprocal plots lying on the Y axis of each plot (Cornish-Bowden, 1974). Interestingly, the values of K_i and K_i' for SL0101 at 120 min pre-incubation were not significantly different (7.81 ± 3.22 and 11.57 ± 6.69, respectively), suggesting that SL0101 is in fact a non-competitive inhibitor.

The lines intersected very close to the X-axis, further suggesting that SL0101 is a non-competitive inhibitor in these conditions.

We have described several families of analogs of SL0101 (chapters 3-6). We sought to determine whether the conformational change induced by SL0101 was unique to this molecule, or whether it was preserved among diverse analogs. To address this hypothesis we tested two SL0101 analogs (fig. 10A-B). Interestingly, both analogs retained the ability to differentially inhibit RSK2Y707A *in vitro*. Therefore, the allosteric regulation of RSK2 kinase activity appears to be a common feature of diverse SL0101 analogs. These results support the notion that SL0101 offers an attractive platform for the synthesis of novel analogs with improved biological properties.

2.4. Discussion

Several selective RSK inhibitors have been described to date, and of those SL0101 remains to be exceptionally specific (Bain et al., 2007, Nguyen, 2008). However, all known inhibitors of the NTKD of RSK are equally potent against all 4 isoforms of RSK. Here, we show for the first time that SL0101 is an isoform-selective inhibitor of RSK1/2 and not RSK3/4. Therefore, SL0101 is the only known isoform-selective inhibitor of the NTKD of RSK. The structural basis for the selectivity of SL0101 against RSK isoforms remains unknown. These results have major implications for the use of SL0101 as a tool compound in studying the functions of RSK. In addition to not inhibiting RSK3 and RSK4, SL0101 has very few off-target kinases, suggesting that the use of this inhibitor in cell-based studies should allow investigating the biological functions of RSK1 and RSK2 with little interference from the other kinases. Therefore,

the effects induced by SL0101 treatment in cells are most likely to be associated with the loss of RSK1 and RSK2 function. At the same time, BI-D1870 is equally potent against all RSK isoforms. As a result, it may elicit different responses in cells than SL0101.

The crystal structure of SL0101 bound to RSK2 NTKD has suggested a very unusual mode of inhibition of the kinase by this molecule. By analyzing the relative positions of catalytic and regulatory residues in the ATP-binding pocket it was suggested that SL0101 was binding to the conformation resembling the autoinhibited "DFG-out" fold of the kinase (Utepbergenov et al., 2012, Taylor and Kornev, 2011). However, it was not a classical autoinhibited form of the kinase, as the inhibitor binding was associated with massive rearrangement of the parts of the kinase that do not undergo the conformational changes between the classical "on" and "off" states (Taylor and Kornev, 2011). Therefore, SL0101 is not likely to be a classical type 2 inhibitor, i.e. an inhibitor that binds to the inactive DFG-out conformation (Zhang et al., 2009). Instead, the conformational change would suggest that SL0101 is an allosteric inhibitor of RSK1/2 NTKD, as defined by its ability to bind to a site different than the typical ATP-binding site.

The measurement of inhibition constants of the free enzyme and enzyme-substrate complex revealed that initially SL0101 is not able to bind to RSK2 NTKD by itself, therefore at 15 min it acts as an uncompetitive inhibitor. When incubated for prolonged time, however, it gains the ability to bind to free enzyme, but without a loss of ability to bind to the enzyme-substrate complex. Therefore, it becomes a non-competitive inhibitor. The crystal structure of RSK2 NTKD with SL0101 does not offer

the explanation to such mechanism. In the classical “DFG-out” conformation the Phe ring is occluding the adenine-binding site in the groove, preventing the binding of ATP (Zhang et al., 2009). Therefore, if SL0101 was a type 2 inhibitor, it would not be able to bind to RSK2-ATP complex. This observation raises the possibility that the crystal structure does not fully recapitulate the binding of SL0101 to RSK2 in solution. It has been noted that the difference in the folds of RSK2 bound to AMP-PNP and SL0101 must most likely involve partial un-folding and re-folding of the kinase (Utepbergenov et al., 2012). Therefore, it is possible that SL0101 in solution binds to one of the transitional states that allow for accommodation of both SL0101 and ATP within the kinase fold.

The crystal structure of the active form of RSK2 NTKD with AMP-PNP showed a unique arrangement of residues involved in ATP binding (Malakhova et al., 2009). The typical αC-helix was replaced in the structure by a novel βB-sheet. This difference changed the pattern of bonds formed between the ATP molecule and amino acid side chains of the groove. In addition, the ATP-binding cleft appeared to have a larger volume, compared to a typical AGC kinase family member. SL0101 bound to RSK2 deep inside the pocket, lodged between the β-strands of the N-lobe (Utepbergenov et al., 2012). Therefore, it is possible that the plasticity of the NTKD of RSK would allow binding of both ATP and SL0101 at the same time. In a basal state RSK NTKD could potentially display relatively disordered, or flexible conformation, with only a small fraction of molecules in a fold that can bind SL0101. ATP binding could stabilize some discrete structure, allowing for simultaneous binding of SL0101. When pre-incubated for an extended period of time with the kinase, SL0101 could slowly bind to and stabilize

this infrequent conformation gradually increasing its population. As a result, in the short pre-incubation only the un-competitive mode of inhibition is present, whereas at longer timepoints the contribution of SL0101 binding to the kinase alone to the overall inhibitory effect would increase. The hypothesis that SL0101 could assist in stabilizing RSK NTKD conformation is supported by the fact that, despite no evidence in the crystal structure of phosphorylation of the conserved Ser227 residue in the activation loop, a large segment of this loop has a very well defined the crystal structure. In contrast, the activation loop of PKA in the absence of this phosphorylation has recently been described to be disordered (Steichen et al., 2012). Therefore, it appears that SL0101 can stabilize the section of the kinase that should normally be disorganized (Utepbergenov et al., 2012).

The results of the kinase activity assays of different RSK2 variants have suggested that the C-terminal portion of the kinase interacts with the NTKD and affects its ability to bind to SL0101. In the absence of the entire C-terminal portion of RSK2, the efficacy of SL0101 against RSK2 is equal at short and long pre-incubation, suggesting equal ability of the inhibitor to bind to the kinase. In the context of a proposed model, the CTKD would therefore enforce the lower frequency of the fold of the NTKD that SL0101 can bind to on its own. As a result, when that inhibition by CTKD is removed, SL0101 can more easily bind to and stabilize the preferred conformation. This interaction of CTKD and NTKD might depend on the active conformation of the CTKD itself, as the activating mutation in the C-terminus causes a decrease in the ability of SL0101 to inhibit the NTKD, compared to the wild-type kinase. The possibility of the two parts of the kinase interacting is supported by two observations. First, the two acetate residues within the sugar moiety of SL0101 are solvent-exposed in the crystal structure of RSK2-

NTKD with SL0101 and do not participate in binding between the two entities (Utepbergenov et al., 2012). The structure of de-acetylated SL0101 bound to RSK2-NTKD is identical to that of SL0101 (Utepbergenov et al., 2012). However, our previous studies have indicated that these two acetates are essential for the ability of SL0101 to bind to RSK, as their loss dramatically increases the IC50 of the inhibitor (Smith et al., 2005; chapter 3). Therefore, additional parts of the kinase not included in the crystal structure have to participate in SL0101 binding to RSK2. The second observation suggesting that the interactions of the CTKD and the NTKD are possible comes from the fact that phosphorylation of Ser227 in the activation loop of the NTKD by itself can only increase the phosphotransfer ability of the kinase to 10% of its maximum. The remaining 90% of the maximum activity is obtained due to the interactions of the phosphorylated hydrophobic motif in the linker region of the kinase with the core of the NTKD (Frodin et al., 2002).

The complex and unusual mode of inhibition of RSK1/2 by SL0101 could explain its remarkable selectivity for other kinases. The active folds of kinases are very highly conserved, therefore inhibitors binding to an active conformation of one kinase are likely to also bind to other kinases (Knight and Shokat, 2005). In contrast, the inactive conformations of kinases display a remarkable diversity of structures (Taylor and Kornev, 2011, Huse and Kuriyan, 2002). As a consequence, the compounds that bind to the conformations other than the classical active fold of the kinase tend to be more selective for their targets and display far less off-target effects (Knight and Shokat, 2005).

Chapter 3

Improving the affinity of SL0101 for RSK using structure-based design

Adapted from:

Mrozowski, R.M., Vemula, R., Wu, V., Zhang, Q., Schroeder, B.R., Hilinski, M.K., Clark, D.E., Hecht S.M., O'Doherty, G.A., Lannigan, D.A. (2013) Improving the affinity of SL0101 for RSK using structure-based design. *ACS Med Chem Lett*, 4: 175-179

Summary

Enhanced activity of the Ser/Thr protein kinase, RSK, is associated with transformation and metastasis, which suggests that RSK is an attractive drug target. The natural product, SL0101 (kaempferol 3-O-(3",4"-di-O-acetyl-α-L-rhamnopyranoside), has been shown to be a specific inhibitor of RSK. However, the K_i for SL0101 is 1 μM with a half-life of less than 30 min *in vivo*. To identify analogues with improved efficacy we designed a set of analogues based on the crystallographic model of SL0101 in complex with the RSK2 N-terminal kinase domain. We identified an analogue with a 5" *n*-propyl group on the rhamnose that has > 40-fold improved affinity for RSK than SL0101 in an *in vitro* kinase assay. This analogue preferentially inhibited the proliferation of the human breast cancer line, MCF-7, versus the normal untransformed breast line, MCF-10A, which is consistent with the results using SL0101. However, the efficacy of the 5" *n*-propyl analogue to inhibit MCF-7 proliferation was only two-fold better than for SL0101, which we hypothesize is due to limited membrane permeability. The improved affinity of the 5" *n*-propyl analogue for RSK will aid in the design of future compounds for *in vivo* use.

3.1. Methods

In vivo studies

Absorption Systems LP (Exton, PA) performed the pharmacokinetic evaluation of SL0101 in male CD-1 mice according to their established protocol.

Purified Recombinant RSK2

Baculovirus containing RSK2 cDNA was prepared using the Bac-to-Bac baculovirus expression system (Invitrogen, Carlsbad, California). His-tagged active RSK2 was expressed in Sf9 cells and purified using NiNTA resin (Qiagen, Valencia, California).

In Vitro Kinase Assay

The assays were performed as previously described (Smith et al., 2005). Briefly, Glutathione-S-transferase (GST)-fusion protein (1 μg) containing the ERα-Ser167 sequence- RLASTND was adsorbed in the wells of LumiNunc 96-well polystyrene plates (MaxiSorp surface treatment). The wells were blocked with 3% tryptone in phosphate-buffered saline. Kinase (5 nM) in 50 μL of kinase buffer (5 mM β-glycerophosphate, pH 7.4, 25 mM HEPES, pH 7.4, 1.5 mM DTT, 30 mM $MgCl_2$, 0.15 M NaCl) and 25 μL of the compound at the indicated concentrations or vehicle was added to each well. Reactions were initiated by ATP (10 μM) and were terminated after 120 min by 500 mM EDTA, pH 7.5. All assays measured the initial velocity of reaction. After extensive washing of wells, a polyclonal anti-ERα-pSer167 antibody (Smith et al., 2005) and HRP-conjugated anti-rabbit antibody (211-035-109, Jackson ImmunoResearch

Laboratories, West Grove, Pennsylvania) were used to detect serine phosphorylation of the substrate. HRP activity was measured using Western Lightning Chemiluminescence Reagent (NEL102, Perkin Elmer Life Sciences) according to the manufacturer's protocol. Maximum responses and the concentrations at half the inhibitory response (IC_{50}) were determined by performing a best-fit analysis of the data (GraphPad Prism).

Proliferation Assays

The assays were performed as previously described (Smith et al., 2005). Briefly, cells were seeded at 2000 cells per well in 96-well tissue culture plates in the appropriate medium as described by American Type Culture Collection. After 24 h, compound or vehicle was added. Cell number was measured 48 h later using CellTiter-Glo™ assay reagent (Promega, Madison, Wisconsin) according to the manufacturer's protocol. Maximum responses and the concentrations of half the effective response (EC_{50}) were determined by performing a best-fit analysis of the data (GraphPad Prism).

Cell-based inhibition assays

The assays were performed as described previously (Smith et al., 2005). Briefly, 250,000 cells were seeded onto 60 mm dishes and after 24 hours the inhibitor treatments were commenced. Compound **7** was used at 25 μM for 24 h, and SL0101 (**1**) was used at 100 μM for 2 hours. 20 minutes before lysing the cells phorbol myristate acetate (PMA) at 500 nM was added to the media. Lysis was performed as described previously (Joel et al., 1998). The lysates were normalized to total protein, electrophoresed and immunoblotted. Antibodies used on cell lysates include anti-(Lys/Arg)X(Lys/Arg)XX(pSer/pThr) motif (9611), anti-eEF2 (2332), anti-peEF2 (2331),

monoclonal anti-cyclin D1 (2926) from Cell Signaling Technology (Danvers, MA), and monoclonal anti-Ran (610341) from BD Tranduction Laboratories (Franklin Lakes, NJ). Secondary antibodies used were donkey anti-rabbit and goat anti-mouse conjugated with horseradish peroxidase (HRP) from Jackson ImmunoResearch Laboratories (West Grove, PA).

General chemistry methods and materials

^{1}H and ^{13}C spectra were recorded on 270 MHz, 400 MHz and 600 MHz spectrometers. Chemical shifts were reported relative to benzene-d_6 (δ 7.16 ppm), $CDCl_3$ (δ 7.26 ppm), CD_3OD (δ 3.31 ppm), acetone-d_6 (δ 2.05 ppm), D_2O (δ 4.80 ppm) for ^{1}H, and benzene-d_6 (δ 127.68 ppm), $CDCl_3$ (δ 77.0 ppm), CD_3OD (δ 49.15 ppm), acetone-d_6 (δ 29.92 ppm) for ^{13}C. Optical rotations were measured with a digital polarimeter at sodium D line (589 nm) and were reported in concentration of g / 100 mL at 25 °C in the solvent specified. Infrared (IR) spectra were obtained on a FT-IR spectrometer. Flash chromatography was performed using the indicated solvent system on silica gel standard grade 60 (230-400 mesh). R_f values are reported for analytical TLC using the specified solvents and 0.25 mm silica gel 60 F254 plates that were visualized by UV irradiation (254 nm) or by staining with KMnO4 stain or *p*-anisaldehyde stain. Ether, tetrahydrofuran, methylene chloride, toluene, and triethylamine were dried by passing through activated alumina (8 x 14 mesh) column with argon gas pressure. Commercial reagents were used without purification unless otherwise noted. Air and/or moisture-sensitive reactions were carried out under an atmosphere of argon/nitrogen using oven/flamed-dried glassware and standard syringe/septum techniques.

General Synthetic Procedures

To a solution of tri-benzyl protected compounds (0.08 mmol) in 2 mL THF-EtOH (1:1) was added 20 mg Pearlman's catalyst (Pd-C, 10%). The reaction mixture was degassed using vacuum at −90 °C and refilling with H_2. This procedure was repeated three times, then the bath was removed and the reaction was warmed up to room temperature. The reaction mixture was stirred under a H_2 atmosphere for 3-4 hours. The reaction mixture was loaded onto silica gel and elution with hexane-EtOAc (7:3 to 1:3) to give deprotected products **1-8** (54 to 91 % yield).

3.2. Results

The family of Ser/Thr protein kinases, RSK, has been implicated in numerous different cancers including breast, lung and prostate cancer (Eisinger-Mathason et al., 2010, Clark et al., 2005, Lara et al., 2011). There are four RSK family members and of these RSK1 and RSK2 promote metastasis. RSK is an unusual kinase in that it contains two non-identical functional kinase domains, an N-terminal (NTKD) and a C-terminal (CTKD) kinase domain (Anjum and Blenis, 2008). The NTKD, which has a high sequence homology between family members, belongs to the AGC kinase family and is responsible for phosphorylation of target substrates. We previously identified that SL0101 (**1**) (Fig. 11A), a kaempferol-α-L-(3",4")-diacylrhamnoside, was a specific inhibitor of the NTKD of RSK, and did not inhibit the two most closely related kinases, p70 S6-inase and mitogen- and stress-activated kinase (Smith et al., 2005). In *in vitro* kinase assays with ~70 kinases, SL0101 (**1**) was found to partially inhibit Aurora B and PIM3 (Doehn et al., 2009, Bain et al., 2007).

Figure 11*. Structure-based design of novel analogues of SL0101 (1)

A) The RSK inhibitor, SL0101 (1), and analogues examined in this study.

B) Pharmacokinetic analysis of SL0101 (1) in male CD-1 mice. AUC/D: area under the curve, extrapolated to infinity and normalized to the dose in mg/kg. C_0 (ng/mL): maximum plasma concentration extrapolated to t=0. C_{max} (ng/mL): maximum plasma concentration. $t_{1/2}$ (h): half-life

C) A hydrophobic pocket within the RSK2 NTKD allows for an extended 5" aliphatic chain on the rhamnose. Molecular docking of analogues 3", 4" di-acetyl versions of 3 and 4 (inset) were performed using the X-ray crystallographic structure of SL0101 in complex with RSK2 NTKD.

* B) performed at Absorption Biosystems

* C) contributed by Michael K. Hilinski

Figure 11

A

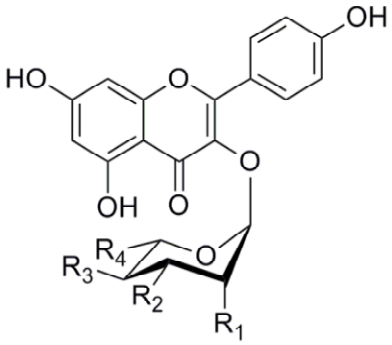

	R_1	R_2	R_3	R_4
1	- OH	- OAc	- OAc	- CH_3
2	- OH	- OH	- OH	- CH_2CH_3
3	- OH	- OH	- OH	- $CH_2CH_2CH_3$
4	- OH	- OH	- OH	- $CH_2CH(CH_3)_2$
5	- OAc	- OH	- OH	- $CH_2CH_2CH_3$
6	- OAc	- OH	- OAc	- $CH_2CH_2CH_3$
7	- OH	- OAc	- OAc	- $CH_2CH_2CH_3$
8	- OAc	- OAc	- OAc	- $CH_2CH_2CH_3$

B

Dose (mg/kg)	AUC/D (ng•h•kg/mL/mg)	C_0 (ng/mL)	C_{max} (ng/mL)	$t_{1/2}$ (h)
1 (iv)	38.7	291		0.15
2.5 (ip)	1023		1851	0.40

C

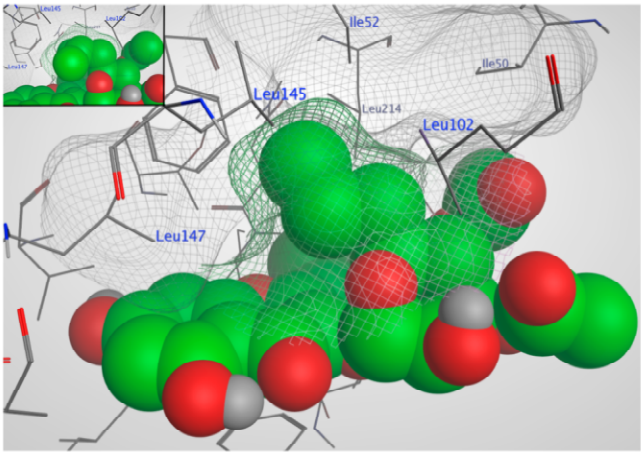

However, these results are not straightforward to interpret because the relative kinase inhibition is dependent on the [ATP] in the assay. In both screens the [ATP] was higher in the RSK kinase assay than in Aurora B and PIM3, which would result in SL0101 (**1**) being less effective against RSK than in the assay conditions used for Aurora B and PIM3.

An effective inhibitor of RSK *in vivo* would be invaluable in the study of RSK function in homeostasis and in disease states. To evaluate the suitability of SL0101 (**1**) for *in vivo* use we analyzed its pharmacokinetic behavior by intravenous (i.v.) and intraperitoneal (i.p.) administration of a single dose into male CD-1 mice. Because of the limited solubility of SL0101 (**1**) a carrier of 1:1:15 Cremophor:EtOH:PBS was required. Regardless of the dosing method, the half-life ($t_{1/2}$) of SL0101 (**1**) was < 30 min (fig. 11B). More importantly, the maximum concentration achieved was ~ 10-fold below that required to completely inhibit proliferation of the breast cancer cell line, MCF-7, in culture (Smith et al., 2005). Thus, SL0101 (**1**) is not suitable for *in vivo* testing and a medicinal chemistry effort is required to identify analogues with improved pharmacokinetic properties, as well as potency and stability.

The crystal structure of SL0101 (**1**) in complex with the RSK2 NTKD has been reported (Utepbergenov et al., 2012). The SL0101 (**1**) binding pocket overlaps with the ATP binding site of the NTKD but is distinct from it, as it is formed by a substantial structural rearrangement of the N-lobe of the kinase domain. The interaction of SL0101 (**1**) with RSK is partially stabilized by hydrogen bonds between the protein and phenolic hydroxyls on the kaempferol backbone in which the hydroxyl groups serve as hydrogen bond donors. Previously, we determined that loss of any of these hydroxyl groups

substantially decreased the affinity of RSK for SL0101 (**1**) (Smith et al., 2007). Furthermore, an analogue in which the hydroxyl groups were O-methylated and therefore could not donate hydrogen bonds did not inhibit RSK (Smith et al., 2007). Thus our previous experience with the SAR of SL0101 (**1**) analogues is in good agreement with the crystallographic model, which supports its use in designing future analogues.

The crystallographic model of the RSK2 NTKD in complex with SL0101 (**1**) indicates that the 5" methyl of the rhamnose only partially fills a hydrophobic pocket (Utepbergenov et al., 2012). We modeled a set of analogues bearing longer aliphatic chains at the 5" position using the docking function of the Molecular Operating Environment (MOE) program. The RSK2 NTKD in complex with SL0101 (**1**) was used as a starting point for the calculations. The kinase was processed and the analogues constructed in the binding pocket from the crystallized inhibitor SL0101 (**1**) using the build function. We performed a docking calculation using the "rigid receptor" presets on both SL0101 (**1**) and the analogues, and the highest-scoring binding pose as determined by the calculated binding free energy in each case was consistent with the crystal structure of the complex. The results clearly show that the longer aliphatic chains occupy a hydrophobic area in the binding pocket unoccupied by any fragment of SL0101 (**1**) (Fig. 11C). Thus, we envisioned a series of C-5" substituted analogues of SL0101 (**2**–**4**, Fig. 11A). The acetyl groups on the rhamnose contribute substantially to the IC_{50} for RSK inhibition as deacetylated SL0101 is ~ 10-fold less potent than SL0101 (Smith et al., 2007). Therefore, we also envisioned a series of analogues in which the number and positioning of the acetyl groups were varied in combination with the 5" n-

propyl group. Efficacy of SL0101 analogues in cell-based assays can be limited by their solubility (Hilinski et al., 2012) so we selected the 5” n-propyl analogue (3) as the parent compound based on its lower LogP compared to 4 (fig. 12).

Previously, we reported both a traditional carbohydrate (Maloney and Hecht, 2005) and a *de novo* asymmetric approach (Shan et al., 2010, Borisova et al., 2010, Guo and O'Doherty G, 2005, Baiga et al., 2008) to SL0101 (**1**) (Shan and O'Doherty, 2006) and several carbohydrate analogues (**1,1a**-**d**, fig. 13A) (Shan and O'Doherty, 2010). While the carbohydrate approach has some real advantages in terms of convergency, the *de novo* approach has the advantage of being amenable to the divergent late stage substitution of the pyranone ring (Elbaz et al., Wang et al., 2011a, Wang et al., 2011b, Wang et al., 2011c, Iyer et al., 2010, Zhou and O'Doherty, 2006, Zhou and O'Doherty, 2007, Zhou and O'Doherty, 2008a). Because of its inherent ability to incorporate C-5” substitution, we decided to further develop the de novo approach to pursue the synthesis and evaluation of the rhamno-sugar of SL0101 analogues **2** - **8**.

Based on or previous experience with SL0101 (**1**), we envisioned the desired target molecules **2**-**8** as being derived from the appropriately substituted pyranones **12a-d** (fig. 13B). Key to the overall efficiency of this approach is that the enone served as precursor for the installation of the desired triol functionality in **2-8** for further acylation.

Figure 12. *In vitro* potency of SL0101 (1) and analogues

IC50: Concentration needed for 50% inhibition of RSK2; the 95% CI is shown in parentheses; n>2 in quadruplicate; p(1): student's t-test compared to SL0101 (1); p(3): student's t-test compared to analogue 3.

Figure 12

compound name	RSK2 IC_{50} [μM]	LogP	*p*(**1**)	*p*(**3**)
SL0101 (**1**)	0.99 (0.74-1.32)	2.11		
2	1.51 (0.45-5.09)	1.64	0.917	
3	0.71 (0.47-1.33)	2.20	0.211	
4	0.48 (0.17-1.33)	2.41	0.073	
5	1.50 (0.90-2.48)	2.90	0.753	0.183
6	0.62 (0.18-2.15)	3.39	0.232	0.804
7	0.02 (0.01-0.04)	3.17	0.007	0.005
8	1.77 (1.24-2.53)	3.87	0.008	0.008

Figure 13*. Synthesis of SL0101 analogues

A) De novo approach to SL0101 (1)

B) Retrosynthetic analysis of SL0101 (1) analogues

C) Synthesis of SL0101 analogues 2-8

*Figure contributed by George O'Doherty.

Figure 13

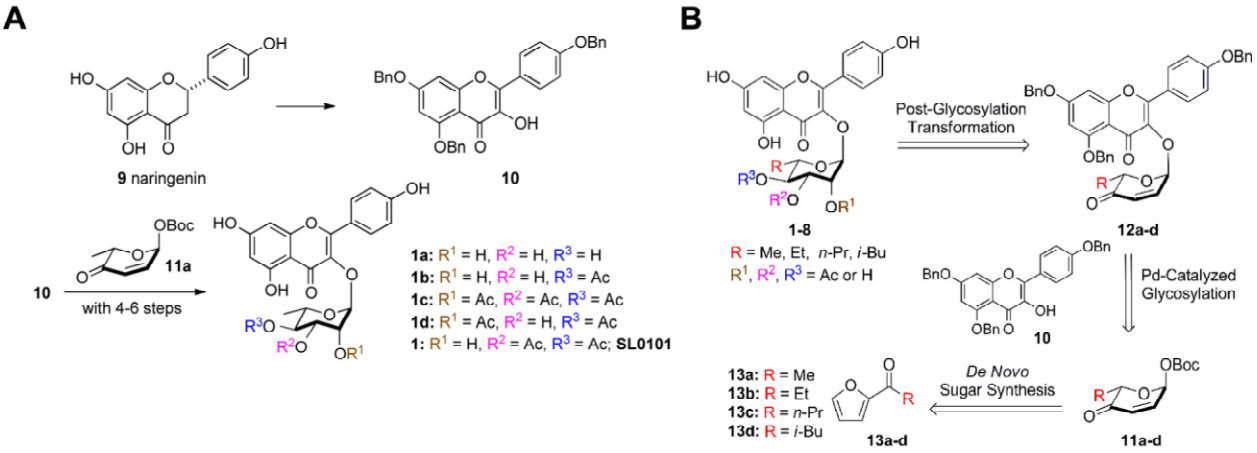

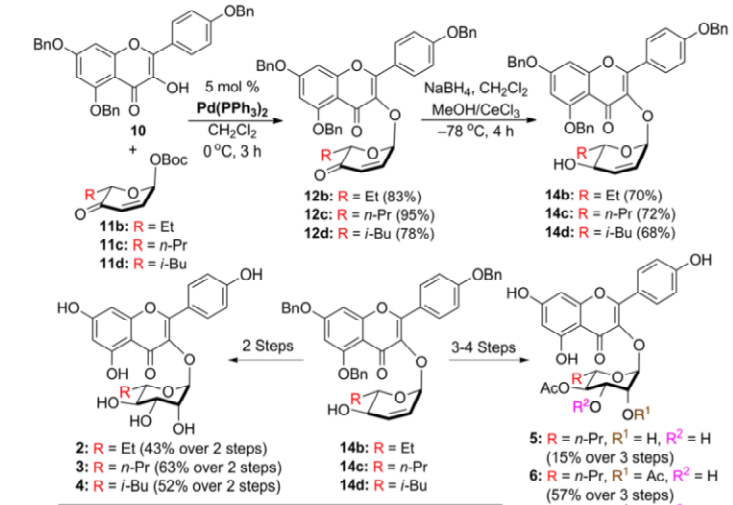

14b to **2**: a, b; **14c** to **3**: a, b; **14d** to **4**: a, b; **14c** to **5**: c, d, b; **14c** to **6**: a, e, b; **14c** to **7**: a, e, f, b; **14c** to **8**: a, g, b.

a) NMO/OsO_4(cat.), *t*-BuOH/Acetone 0 °C, 8 h; b) 10% Pd-C/H_2, THF/EtOH, rt, 3 h; c) Ac_2O/DMAP, Py./CH_2Cl_2, 0 °C, 1 h; d) NMO/OsO_4(cat.), *t*-BuOH/Acetone 0 °C, 24 h; e) *i.* $CH_3C(OMe)_3$, 10% *p*-TsOH in CH_3CN (w/v), 0 °C, 1 h; *ii.* Ac_2O/DMAP, Py./CH_2Cl_2, 0 °C, 1 h; *iii.* 90% HOAc(aq.), 0 °C, 1 h; f) DBU, toluene, 0 °C, 2 h; g) Ac_2O/DMAP, Py./ CH_2Cl_2, 0 °C, 8 h.

$Pd(PPh_3)_2$ = 2.5 mol % $Pd_2(DBA)_3$•$CHCl_3$ and 10 mol% of PPh_3; **DBA** = dibenzylideneacetone; **NMO** = *N*-methylmorpholine-*N*-oxide; **Ac_2O** = acetic anhydride; **DMAP** = 4-dimethylaminopyridine; **Py.** = pyridine; **DBU** = 1,8-diazabicyclo[5.4.0]undec-7-ene.

Similarly, pyranones **12a-d** could be prepared from a palladium-catalyzed glycosylation of aglycon **10** with Boc-pyranones **11a-d** serving as the glycosyl-donor (Babu et al., 2004a, Babu et al., 2006, Babu and O'Doherty G, 2005, Zhou and O'Doherty, 2008b, Guo and O'Doherty, 2008, Yu and O'Doherty, 2008, Wu et al., 2010). Finally, pyranones **11a-d** could be derived from furans **13a-d** (Harris et al., 1999, Harris et al., 2000a, Li et al., 2004, Yu et al., 2011). To accomplish this divergent synthetic effort we planned on preparing all the desired target molecules **2-8** by executing multistep parallel reactions on three key intermediates (**14b-d**).

With the desired coupling partners in hand (**10** and **11b-d**), we first pursued their coupling and diastereoselective transformation into the two divergent points allylic alcohols **14b-d.** Exposure of **11b-d** and **10** to our typical Pd-catalyzed glycosylation procedure (2.5 mol % $Pd_2(DBA)_3$•$CHCl_3$ and 10 mol% of PPh_3) gave the coupling products **12b-d** with complete transfer of anomeric stereochemistry (fig. 13C). A subsequent Luche reduction ($NaBH_4$ at -78 °C) diastereoselectively converted the pyranones **12b-d** into the desired allylic alcohols **14b-d** (dr > 20:1).

We next pursued the direct conversion of allylic alcohols **14b-d** into the desired triols **2-4** with *rhamno*-stereochemistry. This was accomplished in parallel by exposing **14b-d** to typical Upjohn dihydroxylation conditions (NMO/OsO_4 in t-BuOH/acetone). The crude products from the dihydroxylation reactions were filtered through a pad of silica gel (to remove osmium, N-methylmorpholine and its N-oxide (NMO)) and subjected to typical hydrogenolysis conditions (10% Pd/C, 1 atm H_2). To our delight, the three desired SL0101 (**1**) analogues **2-4** could be isolated in pure form after careful silica gel chromatography (43-63% yield).

Buoyed by our success, we next pursued the direct conversion of **14c** into **5-8**, by incorporating selective acylation steps to the previous 2-step sequence. For instance, the allylic alcohol **14c**, with an *n*-Pr-group, was cleanly converted to the C-4 acetylated *rhamno*-diol **5** (i.e. acylation/dihydroxylation/hydrogenolysis) in 15% yield after silica gel chromatography. By simply switching the order of acylation and dihydroxylation, the triacetate **8** was similarly prepared in a 60% overall yield. In contrast, the synthesis of diacetates **6** and **7** required selective diacylation using the orthoester/acylation/hydrolysis/hydrogenolysis protocol to give **6** (57% overall yield). Finally, by incorporating an isomerization step in the sequence (i.e. orthoester/acylation/isomerization/hydrogenolysis) C-3/C-4 diacetate **7** could be prepared in a 25% overall yield.

The affinities of the C5”- substituted analogues for RSK were determined by their ability to inhibit the activity of purified, recombinant RSK2 in an *in vitro* kinase assay (Smith et al., 2005). The data were fit using nonlinear regression analysis. There was a trend toward improving the *in vitro* potency by increasing the chain length, which is consistent with the modeling results indicating that longer chains would be preferred, although the differences did not obtain statistical significance (fig. 12). We have reported a lower IC_{50} for the synthesized SL0101 (**1**) (Smith et al., 2006). However, the IC_{50} is relative and dependent on numerous variables including the batch of purified, recombinant RSK2. Therefore, to accurately evaluate the relative potencies of the various analogues each assay was performed in parallel with SL0101 (**1**).

In the *in vitro* kinase assay, introduction of a single acetyl group as in analogue **5** increased the IC_{50}, but this difference was not statistically significant (fig. 12). Acetyl

groups on the 2”, 3” and 4” position (analogue **8**) doubled the IC_{50} in comparison to the 5” n-propyl (analogue **3**) (fig. 12). Acetyl groups on the 2” and 4” positions (analogue **6**) did not alter the IC_{50}. Surprisingly, analogue **7** with acetyl groups on the 3” and 4” position has an IC_{50} >40-fold lower than SL0101 (**1**) (fig. 12). These results were unexpected because, although previously we had found acetylation to be important, the number or positioning of the acetyl groups was not (Smith et al., 2007). In the crystal structure of SL0101 (**1**) in complex with the RSK2 NTKD the acetyl groups are unresolved (Utepbergenov et al., 2012). However, we speculate that the favorable van der Waals interactions between the 5” *n*-propyl group and hydrophobic residues in the binding pocket restrict the binding orientation of this set of analogues in such a way that only acetyl groups in the 3” and 4” positions can be accommodated without causing unfavorable interactions in the binding pocket.

Analogue **7** was further evaluated for its ability to inhibit the proliferation of the breast cancer cell line, MCF-7, in comparison to SL0101 (**1**). The aqueous solubility of **7** limited the concentrations that could be tested to ≤25 μM. At 25 μM compound **7** was ~50% more potent at inhibiting proliferation than SL0101(**1**)(fig. 14A). To determine whether analogue **7** was specific for RSK we compared the ability of the compound to inhibit proliferation of MCF-7 versus the immortalized, normal breast line, MCF-10A. We have previously found that a preferential ability to inhibit MCF-7 compared to MCF-10A proliferation indicates specific inhibition of RSK (Smith et al., 2005, Smith et al., 2006, Smith et al., 2007, Hilinski et al., 2012). We observed that compound **7** inhibits MCF-7 but not MCF-10A proliferation (Fig. 14B). These results suggest that compound **7** and SL0101 (**1**) have similar specificities.

Figure 14*. Specificity and efficacy of SL0101 (1) and 7 in cell-based assays

A) Efficacy of SL0101 (1) and 7 in MCF-7 cells. Various concentrations of inhibitors were added at time 0 and ATP content was measured after 48 h of treatment. Values are the fold proliferation as a percentage of that obtained with vehicle-treated cells. (n=3 in quadruplicate; bars =SD; * $p<0.05$ in a student's t-test compared to the vehicle. ^ $p<0.05$ in a student's t-test compared to SL0101 (1)).

B) Specificity of analogue 7 for inhibition of RSK activity. Various concentrations of 7 were added to MCF-7 or MCF-10A cells and the assay performed as described in panel A. (n=3 in quadruplicate; bars =SD; * $p<0.05$ in a student's t-test compared to the vehicle).

C) Comparison of compound 7 and SL0101 (1) on altering RSK biomarkers in intact cells. Lysates of MCF-7 cells that were pretreated with inhibitor (SL0101 (100 mM); 7 (25 mM)) and then treated with vehicle (DMSO) or PMA were analyzed by immunoblotting. The arrow indicates a band whose intensity decreases upon treatment of cells with SL0101 (1) and analogue 7.

* Panels A and B contributed by David Clark.

Figure 14

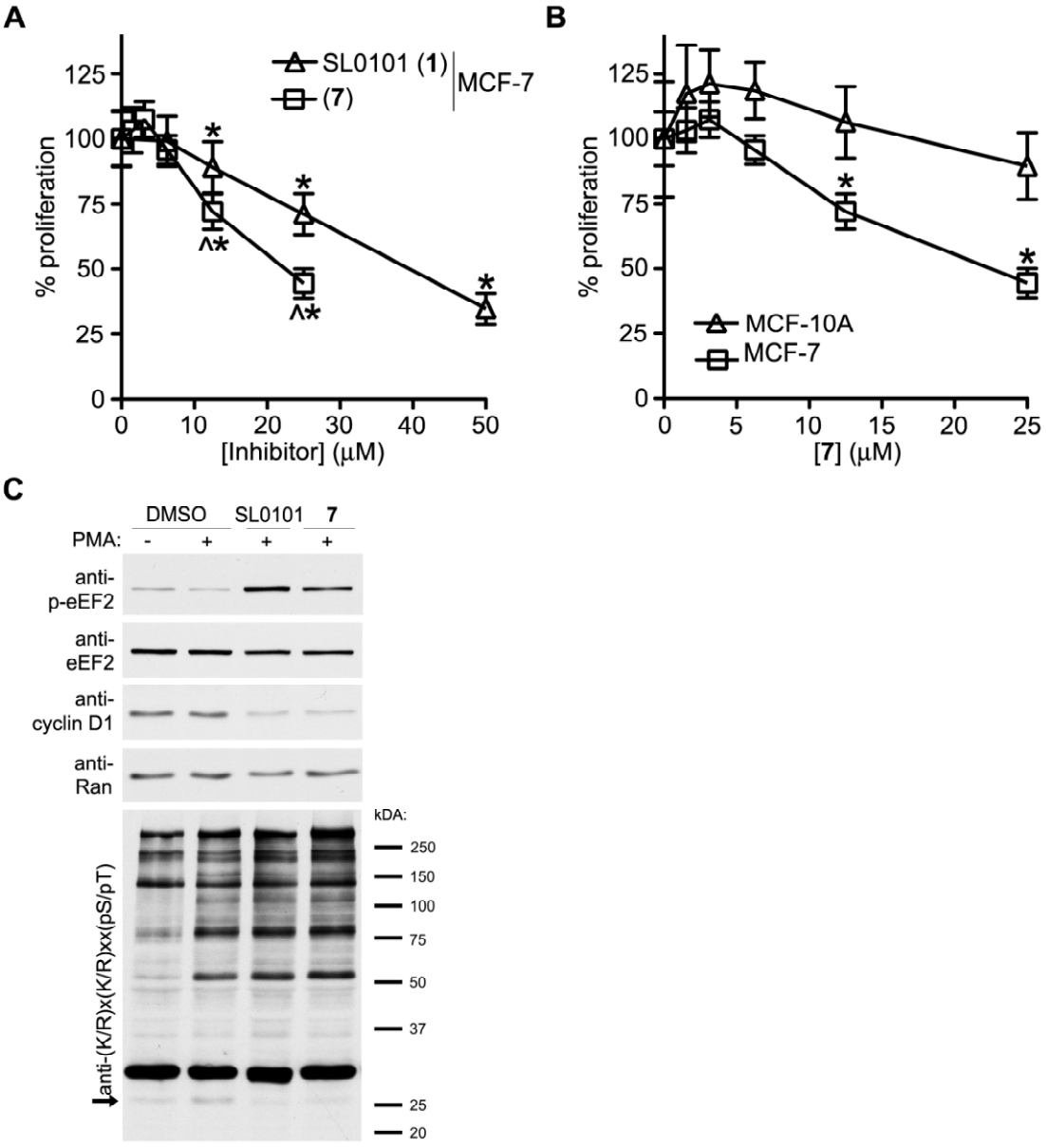
A
SL0101 (1)
(7)
MCF-7
% proliferation
[Inhibitor] (μM)
B
MCF-10A
MCF-7
% proliferation
[7] (μM)
C
DMSO
SL0101
7
PMA:
anti-p-eEF2
anti-eEF2
anti-cyclin D1
anti-Ran
anti-(K/R)x(K/R)xx(pS/pT)
kDA:
250
150
100
75
50
37
25
20

To further examine the specificity of analogue **7** we compared the ability of SL0101 (**1**) and compound **7** to alter the phosphorylation of eukaryotic elongation factor 2 (eEF2). Inhibition of RSK is known to activate EF2 kinase, which phosphorylates eEF2 (Wang et al., 2001a). MCF-7 cells were treated with inhibitor or vehicle and then stimulated with the mitogen, phorbolmyristate acetate (PMA). In the presence of PMA, peEF2 levels decreased as expected as RSK is active and inhibits EF2 kinase. Treatment with SL0101 (**1**) and compound **7** both increased pEF2 levels compared to the PMA control (fig. 14C), which is consistent with inhibition of RSK. We have also found that the levels of the oncogene, cyclin D1, are dependent on RSK activity in MCF-7 cells (Eisinger-Mathason et al., 2008). Consistent with these data SL0101 (**1**) and compound **7** decreased cyclin D1 levels. As a further comparison of the inhibitory profiles of SL0101 (**1**) and analogue **7**, we immunoblotted the lysates with an antibody that recognizes the (Lys/Arg)X(Lys/Arg)XX(pSer/pThr) motif, where X is any amino acid (Anjum and Blenis, 2008). This motif is recognized by a number of kinases including RSK. Treatment with the inhibitors resulted in a decrease in the intensity of a band at ~27 kDa. It is not surprising that we only observed a decrease in a single band as PMA is a potent mitogen that will activate many kinases. The intensities of the bands in the immunoblot were similar between SL0101 (**1**) and analogue **7**. Taken together, these results indicate that SL0101 (**1**) and compound **7** have similar specificities.

In summary, we used structure-based design to identify new SL0101 (**1**) analogues that improve on the *in vitro* potency of SL0101 (**1**). A 5” n-propyl substituent in combination with 3” and 4” acetyl groups (**7**) on the rhamnose improved the *in vitro* affinity for RSK by > 40-fold compared to SL0101 (**1**). Analogue **7** specifically inhibits

RSK but its ability to inhibit the proliferation of the breast cancer cell line, MCF-7, is only 2-fold better compared to SL0101 (**1**), which we hypothesize is due to limited membrane permeability. These studies will provide further guidance in designing a potent SL0101 (**1**) analogue that can be used *in vivo*.

Chapter 4

De novo synthesis and biological evaluation of C6''-substituted C4''-amide analogues of SL0101

Adapted from:

Mrozowski, R.M., Sandusky, Z.M., Vemula, R., Wu, B., Zhang, Q., Lannigan, D.A., O'Doherty, G.A. De novo synthesis and biological evaluation of C6"-substituted C4''-amide analogues of SL0101 (2014) *Org. Lett.*, 16: 5996-5999.

Summary

In an effort to improve upon the *in vivo* half-life of SL0101, C4"-amides/C6"-alkyl substituted analogues of SL0101 were synthesized and evaluated in cell-based assays. The analogues were prepared using a de novo asymmetric synthetic approach, which featured Pd-π-allylic catalyzed glycosylation for the introduction of a C4"-azido group. Surprisingly replacement of the C4"-acetate with a C4"-amide resulted in analogues that were no longer specific for RSK in cell-based assays.

4.1. Methods

Purified recombinant RSK2

Baculovirus expressing RSK2 cDNA was produced using Bac-to-Bac baculovirus expression system (Invitrogen, Carlsbad, CA). His-tagged RSK2 was expressed and activated in Sf9 cells by stimulating with mitogen, phorbol myristate acetate (PMA). Recombinant protein was purified using NiNTA resin (Qiagen, Valencia, CA).

In vitro kinase assays

The assays were performed as previously described (Smith et al., 2005). Briefly, glutathione-S-transferase (GST)- tagged fusion protein (1 μg) containing the ERα-Ser167 sequence RLASTND was adsorbed onto a 96-well MaxiSorp-treated white polystyrene plate (Thermo Scientific Nunc, Roskilde, Denmark). The wells were blocked with 3% tryptone in phosphate-buffered saline. 50 μL of kinase (5 nM) in kinase buffer (25 mM HEPES, 150 mM NaCl, 5 mM β-glycerophosphate, 1.5 mM DTT, 30mM $MgCl_2$, pH 7.4) and 25 μL of the compound at the indicated concentrations were added to each well and incubated for 120 min. The reactions were initiated by adding 25 μL of ATP (final concentration 10 μM) and terminated 20 minutes later by addition of 0.5 M EDTA, pH 8.0. All assays measured initial reaction velocity. The plates were extensively washed and phosphorylation of substrate was detected using rabbit polyclonal anti-ERα-pSer167 antibody (Smith et al., 2005) and horseradish peroxidase (HRP)-conjugated donkey anti-rabbit antibody (Jackson ImmunoResearch Laboratories, West Grove, PA). HRP activity was measured using Western Lightning Plus-ECL

(PerkinElmer Life Sciences, Waltham, MA). Half-inhibitory concentration (IC_{50}) values were calculated using non-linear regression analysis of the data (GraphPad Prism 6).

Proliferation assays

The assays were performed as previously described (Smith et al., 2005). Briefly, MCF-7 cells were seeded at 20,000 cells/well into 24-well tissue culture plates in DMEM low-glucose medium with 5% fetal bovine serum (FBS). Compound or vehicle was added and proliferation was measured 48 hours later using CellTiterGlo assay reagent (Promega, Madison, WI) according to the manufacturer's protocol. Concentration of 50% inhibition in proliferation (IC_{50}) was determined using non-linear regression analysis of the data (GraphPad Prism 6).

Cell-based inhibition assays

The assays were performed as previously described (Smith et al., 2005). Briefly, 200,000 MCF-7 cells were seeded onto a 35 mm dish in DMEM low-glucose medium with 5% FBS. 24 hours later medium was changed for a serum-free medium. 16 hours later vehicle DMSO was added with or without serum, and inhibitors were added in serum-containing medium, for 2 hours. 20 minutes prior to collecting lysates, cells in serum-containing medium were further stimulated with PMA (500 nM). Lysis was performed as described previously (Joel et al., 1998). Equal amounts of total protein were electrophoresed and immunoblotted. Antibodies used for immunoblotting include anti-RxRxx(pS/T) (9611), anti-eEF2 (2332), anti-peEF2 (2331), anti-S6 protein (2217), anti-p-S6 protein (2211) and monoclonal anti-cyclin D1 (2926) from Cell Signaling Technology (Danvers, MA).

General chemistry methods and materials

^{1}H and ^{13}C spectra were recorded on 270 MHz, 400 MHz and 600 MHz spectrometers. Chemical shifts were reported relative to benzene-d_6 (δ 7.16 ppm), $CDCl_3$ (δ 7.26 ppm), CD_3OD (δ 3.31 ppm), acetone-d_6 (δ 2.05 ppm) for ^{1}H, and benzene-d_6 (δ 127.68 ppm), $CDCl_3$ (δ 77.0 ppm), CD_3OD (δ 49.15 ppm), acetone-d_6 (δ 29.92 ppm) for ^{13}C. Optical rotations were measured with a digital polarimeter at sodium D line (589 nm) and were reported in concentration of g/100 mL at 25 ºC in the solvent specified. Infrared (IR) spectra were obtained on a FT-IR spectrometer. Flash chromatography was performed using the indicated solvent system on silica gel standard grade 60 (230-400 mesh). R_f values are reported for analytical TLC using the specified solvents and 0.25 mm silica gel 60 F254 plates that were visualized by UV irradiation (254 nm) or by staining with $KMnO_4$ stain or *p*-anisaldehyde stain. Ethyl ether, tetrahydrofuran, methylene chloride, toluene, and triethylamine were dried by passing through activated alumina (8 x 14 mesh) column with argon gas pressure. Commercial reagents were used without purification unless otherwise noted. Air and/or moisture-sensitive reactions were carried out under an atmosphere of argon/nitrogen using oven/flamed-dried glassware and standard syringe/septum techniques.

4.2. Results

RSK is a family of Ser/Thr kinases, which are downstream effectors of the extracellular signal-regulated kinase 1/2 pathways (Eisinger-Mathason et al., 2010). RSK appears to be involved in the etiology of a number of different cancers and importantly, regulates a motility/invasive gene program (Lara et al., 2011, Doehn et al., 2009).

RSK is a dual kinase domain protein with the N-terminal kinase domain (NTKD) responsible for phosphorylation of target substrates (Anjum and Blenis, 2008). In a screen of botanical extracts SL0101 (**1**), a flavonoid glycoside, was identified as an inhibitor of the NTKD of RSK (Smith et al., 2005). SL0101 (**1**) is a relatively selective inhibitor for RSK with a K_i of ~ 1 μM. From the crystal structure of SL0101 (**1**) complexed with the NTKD isoform of RSK2 (Utepbergenov et al., 2012) and *de novo* synthetic studies (Maloney and Hecht, 2005, Shan and O'Doherty, 2010, Shan and O'Doherty, 2006, Aljahdali et al., 2013, Bajaj et al., 2014) we identified analogues (2 and 3) with C6”-substitutions of the rhamnose that showed improved efficacy in the *in vitro* kinase assays (chapter 3).

SL0101 (**1**) has a short biological half-life *in vivo* (chapter 3), which is presumably due to hydrolysis of the C3”/C4”-acetates which are necessary for high affinity interaction with RSK (Smith et al., 2005). To identify less labile groups that could replace the ester without loss of affinity, we investigated replacing the C4”-acetate with a C4”-acetamide in combination with the C6” substitution that we previously identified (chapter 3). Specifically, we targeted six C4”-acetamide analogues **4a-d** and **5a-b** (fig. 15).

Retrosynthetically, we envisioned that C4”-acetamide substituted analogues **6** could arise from C4”-azido sugar **7a**, which could be prepared from enone sugar **7c** via allylic carbonate **7b** (fig. 16A). Previously we have shown that C4 allylic azides like **7a** could be prepared from C4 allylic carbamates like **7b** via Pd-catalyzed allylic alkylation (Guo and O'Doherty, 2006, Abrams et al., 2008, Borisova et al., 2010). However, this approach was not compatible for pyran rings with a C1 kaempferol group.

Figure 15. C4”-amide analogues of SL0101.

Figure 15

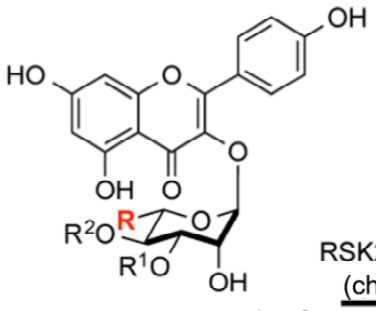

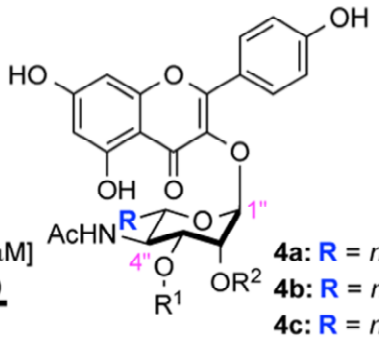

RSK2 IC_{50} [μM] (chapter 3)

1: **R** = Me; **SL0101**, R^1, R^2 = Ac; 0.99
2a: **R** = *n*-Pr, R^1, R^2 = Ac; 0.02
2b: **R** = *n*-Pr, R^1, R^2 = H; 0.71
3a: **R** = *i*-Bu, R^1, R^2 = H; 0.48

4a: **R** = *n*-Pr, R^1 = H, R^2 = H
4b: **R** = *n*-Pr, R^1 = Ac, R^2 = H
4c: **R** = *n*-Pr, R^1 = H, R^2 = Ac
4d: **R** = *n*-Pr, R^1 = Ac, R^2 = Ac
5a: **R** = *i*-Bu, R^1 = H, R^2 = H
5b: **R** = *i*-Bu, R^1 = Ac, R^2 = H

To address this issue, a Pd-glycosylation method was developed for the direct incorporation of a C4 azido sugar.

Our synthesis started with exposure of flavonol **9** and Boc-pyranone **13** to our typical glycosylation conditions (2.5 mol % $Pd_2(DBA)_3$•$CHCl_3$ and 10 mol % of PPh_3 in CH_2Cl_2 at 0 ºC; 95%), which produced glycosylated pyranone **14** with complete a-selectivity (fig. 16B). Reduction of the enone **14** ($NaBH_4$, -78 ºC in CH_2Cl_2/MeOH; 72%) resulted stereoselectively in allylic alcohol **15** (Maloney and Hecht, 2005, Shan and O'Doherty, 2010, Shan and O'Doherty, 2006, Aljahdali et al., 2013, Bajaj et al., 2014). A methyl carbonate leaving group was installed on the allylic alcohol by reaction of **15** with methyl chloroformate to form the C4”-carbonate **16** in 75% yield. Unfortunately, exposure of carbonate **16** to the Sinou conditions ($TMSN_3$, $(Pd(allyl)Cl)_2$/1,4-bis(diphenylphosphino)-butane) failed to afford the desired regio- and stereoisomeric allylic azide **17**. The C-1 kaempferol proved to be the better leaving group, as only products consistent with the hydrolysis at the anomeric position were observed.(Babu et al., 2006, Guppi and O'Doherty, 2007).

To solve this problem, we decided to try reversing the sequence of the two Pd-π-allyl substitution reactions, which required the synthesis of allylic azides **29** and **30** (fig. 16C). This began with a palladium-catalyzed glycosylation (Pd(0)/PPh_3, 1:2) of *p*-methoxybenzyl alcohol with Boc-pyranones **13** and **18** which stereoselectively afforded PMB-pyranones **19** and **20** (95% and 92% respectively). Diastereoselective reduction of the two enones ($NaBH_4$, -78 ºC in CH_2Cl_2/MeOH; 92% and 84%) gave allylic alcohol **21** and **22**. Treatment of the two allylic alcohols with methyl chloroformate in the presence of a catalytic amount of DMAP gave the allylic carbonates **23** and **24** (94% and 90%).

Figure 16*. Synthesis of C4”-amide analogues of SL0101, part 1.

A) Retrosynthesis of C4”-amide SL0101 analogues

B) Unsuccessful approach to C4”-azide sugar 17

C) Synthesis of C4”-azide sugar glycosyl donors 29/30.

*Figure contributed by George O’Doherty.

Figure 16

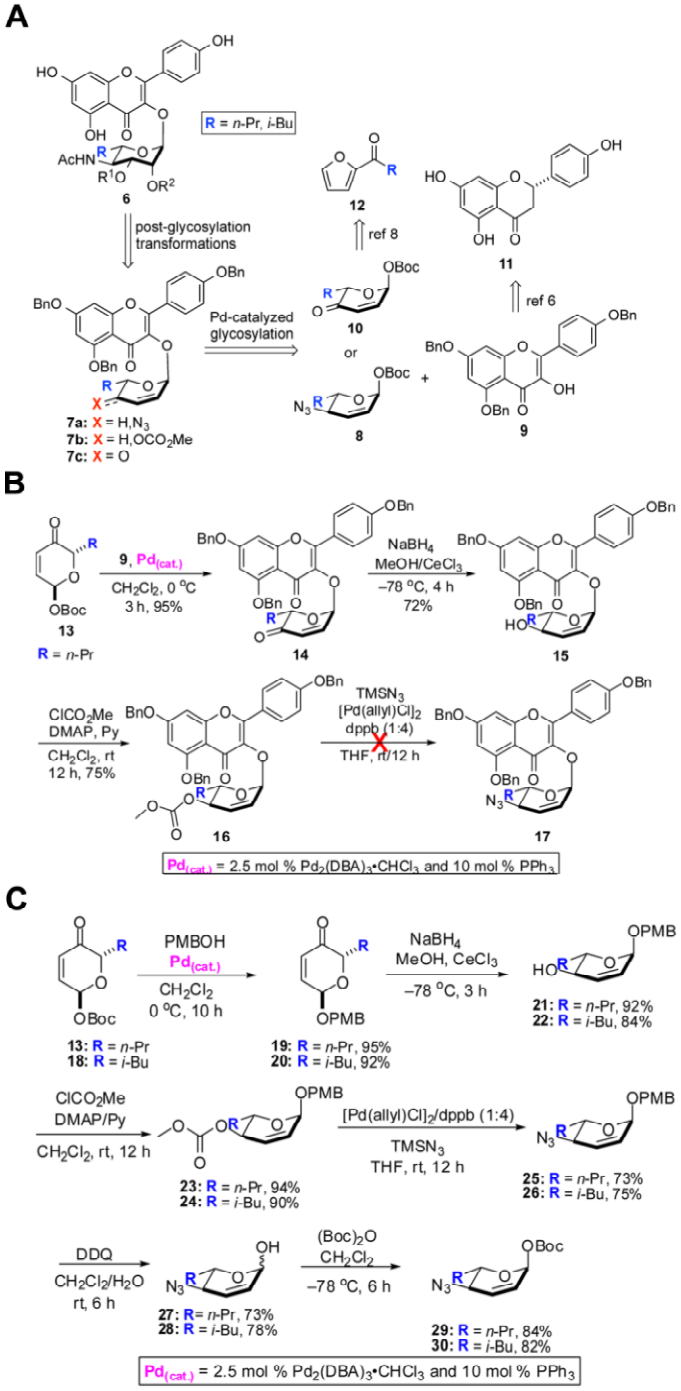
A
R = n-Pr, i-Bu
6
post-glycosylation transformations
Pd-catalyzed glycosylation
7a: X = H,N3
7b: X = H,OCO2Me
7c: X = O
12
ref 8
11
10
or
8
ref 6
9
B
13
R = n-Pr
9, Pd(cat.)
CH2Cl2, 0 °C
3 h, 95%
14
NaBH4
MeOH/CeCl3
–78 °C, 4 h
72%
15
ClCO2Me
DMAP, Py
CH2Cl2, rt
12 h, 75%
16
TMSN3
[Pd(allyl)Cl]2
dppb (1:4)
THF, rt/12 h
17
Pd(cat.) = 2.5 mol % Pd2(DBA)3•CHCl3 and 10 mol % PPh3
C
PMBOH
Pd(cat.)
CH2Cl2
0 °C, 10 h
13: R = n-Pr
18: R = i-Bu
19: R = n-Pr, 95%
20: R = i-Bu, 92%
NaBH4
MeOH, CeCl3
–78 °C, 3 h
21: R = n-Pr, 92%
22: R = i-Bu, 84%
ClCO2Me
DMAP/Py
CH2Cl2, rt, 12 h
23: R = n-Pr, 94%
24: R = i-Bu, 90%
[Pd(allyl)Cl]2/dppb (1:4)
TMSN3
THF, rt, 12 h
25: R = n-Pr, 73%
26: R = i-Bu, 75%
DDQ
CH2Cl2/H2O
rt, 6 h
27: R= n-Pr, 73%
28: R = i-Bu, 78%
(Boc)2O
CH2Cl2
–78 °C, 6 h
29: R = n-Pr, 84%
30: R = i-Bu, 82%
Pd(cat.) = 2.5 mol % Pd2(DBA)3•CHCl3 and 10 mol % PPh3

Figure 17*. Synthesis of C4”-amide analogues of SL0101, part 2.

A) Synthesis of C4”-azido rhamno-sugars 32/33 SL0101 analogues.

B) Synthesis of C4”-amide analogues of SL0101 (4/5).

* Figure contributed by George O’Doherty.

Figure 17

A

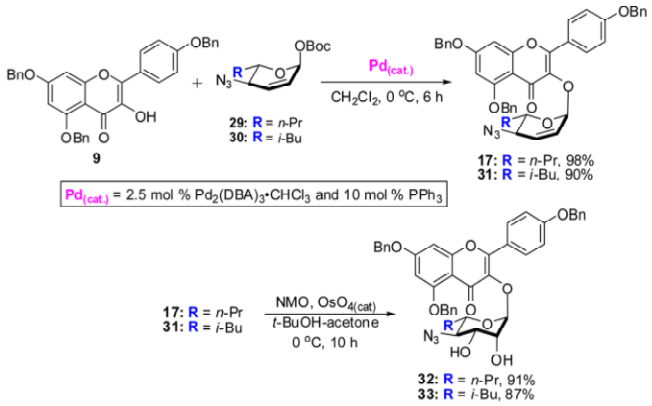
9
29: R = n-Pr
30: R = i-Bu
Pd(cat.)
CH2Cl2, 0 °C, 6 h
17: R = n-Pr, 98%
31: R = i-Bu, 90%
Pd(cat.) = 2.5 mol % Pd2(DBA)3·CHCl3 and 10 mol % PPh3
17: R = n-Pr
31: R = i-Bu
NMO, OsO4(cat)
t-BuOH-acetone
0 °C, 10 h
32: R = n-Pr, 91%
33: R = i-Bu, 87%

B

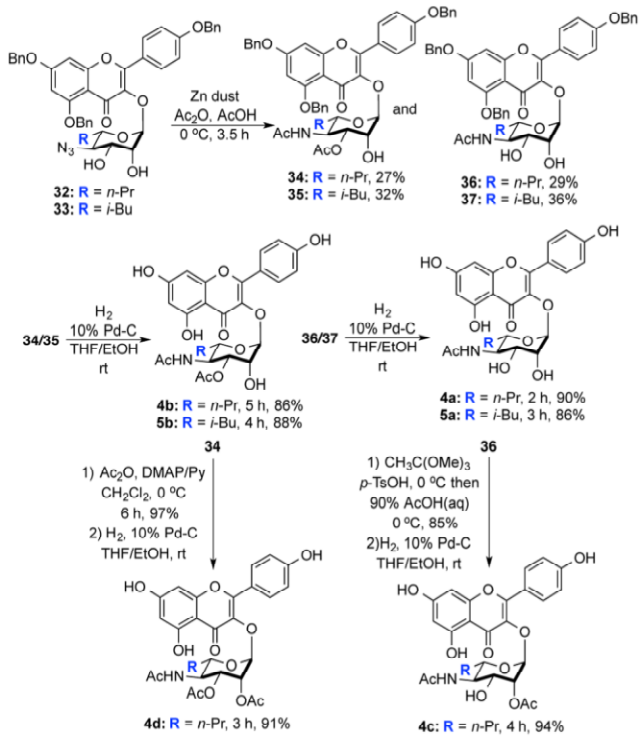
32: R = n-Pr
33: R = i-Bu
Zn dust
Ac2O, AcOH
0 °C, 3.5 h
and
34: R = n-Pr, 27%
35: R = i-Bu, 32%
36: R = n-Pr, 29%
37: R = i-Bu, 36%
34/35
H2
10% Pd-C
THF/EtOH
rt
4b: R = n-Pr, 5 h, 86%
5b: R = i-Bu, 4 h, 88%
36/37
4a: R = n-Pr, 2 h, 90%
5a: R = i-Bu, 3 h, 86%
34
1) Ac2O, DMAP/Py
CH2Cl2, 0 °C
6 h, 97%
2) H2, 10% Pd-C
THF/EtOH, rt
4d: R = n-Pr, 3 h, 91%
36
1) CH3C(OMe)3
p-TsOH, 0 °C then
90% AcOH(aq)
0 °C, 85%
2)H2, 10% Pd-C
THF/EtOH, rt
4c: R = n-Pr, 4 h, 94%

Figure 18*. Evaluation of *in vitro* and cell-based potency of SL0101 (1) and analogues.

A) *In vitro* potency of SL0101 (1) and analogues. RSK2 IC50: concentration needed for 50% RSK2 inhibition (n > 2; quadruplicate: mean, S.D.; p: Student's t test compared to SL0101).

B) Inhibition of MCF7 proliferation at 100 mM SL0101 (1) and analogues. MCF7 proliferation: (n > 2; triplicate: mean, S.D.; * Student's t-test compared to control; # Student's t test compared to SL0101). $p < 0.01$ significant

C) Compound 4d significantly inhibits proliferation of MCF7 and MCF10A cells. n > 2; triplicate: mean, S.D.; * Student's t-test compared to control.

D) RSK biomarkers comparison of 4d and 1. Comparison of analogue 4d and SL0101 (1) was made against known RSK biomarkers in intact cells. MCF-7 cells were pre-treated with 4d at the indicated concentrations and then treated with vehicle or PMA. Lysates were analyzed by immunoblotting. The motif, (K/R)x(K/R)xx(pS/pT), is recognized by a number of kinases, including RSK. The arrows indicate bands whose intensity is altered upon treatment of cells with SL0101 (1).

* Panels B and C contributed by Deborah Lannigan.

Figure 18

A

compound name	RSK2 IC_{50} [μM]	RSK2 IC_{50} *p*(**1**)
SL0101 (**1**)	1.04 ± 0.60	
4a	0.76 ± 0.43	0.17
4b	0.23 ± 0.07	<0.01
4c	0.11 ± 0.09	<0.01
4d	0.44 ± 0.39	0.02
5a	2.33 ± 0.88	<0.01
5b	0.32 ± 0.18	<0.01

B

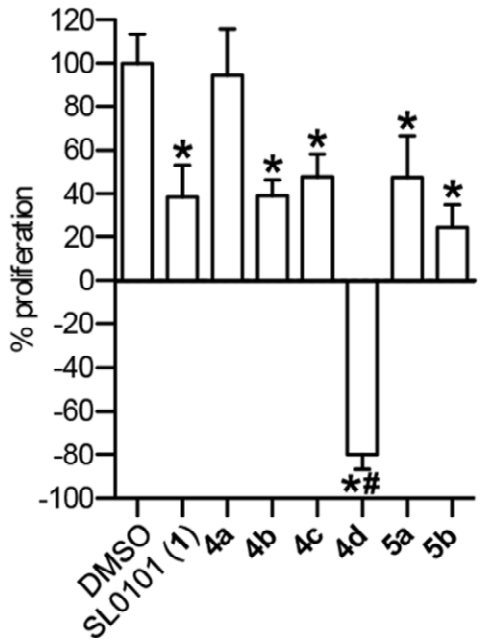

C

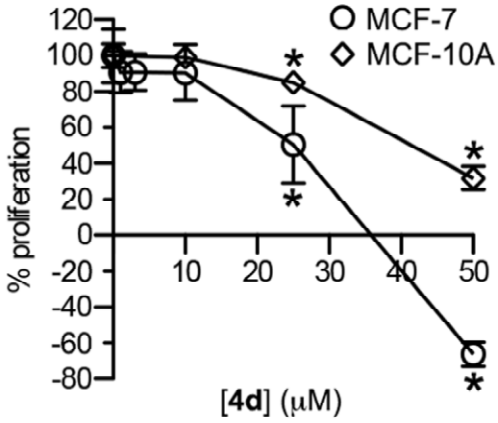

D

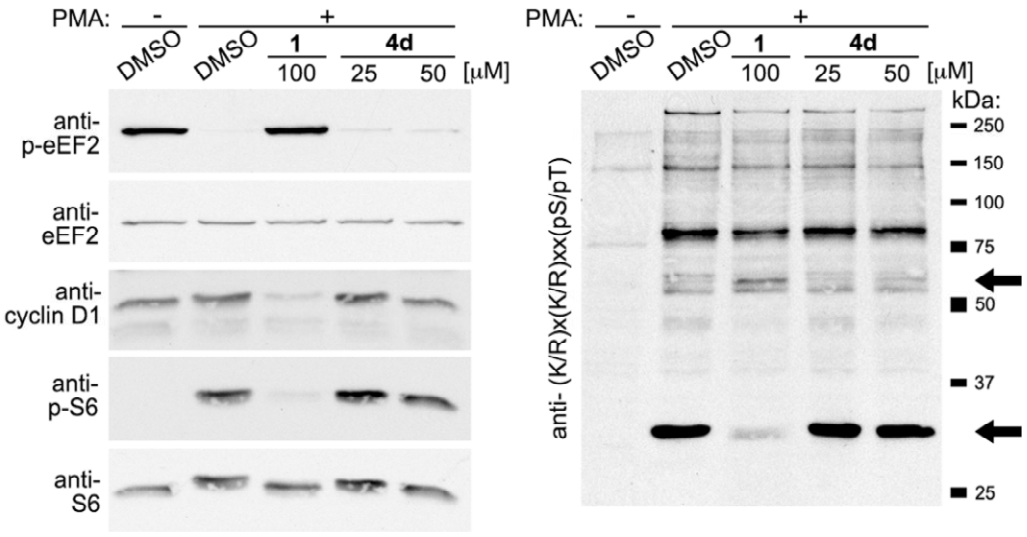

Exposure of the carbonates to the Sinou conditions (TMSN3, $(Pd(allyl)Cl)_2$/1,4-bis(diphenylphosphino)-butane) regio- and stereospecifically afforded the desired allylic azides 25 and 26 (73% and 75%). An oxidative PMB deprotection (DDQ/H_2O) of 25 and 26 provided anomeric alcohols 27 and 28 as a 13:1 mixture of anomers in 73% and 78% yields. The following Boc-protection of the two alcohols produced the key azido containing intermediates 29 and 30 in 84% and 82% yields and with excellent diastereoselectivity.

To our delight, exposure of sugar donor Boc-allylic azides **29** and **30** and acceptor **9** to our typical Pd-catalyzed glycosylation condition provided our desired glycosylated allylic azides **17** and **31** in excellent yield (98% and 90%) with complete α-selectivity and no sign of hydrolysis at the anomeric position. Exposure of the two allylic azides to Upjohn conditions (OsO_4/NMO; 91% and 87%) stereoselectively converted them into the two rhamno-diols **32** and **33**, which are poised for further manipulation into the desired SL0101 analogues (fig. 17A).

We next investigated the reduction and acylation of azido/diols **32** and **33** (fig. 17B) (Maloney and Hecht, 2005, Shan and O'Doherty, 2010, Shan and O'Doherty, 2006, Aljahdali et al., 2013, Bajaj et al., 2014). Fortuitously, both the C4 acylated amides **36** and **37** and C3/C4 bis-acylated products **34** and **35** were generated at a ~1:1 mixture in one pot from the reduction of **32** and **33** with zinc dust in the presence of acetic anhydride and acetic acid. Thus, the reduction acylation of **32** gave the desired C4”-acetamides **36** (29%) and **34** (27%), whereas the reduction acylation of **33** gave the desired C4”-acetamides **37** (36%) and **35** (32%).

The intermediates **34**-**37** were globally deprotected by an exhaustive hydrogenolysis, which produced four of the desired analogues. Thus, exposure of **34** and **35** to typical hydrogenolysis conditions (1 atm. of hydrogen with Pearlman's catalyst (Pd/C)) furnished **4b** and **5b** in good yields (86% and 88%, respectively). Exposure of **36** and **37** to similar hydrogenolysis conditions furnished **4a** and **5a** in good yields (90% and 86%, respectively). Finally the last two analogues **4c** and **4d** were prepared by an acylation deprotection sequence. The peracylated product **4d** was prepared from **34** in 91% overall yield by bis-acylation (Ac_2O, DMAP/Py; 97%) and exhaustive hydrogenolysis. Similarly, the C2 acylated product **4c** was prepared from **36** via an ortho-ester mediated C2-acylation ($CH_3C(OMe)_3$, 10% *p*-TsOH in CH_2Cl_2; then excess 90% AcOH/H_2O; 85%) and per-hydrogenolysis (94% overall yield).

The efficacy of the analogues **4a-d** and **5a-b** to inhibit RSK2 activity was determined in an *in vitro* kinase assays using purified recombinant RSK2 (fig. 18A) (Smith et al., 2005). The data were fit using nonlinear regression analysis. In the *n*-Pr series **4b** and **4c** with a single acetate at C3" or C2"-position, had significantly lower IC_{50}'s compared to SL0101 (**1**). However, when compared with our best analogue **2a**, (C3"/C4"-diacetate, fig. 15) the related C4"-acetamide **4b** had a 10-fold increase in IC_{50} (chapter 3). The IC_{50}'s for **4a** with no C2"- or C3"- acetate and **4d** with two acetates were not statistically different from that of SL0101 (**1**). These results are similar to those obtained in the series in which the acetyl group was at the C4" position (chapter 3). In the isobutyl series the C3"-acetate **5b** had a three-fold improved IC_{50} compared to that of SL0101 (**1**), whereas, **5a** with no C2"- or C3"- acetate had a much poorer IC_{50} than SL0101 (**1**). These data suggest that in the *n*-Pr-series, the C"4-acetamide can replace

the C”4-acetate without dramatically compromising the affinity of the analogues for RSK2.

The six analogues were evaluated for their ability to decrease proliferation of the breast cancer cell line, MCF-7 (fig. 18B). Initially, each analogue was tested at a dose of 100 μM and compared to SL0101 (**1**). Analogue **4d** was the only analogue that inhibited proliferation to a greater extent than SL0101 (**1**) (fig. 18B). A dose response curve with **4d** showed that cytostasis occurred at ~ 35 μM and substantial cell death occurred at ~ 50 μM (fig. 18C). For comparison SL0101 (**1**) at 100 μM (maximum soluble concentration in biological media) induces an ~ 60% reduction in proliferation. To evaluate whether **4d** was specific for RSK, we compared its anti-proliferative effects in MCF-7 cells versus MCF-10A, an immortalized nontransformed human breast cell line. We previously found that a preferential ability to inhibit MCF-7 compared to MCF-10A proliferation correlates with specificity for RSK inhibition (Smith et al., 2005, Smith et al., 2007, Hilinski et al., 2012, Smith et al., 2006, chapter 3). At 25 μM **4d** inhibited proliferation of MCF-7 cells by 50% and marginally inhibited MCF-10A proliferation (fig. 18C). However, at 50 μM of **4d**, a cytotoxic dose in MCF-7 cells, proliferation of MCF-10A cells was inhibited by 70%. Thus **4d** shows a very limited ability to preferentially inhibit MCF-7 proliferation and survival compared to MCF-10A cells. These results suggest that **4d** is not a specific RSK inhibitor in intact cells.

To further evaluate the specificity of **4d** at inhibiting RSK we compared the efficacy of SL0101 (**1**) and **4d** to alter the phosphorylation of known RSK substrates. We chose to test **4d** at both cytostatic (25 μM) and cytotoxic (50 μM) concentrations. To

increase the phosphorylation of substrates MCF-7 cells were stimulated with the mitogen, phorbol myristate acetate (PMA) after a pre-treatment with inhibitor or vehicle. RSK phosphorylates and inhibits the activity of eukaryotic elongation factor 2 (eEF2) kinase (Wang et al., 2001a). Thus inhibition of RSK relieves the inhibition of eEF2 kinase, which results in an increase in phosphorylation of the eEF2 kinase substrate, eEF2. As expected, activation of RSK by PMA led to a decrease in eEF2 phosphorylation and inhibition of RSK with SL0101 (**1**) increased eEF2 phosphorylation compared to the PMA control (fig. 18D).

Ribosomal protein S6, a component of the 40S ribosomal subunit, is phosphorylated by RSK (Erikson and Maller, 1985), and in agreement with these data SL0101 (**1**) inhibits PMA-induced phosphorylation of S6. We have also found that RSK regulates the levels of the oncogene, cyclin D1, in MCF-7 cells (Eisinger-Mathason et al., 2008). Consistent with these observations SL0101 (**1**) inhibited cyclin D1 levels. In contrast with our observations with SL0101 (**1**), the analogue **4d** did not alter the phosphorylation status of eEF2, S6 or the levels of cyclin D1 (fig. 18D). To further investigate the ability of **4d** to inhibit RSK in intact cells, we immunoblotted the lysates with an antibody against the phosphorylation motif that is recognized by numerous kinases, including RSK. Treatment with SL0101 increased the phosphorylation of a band ~ 60 kDa and decreased the intensity of a band at ~ 27 kDa. Analogue **4d** did not alter the phosphorylation pattern compared to the PMA control. Consistent with these results we observed that analogue **4b** (100 μM) did not alter the phosphorylation of RSK biomarkers or cyclin D1 levels in intact cells (data not shown). These results suggest that the amide analogues of SL0101 (**1**) are not specific for RSK.

In conclusion, using de novo synthesis C4”-acetamide analogues of SL0101 with a C”6 substitution were prepared and evaluated as RSK inhibitors. Analogues with improved *in vitro* kinase inhibitory activity were identified. However, this increase in activity came at a loss of selectivity for RSK. Thus an acetate at the C4” position appears to be a requirement to maintain specificity for RSK inhibition.

Chapter 5

Synthesis and Structure-Activity-Relationship Study of 5a-Carbasugar Analogues of SL0101

Adapted from:

Li, M., Li, Y., Mrozowski, R.M., Sandusky, Z.M., Shan, M., Song, X., Wu, B., Zhang, Q., Lannigan, D.A., O'Doherty, G.A. (2014) Synthesis and Structure-Activity-Relationship Study of 5a-Carbasugar Analogues of SL0101. *ACS Med. Chem. Lett*. 6: 95-99

Summary

The Ser/Thr protein kinase, RSK, is associated with oncogenesis and therefore, there are ongoing efforts to develop RSK inhibitors that are suitable for use *in vivo*. SL0101 is a natural product that demonstrates selectivity for RSK inhibition. However, SL0101 has a short biological half-life *in vivo*. To address this issue we designed a set of eight cyclitol analogues, which should be resistant to acid catalyzed anomeric bond hydrolysis. The analogues were synthesized and evaluated for their ability to selectively inhibit RSK *in vitro* and in cell-based assays. All the analogues were prepared using a stereo-divergent palladium-catalyzed glycosylation/cyclitolization for installing the aglycon. The L-cyclitol analogues were found to inhibit RSK2 in *in vitro* kinase activity with a similar efficacy to that of SL0101, however, not specific for RSK in cell-based assays. In contrast, the D-isomers showed no RSK inhibitory activity in *in vitro* kinase assay.

5.1. Materials and Methods

Purified recombinant RSK2

Baculovirus encoding His-tagged RSK2 cDNA was generated using the Bac-to-Bac Baculovirus Expression System (Invitrogen, Carlsbad, CA). Recombinant RSK2 was expressed in Sf9 cells and activated by stimulation with phorbol 12-myristate 13-acetate (PMA). Protein was purified using the Ni-NTA Spin Kit (Qiagen, Valencia, CA).

In vitro kinase assays

The assays were performed as previously described (Smith et al., 2005). Briefly, glutathione S-transferase (GST) ERα Serine167 fusion protein containing the amino acid sequence RRRLA**S**TNDKG was adsorbed in the wells (1 μg/well) of MaxiSorp-treated LumiNunc 96-well white polystyrene plates (Thermo Scientific, Roskilde, Denmark). The wells were blocked with 3% tryptone in PBS and stored at 4°C. Kinase (5 nM) in kinase buffer (25 mM HEPES, 150 mM NaCl, 5 mM β-glycerophosphate, 1.5 mM DTT, 30mM $MgCl_2$, pH 7.4) and 1% bovine serum albumin was added to each well. Reactions were incubated for 120 minutes in the presence of vehicle or inhibitor at indicated concentrations. Reactions were then initiated by the addition of ATP (10 μM) for 20 minutes. The reactions were terminated by addition of EDTA (500 mM, pH 8.0). The plates were washed and phosphorylation was measured using rabbit polyclonal anti-ERα phospho-Serine167 antibody (Smith et al., 2005) followed by horseradish peroxidase (HRP)-conjugated donkey anti-rabbit antibody (Jackson ImmunoResearch Laboratories, West Grove, PA). Western Lightning Enhanced Chemiluminescent Reagent Plus (PerkinElmer Life Sciences, Waltham, MA) was used to measure HRP

activity. To determine IC_{50} values, non-linear regression analysis was performed using GraphPad Prism version 6.0a (La Jolla, CA).

Proliferation assays

The assays were performed as previously described (Smith et al., 2005). Briefly, MCF-7 or MCF-10A cells were seeded at a density of 200,000 cells per well in 24-well tissue culture treated plates. Inhibitor or vehicle was added and proliferation was measured after 48 hours using CellTiterGlo reagent (Promega, Madison, WI) according to the manufacturer's protocol. To determine IC_{50} values, non-linear regression analysis was performed using GraphPad Prism version 6.0a (La Jolla, CA).

Cell-based inhibition assays

The assays were performed as previously described (Smith et al., 2005). Briefly, 250,000 MCF-7 cells were seeded onto a 35-mm tissue culture dish. The next day the medium was replaced with serum-free medium. After 16 hours, the medium was changed for serum-free medium with DMSO, serum-containing medium with DMSO, or serum-containing medium with inhibitor. Cells were treated for 2 hours before stimulation with PMA (500 nM) for 20 minutes. Cell lysis was performed as previously described (Joel et al., 1998). Lysates were normalized for total protein, electrophoresed, and immunoblotted. Antibodies used for immunoblotting include; anti-(K/R)X(K/R)XX(pS/pT) motif (9611), anti-eEF2 (2332), anti-phospho-eEF2 (2331), anti-cyclin D1(2926), anti-S6 (2217), and anti-phospho-S6 (2211) from Cell Signaling Technology (Danvers, MA). Secondary antibodies used were HRP-conjugated donkey

anti-rabbit and goat anti-mouse (Jackson ImmunoResearch Laboratories, West Grove, PA).

General chemistry methods and materials

^{1}H and ^{13}C spectra were recorded on 400 MHz and 500 MHz spectrometers. Chemical shifts were reported relative to $CDCl_3$ (δ 7.26 ppm), CD_3OD (δ 3.31 ppm), acetone-d_6 (δ 2.05 ppm) for 1H, and $CDCl_3$ (δ 77.0 ppm), CD_3OD (δ 49.15 ppm), acetone-d_6 (δ 29.92 ppm) for 13C. Optical rotations were measured with a digital polarimeter at sodium D line (589 nm) and were reported in concentration of g/100 mL at 25 ºC in the solvent specified. Infrared (IR) spectra were obtained on a FT-IR spectrometer. Flash chromatography was performed using the indicated solvent system on silica gel standard grade 60 (230-400 mesh). *Rf* values are reported for analytical TLC using the specified solvents and 0.25 mm silica gel 60 F254 plates that were visualized by UV irradiation (254 nm and 365 nm) or by staining with $KMnO_4$ stain or *p*-anisaldehyde stain. Ethyl ether, tetrahydrofuran, methylene chloride, toluene, and triethylamine were dried by passing through activated alumina (8 x 14 mesh) column with argon gas pressure. Commercial reagents were used without purification unless otherwise noted. Air and/or moisture-sensitive reactions were carried out under an atmosphere of argon/nitrogen using oven/flamed-dried glassware and standard syringe/septum techniques. Melting points are uncorrected. Matrix-assisted laser desorption ionization time-of-flight (MALDI-TOF) mass spectra were obtained using α-cyano-4-hydroxycinnamic acid (CCA) as the matrix on a MALDI-TOF mass spectrometer.

5.2. Results

The Ser/Thr kinases, RSK, have emerged as a potential drug target for numerous cancers (Eisinger-Mathason et al., 2010). A number of RSK inhibitors have been identified (Aronchik et al., 2014, Cohen et al., 2007, Cohen et al., 2005, Nguyen et al., 2006, Bain et al., 2007, Costales et al., 2014, Zhong et al., 2013, Doehn et al., 2009, Utepbergenov et al., 2012), and of these the kaempferol L-rhamnoside SL0101 (**1a**) is the only allosteric inhibitor of RSK (fig. 19A) (chapter 2)(Utepbergenov et al., 2012), which most likely accounts for its specificity (Bain et al., 2007). RSK is unusual in that it contains two nonidentical kinase domains (Anjum and Blenis, 2008).

On the basis of the crystal structure of SL0101 (**1a**) in complex with the RSK2 N-terminal kinase domain (NTKD) we generated the derivative, C3”/C4”-diacetate with a C6”-n-propyl substituent **2**, which has a 50-fold higher affinity for RSK than SL0101 (**1a**) (chapters 3-4). In an effort to further explore the structure activity relationship of SL0101 (**1a**) as it relates to RSK1-2 inhibition and anticancer activity, we targeted for synthesis cyclitol (aka, 5a-carbasugar) analogues of SL0101 (e.g., **3** and **4,** 19B). We hypothesized that the cyclitol analogues (**3a-c**) (i.e., *sans*-anomeric stabilization) would serve as exact conformational mimics of the natural sugar; whereas the enantiomeric analogues (**ent)-3a-c** serve as control molecules. Finally, to further test the importance of the C6” alkyl group, we envisioned preparing and evaluating the desmethyl cyclitol analogue **4**.

Figure 19. Structures of SL0101, top analogue 2 and D-/L- analogues 1-4.

A) Structures of SL0101 (1) and top analogue 2.

B) Structure of D-/L- SL0101 analogues 1-4.

Figure 19

A

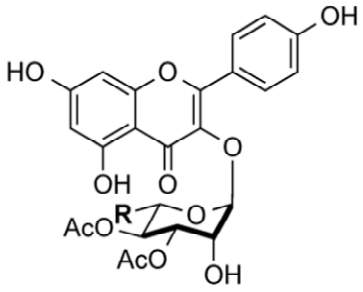

1a: R = Me; **SL0101**: 0.99 μM (IC_{50})
2: R = *n*-Pr; **Best Analogue**: 0.02 μM (IC_{50})

B

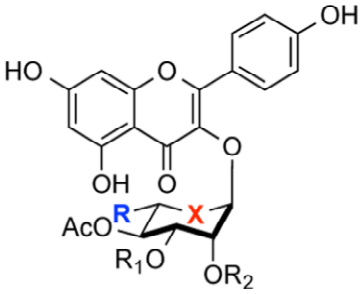

1a: R = Me, X = O, R^1 = Ac, R^2 = H
1b: R = Me, X = O, R^1 = H, R^2 = H
1c: R = Me, X = O, R^1 = H, R^2 = Ac
3a: R = Me, X = CH_2, R^1 = Ac, R^2 = H
3b: R = Me, X = CH_2, R^1 = H, R^2 = H
3c: R = Me, X = CH_2, R^1 = H, R^2 = Ac
4: R = H, X = CH_2, R^1 = Ac, R^2 = H

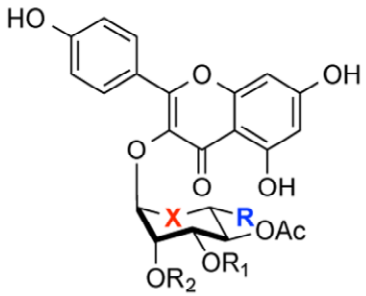

(***ent***)**-1a:** R = Me, X = O, R^1 = Ac, R^2 = H
(***ent***)**-1b:** R = Me, X = O, R^1 = H, R^2 = H
(***ent***)**-1c:** R = Me, X = O, R^1 = H, R^2 = Ac
(***ent***)**-3a:** R = Me, X = CH_2, R^1 = Ac, R^2 = H
(***ent***)**-3b:** R = Me, X = CH_2, R^1 = H, R^2 = H
(***ent***)**-3c:** R = Me, X = CH_2, R^1 = H, R^2 = Ac
(***ent***)**-4:** R = H, X = CH_2, R^1 = Ac, R^2 = H

Figure 20*. Synthesis of carbasugar analogues of SL0101 (1a)

A) Enantiodivergent synthesis of SL0101 analogues 1 and 3.

B) Enantiodivergent cyclitolization of aglycon 7

C) Synthesis of SL0101 cyclitol analogue 4

D) Synthesis of SL0101 cyclitol analogue (ent)-4

* Figure contributed by George O'Doherty.

Figure 20

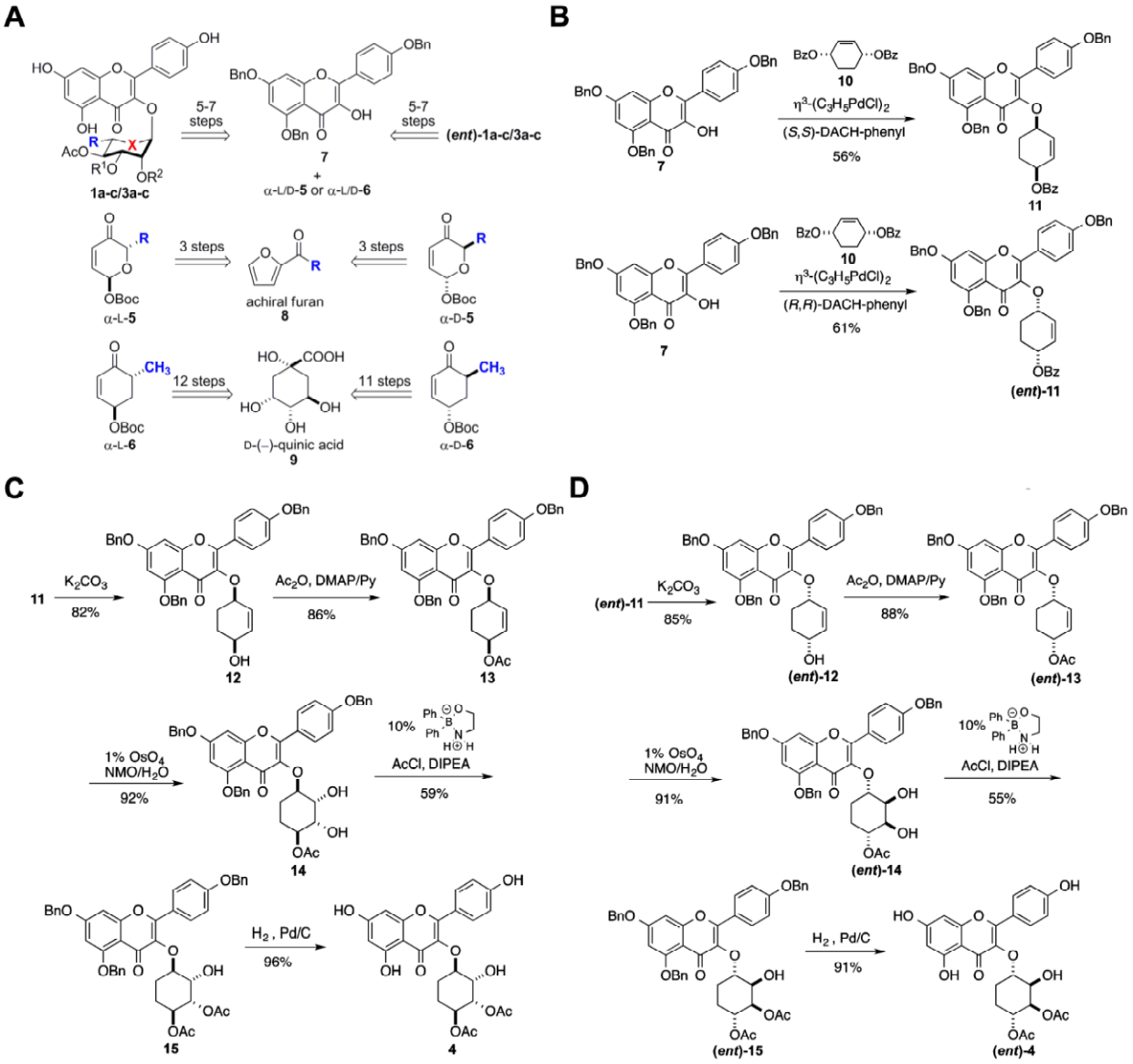
A
1a-c/3a-c
5-7 steps
7
+
α-L/D-5 or α-L/D-6
5-7 steps
(ent)-1a-c/3a-c
3 steps
α-L-5
achiral furan
8
3 steps
α-D-5
12 steps
α-L-6
D-(−)-quinic acid
9
11 steps
α-D-6
B
7
10
η3-(C3H5PdCl)2
(S,S)-DACH-phenyl
56%
11
(R,R)-DACH-phenyl
61%
(ent)-11
C
11
K2CO3
82%
12
Ac2O, DMAP/Py
86%
13
1% OsO4
NMO/H2O
92%
14
10%
AcCl, DIPEA
59%
H2, Pd/C
96%
15
4
D
(ent)-11
85%
(ent)-12
88%
(ent)-13
91%
(ent)-14
55%
91%
(ent)-15
(ent)-4

We have been developing practical and generalizable approaches to both pyranose and 5a-carbasugar and have reported synthetic approaches to SL0101 and its derivatives (Bajaj et al., 2014, Harris et al., 1999, Harris et al., 2000b, Babu et al., 2004b, Guo and O'Doherty, 2007, Zhou and O'Doherty, 2008b). The general approach to these analogues is outlined in fig. 20A. The technology that enables this approach was the use of Pd-catalyzed glycosylation (Shan et al., 2010, Shan and O'Doherty, 2008, Babu and O'Doherty, 2003, Guo and O'Doherty, 2008) or cyclitolisation (Shan and O'Doherty, 2006, Shan and O'Doherty, 2010) and subsequent post-glycosylation transformations. Using the Pd-catalyzed glycosylation, the desired pyranose analogues **1a-c** and **(ent)-1a-c** were produced in five to seven steps from pyranones α-L-5 and α-D-5, respectively. Using the related Pd-catalyzed cyclitolization and in the same number of steps, the desired cyclitol analogues **3a-c** and **(ent)-3a-c** were produced from the corresponding enones α-L-6 and α-D-6.

Key to the success of this approach is the reliance of an enantio-divergent (i.e., D/L) and highly stereo-controlled synthesis of both glycosyl- and cyclitol-donors from readily available intermediates (**8** and **9**, fig. 20A). For instance, the pyranose glycosyl-donors were readily prepared in three steps from achiral acylfuran intermediate **8**. In contrast, the carbasugar cyclitol-donors **6** were significantly more difficult to prepare. Like the pyranones **5**, the cyclitols **6** can also be prepared from a single intermediate, D-quinic acid **9**. Thus in 11 steps, D-quinic acid can be converted into α-D-enone **α-D-6**, whereas, in a related 12 step sequence quinic acid can be also converted into its enantiomeric enone, **α-L-6**.

With access to the cyclitol analogues **3**, we next pursued the de novo asymmetric synthesis of the des-methylcycltiol analogues **4** and **(ent)-4** (fig. 20C,D). Interestingly, the removal of the C6”-methyl group greatly simplifies the analogue synthesis. The simplicity of this approach is enabled by the use of the Trost asymmetric allylation of 7 with meso-1,4-bis-benzoate **10** to form either enantiomer of cyclitol **11** (Trost and Van Vranken, 1996, Trost and Crawley, 2003, Trost et al., 2006). Thus by appropriate choice of the chiral ligand, cyclitol **11** (via (*S,S*)-DACH) or its enantiomer **(ent)-11** (via (*R,R*)-DACH) can be prepared in only one stereo-divergent step. The enantiomeric excess of **12** and **(ent)-12** were determined to be >96% ee by Mosher ester analysis. This was accomplished by converting **12** and **(ent)-12** into their corresponding Mosher ester and integrating resolved diastereomeric vinyl protons in the ^{1}H NMR.

With the C1”/C4” stereochemistry installed in **11**, the C4” benzoate was transformed into an acetate (fig. 20C), via a hydrolysis and acylation sequence (**11** to **13**). Using an Upjohn dihydroxylation (1% OsO_4/NMO), the C2”/C3”-hydroxyl groups were stereoselectively installed in **14**. The required C-3” acetate was regioselectively installed by means of the Taylor catalysis (**14** to **15**). Finally hydrogenolysis was used for a global per-debenzylation of **15** to give the desired cyclitol analogue **4**. Using an identical sequence, the enantiomer **11** was converted into the enantiomeric analogue **(ent)-4** (fig. 20D).

Using purified recombinant enzyme in an *in vitro* kinase assay, the analogues **(ent)-1a**, **3a-c**, **(ent)-3a-3c**, **4** and **(ent)- 4** were evaluated for their ability to inhibit RSK2 kinase activity (Smith et al., 2005). Nonlinear regression analysis was used to fit the data (fig. 21A). Regardless of substitution, we found an absolute requirement for the L-

isoform, as none of the D-isoforms displayed any RSK2 kinase inhibitory activity at concentrations < 30 μM.

Interestingly, we found that replacing the ring oxygen in the rhamnose ring with a methylene did not interfere with *in vitro* RSK2 inhibitory activity (fig. 21A). In fact, the cyclitol analogue **3a** was a slightly better inhibitor of RSK than SL0101, albeit the difference is unlikely to be biologically meaningful. In contrast, the cyclitols with varied acetate substitution (**3b** and **3c**) had higher IC_{50}'s. This trend was consistent to what was observed for the related rhamnose sugar analogues (**1b** and **1c**) (Smith et al., 2006). The C6" methyl group proved to be important for activity, as the desmethyl analogue **4** was a poor inhibitor. Even in the less active desmethyl series, the important of the sugar absolute stereochemistry could be seen, as the **4** was significantly more active than its enantiomer **(*ent*)-4**. This result is consistent with our crystal structure of the RSK2 NTKD/SL0101 complex. Specifically, we observed SL0101 in a specific 3D orientation with the C6" methyl group residing in a key hydrophobic pocket (Utepbergenov et al., 2012) and that alkyl substitution of the C6" alkyl group (Me to *n*-Pr) increased the affinity for RSK2 (chapter 3).

The ability of the analogues to inhibit the proliferation of the breast cancer cell line, MCF-7, was compared to that obtained with the immortalized non-transformed human breast cell line, MCF-10A. We have found that a preferential ability to inhibit MCF-7 compared to MCF-10A proliferation correlates with RSK inhibition (Smith et al., 2005, Smith et al., 2007, Smith et al., 2006). The cyclitol analogue **3b** inhibited both cell lines to the same extent, which suggests that it does not specifically inhibit RSK (fig. 21B).

Figure 21*. Evaluation of *in vitro* and cell-based potency of SL0101 analogues.

A) *In vitro* potency of SL0101 (1a) and analogues. RSK2 IC50: concentration needed for 50% RSK2 inhibition (n > 2; quadruplicate: mean; S.D., p(1a) Student's t test compared to SL0101(1a)). N.D.: no inhibition detected.

B) C3″,C4″ acetates are essential for preferential inhibition of MCF-7 proliferation. The inhibitors were added at time 0, and ATP content was measured after 48 h of treatment. Values are the fold proliferation as a % of the control (n ≥ 2 in triplicate; mean, S.D.; *p < 0.01 in a Student's t test compared to the appropriate cell line in the presence of vehicle).

C) Efficacy and specificity of analogue 3a for inhibition of RSK. As described in Figure B (n ≥ 2 in triplicate; mean, S.D.; *p < 0.01 in a Student's t test compared to control).

D) Efficacy and specificity of analogue 3c for inhibition of RSK. As described in Figure B (n ≥ 2 in triplicate; mean, S.D.; *p < 0.01 in a Student's t test compared to control).

*Figure contributed by Zachary Sandusky.

Figure 21

A

compound name	RSK2 IC_{50} [μM]	RSK2 IC_{50} *p*(**1**)
SL0101 (**1a**)	0.37 ± 0.13	
(***ent***)**-1a**	N.D.	
3a	0.27 ± 0.15	0.0404
(***ent***)**-3a**	N.D.	
3b	1.23 ± 0.62	<0.0001
(***ent***)**-3b**	N.D.	
3c	1.60 ± 0.66	<0.0001
(***ent***)**-3c**	N.D.	
4	8.93 ± 1.02	<0.0001
(***ent***)**-4**	N.D.	

B

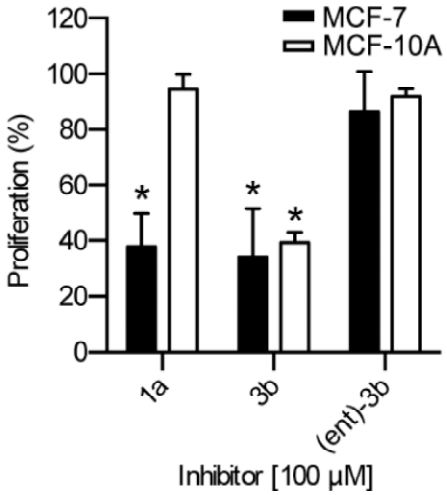

C

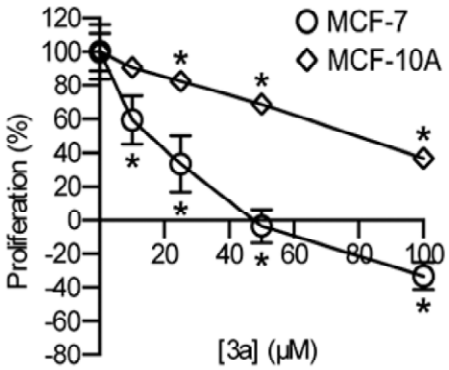

D

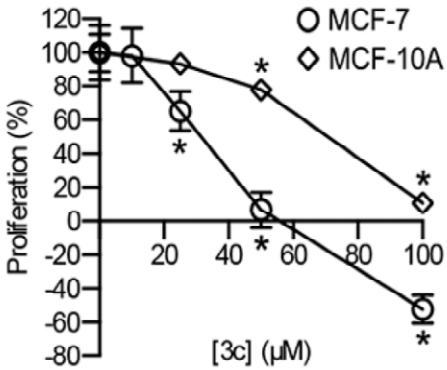

Figure 22. Evaluation of 3a and 3c as RSK-specific inhibitors in MCF-7 cells.

A) Comparison of analogues 3a and 3c and SL0101 (1a) against known RSK biomarkers in intact cells. MCF-7 cells were treated with PMA after pretreatment with the indicated inhibitors. Lysates of the cells were immunoblotted.

B) The motif, (K/R)x(K/R)xx(pS/pT), is recognized by a number of kinases, including RSK and AKT. The arrows indicate bands whose intensity is altered upon treatment of cells with SL0101 (1).

C) The motif, (K/R)(K/R)x(pS/pT), is recognized by a number of kinases, including RSK and PKA. The arrows indicate bands whose intensity is altered upon treatment of cells with SL0101 (1).

D) The motif, (K/R)x(pS/pT)Φ(K/R), is recognized by a number of kinases, including RSK and PKC.

E) Global changes in phosphorylated Tyr residues do not differ between SL0101 and 3a and 3c.

Figure 22

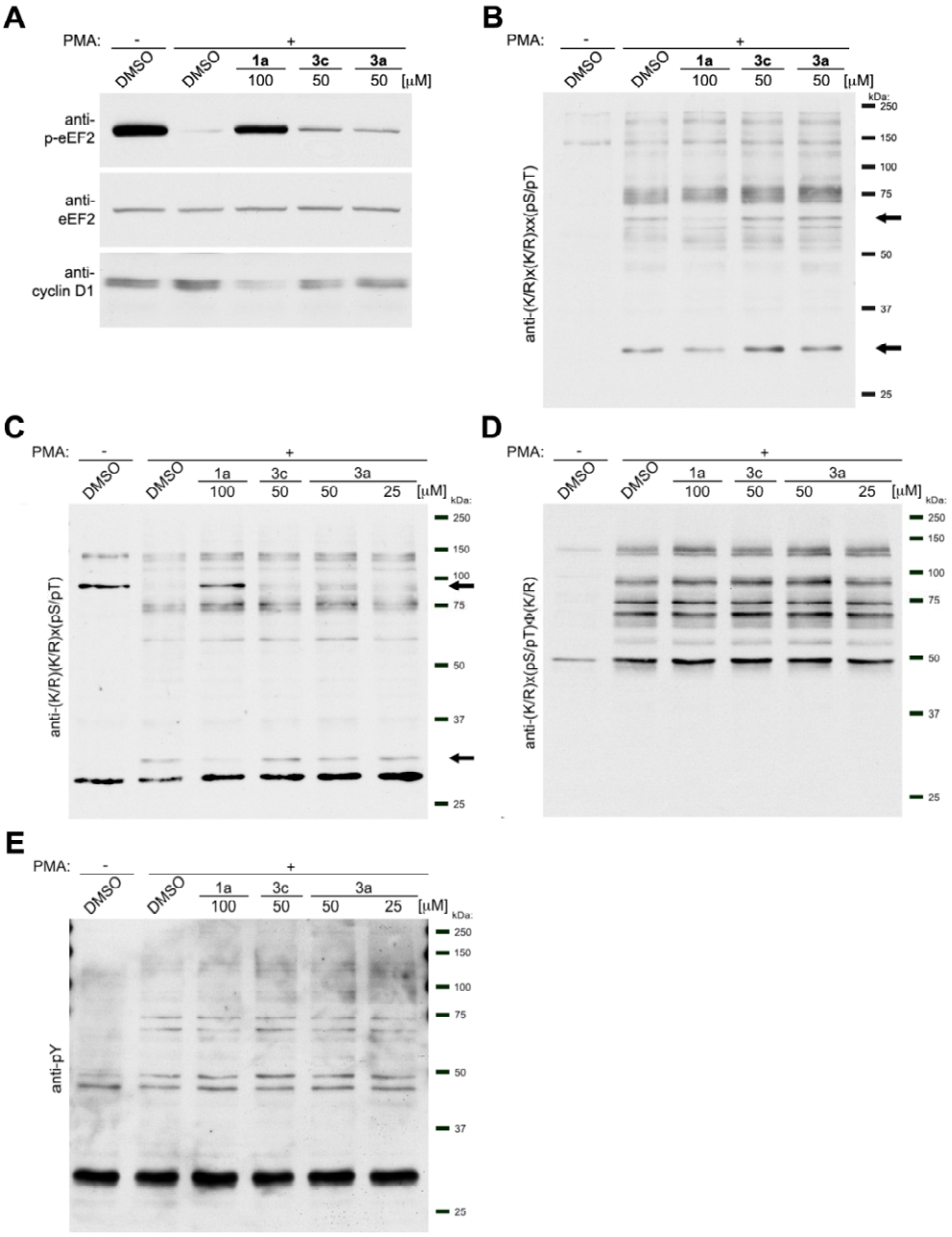
A
PMA: - +
DMSO DMSO 1a 3c 3a
100 50 50 [μM]
anti-p-eEF2
anti-eEF2
anti-cyclin D1
B
PMA: - +
DMSO DMSO 1a 3c 3a
100 50 50 [μM]
kDa:
250
150
100
75
50
37
25
anti-(K/R)x(K/R)xx(pS/pT)
C
PMA: - +
DMSO DMSO 1a 3c 3a
100 50 50 25 [μM]
kDa:
250
150
100
75
50
37
25
anti-(K/R)(K/R)x(pS/pT)
D
PMA: - +
DMSO DMSO 1a 3c 3a
100 50 50 25 [μM]
kDa:
250
150
100
75
50
37
25
anti-(K/R)x(pS/pT)Φ(K/R)
E
PMA: - +
DMSO DMSO 1a 3c 3a
100 50 50 25 [μM]
kDa:
250
150
100
75
50
37
25
anti-pY

In contrast, the enantiomer **(*ent*)-3b** showed no inhibition of either cell line. At 25 μM the analogue **3a** inhibited MCF-7 proliferation by ~ 60% but also significantly inhibited MCF- 10A proliferation (fig. 21C). For comparison, at 100 μM SL0101 (**1a**) inhibited MCF-7 proliferation by ~ 60% but had no effect on MCF-10A proliferation (fig. 21B).

Both analogues **3a** and **3c** were able to completely inhibit proliferation of MCF-7 cells at ~ 50 μM but they also significantly inhibited MCF-10A proliferation at that concentration (fig. 21C,D). For both **3a** and **3c** the dose response differed by ~ 3- fold between MCF-7 and MCF-10A cells. This modest differential effect suggests that the inhibitors are not specific for RSK, as we have found that MCF-10A proliferation is not dependent on RSK.

To further investigate the specificity of **3a** and **3c** for inhibition of RSK we determined their ability to inhibit known RSK substrates in comparison to SL0101. We tested the compounds **3a** and **3c** at 50 μM, which is the cytostatic concentration. Lysates were generated from MCF-7 cells that had been treated with the mitogen, phorbol myristate acetate (PMA) after a pre-treatment with inhibitor or vehicle. Inhibition of RSK is known to result in an increase in the phosphorylation of eukaryotic elongation factor 2 (p-eEF2) via release of the RSK-induced repression of eEF2 kinase (Wang et al., 2001b). As expected SL0101 dramatically enhanced p-eEF2 levels but **3a** and **3c** induced only a minor increase (fig. 22A). To further evaluate whether the analogues could alter RSK biomarkers we used an antibody against a phosphorylation motif, which is recognized by numerous kinases, including RSK. SL0101 decreased the intensity of a

band at ~ 65 and ~ 27 kDa but **3a** and **3c** did not alter the phosphorylation pattern compared to the PMA control (fig. 21B). We have also determined that RSK regulates the levels of the oncogene, cyclin D1 (Eisinger-Mathason et al., 2008). In agreement with our previous observations SL0101 decreased cyclin D1 levels but **3a** and **3c** had no effect (fig. 22A). We conclude that **3a** and **3c** are not specific for RSK inhibition in cell-based assays.

To obtain insight into kinases that **3a** and **3c** could target we used antibodies that detect the phosphorylation motif of protein kinase A (PKA), protein kinase C (PKC), and tyrosine kinases. Cyclitols **3a** and **3c** did not alter the phosphorylation pattern obtained with antibodies to the PKC and tyrosine kinase phosphorylation motifs (fig. 22D-E). However, **3a** and **3c** resulted in the partial increase in the intensity of a band at ~90 kDa. In contrast, SL0101 dramatically increased the intensity of this band compared to PMA (fig. 22C). The PKA motif antibody is able to detect phosphorylations generated by RSK, and therefore, observing changes with SL0101 is expected. On the basis of our immunoblot analysis, **3a** and **3c** do not inhibit kinases that prefer an Arg at the -5 position but do inhibit kinases that prefer an Arg at the -3 and -2 positions from the Ser or Thr phosphorylation site. This information narrows down the possible candidate kinases from within the AGC kinase family that **3a** and **3c** target.

In conclusion, using a Pd-catalyzed glycosylation or cyclitolization in combination with post-glycosylation transformation, an enantiomerically diverse set of SL0101 analogues were prepared and evaluated as RSK inhibitors. Replacement of the L-rhamno-sugar with a L-rhamno-5a-carbasugar did not substantially alter the ability of the analogues to inhibit RSK kinase activity *in vitro*; however, the compounds

demonstrated off-target effects in cell-based assays. Further efforts aimed at identifying cyclitol analogues that specifically target RSK inhibition are ongoing and will be reported in due course.

Chapter 6

Identification of potential novel RSK1-interacting proteins and phosphorylation targets in breast cancer

Summary

The RSK family of Ser/Thr protein kinases consists of four isoforms that are products of separate genes and share very high degree of sequence similarity. RSK is activated by the extracellular signal regulated kinase ERK1/2 in response to various stimuli, including growth factors, cytokines and neurotransmitters. RSK1 and RSK2 were found to be frequently overexpressed in cancers and were shown to promote proliferation and migration of multiple cancer cell types. Therefore, RSK1 and RSK2 are thought to be tumor promoters. RSK3 and RSK4 appear to have opposite effects on tumor growth and are thought to be tumor suppressors. However, the specific mechanisms controlled by individual RSK isoforms are not very well understood. We set out to characterize the specific functions of RSK1 though identification of novel interacting partners by means of high-throughput proteomics. In order to achieve this goal, we utilized a labeling approach in intact cells. We discovered that a portion of RSK1, and not RSK2, associates with intracellular membranes in multiple cell lines. We identified potential interacting partners of RSK1 that localized to ribosomes, mitochondria and endoplasmic reticulum membranes. Therefore, RSK1 could regulate protein synthesis, as well as energy homeostasis.

6.1. Introduction

The Mitogen Activated Protein Kinase (MAPK) pathway represents the critical element of the signaling network regulating cellular growth and proliferation (Meloche and Pouyssegur, 2007). This cellular pathway is very frequently deregulated in a variety of cancers and therefore has been extensively studied as a potential target for therapeutic intervention (Sebolt-Leopold and Herrera, 2004). However, MAPK pathway modulates a wide variety of downstream targets, and some of these targets are important for the survival and growth of normal proliferating cells, such as those in the skin and gut epithelium. (Sebolt-Leopold and Herrera, 2004). Therefore, an alternative strategy is to inhibit downstream effectors of the MAPK pathway that mediate pro-survival signals in cancer cells. One of such classical effectors of the pathway is the p90 RSK family of kinases (Anjum and Blenis, 2008).

RSK is a family of Ser/Thr protein kinases activated by ERK1/2 signaling in response to various stimuli, including growth factors, peptide hormones and neurotransmitters (Romeo et al., 2012). The four members of the family share a very high degree of peptide similarity, but are products of separate genes. With the exception of RSK4, which was found to be constitutively active in cells, all RSK isoforms are activated in a similar mechanism downstream of the MAPK pathway (Romeo et al., 2012). However, RSK isoforms appear to perform non-overlapping, and sometimes opposing functions in cells (Lara et al., 2013). It is increasingly appreciated that, whereas RSK1 and RSK2 serve pro-tumorigenic and pro-metastatic functions, RSK3 and RSK4 appear to be putative tumor suppressors (Lara et al., 2013). In addition, even though all four isoforms of RSK are often expressed in one cell, it has been observed

that these isoforms can have distinct intracellular localizations (Heffron and Mandell, 2005, Eisinger-Mathason et al., 2008, Lara et al., 2013). Therefore, different RSK isoforms can interact with and phosphorylate distinct cellular targets. However, the paucity of isoform-specific antibodies recognizing the active phosphorylated forms of RSK, as well as lack of isoform-specific small molecule inhibitors have hindered the efforts to characterize the divergent signaling landscapes of RSK isoforms.

A novel method of labeling of interacting proteins in intact cells has recently been characterized (Hung et al., 2014, Rhee et al., 2013). In this method, a promiscuous ascorbate peroxidase APEX was fused with a short peptide targeting it to the mitochondria, or the mitochondrial intramembrane space, and expressed in HEK cells. In response to biotin-phenol and hydrogen peroxide APEX peroxidase oxidized biotin-phenol to form a phenoxyl radical (Martell et al., 2012). This radical could rapidly attach to electron-negative amino acid side chains of proteins, such as Tyr, Trp, His and Cys (Amini et al., 2002). Due to its very short half-life (< 1ms) and very small labeling radius (< 20 nm) the phenoxyl radical labeled only proteins that were in a very close proximity to APEX (Rhee et al., 2013). Therefore, APEX could aid in identifying proteins that only transiently interacted with a fusion protein, as well as stably bound partners. The biotinylated proteins can then be affinity-purified using streptavidin, and analyzed by liquid chromatography mass spectrometry (LC/MS). These studies provided very detailed analysis of the proteins localized to the mitochondria, as well as the topology of the mitochondrial transmembrane protein complexes.

Given the limited knowledge of the isoform-specific downstream targets of RSK1, as well as the increasing evidence for the role of RSK1 in promoting tumorigenesis and

invasiveness (Larreaa et al., 2009, Lara et al., 2011), we set out to characterize the RSK1 interactome in breast cancer cells. We decided to employ the APEX-mediated labeling of RSK1-interacting partners in intact cells. This method allowed us to investigate proteins that bind in a stable, as well as transient fashion, as in the case of the kinase substrates. We discovered that a significant fraction of RSK1 was stably associated with intracellular membranes in multiple cell lines. Contrary to RSK1, RSK2 was found exclusively in the cytosol. Through mass spectrometry analysis of labeled proteins we identified potential RSK1-binding partners in the ribosomes, as well as mitochondrial and endoplasmic reticulum membranes. Therefore, RSK1 could regulate such cellular processes as protein synthesis and energy production.

6.2. Materials and methods

Plasmids and lentiviral production

Plasmids used for lentivirus production, pSPAX2 and pMD2G, were generously provided by D. Trono (Swiss Federal Institute of Technology, Lausanne, Switzerland). pLentiPuro plasmid was generously provided by I. Macara (Vanderbilt University, Nashville, TN). pcDNA3-mito-APEX was purchased from AddGene (Cambridge, MA). APEX was cloned into pLentiPuro and the virus was produced according to a previously described protocol (McCaffrey and Macara, 2009).

Reagents and antibodies

Mitochondria isolation kit from cell lines and streptavidin-conjugated magnetic beads were purchased from ThermoScientific (Rockfolrd, IL). AlexaFluor488-conjugated streptavidin was purchased from Life Technologies (Carlsbad, CA). Ponceau S stain

concentrate, PMSF, protease inhibitor cocktail, sodium azide, sodium ascorbate, Trolox and 30% hydrogen peroxide were from Sigma (St. Louis, MO). Biotin-phenol conjugate was synthesized in-house according to previously published protocol (Rhee et al., 2013), and purchased from Berry and Associates (Ann Arbor, MI). RapiGest was purchased from Waters Corporation (Milton, MA). Bovine serum albumin (BSA) was from Roche (Germany). The antibodies used in the study were: rabbit anti-RSK1, mouse monoclonal anti-RSK2 and goat anti-EEA1 from Santa Cruz Biotechnology (Santa Cruz, CA); mouse anti-catalase, mouse anti-MTCO2 and mouse anti-VDAC1 from AbCam (Cambridge, MA); mouse monoclonal anti-Ran and mouse anti-PanERK from BD Biosciences (San Jose, CA); rabbit anti-pThr359/pSer363-RSK from Cell Signaling Technology (Danvers, MA); mouse anti-V5 and Alexa546-conjugated goat anti-mouse were from Life Technologies (Carlsbad, CA).

Cell culture and treatments

MCF7, MCF10A and HEK293T cell lines were cultured according to the instructions from the American Type Culture Collection. For viral transductions, cells were passaged and resuspended in full growth medium, and appropriate amount of virus was added at MOI 1.5. Cells were seeded onto a 12-well plate at 100,000 cells/well and grown for 2 days, followed by a passage for experiments. For serum starvation, cells were washed 3 times with phosphate buffered saline and fresh serum-free medium was added for 16 hours. Cells were then stimulated with 500 mM phorbol myristate acetate (PMA) in fresh serum-containing growth medium for 20 minutes, and lysates were collected. Lysis was done in boiling 4% SDS loading buffer (120 mM Tris pH 6.8, 200 mM DTT, 10% glycerol).

Cellular fractionation

Mitochondria isolation kit was used for cellular fractionation, according to manufacturer's instructions. All steps were preformed at 4 °C. $10*10^6$ cells were washed 3 times with ice-cold PBS, lysed in mitochondria isolation buffer A and homogenized by 80 strokes in Dounce homogenizer. Lysate was combined with buffer B and centrifuged at 700 g for 10 min to separate nuclei and plasma membrane, as well as unlysed cells. 5 mM EDTA was added to the supernatant at this step to prevent aggregation of proteins in subsequent centrifugations. The supernatant was centrifuged for 10 min at 700 g and the heavy mitochondrial pellet was separated. The supernatant was centrifuged at 16000 g for 15 min to separate light mitochondrial pellet. The supernatant was subjected to an ultracentrifugation at 100000 g for 1 h and the microsomal pellet was separated. Each pellet was washed once in the buffer A/B mixture and repelleted. All fractions were lysed by boiling for 5 min in lysis buffer and electrophoresed.

Immunofluorescence

For immunofluorescene imaging, MCF7 cells were seeded onto poly-L-lysine coated glass coverslips and 2 days later biotin-phenol was added in fresh growth medium for 16 hours. 1 mM hydrogen peroxide was added to cells for 15 min, and the labeling was terminated by 3 washes with quencher buffer (PBS pH 7.4 with 10 mM sodium ascorbate, 10 mM sodium azide and 5 mM Trolox). Cells were fixed with 4% para-formaldehyde in PBS pH 7.4 for 15 min and permeabilized with 0.0025% digitonin in PBS for 10 min. Coverslips were blocked with 10% BSA. Primary antibody against V5 tag was incubated for 16 h at 4 °C in 3% BSA in PBS, and secondary antibody together

with Alexa546-conjugated streptavidin were incubated for 1 hour at room temperature. Cells were imaged on 510-META confocal microscope using 63X apochromat lens (N.A. 1.4) (Zeiss, Germany).

In vivo biotin labeling

The protocol was adapted from (Rhee et al., 2013). Briefly, a 80% confluent late of MCF7 cells was treated with 50 mM biotin-phenol in growth medium for 16 h, followed by 15 min stimulation with 1 mM hydrogen peroxide in fresh growth medium. Labeling was terminated with 3 washes with ice-cold quencher buffer. Cells were lysed in 200 μL of ice-cold RIPA lysis buffer (50 mM Tris pH 7.2, 150 mM NaCl, 0.1% SDS, 0.5% sodium deoxycholate, 1% Triton-X100, 1X protease inhibitor cocktail, 1mM PMSF, 10 mM sodium azide, 10 mM sodium ascorbate, 5 mM Trolox) on ice for 5 min, followed by shearing the lysate by passing 3 times through 27G needle. The lysate was snap-frozen in liquid nitrogen and stored in -80 °C until further steps.

Affinity purification of biotinylated proteins

50 μL of streptavidin bead slurry was washed 3 times with RIPA lysis buffer and cell lysate from ~$7*10^6$ cells was added. The beads were incubated in a rotator for 1 h at 4 °C and the lysate was separated from the beads. The procedure was repeated 2 more times with fresh aliquots of beads, to generate 3 fractions of biotinylated proteins. Each aliquot was washed 2 times in ice-cold RIPA buffer, one time with 2 M urea in 10 mM Tris pH 8.0 and 2 more times with RIPA buffer. The beads were then washed 5 times in 100 mM ammonium bicarbonate pH 7.4 and stored in ammonium bicarbonate at 4 °C until further processing.

Sample processing for mass spectrometry

The affinity-purified biotinylated proteins bound to the beads were reduced with DTT and alkylated with iodoacetamide as previously described (Schroeder et al., 2004). The beads were subjected to a 10 min trypsin digest (1:20 trypsin:protein ratio by mass) at room temperature in 2 M urea. The digest was quenched with glacial acetic acid and stored at -40 °C for downstream applications.

Mass spectrometry

5% of the sample was pressure-loaded onto 360 μm outer diameter, 75 μm inner diameter fused-silica microcapillary pre-column (Polymicro Technologies) packed with 6 cm of irregular C_{18} resin (YMC, Kyoto, Japan) and washed with approximately 20 column volumes of 0.1% v/v acetic acid. The pre-column was then connected to a 360 μm outer diameter, 50 μm inner diameter fused-silica analytical column (Polymicro Technologies) packed with 6 cm of C_{18} resin, 5 μm, 120 A (YMC, Kyoto, Japan) and equipped with a laser-pulled electrospray emitter tip (P-2000, Sutter Instruments) (Martin et al., 2000).

Nanoflow (60 nL/min) reverse-phase HPLC was used to elute the sample, and micro-electrospray ionization was used to ionize it. The Fourier transform hybrid mass spectrometers (LTQ-FTMS and LTQ-Orbitrap, Thero Scientific) were used for sample analysis. Mass spectrometers were equipped with either electron-transfer dissociation (ETD) or collisionally activated dissociation (CAD). The instrument method was employed in a data-dependent manner to select abundant precursor ions for fragmentation. Qual Browser software (Thermo Fisher Scientific) was used for data

analysis, and peptides were searched against human RefSeq database using OMSSA, assuming a maximum of 3 missed trypsin cleavage sites.

6.3. Results

The exact cellular localization of RSK1 in epithelial cells is unknown. RSK1 has been suggested to transiently localize to the plasma membrane upon activation, and subsequently translocate to the nucleus (Richards et al., 2001). However, other groups have shown that RSK1 does not localize to the nucleus in MCF7 cells and in mouse brain tissue sections (Eisinger-Mathason et al., 2008, Heffron and Mandell, 2005). Given the lack of success in using RSK1-specific antibodies in immunofluorescence, and a diffuse pattern of RSK1 signal in fluorescently tagged overexpression experiments, we decided to perform sub-cellular fractionations. The outline of the protocol is presented in fig. 23A. We used a series of differential centrifugations of whole-cell lysates collected by homogenization in a high-density iso-osmotic buffer. Three membrane fractions, along with the cytosol, were collected. The heavy mitochondrial fraction contained most of the cellular mitochondria, as evidenced by the presence of mitochondrial markers MTCO2 and VDAC1 in the fraction (fig. 23B). Light mitochondria and microsomes contained EEA1 and catalase, the markers of endosomes and peroxisomes, respectively. Ran was used as a cytoplasmic protein marker, and was almost exclusively found in the cytosolic fraction, indicating that the membrane-bound tractions were not contaminated with cytosolic proteins. Interestingly, we detected RSK1 in all membrane-bound fractions, in addition to a cytosolic pool (fig. 23B). This distribution was in stark contrast to that of RSK2, which was exclusively found in the cytosol.

Figure 23. RSK1, and not RSK2, associates with intracellular membranes in normal and transformed breast epithelial cells.

A) A flow-chart demonstrating the sub-cellular fractionation protocol used in the experiments.

B) Sub-cellular fractionation of MCF7 cells demonstrates that RSK1 stably associates with intracellular membranes. $10*10^6$ cells were fractionated according to protocol outlined in A), electrophoresed and immunoblotted.

C) Sub-cellular fractionation of MCF10A cells demonstrates that RSK1 stably associates with intracellular membranes. $10*10^6$ cells were fractionated according to protocol outlined in A), electrophoresed and immunoblotted.

Figure 23

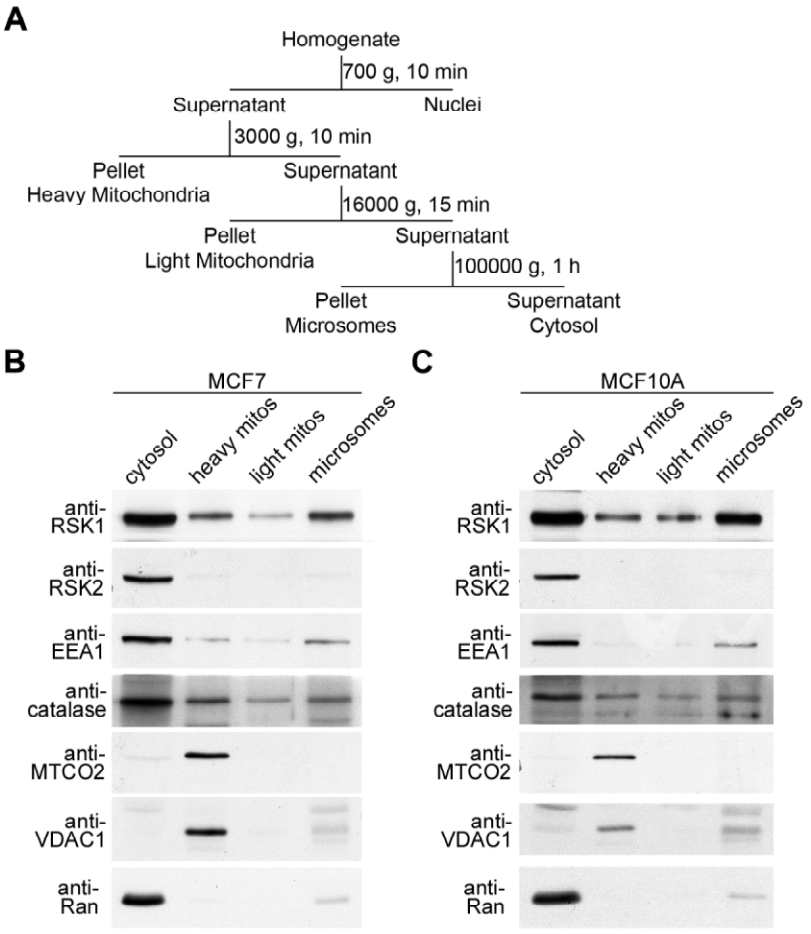
A
Homogenate
700 g, 10 min
Supernatant
Nuclei
3000 g, 10 min
Pellet
Heavy Mitochondria
Supernatant
16000 g, 15 min
Pellet
Light Mitochondria
Supernatant
100000 g, 1 h
Pellet
Microsomes
Supernatant
Cytosol
B
MCF7
cytosol
heavy mitos
light mitos
microsomes
anti-RSK1
anti-RSK2
anti-EEA1
anti-catalase
anti-MTCO2
anti-VDAC1
anti-Ran
C
MCF10A
cytosol
heavy mitos
light mitos
microsomes
anti-RSK1
anti-RSK2
anti-EEA1
anti-catalase
anti-MTCO2
anti-VDAC1
anti-Ran

Given that each fraction was produced by further centrifugation of the supernatant from the previous step, and the pellets were washed to remove contaminations, we concluded that RSK1 was stably associated with membrane-bound compartments in the cells. One of these compartments could be mitochondria, as these organelles were heavily enriched in the heavy mitochondrial fraction. However, it is not the only compartment, as almost the third of the RSK1 signal was found in the microsomes, which do not contain mitochondria. RSK1 distribution does not follow closely any of the markers, suggesting that it does not associate with just one specific compartment. Another potential localization of RSK1 would be the endoplasmic reticulum (ER). The ER stain was not included in the fractionation analysis. A subpopulation of ER membranes is decorated by ribosomes, and RSK has been shown to associate with actively translating ribosomes (Angenstein et al., 1998). ER localization could explain apparent diffuse localization of the fluorescent signal in the overexpression experiments, since the cytosolic RSK1 would overlay the fine reticular pattern of the ER and prevent clear distinguishing of this localization.

In order to investigate if RSK1 association with the membranes is not limited to MCF7 cells, we performed analogous experiments in the MCF10A cell line. Consistent with the results obtained in MCF7 cells, RSK1 was distributed between all four fractions in the cells, and the staining pattern did not closely follow the distribution of mitochondria, microsomes or endosomes (fig. 23C). Therefore, we conclude that in epithelial cell lines a significant proportion of RSK1 is stably associated with intracellular membranes, and this distribution is not shared by RSK2.

Figure 24. RSK1-APEX is properly activated and localized, and functional in MCF7 cells.

A) RSK1-APEX is expressed and properly activated in MCF7 cells. Cells were serum-starved overnight and either untreated or treated with 500 nM PMA in serum-containing medium. The lysates were electrophoresed and immunoblotted.

B) RSK1-APEX follows the sub-cellular distribution of the endogenous protein. MCF7 cells expressing RSK1-APEX were fractionated according to the protocol in fig. 23A, electrophoresed and immunoblotted.

C) RSK1-APEX is capable of biotinylation in intact cells. RSK1-APEX expressing MCF7 cells were treated with or without 500 μM biotin-phenol for 1 h and stimulated with 1 mM hydrogen peroxide for 1 h. Whole-cell lysates were electrophoresed and biotinylations were detected using HRP-conjugated streptavidin. The nitrocellulose membrane was stained with Ponceau S prior to streptavidin binding to assess the total protein amounts.

D) MCF7 cells contain endogenously biotinylated proteins, and RSK1-APEX biotinylates multiple proteins in intact cells. MCF7 cells expressing RSK1-APEX were treated with or without biotin-phenol for 16 h and stimulated with hydrogen peroxide for 15 min. Cells were fixed, immunostained, and imaged using fluorescence confocal microscopy.

Figure 24

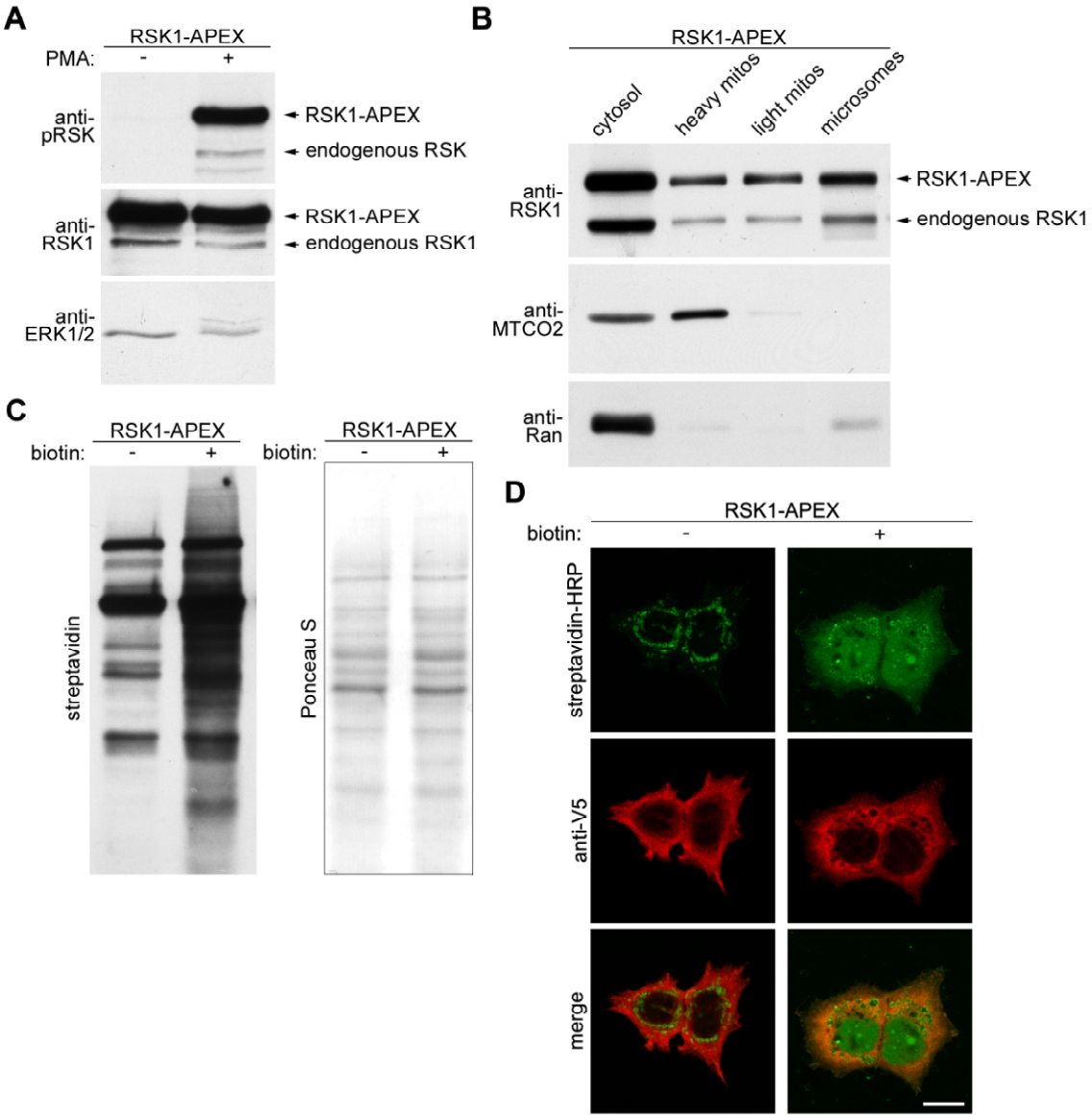
A
RSK1-APEX
PMA:
-
+
anti-pRSK
RSK1-APEX
endogenous RSK
anti-RSK1
RSK1-APEX
endogenous RSK1
anti-ERK1/2
B
RSK1-APEX
cytosol
heavy mitos
light mitos
microsomes
anti-RSK1
RSK1-APEX
endogenous RSK1
anti-MTCO2
anti-Ran
C
RSK1-APEX
biotin:
-
+
streptavidin
RSK1-APEX
biotin:
-
+
Ponceau S
D
RSK1-APEX
biotin:
-
+
streptavidin-HRP
anti-V5
merge

In order to identify the RSK1-specific interacting partners and phosphorylation targets, we decided to employ the APEX-mediated biotin labeling in intact cells (Rhee et al., 2013, Hung et al., 2014). We chose to perform the study using human estrogen receptor positive breast cancer cell line, MCF7. Our previous studies have shown that inhibition of RSK by the small molecule, SL0101, reduces proliferation in this cell line, while the non-transformed breast epithelial cell line, MCF10A, is not sensitive to RSK inhibition (Smith et al., 2005; chapters 3-5 and appendix). RSK1 was ectopically expressed as a fusion protein with the APEX peroxidase attached at the C-terminus. The construct was delivered using a lentiviral platform that allows integration of the cDNA of the overexpressed protein with the host genome (Wiznerowicz and Trono, 2005). RSK1-APEX was expressed at a high level compared to the endogenous RSK1 (fig. 24A). Stimulation with a potent mitogen, PMA, activates RSK, which is evidenced by the phosphorylation of RSK on multiple sites, including Thr359 and Ser363 (Roux et al., 2003). We serum-starved cells overnight to reduce the basal level of RSK activation, and stimulated cells with PMA for 20 minutes. As expected, we did not detect endogenous RSK phosphorylation at Thr359/Ser363 in unstimulated cells. PMA stimulation caused phosphorylation of RSK on Thr359/Ser363. RSK1-APEX was not phosphorylated in unstimulated cells, and a strong phosphorylation signal was detected in RSK1-APEX after PMA stimulation. These results show that RSK1-APEX is active and this activity is properly regulated in cells. For all subsequent experiments, in order to reduce the amount of overexpression of RSK1-APEX, we reduced the time between viral transduction and collection of the lysates.

RSK1-APEX closely followed the distribution of endogenous protein in fractionation experiments (fig. 24B). Therefore, we concluded that in addition to proper activation, RSK1-APEX localizes to the appropriate compartments. It is also important to note that we were able to reduce the level of over-expression of RSK1-APEX to the amounts comparable to those of the endogenous protein. These results together indicate that RSK1-APEX is an appropriate construct to study the properties of the endogenous protein.

We assessed the activity of APEX in cells expressing the RSK1-APEX construct. Initially, the cells were treated with 500 μM biotin-phenol for 1 hour, which is the incubation time reported in previous studies using HEK cells (Hung et al., 2014, Rhee et al., 2013). To ensure maximum signal we stimulated cells with hydrogen peroxide for 1 hour. In cells not treated with biotin-phenol, we detected a number of endogenously biotinylated proteins (fig. 24C). These observations are consistent with the fact that mammalian cells express several enzymes that possess biotin as a prosthetic group in the active site, including pyruvate carboxylase, propionyl-CoA carboxylase and acetyl-CoA carboxylase (Knowles, 1989). A dramatic increase in biotinylation signal was detected in cells expressing RSK1-APEX, confirming that the peroxidase is capable of catalyzing biotinylation of multiple proteins in intact cells (fig. 24C).

We assessed cellular biotinylations by immunofluorescence imaging. In order to detect the ectopically expressed RSK1-APEX we used a V5-tag that is encoded in the linker between RSK1 and APEX. The anti-V5 antibody allowed us to identify cells expressing RSK1-APEX and the intracellular localization of this protein. RSK1 was present in the cytoplasm and did not localize to the nucleus (fig. 24D), which is

consistent with previously reported inability of RSK1 to enter this cellular compartment (Eisinger-Mathason et al., 2008, Heffron and Mandell, 2005). Cytoplasmic stain of RSK1-APEX represented a diffuse pattern with no clear compartmentalization. We then used fluorescently labeled streptavidin to detect biotinylated proteins. Untreated cells displayed a distinct biotinylation staining pattern in a discrete cellular compartment, whereas the majority of cytoplasm and the nucleus were devoid of biotinylated proteins. These results are consistent with the fact that the majority of endogenously biotinylated proteins in mammalian cells reside in the mitochondria, where they participate in various metabolic processes (Coene et al., 2008). When cells were loaded with biotin-phenol and stimulated with hydrogen peroxide, extensive biotinylation was detected, both in the cytoplasm and in the nucleus (fig. 24D). Therefore, we conclude that the RSK1-APEX construct is active and capable of labeling multiple proteins in diverse cellular compartments in intact cells. Since we did not detect RSK1-APEX in the nucleus, the presence of biotinylation in this compartment most likely is due to nuclear translocation of proteins that became labeled in the cytoplasm by RSK1-APEX.

In order to optimize the labeling conditions of RSK1-APEX interacting partners, we tested several different treatment regimens. First, since biotin-phenol is an essential substrate for APEX, we investigated the optimum incubation time for efficient loading of this reagent to the cells. We have already seen that loading with biotin-phenol for one hour, followed by 1 hour of hydrogen peroxide stimulation, was sufficient to induce extensive biotinylation (fig. 24C). We tested the condition in which the pre-incubation with biotin-phenol was extended to 2 hours. In this condition as well, the cellular proteins were extensively biotinylated (fig. 25A).

Figure 25. Biotinylated proteins can be affinity-purified using streptavidin-magnetic beads.

A) 16 h pre-incubation with biotin-phenol ensures maximum coverage of biotinylation pattern in MCF7 cells. RSK1-APEX expressing cells were loaded with biotin-phenol and stimulated with hydrogen peroxide for indicated times. Lysates were electrophoresed and probed with HRP-conjugated streptavidin. Prior to biotin detection, the membrane was stained with Ponceau S.

B) 15 min stimulation with hydrogen peroxide is sufficient to induce maximum coverage of biotinylation pattern in MCF7 cells. RSK1-APEX expressing cells were loaded with biotin-phenol and stimulated with hydrogen peroxide for indicated times. Lysates were electrophoresed and probed with HRP-conjugated streptavidin. Prior to biotin detection, the membrane was stained with Ponceau S.

C) Biotinylated proteins can be eluted off the beads using RapiGest or SDS boiling. RSK1-APEX expressing cells were loaded with biotin-phenol and stimulated with hydrogen peroxide. Biotinylated proteins were affinity-purified using streptavidin magnetic beads, followed by boiling the beads for 10 min with buffers containing indicated detergent. The samples were electrophoresed, stained with Ponceau S and probed with HRP-conjugated streptavidin.

D) Streptavidin beads can be saturated with biotinylated proteins. RSK1-APEX expressing MCF7 cells were treated as in C) and indicated amounts of lysate were incubated with 10 μL of streptavidin bead slurry. The beads were boiled with SDS, electrophoresed and probed with HRP-conjugated streptavidin.

Figure 25

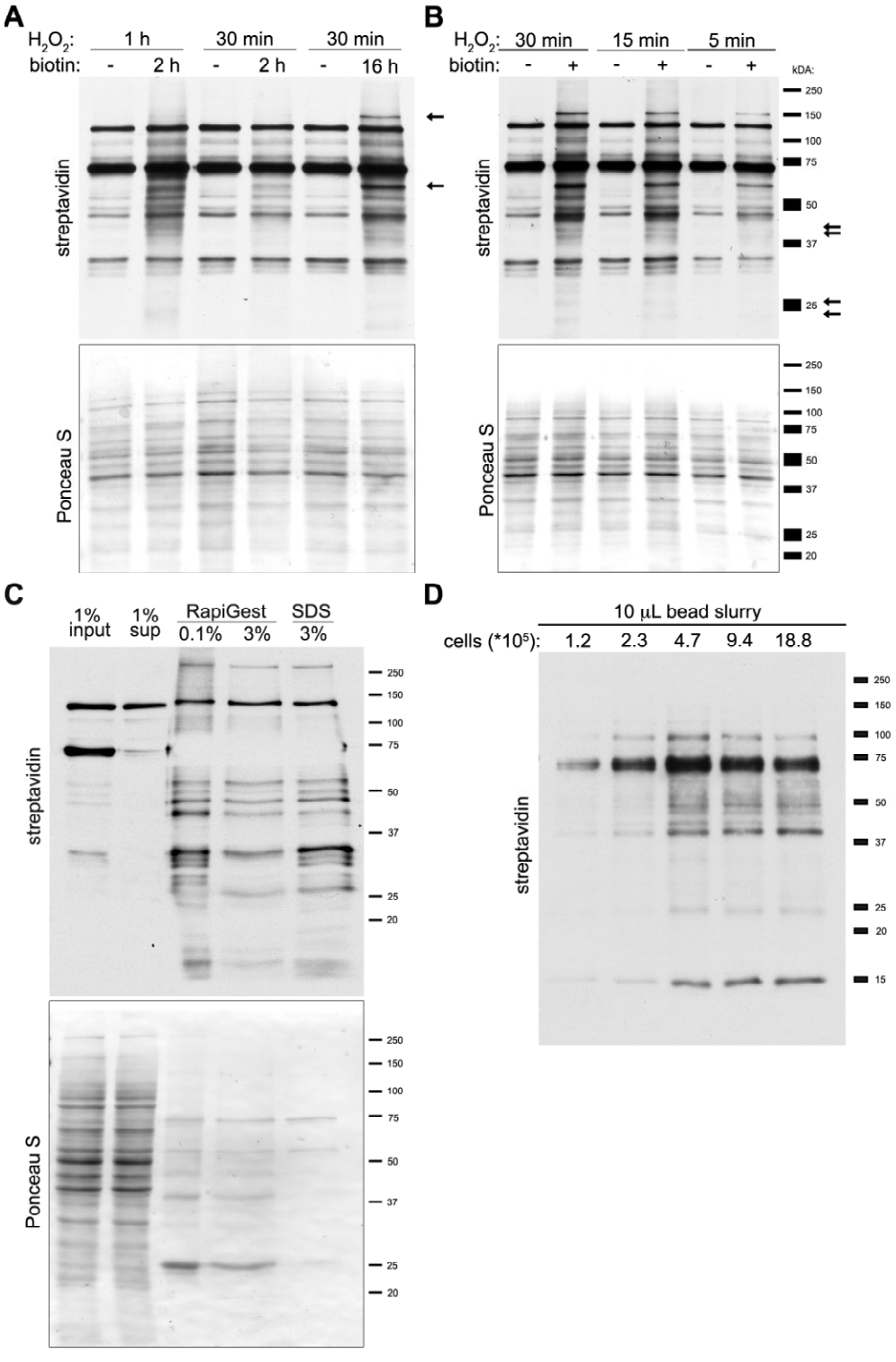
A
H2O2: 1 h 30 min 30 min
biotin: - 2 h - 2 h - 16 h
streptavidin
Ponceau S
B
H2O2: 30 min 15 min 5 min
biotin: - + - + - +
kDA:
250
150
100
75
50
37
25
20
streptavidin
Ponceau S
C
1% input
1% sup
RapiGest 0.1%
SDS 3%
streptavidin
Ponceau S
D
10 µL bead slurry
cells (*10^5): 1.2 2.3 4.7 9.4 18.8
streptavidin
15

We were concerned that a prolonged incubation with hydrogen peroxide can affect the cellular signaling and change the interactome of RSK1, therefore we decided to shorten this treatment condition. When hydrogen peroxide was added to cells for 30 min, it resulted in a decrease in the number and intensity of bands indicating protein biotinylations (fig. 25A). Extending biotin-phenol loading to 16 h prevented that decrease in biotinylation associated with shortened hydrogen peroxide stimulation, suggesting that biotin-phenol levels were the limiting factor in this set of experiments. In addition, we observed the appearance of new bands, and an increase in intensity of some other bands, when biotin-phenol was loaded for 16 hours (fig. 25A, black arrows). Therefore, it appears that this condition allowed for the most extensive detection of RSK1-APEX interacting proteins. We then proceeded to test shorter incubations with hydrogen peroxide, to minimize the cellular perturbations introduced by this oxidative insult. Shortening the hydrogen peroxide treatment to from 30 min to 15 min did not significantly reduce the number of detected bands (fig. 25B). However, when hydrogen peroxide was added for 5 minutes, a number of bands disappeared (fig. 25B, black arrows), and the overall staining intensity was decreased, suggesting that this short incubation was not sufficient to induce full labeling of the RSK1 interactome. Therefore, we identified labeling conditions that ensured sufficient cellular levels of the substrate for APEX, as well as the length of stimulation that induced sufficiently complex and intense labeling.

In order to separate the biotin-labeled proteins from the whole-cell lysate, we decided to employ streptavidin-conjugated magnetic beads. The biotin-streptavidin binding is one of the strongest non-covalent interactions found in nature (Green, 1990),

and in case of wild-type streptavidin can only be disrupted in extremely low pH, high temperature or shear stress (Laitinen et al., 2006, Stayton et al., 1999). Therefore, we chose to boil the beads in 4% SDS containing 2 mM free biotin, as well as in RapiGest, a detergent that can be used for downstream mass spectrometry applications, to elute the proteins off the beads for subsequent Western Blot analysis. We were able to efficiently bind biotinylated proteins and separate them from the rest of the lysate, as evidenced by the lack of biotinylations in the supernatant after the binding reaction (fig. 25C, lane 2). The majority of cellular proteins were still present in the supernatant, which was visualized by the Ponceau S stain of the membrane (fig. 25C, lower panel). We then tested the capacity of the beads to bind biotinylated proteins. 10 μL of bead slurry was incubated with increasing amounts of the lysate from biotin-treated RSK1-APEX expressing cells, corresponding to the indicated cell numbers (fig. 25D). We found that adding more lysate beyond ~$4.7*10^5$ cells did not further increase the amount of bound proteins, indicating that the beads were saturated.

Having identified the conditions for biotin labeling of RSK1-interacting proteins in intact cells, and the conditions for affinity-purifications of these proteins, we proceeded to perform a full-scale experiment, using ~$7*10^6$ cells. The affinity-purified proteins were subjected to on-bead trypsin digestion and subsequent LC/MS analysis, to identify the peptides. We have observed that untreated cells express endogenously biotinylated proteins, and that multiple proteins from untreated cells are pulled down by the streptavidin beads. Therefore, we included a negative control, in which control cells expressing RSK1-APEX were stimulated with hydrogen peroxide but not loaded with biotin-phenol. The beads from both conditions were subjected to the same processing

and analysis, and the resulting peptide lists were cross-referenced. We initially observed a large amount of streptavidin-derived peptides in the tryptic digests, therefore we chose to shorten the length of time trypsin is allowed to digest the peptides on the beads. As a result, we predicted longer peptides, with some trypsin-digest sites remaining uncleaved in the process. Protein mass spectrometry can utilize two methods to generate charged products of peptide fragmentation, the collision-activated dissociation (CAD) and electron transfer dissociation (ETD) (Li and Wysocki, 2012, Syka et al., 2004, Chalkley et al., 2010). The latter method is more amenable to fragmentation and sequencing of larger and more charged peptides (Chalkley et al., 2010). Since we generated incomplete tryptic digests of the proteins on the beads, we utilized both methodologies to analyze the samples by mass spectrometry, and generated two separate peptide lists, one from each method. Therefore, we obtained four lists of peptide fragment spectra.

High-throughput proteomics generates thousands of peptide mass spectra (Washburn et al., 2001). Identification of these peptides requires extensive data analysis, and one of the methods commonly used is the Open Mass Spectrometry Search Algorithm (OMSSA) (Geer et al., 2004). This algorithm compares the experimental peptide mass spectra to those generated by *in silico* digestion of a protein sequence library and assigns the probability of the peptides to be derived from the proteins in that library. The protein hits are scored from the most to the least probable, based on various criteria, such as predicted abundance and homology to other proteins (Geer et al., 2004). We used human protein database based on the latest release of RefSeq to identify the potential proteins. We analyzed the same data against the

database of reverse protein sequences from RefSeq to predict the false discovery rate. We chose the 1% false discovery rate as a significance cutoff in the peptide lists. As a result, we generated four lists of potential protein hits. We then compared the lists of potential proteins from each fragmentation method separately, to subtract the proteins present in the negative control beads from the proteins present in the RSK1-APEX samples. Each method separately yielded 186 proteins present in the RSK1-APEX and not present in the negative control condition (fig. 26A). It is possible that a protein will be present in both conditions, but will be much more abundant in RSK1-APEX samples, compared to the control. In order to account for such possibility we re-assessed the lists of proteins present in both samples. We decided to include in further analysis those proteins that appeared at least 3-fold more abundant in the RSK1 sample, compared to the control, based on the total number of peptides identified in the sample. As a result, we added 23 and 17 proteins to the CAD and ETD lists, respectively. Therefore, we identified 209 and 203 potential RSK1-interacting proteins though either method of peptide analysis. We then compared these two groups to identify proteins found on both lists. As a result, we identified 54 protein candidates that were found through both CAD and ETD methods in the RSK1-APEX sample, and were >3-fold more abundant in this sample than in the control, as measured by the total number of peptides found (fig. 26A).

Since OMSSA is probability-based, it generates a list of potential proteins. These protein hits have to be manually validated to confirm correct identification of the proteins (Nesvizhskii et al., 2007). We manually assessed these protein hits and found that 29 of them represented true hits found in the RSK1-APEX samples and not in the negative

control samples. Further 8 proteins were found in both samples, but were >3-fold more abundant in the RSK1-APEX sample. Taken these results together, we identified 37 potential RSK1-interacting partners (table 1).

In order to better understand the relationship between the identified proteins, we performed functional annotation analysis. This tool allows identifying the gene ontology clusters, or GO-terms, that are significantly enriched in the given list (Harris et al., 2004). As a result, this method of data mining helps predicting what are the common features of the elements in the set. We found that the single most significantly enriched biological function in the list was generation of precursor metabolites and energy. Eight of the 37 proteins were annotated into this cluster (fig. 26B). In terms of cellular components, the most enriched GO-terms were parts of the mitochondrion and ribosome (fig. 26C). Similarly, the molecular function GO-terms contained such terms as the structural constituents of the ribosome and cytochrome C-oxidase. In addition the inorganic cation transmembrane transporter activity was significantly enriched in the protein list. Therefore, the functional annotation strongly suggested that RSK1 might be regulating such cellular processes as protein translation and production of energy, and could perform these functions through changes in electron transport chain activity and inorganic cation transport.

A second approach to analyzing the data was to perform the protein-protein interaction network analysis. We utilized the recently developed online tool that compiles known and predicted interactions between input proteins to generate a functional network (Szklarczyk et al., 2015). Among the 37 proteins we analyzed, we identified 4 putative clusters of interactions (fig. 27).

Table 1. RSK1-APEX-mediated biotinylation identified 37 potential novel RSK1-interacting proteins.

Proteins are sorted by decreasing abundance, as assessed by total number of identified peptides. 54 predicted protein hits were manually validated for presence of peptides in the control and RSK1-APEX samples. RefSeq accession # indicates protein identity predicted by OMSSA. # of validated peptide hits indicates total number of peptides corresponding to this protein found in the peptide spectra. Numbers in brackets indicate number of peptides belonging to this protein found in the negative control sample. Red indicates proteins containing putative RSK phosphorylation sites, RxRxxS/T, or RRxS/T, where R can also be K. Green indicates no consensus RSK phosphorylation sites.

Table 1

RefSeq Accesion #	gene symbol	UniProt Protein Name	# of validated peptide hits
NP_001123630	MYO1B	Unconventional myosin-Ib	5 hits
NP_003365	VDAC1	Voltage-dependent anion-selective channel protein 1	5 hits
NP_001091868	COPA	Coatomer subunit alpha	3 hits
NP_001672	ATP2A2	Sarcoplasmic/endoplasmic reticulum calcium ATPase 2	3 hits
NP_054828	ATAD2	ATPase family AAA domain-containing protein 2	3 hits
NP_000217	KRT9	Keratin, type I cytoskeletal 9	2 hits
NP_001104792	DDX54	ATP-dependent RNA helicase DDX54	2 hits
NP_001129243	RPN2	Dolichyl-diphosphooligosaccharide--protein glycosyltransferase subunit 2	2 hits
NP_001153682	SLC25A13	Calcium-binding mitochondrial carrier protein Aralar2	2 hits
NP_001171712	VDAC2	Voltage-dependent anion-selective channel protein 2	2 hits
NP_001853	COX5B	Cytochrome c oxidase subunit 5B, mitochondrial	2 hits
NP_002287	LBR	Lamin-B receptor	2 hits
NP_000508	HBA2	Hemoglobin subunit alpha	1 hit
NP_001137457	BANF1	Barrier-to-autointegration factor	1 hit
NP_001161803	NDUFB4	NADH dehydrogenase [ubiquinone] 1 beta subcomplex subunit 4	1 hit
NP_001267718	SURF4	Surfeit locus protein 4	1 hit
NP_001284494	UQCRH	Cytochrome b-c1 complex subunit 6, mitochondrial	1 hit
NP_001854	COX6B1	Cytochrome c oxidase subunit 6B1	1 hit
NP_002626	SLC25A3	Phosphate carrier protein, mitochondrial	1 hit
NP_004364	COX6A1	Cytochrome c oxidase subunit 6A1, mitochondrial; Cytochrome c oxidase subunit 6A, mitochondrial	1 hit
NP_006383	NOP56	Nucleolar protein 56	1 hit
NP_006398	ARL6IP5	PRA1 family protein 3	1 hit
NP_038479	MYOF	Myoferlin	1 hit
NP_057049	NDUFA13	NADH dehydrogenase [ubiquinone] 1 alpha subcomplex subunit 13	1 hit
NP_060352	CLN6	Ceroid-lipofuscinosis neuronal protein 6	1 hit
NP_079406	HKDC1	Putative hexokinase HKDC1; Hexokinase	1 hit
NP_115714	LLPH	Protein LLP homolog	1 hit
NP_115784	BAZ1B	Tyrosine-protein kinase BAZ1B	1 hit
NP_940888	RPL7L1	60S ribosomal protein L7-like 1	1 hit
NP_000179	HK1	Hexokinase-1; Hexokinase	18(2)
NP_000958	RPL3	60S ribosomal protein L3	20(5)
NP_001030168	RPL14	60S ribosomal protein L14	8(2)
NP_002408	MKI67	Antigen KI-67	15(5)
NP_056474	RSL1D1	Ribosomal L1 domain-containing protein 1	6(2)
NP_000986	RPL34	60S ribosomal protein L34	3(1)
NP_000987	RPL35A	60S ribosomal protein L35a	4(1)
XP_005252898	MTCH2	Mitochondrial carrier homolog 2	4(1)

Figure 26. 37 potential RSK1-interacting proteins are enriched for constituents of ribosomes and mitochondrial membranes.

A) Analysis of lists of potential proteins generated by OMSSA search from the peptide spectra of RSK-APEX and negative control samples identified 54 most likely interacting partners of RSK1.

B) Biological function gene ontology analysis found a single significantly enriched cluster, the generation of precursor metabolites and energy, containing 8 proteins, in the list of 37 manually validated potential RSK1 interacting partners. Significance cut-off was set at Benjamini <0.05, which is the most stringent criterion in statistical analysis of functional annotation.

C) 37 potential RSK1-iteracting partners are localized to mitochondrial and ER membranes, and to ribosomes. Cellular components and molecular functions gene ontology analysis several significantly enriched clusters in each category. Significance cut-off was set at Benjamini <0.05, and the bar graphs present the –log(p) value for each cluster.

Figure 26

A

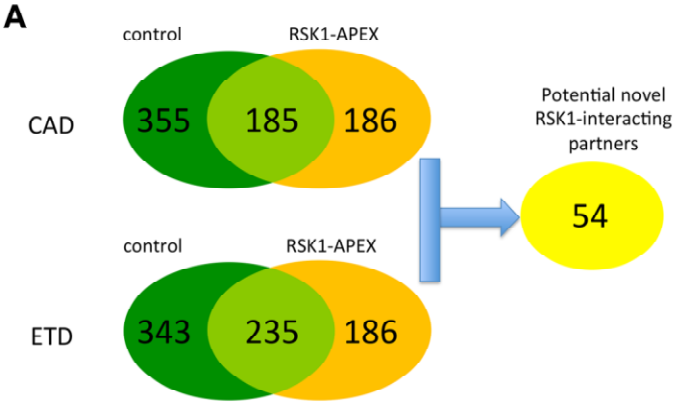

B

cluster name	p value	Benjamini
GO:0006091~generation of precursor metabolites and energy	6.79E-06	0.04

ID	Gene Name
NDUFA13	NADH dehydrogenase (ubiquinone) 1 alpha subcomplex, 13
COX6A1	cytochrome c oxidase subunit VIa polypeptide 1
HK1	hexokinase 1
HKDC1	putative hexokinase HKDC1
NDUFB4	NADH dehydrogenase (ubiquinone) 1 beta subcomplex, 4
SLC25A3	solute carrier family 25 (mitochondrial carrier; phosphate carrier), member 3
SLC25A13	solute carrier family 25, member 13 (citrin)
UQCRH	ubiquinol-cytochrome c reductase hinge protein-like

C

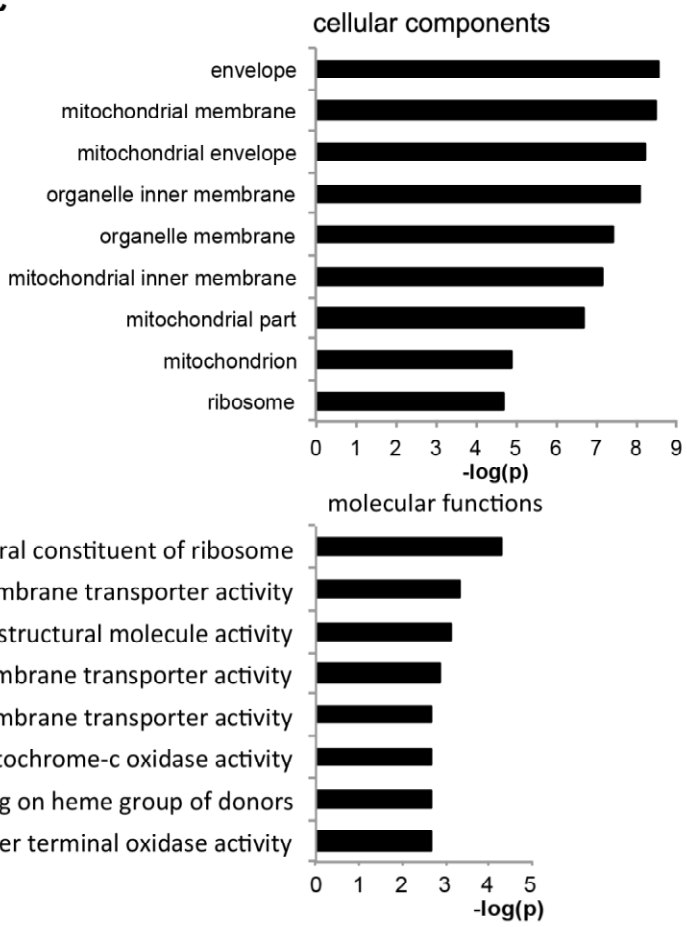

Figure 27. String network analysis identifies 4 putative functional clusters among 37 proteins identified through mass spectrometry.

Each sphere represents one protein from the list of potential RSK1-interacting partners. The thickness of the line connecting the spheres indicates the strength of connection between proteins, based on published and predicted physical and functional interactions.

Figure 27

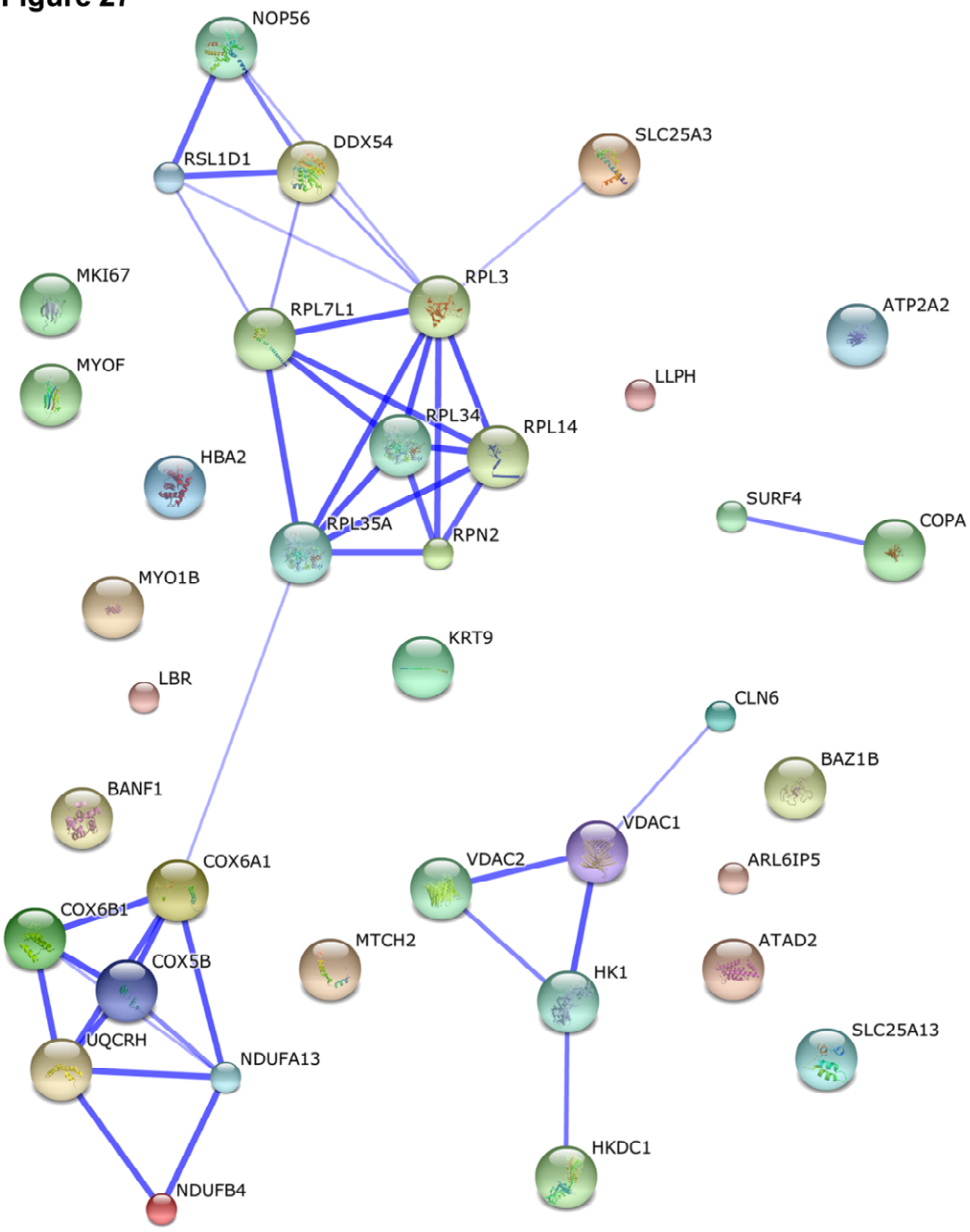
NOP56
DDX54
RSL1D1
SLC25A3
MKI67
RPL3
RPL7L1
ATP2A2
MYOF
LLPH
RPL34
RPL14
HBA2
SURF4
COPA
RPL35A
RPN2
MYO1B
KRT9
LBR
CLN6
BAZ1B
BANF1
VDAC1
COX6A1
VDAC2
ARL6IP5
COX6B1
MTCH2
ATAD2
COX5B
HK1
UQCRH
SLC25A13
NDUFA13
HKDC1
NDUFB4

One cluster consisted of 5 large ribosomal subunit proteins, as well as RPN2, an essential component of ER-associated ribosomes (Crimaudo et al., 1987, Fu and Kreibich, 2000). The second cluster closely linked to the large-ribosomal subunit was a group of 3 proteins involved in ribosome biogenesis, NOP56, RSL1D1 and DDX54. The third cluster consisted of 6 proteins found in the mitochondrial electron transport chain. Finally, the forth cluster contained mitochondrial outer membrane proteins, VDAC1/2, HK1 and HKDC1, as well as an ER-membrane-bound protein CLN6. Taken these results together, the pathway analysis suggested that RSK1 may be involved in regulation of ribosome biogenesis, ER-associated ribosomes, and mitochondrial membrane components. These results are in agreement with the gene ontology analysis presented in fig. 26.

Since RSK1 is a kinase, we hypothesized that among those proteins we could identify the substrates for RSK-mediated phosphorylation. The consensus RSK-phosphorylation motif is known, therefore we analyzed the protein sequences of all 37 hits and identified those that contain this motif. Of 37 proteins, 25 contained at least one potential RSK phosphorylation site (table 1). Therefore, it appears that a large proportion of the identified proteins could be regulated by direct phosphorylation by RSK1.

Taken all the results together, we conclude that RSK1 stably associates with intracellular membranes and potentially interacts with a number of proteins involved in ribosome and mitochondrial synthesis and function. Association of RSK1 with ribosomes has previously been suggested (Angenstein et al., 1998). However,

association of RSK1 with mitochondrial membranes and the ribosome biogenesis machinery represents a novel finding.

6.4. Discussion

We report the first use of APEX labeling to identify potential interacting partners of a protein kinase. We also report the first use of on-bead digestion of streptavidin affinity purified proteins in the APEX method. Previous reports have used in-gel digestion of proteins boiled off the beads with SDS. In previous studies APEX was fused to a mitochondrial localization signal to label all proteins found in this tight cellular compartment (Hung et al., 2014, Rhee et al., 2013). These studies were not designed to interrogate interacting partners of a particular protein, but rather enrich for all proteins found in a given cellular compartment. Incidentally, endogenously biotinylated proteins are known to almost exclusively localize to the mitochondria, and here we confirm this observation using fluorescently-labeled streptavidin for immunofluorescence (fig. 24D). As a result, the endogenously biotinylated proteins were expected to be identified in the procedure and did not confound the interpretation of the results. A new study using a specific APEX fusion protein has very recently been reported (Lam et al., 2015). However, this protein was not used for a high-throughput proteomics study.

We were able to identify RSK1-interactions with the ribosomal components, which is consistent with previous reports. In addition, we identify potential new associations of RSK1 with mitochondria and the endoplasmic reticulum. None of the 37 proteins has ever been directly shown to interact with and be regulated by RSK1. Of those, two proteins, CLN6 and NOP56, were previously identified as potential RSK

substrates through another high-throughput proteomics study (Galan et al., 2014). In this study, RSK1 and RSK2 were either inhibited using BI-D1870, or silenced using siRNA, in HEK293 cell line and a melanoma cell line A375. The changes in protein phosphorylation were analyzed using SILAC, to identify proteins whose phosphorylation status changes upon loss of RSK1/2 expression or activity. Since both RSK1 and RSK2 were silenced and inhibited together, the study did not reveal which isoform was responsible for the observed change in phosphorylation status. CLN6 and NOP56 were not experimentally validated in that study and their role in the context of RSK signaling remains unknown.

Further optimization of the high-throughput proteomics method described in this chapter should yield more extensive list of potential novel RSK1-interacting protein, beyond the 37 proteins we identify. One major area for improvement is reducing the number of non-specific protein hits. We have detected >500 potential proteins binding to the beads in cells not treated with biotin-phenol. Since OMSSA analysis is based on probabilities, this large number could be due to relative low abundances of peptides, lowering the dynamic range of the detection. In fact we did detect a very high abundance of streptavidin-derived peptides, compared to all the other peptides. We speculate that limiting the amount of time the beads are allowed to digest with trypsin could solve this issue. We offer two alternative strategies to obtain this goal. The first possibility is to perform a very brief trypsin digest on the beads, to liberate only the major peptides, followed by separation of these peptides from the beads and re-digestion of the supernatant with trypsin to further cleave proteins into fragments compatible with downstream mass spectrometry analysis. The second option is to boil

the proteins off the beads using the mass spectrometry-compatible detergent RapiGest. This detergent can be decomposed by lowering pH of the solution, which generates the water-soluble denatured protein fraction and a separate hydrophobic phase that can be easily separated. Such denatured proteins in mass spectrometry-competent buffer can then be processed by trypsin and subjected to further analysis.

Chapter 7

RSK regulation of cancer bioenergetics

Summary

The RSK family of Ser/Thr protein kinases consists of four members that share very high sequence homology and are products of separate genes. RSKs are activated by the extracellular signal regulated kinase ERK1/2 in response to various stimuli, including growth factors, cytokines and neurotransmitters. In addition to known functions in promoting survival, proliferation and motility, RSK has been suggested to influence cellular metabolism. RSK was shown to phosphorylate proteins involved in energy homeostasis, such as an mTORC1 component Raptor, kinase Lkb1 and mitochondrial protein Bad. However, the significance of these interactions in the context of metabolism has not been reported. We previously found that breast cancer cells rely on RSK for proliferation, while non-transformed cells do not. Global changes in cellular metabolism are one of the hallmarks of cancer. We hypothesized that the reliance of RSK on proliferation could be associated with the differences in cellular metabolism. We found that RSK inhibition caused a reduction in mitochondrial oxidative phosphorylation, and this effect was specific to transformed cells. Therefore, we hypothesize that inhibition of RSK offers a therapeutic strategy to target metabolic transformation in breast cancer.

7.1. Introduction

Changes in cellular metabolism have long been recognized as one of the hallmarks of cellular transformation (Hanahan and Weinberg, 2011). Early studies have shown that cancer cells derive a significant fraction of their cellular ATP from glycolysis even in the presence of oxygen, a phenomenon known as Warburg effect (Hsu and Sabatini, 2008). However, the Warburg effect does not indicate that cancer cells no longer rely on their mitochondria for survival. It is thought that the decrease in mitochondrial ATP synthesis is caused by depletion of metabolic intermediates from the mitochondria. These metabolites are utilized in the anabolic processes to fuel rapid proliferation (Hanahan and Weinberg, 2011). This phenomenon of metabolic transformation has been proposed to constitute novel therapeutic target in cancer treatment (Tennant et al., 2010).

RSK is a family of four Ser/Thr protein kinases activated by the extracellular signal regulated kinases 1/2 (ERK1/2) (Carriere et al., 2008b). RSK has been extensively studied in the context of pro-survival and pro-growth signaling in a number of cancers, as well as in normal cell homeostasis (Pasic et al., 2011, Romeo et al., 2012, Anjum and Blenis, 2008). Of the four RSK isoforms, only a RSK2 knock-out mouse has been reported in the literature (Laugel-Haushalter et al., 2014). This knock-out displayed a number of defects in metabolism, including lipodystrophy, insulin resistance and increased glycogen synthesis (El-Haschimi et al., 2003, Dufresne et al., 2001). However, the exact mechanism of RSK2-mediated regulation of organismal metabolism has not been elucidated. RSK has been shown to phosphorylate many proteins with known functions in regulating cellular metabolism. For example, RSK was

reported to phosphorylate Lkb1 on residue Ser341 (Sapkota et al., 2001). However, the physiological significance of this phosphorylation in the context of cellular metabolism was not assessed. Later studies revealed that Ser341 phosphorylation of Lkb1 did not affect its ability to interact with the plasma membrane or phosphorylate its downstream target involved in regulation of metabolism, AMPK (Fogarty and Hardie, 2009, Houde et al., 2014). In addition to Lkb1, RSK was shown to phosphorylate GSK and mTOR component Raptor (Carriere et al., 2008a, Sutherland et al., 1993). However, in none of these studies the changes of metabolism in response to RSK perturbation were explored. Therefore, it remains unknown what is the role of RSK in regulating cellular metabolism.

We have developed the first potent, selective inhibitor of RSK, SL0101 (Smith et al., 2005). This inhibitor is remarkably specific for its target (Sapkota et al., 2007), and therefore has been proposed as a promising lead compound for developing RSK inhibitor suitable for *in vivo* studies (chapters 2-5 and appendix). Based on the evidence in the literature that RSK could regulate metabolism, we set out to characterize the effects of inhibiting this kinase on the metabolism of both non-transformed and transformed cell lines. We have previously found that the human estrogen receptor-positive breast cancer cell line, MCF7, was sensitive to RSK inhibition, while a non-transformed human breast epithelial cell line, MCF10A, was not. Therefore, we hypothesized that RSK could differentially regulate cellular metabolism in transformed vs. non-transformed cells.

We have found that RSK inhibition caused a reduction in mitochondrial oxygen consumption in breast cancer cell lines. Consistent with the differences in the effects of

SL0101 on proliferation of normal and breast cancer cell lines, we found that in non-transformed cells RSK inhibition did not decrease oxygen consumption. We observed decreases in mitochondrial superoxide generation, membrane potential and calcium levels in MCF7 cells, consistent with a defect in mitochondrial respiration. Our results provide the first evidence of the differential role of RSK in regulating cellular metabolism in transformed cells. We hypothesize that inhibiting RSK with SL0101 and its analogs could offer therapeutic strategy to specifically target metabolic alterations in cancer.

7.2. Materials and methods

Reagents and antibodies

Mitochondrial stress test kits were purchased from Seahorse Bioscience (North Billerica, MA). BI-D1870 was purchased from Enzo Life Sciences (Farmingdale NY). SL0101 and its enantiomer were synthesized by George O'Doherty (Northeastern University, Boston, MA). 200 mM glutamine and 100 mM pyruvate solutions, as well as glucose and ionomycin were purchased from Sigma (St. Louis, MO). MitoSox Red, TMRM, Rhod-2 and fibronectin from human plasma were purchased from Life Technologies (Carlsbad, CA).

Cell culture and treatments

MCF7, MCF10A and T47D cell lines were cultured according to the instructions from the American Type Culture Collection. For live-imaging experiments, cells were passaged and seeded at 50,000 cells onto 2-well borosilicate glass LabTek slides (Fisher, Rochester, NY). 2 days later, the treatments were commenced. For MitoSox Red imaging, cells were washed 3 times with phosphate-buffered saline (PBS) and

vehicle or 100 μM SL0101 were loaded in serum-free medium for 2 hours. The medium was changed for inhibitor- or vehicle-containing medium with 5 μM MitoSox Red and incubated for 10 minutes. Cells were then washed and fresh serum-free medium with or without inhibitor was added. Cells were imaged by confocal microscopy immediately after the removal of MitoSox Red from the medium.

For TMRM imaging, cells were washed 3 times with PBS and incubated with DMSO or 100 μM SL0101 in serum-free medium without glucose for 2 hours. 1.5 h into the incubation with the inhibitor, TMRM was added at the final concentration of 20 nM. 2 hours into the inhibitor treatment, cells were imaged using confocal microscopy.

For Rhod-2 imaging, cells were washed 3 times with PBS, and 5 μM Rhod-2 in serum-free medium without glucose was added for 50 min. Rhod-2-containing medium was removed and fresh serum-free glucose-free medium with or without 100 μM SL0101 was added. 2 hours later, cells were imaged using confocal microscopy. For ionomycin treatment, cells were treated as described above, and ionomycin was added at final concentration of 20 ng/mL. 10 minutes later, cells were imaged using confocal microscopy.

Mitochondrial stress tests

Mitochondrial stress tests were performed according to manufacturer's protocol. Briefly, cells were passaged and seeded onto 12-well or 96-well seahorse assay plates (Seahorse Bioscience, North Billerica, MA). 96-well plates were coated with 80 μL/well of 5 μg/mL human fibronectin in PBS prior to cell seeding. Cells were seeded at 30,000 or 16,000 cells/well in a 12-well and 96-well plate, respectively, which was confirmed to

be within the linear range of the basal respiration rate for each cell line. For 12-well plates, cells were collected with trypsin and seeded in full growth medium with serum, and 16 hours later medium was changed for unbuffered base medium (pH 7.4) with glucose, glutamine and pyruvate, and with or without the inhibitors. The measurements of oxygen consumption were conducted 2 hours later on Seahorse Xf24 analyzer. For 96-well plates, cells were collected with 10 mM EDTA in PBS and seeded in unbuffered serum-free medium with indicated nutrients. 16 h later, DMSO or 100 μM SL0101 were added in the medium with appropriate nutrients. 1 hour later, the measurements of oxygen consumption rate wee commenced using Seahorse Xf96e analyzer.

7.3. Results

In order to investigate whether RSK is involved in regulation of cellular metabolism, we undertook the effort to characterize the changes in cellular respiration in response to RSK inhibition. To investigate the role of RSK in regulating mitochondrial oxidative phosphorylation the estrogen receptor positive breast cancer cell line, MCF7, was treated with a series of mitochondrial inhibitors and changes in oxygen consumption rate were measured in response to these inhibitors (Brand and Nicholls, 2011). First, to determine basal respiration, the basal oxygen consumption rate was measured in cells incubated in DMEM medium containing glucose, pyruvate and glutamine (fig. 28A). The presence of all three basic nutrients was intended to ensure that the mitochondria operated at the optimum capacity. In the next step oligomycin was added to the medium to inhibit ATP synthase. Blocking the activity of the ATP synthase by oligomycin treatment caused a decrease in oxygen consumption.

The difference between the initial oxygen consumption and the levels of oxygen consumption induced by oligomycin represented oxygen consumption associated with mitochondrial ATP synthesis. The addition of a mitochondrial uncoupler FCCP allowed the electron transport chain to operate at its maximum capacity independent of the activity of the ATP synthase. As a result, an increase in the oxygen consumption was observed. This increase represented the maximum respiratory capacity. Addition of the combination of rotenone and antimycin A, the inhibitors of electron transport chain complexes I and III, respectively, completely blocked electron transport chain, which resulted in an almost complete abrogation of oxygen consumption. The remaining rate of oxygen consumption was therefore associated with non-mitochondrial oxygen consumption. Initial OCR represented basal respiration rate, while OCR following FCCP addition defined the maximum respiration.

Inhibition of RSK by SL0101 caused a 30% reduction in both basal and maximal respiration in MCF7 cells (fig. 28B). In addition, proton leak was increased upon SL0101 treatment. Proton leak can occur through two general mechanisms. First, electrons can pass across the mitochondrial membranes through the protein channels, such as uncoupling proteins (UCP) or the adenine nucleotide translocase (ANT) (Jastroch et al., 2010, Busiello et al., 2015). Alternatively, protons can be carried directly through the mitochondrial membranes, as in the case of the protonophore FCCP (Jastroch et al., 2010). To test whether SL0101 acts as a mitochondrial protonophore, we used an enantiomer of SL0101 (ent-SL0101, fig. 28C). This compound has the same chemical structure as SL0101, but due to a reverse chirality on the anomeric carbon it is biologically inactive (chapter 5).

Figure 28. Inhibition of RSK decreases mitochondrial oxidative phosphorylation in breast cancer cell lines, but not in a non-transformed cell line.

A) Schematic representation of the mitochondrial stress test assay.

B) SL0101 decreases basal and maximal OCR by 30% in the breast cancer cell line MCF7. Combined mean ±SD, N=2 in ≥ quadruplicate, normalized to control basal respiration. * $p<0.01$ Student's t-test

C) Chemical structures of SL0101, ent-SL0101 and cyclitol compound 1

D) Ent-SL0101 does not affect OCR in the breast cancer cell line MCF7. Combined mean ±SD, N=2 in ≥ quadruplicate, normalized to control basal respiration. * $p<0.01$ Student's t-test compared to the control

E) cyclitol-SL0101 [1] decreases basal and maximal OCR in MCF7 cell line by 30%, consistent with the effects of SL0101. Representative graph of N=2, mean ±SD in 12 replicates. * $p<0.01$ (SL0101) in Student's t-test compared to the control; ^ $p<0.01$ ([1]) in Student's t-test compared to the control

F) BI-D1870 decreases basal and maximal OCR by 30% in the breast cancer cell line MCF7. Combined mean ±SD, N=2 in ≥ quadruplicate, normalized to control basal respiration. * $p<0.01$ Student's t-test

G) SL0101 decreases basal and maximal OCR by 30% in the breast cancer cell line T47D. Combined mean ±SD, N=2 in ≥ quadruplicate, normalized to control basal respiration. * $p<0.01$ Student's t-test

H) SL0101 does not affect OCR in the non-transformed breast epithelial cell line MCF10A. Combined mean ±SD, N=2 in ≥ quadruplicate, normalized to control basal respiration. * $p<0.01$ Student's t-test compared to the control

Figure 28

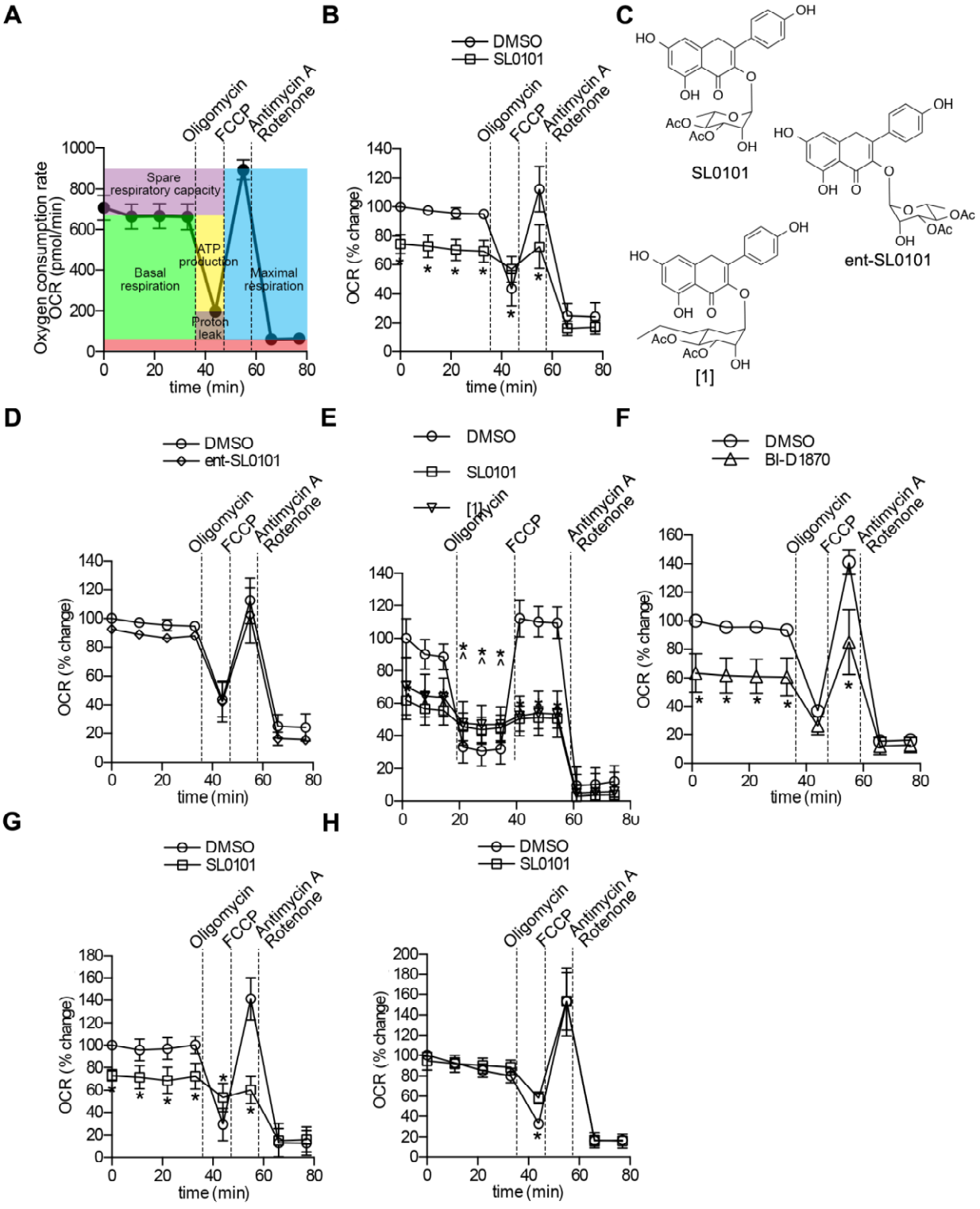
A
B
C
D
E
F
G
H
Oligomycin
FCCP
Antimycin A
Rotenone
Oxygen consumption rate OCR (pmol/min)
Spare respiratory capacity
Basal respiration
ATP production
Proton leak
Maximal respiration
time (min)
DMSO
SL0101
OCR (% change)
SL0101
ent-SL0101
[1]
DMSO
ent-SL0101
DMSO
SL0101
[1]
DMSO
BI-D1870
DMSO
SL0101
DMSO
SL0101

We observed no decrease in oxygen consumption in cells treated with ent-SL0101 (fig. 28D). Therefore, we conclude that SL0101 does not act as a protonophore. A hexose sugar ring is a structural component of both SL0101 and its enantiomer. It is conceivable that these two chemicals could interfere with sugar uptake or utilization in cells independent of their ability to affect RSK activity. To address this possibility we tested a SL0101 derivative in which the rhamnose ring was replaced with a corresponding cyclitol ring (compound [1] in fig. 28C). This compound is a potent inhibitor of RSK both *in vitro* and in cell-based assays (chapter 5). Cyclitol-derivative of SL0101 reduced mitochondrial oxygen consumption in MCF7 cells to the same extent as its parent compound (fig. 28E). Consistent with the effects of SL0101, cyclitol-SL0101 also caused an increase in proton leak. Taken these results together, we conclude that inhibition of RSK caused decreases in basal and maximal OCR, and an increase in proton leak. Since SL0101 is not a protonophore, RSK inhibition could induce an increase in proton leak through the action of mitochondrial ion channels.

To further support the role of RSK signaling in the regulation of mitochondrial oxygen consumption, a structurally unrelated inhibitor of RSK, BI-D1870, was used. Treatment of MCF7 cells with this compound caused a 30% reduction in both basal and maximal respiration (fig. 28F), which is consistent with the effects of SL0101. However, BI-D1870 did not increase proton leak. It is important to note that BI-D1870 and SL0101 have different selectivities against RSK isoforms. BI-D1870 inhibits all four isoforms of RSK, while SL0101 is selective for RSK1/2 (chapter 2). Therefore, it is possible that the biological effects of one of these compounds would not be fully recapitulated by the other inhibitor. SL0101 and BI-D1870 both caused a reduction in basal and maximal

oxygen consumption, indicating that RSK1/2 stimulates these two respiratory rates. It is possible that RSK1/2 is a negative regulator of proton leak, while RSK3/4 counteracts this action of RSK1/2. In such case, inhibition of RSK1/2 would trigger RSK3/4 dependent increase in proton leak. However, BI-D1870 would block the ability of RSK3/4 to enhance proton leak upon RSK1/2 inhibition.

We tested the effects of SL0101 in another ER-positive breast cancer cell line, T47D. Consistent with the results obtained in MCF7 cells, treatment of T47D cells with SL0101 reduced both basal and maximal oxygen consumption rates by 30% (fig. 28G). In addition, proton leak was also increased in these cells upon SL0101 treatment. These results indicated that the role of RSK in regulating mitochondrial function is not unique to MCF7 cells.

We have previously observed that RSK inhibition reduced proliferation of MCF7 cells, but a non-transformed breast epithelial cell line, MCF10A, was not sensitive to a loss of RSK activity (Smith et al., 2005; chapters 3-5 and appendix). We hypothesized that the differential response of cancer vs. non-transformed cell lines could, at least in part, be due to a differential effect of RSK inhibition on mitochondrial oxidative phosphorylation. In order to address this hypothesis we performed a mitochondria stress test in MCF10A cells treated with SL0101. RSK inhibition did not reduce basal and maximal oxygen consumption MCF10A cell line (fig. 28H), which is consistent with the lack of inhibition of proliferation in this cell line upon RSK inhibition. Intriguingly, SL0101 treatment caused a significant increase in proton leak in MCF10A cells. However, SL0101 does not reduce proliferation of this cell line. Proton leak results in a decrease in the efficiency of ATP synthesis in the mitochondria (Jastroch et al., 2010).

However, ATP can be produced by other metabolic processes, such as glycolysis (Jastroch et al., 2010, Fernie et al., 2004). Therefore, although proton leak seems to be commonly increased upon RSK inhibition, the biological significance of this effect remains unknown.

Taken together, these data demonstrate that in breast cancer cell lines RSK promotes mitochondrial respiration. However, RSK signaling is not involved in regulating oxidative phosphorylation in non-transformed breast cells. We have discovered that SL0101 is an isoform-specific inhibitor of RSK1/2, as it does not inhibit RSK3 and RSK4 (chapter 2). Here, we observed the same reduction in mitochondrial oxygen consumption induced by both SL0101 and another RSK inhibitor, BI-D1870, in breast cancer cell lines. Therefore, the observed effects on basal and maximal mitochondrial respiration were due to inhibition of RSK1/2, and did not involve RSK3 and RSK4. These results uncovered a novel function of RSK1/2 in regulating cancer cell metabolism. This discovery opens a new possibility of targeting breast cancer by specific inhibition of cancer bioenergetics. It remains to be determined which of the two isoforms of RSK1/2 is responsible for the observed mitochondrial phenotypes.

The experiments described above were conducted in the presence of glucose, glutamine and pyruvate. All 3 of these substrates enter the tricarboxylic acid (TCA) cycle in the mitochondria (Fernie et al., 2004). We sought to determine whether inhibition of RSK1/2 resulted in a decrease in utilization of one of the nutrients to a greater extend than the others. First, we treated cells with full medium, or basal medium with glutamine alone (fig. 29A). In control cells, glutamine alone induced the same basal OCR as the full medium, but maximal OCR was reduced, compared to the full medium.

In the presence of pyruvate alone, basal OCR was increased by 60%, compared to full medium, as was equal to the maximal OCR in this condition (fig. 29B). Glucose alone maintained basal OCR levels comparable to those of the full medium, but was not sufficient to increase the maximal OCR above the basal levels (fig. 29C). In all 3 conditions, SL0101 suppressed basal OCR in the presence of individual substrate by 20%, compared to the full medium control. In addition, pyruvate-stimulated increase in basal OCR above the levels in full medium was blocked by SL0101 (fig. 29B). IN the presence of SL0101, each substrate alone was unable to bring the maximal OCR above the basal levels in this condition. The presence of all 3 substrates in combination with SL0101 was only sufficient to raise the maximal OCR to the basal levels in the full medium control. In summary, SL0101 inhibited utilization of all 3 substrates, and the biggest decrease in basal OCR was in the presence of pyruvate alone. Therefore, inhibition of RSK caused a decrease in the utilization of all 3 substrates individually, and adding back all those substrates was not sufficient to rescue the maximal OCR levels.

We sought to determine if the decrease in oxidative phosphorylation seen upon loss of RSK1 and RSK2 activity was sufficient to trigger a biologically relevant change in cellular metabolism. Mitochondrial respiration is coupled to ATP synthesis through the proton gradient generated by the electron transport chain (ETC) in the inner mitochondrial membrane (Dimroth et al., 2003, Dimroth et al., 2000). ETC is a supercomplex composed of four complexes transporting electrons from NADH and succinate onto molecular oxygen, with a simultaneous exclusion of protons from the mitochondrial matrix. A small amount of electrons carried by complexes I and III can prematurely leak to molecular oxygen to generate superoxide, a main mitochondrial

reactive oxygen species. Therefore, superoxide is a by-product of mitochondrial respiration (Drose and Brandt, 2012). Since loss of RSK activity caused a decrease in oxygen mitochondrial respiration, we hypothesized that the amount of mitochondrial superoxide generated by cells was changed. To test this possibility, a mitochondria-localized fluorescent superoxide sensor MitoSox Red was used. This indicator is rapidly and selectively targeted to mitochondria in live cells, where is specifically reacts with superoxide, but not other reactive oxygen species. The chemical modification caused by superoxide activates red fluorescence, which can be measured by confocal microscopy. Consistent with the role of RSK in stimulating oxygen consumption by mitochondria, SL0101 treatment in MCF7 cells caused an 80% reduction in MitoSox Red fluorescence intensity (fig. 30A).

Maximal OCR rate defines a condition in which the ETC can operate at its maximum capacity (Brand and Nicholls, 2011). RSK1/2 inhibition caused a decrease in this level, suggesting that loss of RSK1/2 activity reduced the function of the ETC. Since ETC generates the proton gradient across the mitochondrial membrane, we hypothesized that SL0101 treatment caused a decrease this membrane potential. In order to measure the changes in mitochondrial proton gradient we employed a fluorescent indicator, tetramethylrhodamine methyl ester (TMRM). This fluorescent dye accumulates in the mitochondria in a process dependent on the mitochondrial membrane potential. We performed the experiment is MCF7 cells treated with SL0101 and loaded with 20 nM TMRM.

Figure 29. RSK inhibition reduces oxidative phosphorylation in the presence of each of the substrates.

A) SL0101 reduces basal and maximal OCR in MCF7 cells both in the presence of glutamine alone, and all 3 nutrients. Representative experiment of n=2 in 12 replicates, mean±SD.

B) SL0101 reduces basal and maximal OCR in MCF7 cells both in the presence of pyruvate alone, and all 3 nutrients. Representative experiment of n=2 in 12 replicates, mean±SD.

C) SL0101 reduces basal and maximal OCR in MCF7 cells both in the presence of glucose alone, and all 3 nutrients. Representative experiment of n=2 in 12 replicates, mean±SD.

Figure 29

A

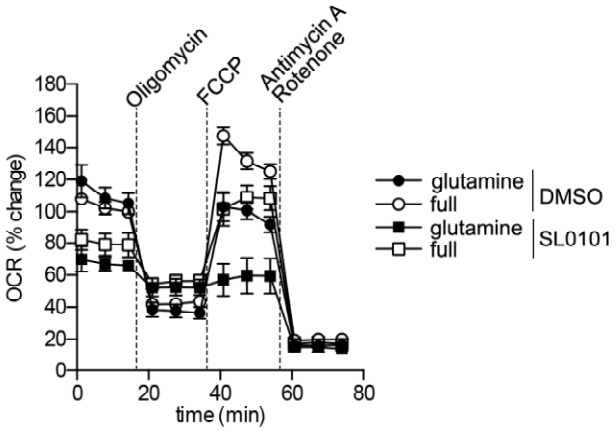

B

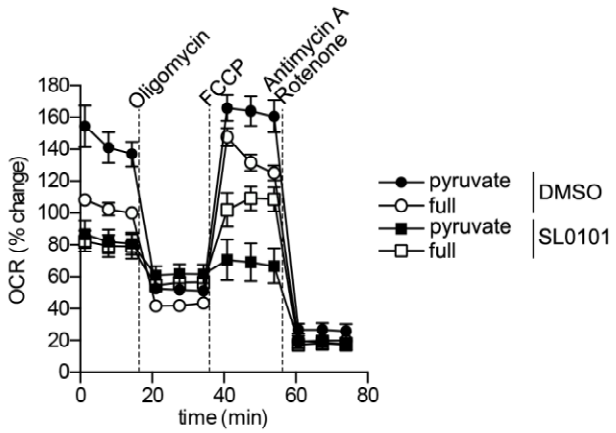

C

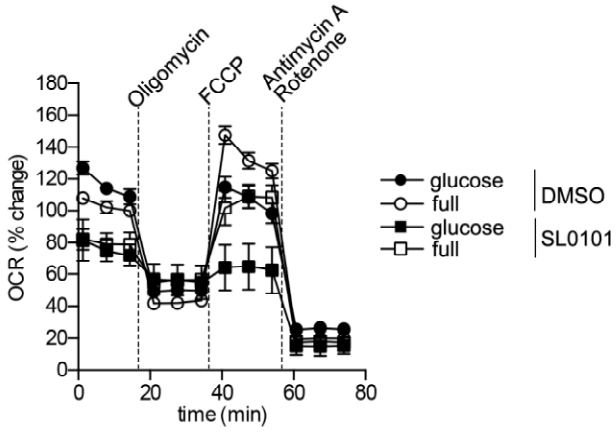

RSK inhibition caused a ~70% decline in TMRM fluorescence intensity, compared to the DMSO vehicle control, suggesting a decrease in the mitochondrial membrane potential upon the loss of RSK activity (fig. 30B). These observations further support the role of RSK in maintaining the activity of the ETC in MCF7 cells. It is possible that SL0101 interfered with the ability of TMRM to enter and be accumulated in cells. The experimental setup we used did not test for this possibility. Therefore, the results of the TMRM imaging need to be interpreted with caution.

Mitochondrial oxidative phosphorylation is coupled to the ability of the mitochondria to maintain a concentration gradient of the calcium ions across the mitochondrial inner membrane (Williams et al., 2013). Calcium ion concentration is kept very low in the cytosol, while the endoplasmic reticulum and mitochondria provide a major storage site for these ions. When mitochondria become depolarized, they release stored calcium ions to the cytoplasm, which can trigger various cellular processes, including apoptosis (Smaili et al., 2000). Therefore, the ability of the mitochondria to maintain calcium stores is linked to the mitochondrial membrane potential and the activity of the electron transport chain. We hypothesized that the decrease in mitochondrial ETC activity and membrane potential upon loss of RSK activity could result in a decrease in the calcium ion concentration in the mitochondrial matrix. In order to test this hypothesis we used Rhod-2, a fluorescent calcium indicator. This rhodamine dye derivative accumulates in the mitochondria where upon calcium ion binding it becomes fluorescent. Therefore, it can be used to measure the concentration of this metal ion in mitochondria. SL0101 caused a 90% decrease in fluorescence intensity of Rhod-2 (fig. 30C).

Figure 30. RSK inhibition decreases superoxide levels, membrane potential and calcium levels in the mitochondria in transformed cells.

A) RSK inhibition decreases mitochondrial superoxide levels in MCF7 cells. Cells were treated for 2 hours with or without SL0101, and MitoSox Red was loaded for 10 min and imaged by live confocal microscopy. Combined normalized fluorescence intensity per cell, N=3, Student's t-test.

B) RSK inhibition decreases mitochondrial membrane potential levels in MCF7 cells. Cells were treated for 2 hours with or without SL0101, and TMRM was loaded for 30 min and imaged by live confocal microscopy. Combined normalized fluorescence intensity per cell, N=3, Student's t-test.

C) RSK inhibition decreases mitochondrial calcium levels in MCF7 cells. Cells were loaded for 50 min with Rhod-2 and treated for 2 hours with or without SL0101. Cells were imaged by live confocal microscopy. Combined normalized fluorescence intensity per cell, N=3, Student's t-test.

D) RSK inhibition does not affect mitochondrial calcium levels in MCF10A cells. Cells were loaded for 50 min with Rhod-2 and treated for 2 hours with or without SL0101. Cells were imaged by live confocal microscopy. Combined normalized fluorescence intensity per cell, N=2, Student's t-test.

Figure 30

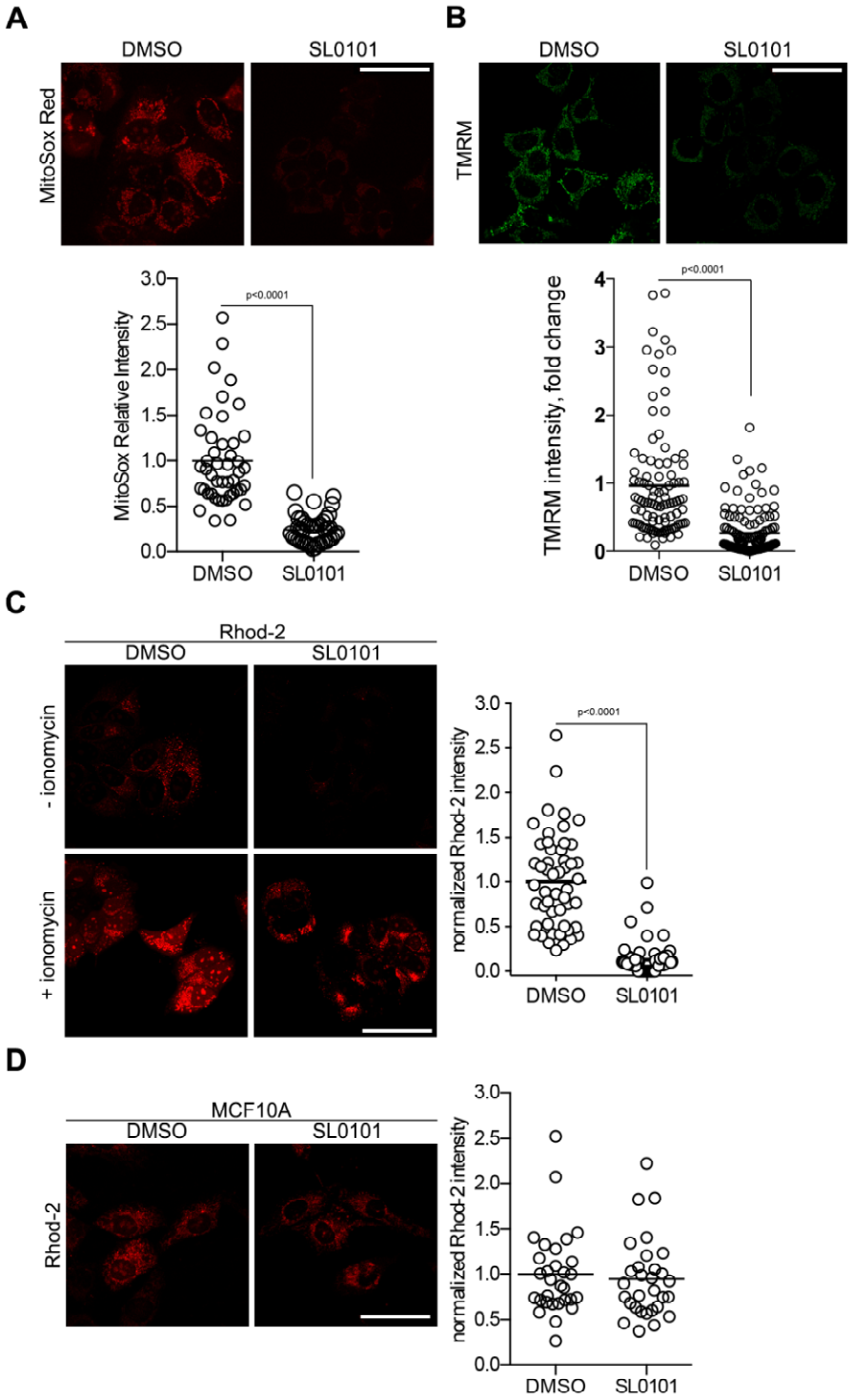
A
DMSO
SL0101
MitoSox Red
MitoSox Relative Intensity
p<0.0001
B
TMRM
TMRM intensity, fold change
C
Rhod-2
- ionomycin
+ ionomycin
normalized Rhod-2 intensity
D
MCF10A

To prove that the loss of Rhod-2 fluorescence upon SL0101 treatment was due to a decrease in mitochondrial calcium ions, and not due to the drug interfering with the fluorophores, cells were treated with the calcium ionophore, ionomycin. Ionomycin treatment caused a rapid increase in Rhod-2 fluorescence in both DMSO and SL0101 treated cells, providing evidence that Rhod-2 dye was able to respond to the increase in mitochondrial calcium ion concentration. The results indicate that RSK inhibition by SL0101 causes a decrease in mitochondrial calcium ion levels. These observations provide further support for the role of RSK in stimulating the activity of the electron transport chain.

We have found that RSK activity was dispensable for the regulation of oxidative phosphorylation in non-transformed cell line, MCF10A. To further support this hypothesis we measured the mitochondrial calcium levels in MCF10A cells treated with SL0101. Consistent with the observation that RSK inhibition in this cell line did not affect mitochondrial oxygen consumption, SL0101 treatment did not affect the mitochondrial calcium levels in these cells (fig. 30D). These results provided further evidence for a divergent role of RSK signaling in regulating mitochondrial respiration between breast cancer and non-transformed breast epithelial cell lines.

7.4. Discussion

The specific role of RSK1 and RSK2 in regulating caner bioenergetics remains to be described. Based on our results there are several potential processes whose perturbations could lead to observed phenotypes. One possibility is that RSK1/2 regulates the activity of the ETC complexes. Interestingly, our results of the RSK1

interactome analysis suggested that this kinase might interact with several components of the ETC complexes: complex I (NDUFB4), complex III (UQCRH) and complex IV (COX5B, COX6A) (chapter 6). An alternative mechanism could involve regulation of the activity of the TCA cycle. In this case, SL0101 treatment would lead to a reduction in the production of NADH and succinate, which constitute the substrates for the ETC. As a result, oxygen consumption and the proton transfer across the mitochondrial membrane would decline. Hence, the mitochondrial membrane potential would decrease, which in turn would result in the decrease in mitochondrial calcium levels.

The regulation of the TCA cycle could involve RSK phosphorylating and thereby changing the activity of the metabolic enzymes involved in the cycle. This mechanism would have to involve RSK translocating into the mitochondrial matrix, as this is the site where the TCA cycle enzymes reside in. Conversely, RSK could phosphorylate a regulator of the activity of the TCA cycle enzyme that can translocate between cytoplasm and the mitochondrial matrix. Interestingly, it has become increasingly appreciated that transformation involves changes in both expression and activities of multiple metabolic enzymes, including those involved in the TCA cycle (Desideri et al., 2015). For example, it has recently been shown that alteration in the enzyme mitochondrial aconitase 2 (ACO2) could contribute to tumorigenesis in renal cancer (Ternette et al., 2013). Therefore, the ability of RSK to affect the activities of the ETC complexes remains a possibility that should be further explored.

As mentioned above, we observed a decrease in mitochondrial calcium levels in MCF7 cells upon RSK inhibition. This decrease could be a consequence of a decline in the activity of the ETC complex. However, mitochondrial calcium level has long been

recognized a critical regulator of the activity of the TCA cycle (Williamson and Cooper, 1980). The activities of multiple TCA cycle enzymes dramatically decrease upon a decline in calcium ion concentration. Therefore, in addition to being a consequence of a loss in mitochondrial membrane polarization, a drop in mitochondrial calcium could be a source of a decrease in mitochondrial function. Calcium is transported into mitochondria through the mitochondrial calcium uniporter MCU (Baughman et al., 2011). It has been shown that the activity of this ion channel can be regulated by other proteins, such as MICU1 (Perocchi et al., 2010) and MCUR1 (Mallilankaraman et al., 2012a, Mallilankaraman et al., 2012b). It is possible that RSK could regulate mitochondrial respiration though the changes in the activity of the mitochondrial calcium uniporter, either directly or through the MCU-regulating proteins. Interestingly, we have indentified potential interactions of RSK1 with proteins involved in ion homeostasis in the mitochondria and endoplasmic reticulum, including VDAC1 and VDAC2, ATP2A2, SLC25A13 and SLC25A3 (chapter 6).

In conclusion, we have discovered a novel role of RSK1 and RSK2 in regulating bioenergetics in breast cancer. This role is specific to transformed epithelial cells, as mitochondrial oxidative phosphorylation in the MCF10A cell line does not depend on RSK signaling. These observations uncover an exciting new opportunity to selectively target growth and survival of cancer cells versus normal epithelium.

Chapter 8

General discussion

The ability to sense the changes in the environment and to adapt to these alterations is one of the fundamental properties of living systems. One of the major groups of proteins involved in these processes is the family of extracellular signal regulated kinases (ERK). The function of this particular family of proteins is to integrate the various mitogenic signals into a specific biological response of the cell, such as increased cellular proliferation, survival and differentiation. These end goals are achieved by the modulation of the downstream effectors of ERK with specialized functions. The RSK family of kinases has been recognized as one of the major downstream effectors of ERK. Many molecular functions of RSK have been described to date, and disregulation of some of these functions has also been demonstrated to contribute to various pathologies, including cancer. Therefore, there is an ongoing interest to better understand how RSK kinases execute the specific biological tasks dictated by mitogenic signals, and whether these functions represent potential targets for the therapeutic intervention in various pathologies driven by inappropriate ERK signaling.

RSK signaling downstream of the ERK family of kinases is complicated by the existence of four functionally non-redundant, yet structurally very similar isoforms. Of those, only RSK2 has been knocked out in the genetically engineered mouse model. Therefore, our full understanding of the complex biology of RSK is limited by the

relatively scarce in vivo data for individual RSK functions. Taken all these factors together, there is a need to develop small molecule inhibitors of RSK that could be used to study the biological functions of this family of kinases in vivo, both in the context of normal homeostasis and in the various disease states. It s also increasingly appreciated that in order to better understand the in vivo functions of RSK, the tools to study the biology of the individual isoforms of RSK have to be developed.

Driven by the need to establish such methods to study specific functions of RSK in vivo, in particular in the context of breast cancer, we undertook the efforts to better characterize the previously reported small molecule inhibitor of RSK, SL0101. The section 8.1 of this dissertation summarizes the findings and demonstrate how these results allow us to rationalize a novel SL0101 analog with superior properties in vivo. Here, we also report a previously overlooked selectivity of SL0101 for RSK1/2 isoforms, which distinguishes this compound from other published small molecule inhibitors of RSK kinases.

Among the plethora of biological affects that have been proposed to be regulated by RSK, the cellular energy homeostasis has remained a relatively understudied function of this family of kinases. Although several potential mechanisms of RSK regulation of these processes have been postulated, the biological consequence of RSK inhibition on cellular energy homeostasis has remained unexplored. Driven by this paucity of experimental data, and previous unpublished observations from our laboratory, we set out to investigate the effects of RSK1/2 inhibition on cellular energy homeostasis. We show for the first time that RSK1/2 are involved in stimulation of the cellular energy production specifically in the mitochondria, and that this mechanism

appears to be confined to transformed cell lines. The results of these studies are summarized in section 8.2 of this dissertation.

8.1. SL0101 analogs as potential therapeutic agents to inhibit RSK1/2 *in vivo*

8.1.1. Conclusions of chapters 2-5: SL0101 is a prototypical member of a family of isoform-specific allosteric inhibitors of RSK1/2

RSK family of kinases constitutes well-established downstream effectors of the mitogenic ERK signaling. Multiple studies have characterized the role of these kinases in regulating cellular proliferation, survival and motility. Consistent with the importance of these proteins in stimulating these cellular processes, RSK kinases have been found to be often misregulated in a variety of cancers. As a result, there has been an ongoing effort to identify new inhibitors of RSK. Several compounds have previously been described as RSK inhibitors, and some of these molecules have proven very useful in mechanistic studies of RSK in tissue culture systems. However, all these molecules suffer from limited applicability *in vivo*. As a result, many of the described functions of RSK characterized in cell-based assays are yet to be translated to clinically relevant *in vivo* observations.

Here, we investigated the properties of one RSK inhibitor, the natural compound SL0101. Previous studies have described remarkable kinase selectivity of SL0101 for RSK, and the basis of this selectivity has not been very well understood. The crystal structure of RSK bound to SL0101 suggested a very unusual mode of inhibition of the enzyme employed by the compound, indicating the potential that SL0101 is an allosteric inhibitor of RSK. We provide the *in vitro* enzyme kinetics data in support of this model

(chapter 2). Our studies indicate that SL0101 acts as a non-competitive inhibitor of RSK, and this mode of inhibition likely involves stabilization of the unique conformation of the kinase that has been suggested by the crystallography studies. Additionally, we discover unexpected selectivity of SL0101 for RSK1/2, which differentiates this compound from other previously characterized RSK inhibitors, including BI-D1870.

Selectivity of small molecule kinase inhibitors is often a major concern in developing new ways of targeting specific kinases (Vieth et al., 2004, Knight and Shokat, 2005). Small molecules that inhibit the active state of the kinase tend to be able to bind in a similar fashion to multiple targets, hence displaying a relatively poor selectivity profile (Knight and Shokat, 2005). On the other hand, inhibitors that target conformations different than the active fold of the kinase are typically much more selective for their target. SL0101 is a glycosylated form of flavonoid kaempferol, kaempferol no-specifically binds to active conformations of multiple kinases (Calderon-Montano et al., 2011). Consequently, SL0101 was assumed to be an ATP-competitive inhibitor of the active state of RSK kinases. This assumption stayed in contrast to the remarkable selectivity of SL0101 for other kinases, suggesting that the binding properties of SL0101 could be different than anticipated. Together with the previous X-ray crystallography studies, our current results offer an explanation to this discrepancy.

Unique characteristics of SL0101 as a highly selective allosteric inhibitor of RSK1/2 have encouraged us to investigate the possibility of improving its poor *in vivo* properties. Our goal was to identify a derivative compound with superior *in vitro* affinity for the target, as well as greatly extended stability in cell-based assays, and with preserved selectivity for the target. To this end, we characterized three chemical

alterations to the SL0101 molecule that significantly improved one or more of these properties of the parent compound. The C6''-n-propyl modification conferred a fifty-fold increase in the *in vitro* affinity of SL0101 for RSK2, while preserving its selectivity for the target kinases (chapter 3). We discovered that replacing the rhamnose sugar constituent within the SL0101 molecule with a corresponding cyclitol resulted in the greatest increase in its ability to reduce proliferation of the breast cancer cell line, MCF-7 (chapter 5). However, this modification also negatively affected the selectivity profile of SL0101. Finally, we identified the carbamate modification to the acetyl groups within the sugar ring of SL0101 that preserved its *in vitro* affinity for RSK2, as well as the selectivity profile in cell-based assays (appendix 1).

Despite the loss of selectivity for RSK exhibited by the some analogs of SL0101 (chapters 4 and 5), these compounds help define the biological space that can be occupied by RSK inhibitors. These inhibitors help us understand what modifications can be accommodated by the features of the target kinase. We can use this information to combine the modifications that confer desired properties to the analog into one molecule. For example, we anticipated that the cyclitol analog of SL0101 would be more stable *in vivo*, since it modifies the chemical character of the bond linking the sugar and kaempferol parts of the molecule (chapter 5). However, this modification caused a decrease in selectivity of the analog for RSK. At the same time, the analog was a much more potent inhibitor of MCF7 cell proliferation, compared to the parent compound. The shift in cell-based IC50 could suggest an increase in bioavailability of the inhibitor. On the other hand, the increased sensitivity to the inhibitor could be due to its off-target effects, inhibiting other pathways essential for the growth and survival of this cell line.

Combining the cyclitol modification of SL0101 with the modification that greatly improved the affinity of SL0101 for RSK could potentially overcome that loss of inhibitor selectivity. We are now in the advanced stages of validating such compound and indeed have seen a restoration of the kinase selectivity of the cyclitol analog (unpublished data). We have also seen an increase in stability of the compound in cell-based assays, consistent with the predicted stabilization of the molecule by the cyclitol modification. However, we did not know whether the two modifications together would act as we predicted until the new analog was tested.

The fact that, unlike BI-D1870, SL0101 does not inhibit RSK3/4 has important implications for the use of these compounds in mechanistic studies of the biological functions of the RSK family of kinases. It is now becoming increasingly appreciated that individual RSK isoforms may perform divergent functions. Therefore, inhibiting a subset of the members of this family may have different biological effects than reducing the activity of all four isoforms. Such differences could represent the functions of RSK3/4, as these two kinases are affected by BI-D1870, and not by SL0101. Indeed, inconsistencies between the biological effects of BI-D1870 and SL0101 have previously been reported (Chen and Mackintosh, 2009, Roffe et al., 2015).

8.1.2. Emerging questions from chapter 2: allosteric inhibition of RSK1/2

Our results strongly suggest that the ability of SL0101 to bind to and inhibit the NTKD of RSK1/2 is influenced by the CTKD of these proteins. The notion that the activity of the NTKD is regulated by the C-terminal segments of the protein is also supported by two previous observations. First, the phosphorylation of the conserved

residue Ser 227 in the activation loop is not sufficient for a full activation of the RSK2 NTKD. In addition to this activating phosphorylation, the hydrophobic motif from within the linker between the two kinase domains of RSK has to interact with the active site of the NTKD (Frodin et al., 2002). Second, our crystal structure of SL0101 bound to the NTKD of RSK2 showed that the two acetate residues within the sugar ring of SL0101 were not involved in inhibitor binding to the kinase (Utepbergenov et al., 2012). However, these two acetates appear to be crucial for SL0101 affinity for full-length RSK2 *in vitro* (chapters 3-5).

Taken all these observations together, we argue that the changes in RSK NTKD kinase activity in response to SL0101 binding represent a complex mechanism involving multiple parts of the polypeptide chain, in addition to the kinase domain itself. Interestingly, while the N- and C-terminal kinase domains of all RSK isoforms are ~90% identical, the linker between the kinase domains and the C- and N-terminal extensions are much more divergent (Carriere et al., 2008b). Therefore, the isoform-selectivity of SL0101 for RSK1/2 and not RSK3/4 can potentially be dictated by the C-terminal part of these kinases. This possibility could be tested by assessing the ability of SL0101 to inhibit the isolated NTKDs of RSK3 and RSK4. If the isolated kinase domains are inhibited by SL0101, the features of the kinases conferring the isoform-selectivity of SL0101must be contained in the sequences outside these domains.

The understanding of the mechanisms governing kinase activity comes from extensive studies of the cAMP-dependent protein kinase (PKA) that spans the last two decades (Taylor et al., 2013). The example of PKA shows that regulatory domains within the kinase itself, as well as other proteins, can allosterically modulate the activity

of the kinase (Taylor et al., 2012). Our studies of SL0101 binding to and inhibition of RSK1 and RSK2 now suggest a similar complexity of regulation of RSK kinase activity. In addition to a known function in the phosphorylation and activation cascade of RSK, the C-terminal part of this kinase can also act as an allosteric modulator of the NTKD activity. This allosteric regulation could be conserved between RSK1 and RSK2, and not RSK3 and RSK4, explaining the lack of inhibition of the latter two kinases with SL0101. Importantly, unlike other isoforms, RSK4 appears to be constitutively active even in the absence of the mitogen stimulation, and the mechanism of this activation remains elusive (Dummler et al., 2005). Therefore, there is evidence of a differential regulation of kinase activity between the RSK isoforms.

Our full understanding of the complex regulation of RSK activity is limited by the lack of success in solving the structures of the full-length enzyme. Multiple attempts to crystallize both RSK kinase domains together have proven unsuccessful. So far, only the structures of the isolated CTKD and NTKD of RSK1 and RSK2 are known (Malakhova et al., 2009, Utepbergenov et al., 2012, Ikuta et al., 2007, Malakhova et al., 2008, Alexa et al., 2015). Therefore, it remains unknown how all the parts of the kinase could affect the overall activity of the enzyme. However, the results of our studies highlight the importance of fully elucidating this mechanism. With the advancement in the area of structural biology beyond crystallography, such studies are becoming possible. For example, the differences in the interactions of the NTKD and the CTKD between the active and inactive states of RSK isoforms, as well as between the ATP-bound and SL0101-bound kinases, could be investigated using small angle X-ray scattering (Vestergaard and Sayers, 2014, Hennig and Sattler, 2014). Cryo-electron

microscopy could also offer a method of investigating the changes in RSK protein conformation between different active and inhibited states (Cheng, 2015). Interrogating the structures of the full-length proteins could help us better understand the complex regulation of RSK kinase activity, as well as effects of small-molecule inhibitors.

The ability of cancer cells to leave the primary tumor mass and colonize distant sites, called metastasis, is its most deadly feature (Sethi and Kang, 2011), accounting for more than 90% of cancer-related mortality (Hanahan and Weinberg, 2011, Chaffer and Weinberg, 2011, Steeg, 2006). As summarized in chapter 1, RSK has been shown to regulate a variety of processes involved in cancer cell metastasis, in addition to survival and growth of primary tumors. Therefore, RSK has been proposed as a very promising new target for inhibition of metastasis (Sulzmaier and Ramos, 2013). The therapeutic potential of small-molecule inhibition of RSK to block metastasis has recently been demonstrated *in vivo* for the first time. In this study, RSK inhibitor fmk decreased metastatic potential of the mouse xenograft of human head and neck squamous cell carcinoma (HNSCC) (Li et al., 2013). *In vitro* studies of RSK inhibitors, as well as RSK knock-down experiments in cell lines and in xenograft models suggest that the function of RSK as a promoter of metastasis is not limited to HNSCC, but can be a common feature of many types of cancers, especially those driven by hyperactive Ras/MAPK pathway. The unpublished results from our laboratory also indicate the role of RSK1 and RSK2 in promoting metastasis in the xenograft model of aggressive breast cancer. Therefore, developing RSK inhibitors offers a great promise for new therapies targeting the metastatic cascade.

Based on the structure-activity relationship studies described in chapters 3-5, we hypothesize that the cyclitol-C6'-n-propyl analog of SL0101 could be a superior inhibitor of RSK *in vivo*. The future work will require full validation of this compound in vivo. A preliminary study in an experimental model of breast cancer metastasis in mouse we have recently completed suggests that indeed the new analog is capable of eliciting desired effects on RSK *in vivo* (unpublished data). The design of this inhibitor would not have been possible without characterizing the individual modifications of SL0101 in the studies descried in chapters 3-5.

Since RSK appears to be a major effector of ERK signaling, the potential benefits of using RSK inhibitors in cancer therapy could be extended to tumors driven by hyperactive Ras-MAPK axis. Melanoma is an excellent example of a disease is driven by inappropriate signaling mediated by this pathway (Homet and Ribas, 2014). At least 70% of all melanomas are driven by defined activating mutations in the pathway (Gray-Schopfer et al., 2007). Due to the dependency of a large fraction of melanomas on the activating mutation in BRAF, these tumors have been successfully targeted by small-molecule inhibitors of this kinase (Chapman et al., 2011, Hauschild et al., 2012). However, recent results suggest that both de novo and acquired resistance to mutant BRAF inhibitors in melanoma is frequently associated with re-activation of the MAPK pathway through various mechanisms (Fedorenko et al., 2015, Lito et al., 2013). Interestingly, RSK is frequently activated in melanomas (Old et al., 2009). Therefore, RSK inhibition could offer an attractive target in melanomas, particularly as a combination treatment with mutant BRAF inhibitors.

It is very important to highlight that the four RSK isoforms may have non-overlapping, and even opposing functions. There is ample evidence that RSK2 acts as a mediator of tumor-promoting signaling in multiple cancers (chapter 1). In addition to promoting survival and proliferation, it also participates in the pro-motile and pro-invasive cellular program in these cancers. The literature concerning RSK1 functions in promoting cell invasiveness almost unanimously characterizes it as a positive regulator of motility. The exception is one publication, in which silencing of RSK1 in lung cancer cell lines decreased motility and invasiveness (Lara et al., 2011). This study also indicated that the protein expression of RSK1 is decreased in non-small cell lung cancer (NSCLC) metastases, compared to the primary tumor samples from the same patients. Therefore, it is possible that the role of RSK1 in conferring invasive phenotype may be cell-type specific.

Contrary to RSK1 and RSK2, RSK3 and RSK4 have been suggested to serve a putative tumor suppressor function. For example, RSK3 was found to be down-regulated in ovarian cancer, and re-expression of RSK3 in ovarian cancer cell lines led to cell cycle arrest and apoptosis (Bignone et al., 2007). The role of RSK3 in promoting cancer cell motility and invasiveness has never been investigated. RSK4 has been shown to be decreased in colon and renal tumors, and low expression of RSK4 was correlated with poor outcome in colorectal tumors (Lopez-Vicente et al., 2009, Cai et al., 2014). RSK4 was shown to be a negative regulator of invasiveness in an aggressive breast cancer cell line (Thakur et al., 2008). However, RSK3 and RSK4 were also suggested to drive resistance to PI3K inhibitors in a breast cancer cell line (Serra et al., 2013). In addition, existence of multiple splice variants of RSK4 has complicated the

interpretation of the studies investigating expression of this protein in cancer samples (Sun et al., 2013). Therefore, our current knowledge of the functions of these two RSK isoforms is not sufficient to make predictions on their roles in cancer etiology. Potentially divergent functions of RSK isoforms in regulating cancer metastasis highlight the importance of developing isoform-selective inhibitors of this family of kinases. SL0101 and its derivatives offer such possibility for the first time.

8.2. RSK1/2 regulation of cancer cell bioenergetics

8.2.1. Conclusions of chapters 6 and 7: RSK1/2 regulate energy homeostasis in transformed epithelial cell lines

Previous studies of phenotypes observed in RSK2 knock-out mice, as well as phosphorylation targets of RSK in cell lines, have implicated the potential roles of RSK1/2 in regulating cellular energy homeostasis. However, the exact mechanisms of RSK1/2 involvement in cellular energy balance have never been elucidated. Understanding the exact functions of RSK1 and RSK2 has is complicated by the paucity of definitive studies characterizing the isoform-specific functions of these proteins. Therefore, we set out to establish a systematic approach to investigate the interacting partners and phosphorylation targets of individual RSK isoforms.

In order to better understand the biological functions of RSK1, we developed a high throughput proteomics method to discover new interacting partners of this protein in intact cells. We set out to modify the method based on APEX peroxidase-mediated labeling of transient and stable interacting partners in intact cells, which has recently been described (Rhee et al., 2013, Hung et al., 2014). The novelty in our approach was

two-fold. First, nobody has published using this technique to investigate the interacting partners of a specific protein. Second, the previous studies using this method have relied on in-gel digestion of electrophoretically separated proteins enriched by the labeling. We decided to perform digestion of the labeled proteins on the beads. We identified 37 potential RSK1-binding proteins with known functions in regulating protein synthesis, as well as in mitochondrial energy homeostasis (chapter 6). Even in such a short list we found two proteins that have previously been reported in another proteomics study of RSK targets, NOP56 and CLN6. Importantly, that study used a very different method of identifying potential new RSK targets (Galan et al., 2014).

Our results of the proteomics study provide additional piece of evidence suggesting a potential role of RSK proteins in regulating cellular energy homeostasis. Therefore, we investigated the involvement of RSK1/2 in maintaining mitochondrial function. We found that RSK1/2 inhibition significantly decreased mitochondrial oxidative phosphorylation, and this reduction was associated with decreases in several markers of mitochondrial fitness (chapter 7). Intriguingly, oxidative phosphorylation in non-transformed breast epithelial cell line, MCF-10A, was insensitive to RSK1/2 inhibition. These observations add to the repertoire of cellular functions of RSK1/2 that contribute to a well-documented preferential dependence of transformed cells on RSK for their survival.

Decades of extensive studies in various mammalian systems have established that cellular energy demand is matched by ATP production, such that at steady state the cellular ATP levels remain constant (Wieser and Krumschnabel, 2001, Buttgereit and Brand, 1995, Schmidt et al., 1991). The three main energy consumption processes

in mammalian cells are protein synthesis, sodium/potassium antiport and calcium transport, with protein synthesis accounting for between 20-50% of total ATP consumption, depending on cell type (Rolfe and Brown, 1997, Wieser and Krumschnabel, 2001). In addition to these processes involved in basic cellular homeostasis, actin dynamics associated with migration was found to constitute a major pathway of energy consumption (Desai et al., 2013). Importantly, RSK signaling has well-established roles in potentiating all these processes (fig. 31). As a result, activation of RSK puts increased stress on cellular energy balance. Therefore, it is conceivable that RSK could act to stimulate cellular energy production to meet this increased demand. Several kinases integrating signals to regulate both protein expression and energy production have previously been identified. Among those are such enzymes as PDK1, which is involved in activation cascades of multiple pro-survival kinases, including RSK, as well as phosphorylation and regulation of activity of pyruvate dehydrogenase, a critical enzyme involved in glucose metabolism (Cairns et al., 2011). In addition, kinase complex mTOR was shown to regulate amino acid metabolism and rates of protein synthesis in response to nutrient availability (Mayer and Grummt, 2006, Jewell et al., 2013, Jewell and Guan, 2013).

Figure 31. RSK regulates both energy production and consumption in breast cancer cells.

Figure 31

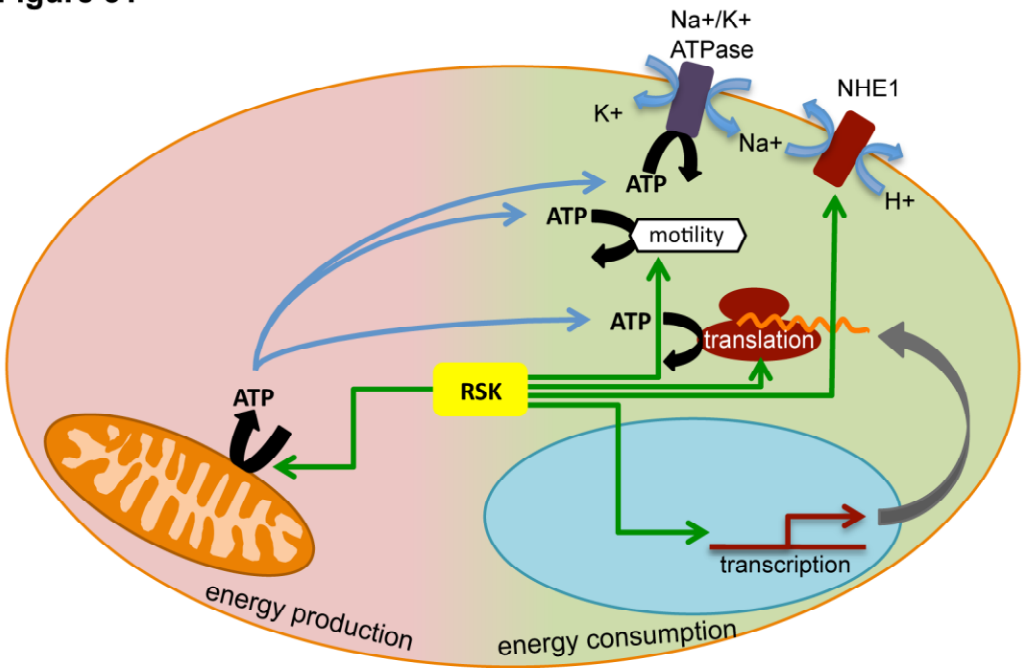
Na+/K+
ATPase
K+
ATP
NHE1
Na+
H+
ATP
motility
ATP
translation
RSK
ATP
transcription
energy production
energy consumption

To summarize, the findings that RSK1 could regulate both protein translation at ribosomes and energy metabolism in mitochondria in breast cancer cells point to a possibility that RSK1 is a critical mediator of cellular resource management. RSK1 could act to integrate cellular signaling downstream of growth factors to coordinate energy production and consumption. Targeting RSK could offer a possibility to induce cancer cell death through the disruption of the bioenergetic balance of these cells. This mechanism adds to the repertoire of known functions of RSK in regulating proliferation, survival and motility of cancer cells, further reinforcing the potential of targeting these kinases in the treatment of cancer.

9.2.2. Emerging questions from chapters 6 and 7: Regulation of cancer bioenergetics by RSK1/2

We found a striking difference in the distribution of RSK1 and RSK2 between the cytoplasmic compartments. RSK1 appeared to be associated with intracellular membranes in a stable fashion. Since its localization is so different from that of RSK2, it is conceivable that these two kinases would phosphorylate different targets. In addition, RSK1 does not posses any known features that would allow it to stably bind to the lipid bilayers, therefore we expected it would be anchored to the membranes through interactions with other proteins.

Although the method we developed still requires further optimization, it has already yielded very interesting results. The main problem that still needs to be resolved is a relatively low dynamic range of the method, giving a long list of potential proteins with relatively low confidence in the detection of each of these proteins. We are

confident, however, that with the improvements in the processing of affinity-purified proteins samples we can increase the dynamic range of the assay.

We will pursue further optimization of the labeling approach to interrogating the RSK1-interactome in intact cells. The results of the high-throughput proteomics will be analyzed using a variety of bioinformatics tools, to identify functional clusters and nodes connecting these clusters. These nodes will represent the most promising potential targets of RSK1 regulation. The validation of the hits will encompass a variety of biochemical and cell biology approaches, including assessment of total protein and phosphorylation levels upon RSK1 knock-down or inhibition, as well as immunoprecipitations and investigations of sub-cellular distribution.

The mechanism by which RSK inhibitors could elicit the decrease in mitochondrial metabolism remains unknown. However, the proteomics approach described in chapter 7 offers a method to identify this mechanism. In view of the preliminary findings that RSK1 can potentially interact with mitochondrial proteins involved in oxidative phosphorylation, the identification of the mechanism becomes a real possibility. When applied to non-transformed cells, this method could also help explain the differential ability of RSK to regulate oxidative phosphorylation specifically in transformed cells.

In addition to mitochondria, endoplasmic reticulum provides a major cellular reservoir of calcium ions, and the two sites dynamically communicate with each other to maintain cellular homeostasis of these ions (Kaufman and Malhotra, 2014, Naon and Scorrano, 2014). Interestingly, ER proteins were identified in our initial screen of

potential RSK1-interacting partners (chapter 7). Therefore, RSK1 could regulate the function of both compartments. Such possibility should be further investigated. For example, the ER-mitochondria contact sites could be imaged using super-resolution microscopy or electron microscopy.

It is important to note that this cell line displays high spare respiratory capacity, compared to breast cancer cell lines MCF-7 and T47D (fig. 32). This respiratory reserve is thought to represent the flexibility of cells to changes in energy demand (Fern, 2003). Lower respiratory capacity in breast cancer cell lines suggests that these cells are experiencing high energy demand, and are forced to operate close to the upper limit of a possible energy output. Inhibition of RSK would prevent cells from accessing this spare capacity, lowering energy production below the critical threshold required to sustain proliferation. In MCF-10A cells, however, the basal energy demand is low enough that the spare capacity does not have to be employed, and RSK inhibition does not affect the basal oxygen consumption rate. Consistent with the role of the respiratory reserve in cell proliferation and survival, reduced spare respiratory capacity has been shown to correlate with increased susceptibility to death induced by various types of stress in multiple cell types (Sriskanthadevan et al., 2015, Nickens et al., 2013, Choi et al., 2009, Zhu et al., 2012).

The changes in mitochondrial metabolism should be further investigated in the context of multiple cell lines. The studies should encompass measurements of enzymatic activities of mitochondrial ETC complexes. Changes in cellular distribution of the calcium stores should also be investigated. The studies conducted so far included small-molecule inhibition of RSK. The individual roles of RSK1 and RSK2 in this context

have to be further investigated. Each isoform should be knocked down individually, and a double knock-down should be performed. The mitochondrial phenotypes, such as membrane polarization, superoxide production and calcium levels should then be assessed. The knock-down studies should be accompanied by re-expression of RSK1 and RSK2, to evaluate the specificity of the knock-down short hairpins.

Studies of RSK1/2 function in regulating oxidative phosphorylation in various cell types could help us understand whether the functions of RSK in regulating mitochondria is a unique feature of transformed cells, or is it shared by other cell types, particularly those with high energy demand, like muscle cells and neurons. In addition to ATP synthesis, proton gradient established by oxidative phosphorylation is used for heat generation by brown and beige adipose tissue (Wu et al., 2015). Interestingly, lipodystrophy has been reported in RSK2 knock-out mice, suggesting a role of this protein in the normal function of this tissue (El-Haschimi et al., 2003). Therefore, the studies of RSK in these cell types are warranted.

Appendix

Analogs of the RSK inhibitor SL0101: Optimization of *in vitro* biological stability

Adapted from:

Hilinski, M.H., Mrozowski, R.M., Clark, D.E., Lannigan, D.A. (2012) Analogs of the RSK inhibitor SL0101: Optimization of *in vitro* biological stability. *Bioorg. Med. Chem. Lett.* 22: 3244-3247

Summary

The Ser/Thr protein kinase, RSK, is important in the etiology of tumor progression including invasion and motility. The natural product kaempferol-3-O-(3”,4”-di-O-acetyl-α-L-rhamnopyranoside), called SL0101, is a highly specific RSK inhibitor. Acylation of the rhamnose moiety is necessary for high affinity binding and selectivity. However, the acetyl groups can be cleaved by esterases, which accounts for the poor *in vitro* biological stability of SL0101. To address this problem a series of analogs containing acetyl group replacements were synthesized and their *in vitro* stability evaluated. Monosubstituted carbamate analogs of SL0101 showed improved *in vitro* biological stability while maintaining specificity for RSK. These results should facilitate the development of RSK inhibitors derived from SL0101 as anticancer agents.

A.1. Materials and Methods

Kinase Assays

Glutathione-S-transferase (GST)-fusion protein (1 μg) containing the ERζ-Ser167 sequence- RLASTND was adsorbed in the wells of LumiNunc 96-well polystyrene plates (MaxiSorp surface treatment). The wells were blocked with sterile 3% tryptone in phosphate-buffered saline. Kinase (5 nM) in 50 μL of kinase buffer (5 mM β-glycerophosphate, pH 7.4, 25 mM HEPES, pH 7.4, 1.5 mM DTT, 30 mM $MgCl_2$, 0.15 M NaCl) was dispensed into each well. 25 μL of the compound at the indicated concentrations or vehicle was added and reactions were initiated by the addition of 25 μL of ATP to a final ATP concentration of 10 μM. Reactions were terminated after 120 min by addition of 75 μL of 500 mM EDTA, pH 7.5. All assays measured the initial velocity of reaction. After extensive washing of wells, a polyclonal phosphospecific anti-ERζ-pSer167 antibody and HRP-conjugated anti-rabbit antibody (211-035-109, Jackson ImmunoResearch Laboratories, West Grove, Pennsylvania) were used to detect serine phosphorylation of the substrate. HRP activity was measured using Western Lightning Chemiluminescence Reagent (NEL102, PerkinElmer Life Sciences) according to the manufacturer's protocol. Maximum and minimum activity is the relative luminescence detected in the presence of vehicle and 500 mM EDTA, respectively. His-tagged active RSK was expressed in Sf9 cells and purified using NiNTA resin (Qiagen, Valencia, California). Baculovirus was prepared using the Bac-to-Bac baculovirus expression system (Invitrogen, Carlsbad, California). Maximum responses and the concentrations at half the inhibitory response (IC_{50}) were determined by performing a best-fit analysis of

the data (GraphPad Prism).

Cell Culture

For proliferation and stability studies cells were seeded at 2000 cells per well in 96-well tissue culture plates in the appropriate medium as described by American Type Culture Collection. After 24 h, the medium was replaced with medium containing compound or vehicle as indicated. Cell viability was measured 48 h later (proliferation studies) or 48 h, 96 h, and 144 h later (stability studies) using CellTiter-Glo™ assay reagent (Promega, Madison, Wisconsin) according to the manufacturer's protocol. Maximum responses and the concentrations of half the effective response (EC_{50}) were determined by performing a best-fit analysis of the data (GraphPad Prism). For specificity studies, cells were seeded at 1 x 10^5 cells/60 mm dish. After 24 h incubated with compound or vehicle for 2 h, 48 h, or 96 h. Cells were lysed with boiling SDS-sample buffer without dithiothreitol (DTT). The lysates were normalized for total protein, and DTT was added to an aliquot, which was electrophoresed and immunoblotted. Antibodies used on cell lysates included anti-eEF2 (2332) and anti-Cyclin D1 (2926) from Cell Signaling Technologies.

Chemistry

Unless otherwise noted, reagents and solvents were of reagent grade and used without further purification. Anhydrous tetrahydrofuran and *N*,*N*-dimethylformamide were purchased from Sigma-Aldrich. All reactions involving air- or moisture-sensitive reagents or intermediates were performed under a nitrogen atmosphere. Flash chromatography was performed using Fisher 70 – 230 mesh silica gel. Analytical TLC

was performed using 0.25 mm Merck KGaA silica gel 60 plates that were visualized by irradiation (254 nm) or by staining with Hanessian's stain (CAM). ^{1}H and ^{13}C NMR spectra were obtained using 300 and 500 MHz Varian instruments. Chemical shifts are reported in parts per million (ppm δ) referenced to the residual ^{1}H resonance of the solvent (CDCl3, 7.26 ppm; acetone-d6 2.09 ppm). ^{13}C spectra were referenced to the residual ^{13}C resonance of the solvent (CDCl3, 77.3 ppm; acetone-d6 29.9 ppm). Splitting patterns are designated as follows: s, singlet; br, broad; d, doublet; dd, doublet of doublets; t, triplet; q, quartet; m, multiplet. High-resolution mass spectra were obtained from the Michigan State University-NIH Mass Spectrometry Facility.

A.2. Results

The members of the p90 ribosomal S6 kinase (RSK) family of Ser/Thr protein kinases have been shown to play a role in a number of different cancers as key drivers of proliferation and metastasis (Eisinger-Mathason et al., 2010, Doehn et al., 2009, Smolen et al., 2010, Cho et al., 2007, Clark et al., 2005, Kang et al., 2007a, Kang et al., 2010, Kang et al., 2009). These discoveries have been enabled in part by our report of the identification and isolation of the RSK inhibitor SL0101 (**1**, fig. A1) (Smith et al., 2005). SL0101 is a flavonoid glycoside (kaempferol 3-O-(3",4"-di-O-acetyl- α-L-rhamnopyranoside)) isolated from *Forsteronia refracta*, a variety of dogbane found in the South American rainforest. SL0101 is highly specific for RSK, inhibiting RSK1/2 but not unrelated kinases nor the closely related kinases MSK1 and p70S6K1 (Doehn et al., 2009, Smith et al., 2005, Bain et al., 2007). SL0101 inhibits the proliferation of breast and prostate cancer lines but not their normal counterparts even though it inhibits RSK activity in all the lines (Eisinger-Mathason et al., 2010, Clark et al., 2005, Smith et al.,

2005). Thus it appears that some cancer cells have become addicted to RSK, which suggests that RSK may be a potential new target for cancer therapeutics. SL0101, owing to its exquisite specificity, is a compelling lead compound from which to begin the process of identifying drug-like RSK inhibitors.

We and others have reported the total synthesis and biological evaluation of SL0101 and a number of analogs, with the ultimate goal of developing an anticancer drug that targets RSK (Maloney and Hecht, 2005, Smith et al., 2006, Smith et al., 2007, Shan and O'Doherty, 2006, Shan and O'Doherty, 2010). These analogs have provided key information about the SAR of both the aglycone and carbohydrate portions of the natural product. In the course of this work we discovered that the 3" and 4" acetyl groups of the carbohydrate are critical for potency and specificity for RSK (Smith et al., 2007). TriOH-SL0101 (**2**), lacking these acetyl groups, is 12-fold less potent for inhibition of RSK *in vitro* and does not inhibit the growth of cancer cell lines, likely due to poor membrane permeability (Smith et al., 2007). These results indicate that SL0101 is not a suitable candidate for *in vivo* evaluation, as hydrolysis of the acetates by esterases would generate a less potent inhibitor.

An analog that replaces these acetates with ethyl ethers (**3**) inhibits RSK with potency roughly equivalent to SL0101 (Smith et al., 2007). We previously determined that the specificity of SL0101 and its analogs for RSK could be evaluated by their preferential ability to inhibit the growth of the human breast cancer line, MCF7, compared to the normal human breast line, MCF-10A (Smith et al., 2006). Unexpectedly, we observed that the ethyl ether analog **3** inhibited both lines to a similar extent, which indicates that it has a decreased specificity for RSK (Smith et al., 2007).

Figure A1*. The RSK inhibitor SL0101 and two previously reported analogs.

*Figure contributed by Michael Hilinski.

Figure A1

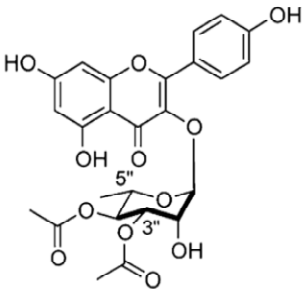

1 (SL0101)

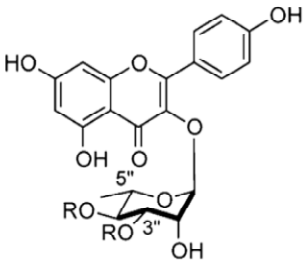

2 R = H
3 R = Et

Figure A2*. Synthesis of a bis-ketone analog of SL0101.

*Figure contributed by Michael Hilinski.

Figure A2

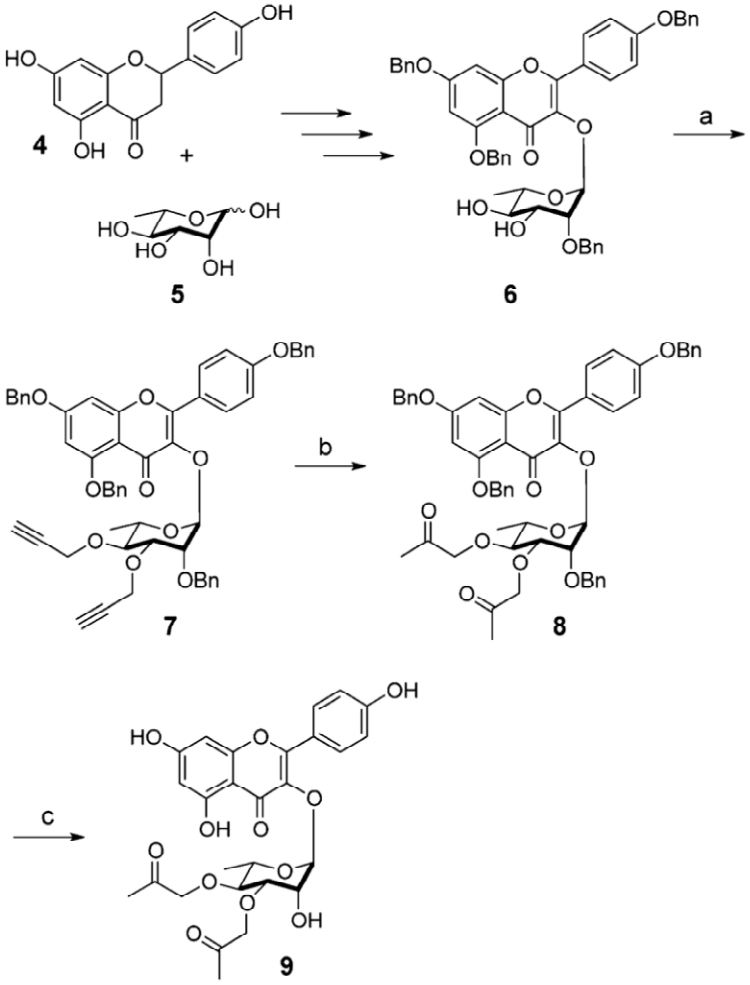

Figure A3*. General scheme for the preparation of carbamate analogs of SL0101..

*Figure contributed by Michael Hilinski.

Figure A3

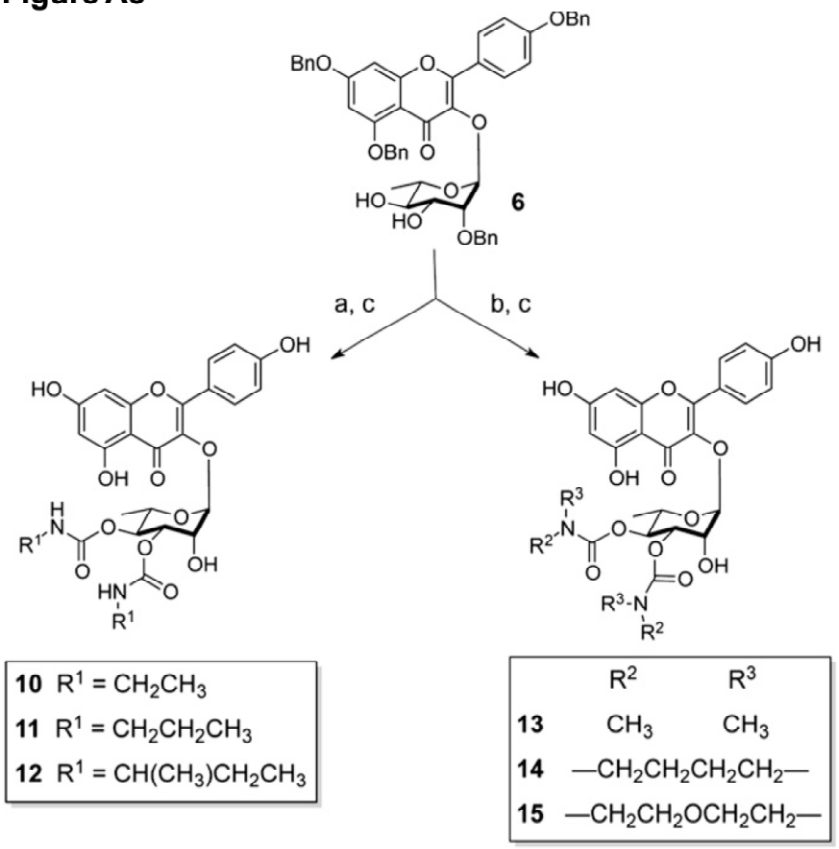

10 $R^1 = CH_2CH_3$

11 $R^1 = CH_2CH_2CH_3$

12 $R^1 = CH(CH_3)CH_2CH_3$

	R^2	R^3
13	CH_3	CH_3
14	$—CH_2CH_2CH_2CH_2—$	
15	$—CH_2CH_2OCH_2CH_2—$	

Figure A4*. Evaluation of *in vitro* and cell-based efficacy and stability of SL0101 analogs.

A) Potency of analogs in *in vitro* kinase and MCF7 cell-based assays. IC50 is concentration needed for 50% inhibition; the 95% CI is shown in parentheses; n=3 in triplicate. * $p<0.05$. PS; partially soluble.

B) *In vitro* determination of analog stability. The inhibitor (100 μM) was added to MCF7 cells at time 0 and percentage of growth determined for the indicated time points. (n= 3 in quadruplicate, #$p \leq 0.05$ at 48 h when compared to vehicle at 48 h, *$p \leq 0.05$ when compared to 48 h treatment with the same analog).

C) Persistence of RSK inhibition. MCF7 cells were treated with SL0101 or the more stable analogs 11 and 12 (100 μM). At the indicated time in hours (h) the cells were lysed and the lysates immunoblotted. Each analog was analyzed on a single membrane with SL0101. White space indicates sections of the membrane that were cropped to remove unnecessary lanes

D) Inhibition of growth of MCF-10A versus MCF7 cells by SL0101 and select analogs. The inhibitor concentration was 50 μM. (n = 3 in quadruplicate, *$p \leq 0.05$ when compared to vehicle).

*Panels B,C,D contributed by David Clark.

Figure A4

A

compound name	RSK2 IC_{50} [μM]	MCF-7 IC_{50} [μM]
SL0101 (**1**)	0.583 (0.489-0.696)	45.6 (42.7-48.8)
9	0.252 (0.189-0.336)*	34.1 (30.1-38.5)*
10	1.13 (0.876-1.46)*	77.0 (71.6-82.7)*
11	0.869 (0.649-1.16)	46.4 (43.2-50.0)
12	1.92 (1.29-2.86)*	53.3 (50.6-56.2)*
13	0.493 (0.355-0.684)	PS
14	0.356 (0.255-0.496)	PS
15	1.43 (1.09-2.04)*	>100

B

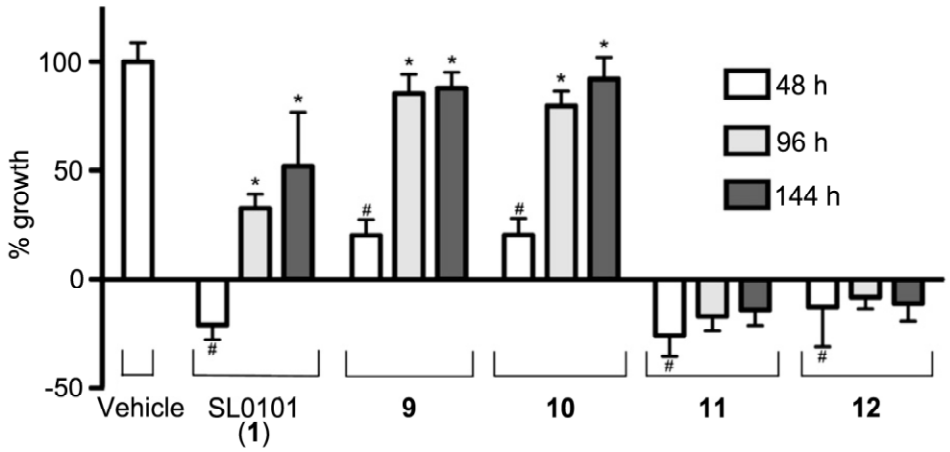

C

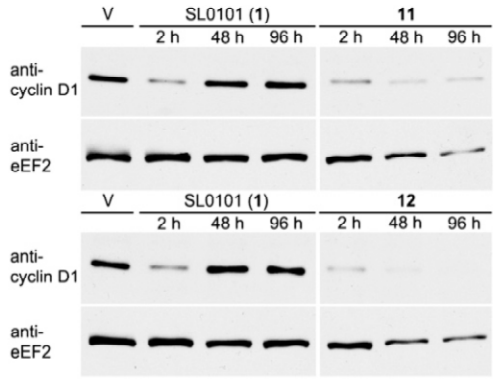

D

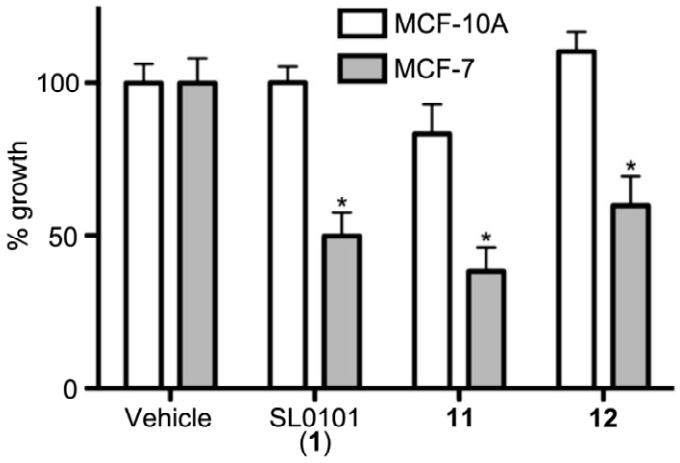

These results demonstrate that the acetates are a key modulator of specificity and thus a more carefully considered approach is necessary to identify suitable replacements. Accordingly, we have focused our efforts on identifying analogs bearing replacements for the acetates that confer greater biological stability without decreasing potency or specificity for RSK. Herein we present our approach, which has led to the identification of SL0101 analogs that are both specific for RSK and more biologically stable *in vitro* than the parent compound.

The only structural difference between the diethyl analog **3** and the diacetyl parent compound is the replacement of two methylenes with two carbonyl groups. It is surprising that such a seemingly small structural feature can regulate specificity for RSK. To recover this specificity, in the design of new analogs we sought to better mimic the acetates and particularly the acetate carbonyls, sterically and electronically, in a way that would confer a greater resistance to metabolism by esterases. In one approach we investigated the dependence of potency and specificity on the relative position of the carbonyl group. To this end we prepared an analog **9** in which the acetates are replaced by alkoxyacetones (fig. A2), moving the carbonyl group one carbon further from the carbohydrate ring and replacing the labile ester bond with an ether bond. The desired functionality could be installed at a late stage in the synthesis of the analog. Alkylation of known diol **6** (Smith et al., 2007) with propargyl bromide provided bis-alkyne **7**, which after mercury-catalyzed hydration provided bis-ketone **8**. Removal of the benzyl ether protecting groups by hydrogenolysis using Pearlman's catalyst provided the completed analog **9**.

In a second approach we retained the acetate carbonyl in the correct position but in a more biologically stable form in a series of analogs in which we replaced the acetates with bioisosteric mono- or disubstituted carbamates. Late-stage installation of the carbamate was desirable for maximum synthetic efficiency. Thus, carbamoylation of diol **6** with the appropriate isocyanate or diaklycarbamoyl chloride followed by hydrogenolysis of the benzyl ethers provided mono- or dialkylated carbamates **10–15** (fig. A3).

The ability of all new analogs to inhibit RSK activity was determined in an *in vitro* kinase assay and compared with the parent compound **1** (fig. A4A). The ketone analog **9** was twofold more potent than **1** at inhibiting RSK2. Analogs **11**, **13**, and **14** were as potent as SL0101 (**1**), and analogs **10**, **12**, and **15** were slightly (two to threefold) less potent. Overall, we found that the ability of an analog to inhibit RSK was not greatly influenced by the structure of the acetate replacement, which is consistent with previous observations.

We also determined the ability of all new analogs to inhibit MCF7 cell proliferation (fig. A4A). The ketone analog **9** was again the most potent of the new analogs. The three monosubstituted carbamates, analogs **10-12**, were similarly potent to the parent compound, with a trend toward improved potency with increasing lipophilicity of the carbamate substituent, presumably due to improved membrane permeability. In the disubstituted carbamate series, the dimethyl analog **13** and 1-pyrrolidinyl carbamate analog **14** exhibited poor solubility in cell culture media and therefore their ability to inhibit cell growth was not determined. The morpholino bis-carbamate **15** showed

improved solubility but was unable to inhibit cell proliferation despite its ability to inhibit RSK in the *in vitro* kinase assay, most likely due to poor membrane permeability.

Analogs that inhibited MCF7 cell proliferation were evaluated along with **1** for their stability in a MCF7 cell-based assay. The inhibitor was added when the cells were plated and proliferation analyzed at various time points to determine the persistence of the inhibitory effect. SL0101 (**1**) was able to inhibit MCF7 proliferation for 48 h (fig. A4B). However, at longer time points the cells began to proliferate indicating that SL0101 was no longer effective, which we hypothesize is due to degradation of the inhibitor by esterases to the inactive triol **2**. Treatment of cells with either the bis-ketone analog **9** or the ethyl carbamate analog **10** did not result in sustained growth inhibition, indicating poor *in vitro* stability of these analogs. As the 3” and 4” substituents of analog **9** are non-hydrolyzable, its poor stability was initially surprising. However, MCF7 cells express aldo-keto reductases (AKRs), well known to be Phase I metabolizing enzymes for a variety of drugs bearing carbonyl groups (Ruiz et al., 2011, Jin and Penning, 2007). Thus an alternative metabolic pathway is available to analog **9** whereby one or both ketones could be reduced by AKRs to secondary alcohols, leading either directly to a less potent RSK inhibitor or indirectly as the secondary alcohols could be further metabolized by conjugation (Jin and Penning, 2007).

Encouragingly, the more lipophilic monosubstitued carbamate analogs **11** and **12** demonstrated improved *in vitro* stability, as cells treated with these compounds did not proliferate over the full time course (fig. A4B). We further examined the stability of analogs **11** and **12** by determining whether cyclin D1 levels were inhibited (fig. A4C). Previously, we found that SL0101 inhibits proliferation in breast cancer cell lines by

inducing a cell cycle block in G1, which is due to RSK regulation of cyclin D1 levels (Eisinger-Mathason et al., 2010, Eisinger-Mathason et al., 2008). In agreement with the MCF7 stability results we observed that SL0101 decreased the levels of cyclin D1 at 48 h compared to the control, but that cyclin D1 levels began to increase at later time points, indicating degradation of the inhibitor. However, cyclin D1 levels remained low in cells treated with **11** or **12**, indicating persistent inhibition of RSK and therefore improved biological stability of the carbamate analogs over the parent compound. Taken together, these results indicate that analogs **11** and **12** have improved stability over SL0101 (**1**).

We then investigated whether our strategy of reintroducing the carbonyl group improved the specificity of **11** and **12** relative to the diethyl analog **3** (Smith et al., 2007). We have previously shown that the specificity of an analog for RSK can be evaluated by determining its antiproliferative activity in both MCF-10A and MCF7 cells, with the most specific analogs showing no inhibition of MCF-10A but substantial inhibition of MCF7 proliferation, due to the differential dependence of the growth of these cell lines on RSK (Smith et al., 2005, Smith et al., 2006). We have also previously shown that while SL0101 does not inhibit the growth of MCF-10A cells up to a concentration of 100 μM, the diethyl analog **3** significantly inhibits the growth of MCF-10A cells, indicating reduced specificity for RSK (Smith et al., 2007). We found that analogs **11** and **12**, like SL0101 (**1**), significantly inhibited the growth of MCF7 cells but did not significantly inhibit the growth MCF-10A cells (fig. A4D). These results suggest that analogs **11** and **12**, like SL0101 (**1**), specifically inhibit RSK (Doehn et al., 2009, Smith et al., 2005, Bain et al., 2007). The only significant differences in biological activity between the two

compounds are slightly improved potencies for **11** versus **12** in both the kinase and MCF7 cell proliferation assays. As these small differences are unlikely to be physiologically important, either carbamate modification should render an analog suitable for *in vivo* evaluation.

In summary, the C3” and C4” acetates on the carbohydrate moiety of SL0101 are required for both potent and specific inhibition of RSK but we predict that they would be metabolized rapidly by esterases *in vivo*, a fact which is supported by the poor biological stability of the natural product *in vitro*. Thus, SL0101 is not suitable for *in vivo* evaluation and analogs with improved stability are needed. The number of suitable replacements for these acetates that would confer greater biological stability is surprisingly limited as a simple change from acetyl to ethyl leads to a reduction in specificity for RSK. As a solution to this problem, bioisosteric replacement of the acetates by carbamates provided analogs that are more biologically stable than SL0101 *in vitro* and are as specific as SL0101 for RSK. These modifications along with others aimed at further improving the stability and potency of SL0101 analogs are currently being investigated in our laboratory with the goal of identifying a RSK inhibitor that could be advanced to preclinical testing.

References

ABRAMS, J. N., BABU, R. S., GUO, H., LE, D., LE, J., OSBOURN, J. M. & O'DOHERTY, G. A. 2008. De novo asymmetric synthesis of 8a-epi-swainsonine. *J Org Chem,* 73**,** 1935-40.

ADRIAN, F. J., DING, Q., SIM, T. B., VELENTZA, A., SLOAN, C., LIU, Y., ZHANG, G. B., HUR, W., DING, S., MANLEY, P., MESTAN, J., FABBRO, D. & GRAY, N. S. 2006. Allosteric inhibitors of Bcr-abl-dependent cell proliferation. *Nature Chemical Biology,* 2**,** 95-102.

ALESSI, D. R., JAMES, S. R., DOWNES, C. P., HOLMES, A. B., GAFFNEY, P. R., REESE, C. B. & COHEN, P. 1997. Characterization of a 3-phosphoinositide-dependent protein kinase which phosphorylates and activates protein kinase Balpha. *Current Biology,* 7**,** 261-9.

ALEXA, A., GOGL, G., GLATZ, G., GARAI, A., ZEKE, A., VARGA, J., DUDAS, E., JESZENOI, N., BODOR, A., HETENYI, C. & REMENYI, A. 2015. Structural assembly of the signaling competent ERK2-RSK1 heterodimeric protein kinase complex. *Proc Natl Acad Sci U S A,* 112**,** 2711-6.

ALJAHDALI, A. Z., SHI, P., ZHONG, Y. & O'DOHERTY, G. A. 2013. De novo asymmetric synthesis of the pyranoses: from monosaccharides to oligosaccharides. *Adv Carbohydr Chem Biochem,* 69**,** 55-123.

AMINI, F., KODADEK, T. & BROWN, K. C. 2002. Protein affinity labeling mediated by genetically encoded peptide tags. *Angew Chem Int Ed Engl,* 41**,** 356-9.

ANGENSTEIN, F., GREENOUGH, W. T. & WEILER, I. J. 1998. Metabotropic glutamate receptor-initiated translocation of protein kinase p90rsk to polyribosomes: A possible factor regulating synaptic protein synthesis. *Proceedings of the National Academy of Sciences of the United States of America,* 95**,** 15078-15083.

ANJUM, R. & BLENIS, J. 2008. The RSK family of kinases: emerging roles in cellular signalling. *Nat Rev Mol Cell Biol,* 9**,** 747-58.

ANJUM, R., ROUX, P. P., BALLIF, B. A., GYGI, S. P. & BLENIS, J. 2005. The tumor suppressor DAP kinase is a target of RSK-mediated survival signaling. *Current Biology,* 15**,** 1762-1767.

ARIAS, J., ALBERTS, A. S., BRINDLE, P., CLARET, F. X., SMEAL, T., KARIN, M., FERAMISCO, J. & MONTMINY, M. 1994. Activation of Camp and Mitogen Responsive Genes Relies on a Common Nuclear Factor. *Nature,* 370**,** 226-229.

ARONCHIK, I., APPLETON, B. A., BASHAM, S. E., CRAWFORD, K., DEL ROSARIO, M., DOYLE, L. V., ESTACIO, W. F., LAN, J., LINDVALL, M. K., LUU, C. A., ORNELAS, E., VENETSANAKOS, E., SHAFER, C. M. & JEFFERSON, A. B. 2014. Novel Potent and Selective Inhibitors of p90 Ribosomal S6 Kinase Reveal the Heterogeneity of RSK Function in MAPK-Driven Cancers. *Molecular Cancer Research,* 12**,** 803-812.

ARTHUR, J. S. C. 2008. MSK activation and physiological roles. *Frontiers in Bioscience,* 13**,** 5866-5879.

AVKIRAN, M., COOK, A. R. & CUELLO, F. 2008. Targeting Na+/H+ exchanger regulation for cardiac protection: a RSKy approach? *Curr Opin Pharmacol,* 8**,** 133-40.

BABU, R. S., GUPPI, S. R. & O'DOHERTY, G. A. 2006. Synthetic studies toward mannopeptimycin-E: synthesis of the O-linked tyrosine 1,4-alpha,alpha-manno,manno-pyranosyl pyranoside. *Org Lett,* 8**,** 1605-8.

BABU, R. S. & O'DOHERTY G, A. 2005. Palladium catalyzed glycosylation reaction:De-novo synthesis of trehalose analogues. *J Carb Chem,* 24**,** 169-177.

BABU, R. S. & O'DOHERTY, G. A. 2003. A palladium-catalyzed glycosylation reaction: the de novo synthesis of natural and unnatural glycosides. *Journal of the American Chemical Society,* 125**,** 12406-7.
BABU, R. S., ZHOU, M. & O'DOHERTY, G. A. 2004a. De novo synthesis of oligosaccharides using a palladium-catalyzed glycosylation reaction. *J Am Chem Soc,* 126**,** 3428-9.
BABU, R. S., ZHOU, M. & O'DOHERTY, G. A. 2004b. De novo synthesis of oligosaccharides using a palladium-catalyzed glycosylation reaction. *Journal of the American Chemical Society,* 126**,** 3428-9.
BAIGA, T. J., GUO, H., XING, Y., O'DOHERTY, G. A., DILLIN, A., AUSTIN, M. B., NOEL, J. P. & LA CLAIR, J. J. 2008. Metabolite induction of Caenorhabditis elegans dauer larvae arises via transport in the pharynx. *ACS Chem Biol,* 3**,** 294-304.
BAIN, J., MCLAUCHLAN, H., ELLIOTT, M. & COHEN, P. 2003. The specificities of protein kinase inhibitors: an update. *Biochemical Journal,* 371**,** 199-204.
BAIN, J., PLATER, L., ELLIOTT, M., SHPIRO, N., HASTIE, C. J., MCLAUCHLAN, H., KLEVERNIC, I., ARTHUR, J. S. C., ALESSI, D. R. & COHEN, P. 2007. The selectivity of protein kinase inhibitors: a further update. *Biochemical Journal,* 408**,** 297-315.
BAJAJ, S. O., SHARIF, E. U., AKHMEDOV, N. G. & O'DOHERTY, G. A. 2014. asymmetric synthesis of the mezzettiaside family of natural products via the iterative use of a dual B-/Pd-catalyzed glycosylation. *Chem Sci,* 5**,** 2230-2234.
BANNISTER, A. J. & KOUZARIDES, T. 1995. CBP-induced stimulation of c-Fos activity is abrogated by E1A. *Embo Journal,* 14**,** 4758-62.
BARTKOVA, J., HOREJSI, Z., KOED, K., KRAMER, A., TORT, F., ZIEGER, K., GULDBERG, P., SEHESTED, M., NESLAND, J. M., LUKAS, C., ORNTOFT, T., LUKAS, J. & BARTEK, J. 2005. DNA damage response as a candidate anti-cancer barrier in early human tumorigenesis. *Nature,* 434**,** 864-70.
BASU, A. & ROWAN, B. G. 2005. Genes related to estrogen action in reproduction and breast cancer. *Frontiers in Bioscience,* 10**,** 2346-72.
BAUGHMAN, J. M., PEROCCHI, F., GIRGIS, H. S., PLOVANICH, M., BELCHER-TIMME, C. A., SANCAK, Y., BAO, X. R., STRITTMATTER, L., GOLDBERGER, O., BOGORAD, R. L., KOTELIANSKY, V. & MOOTHA, V. K. 2011. Integrative genomics identifies MCU as an essential component of the mitochondrial calcium uniporter. *Nature,* 476**,** 341-5.
BESSON, A., GURIAN-WEST, M., SCHMIDT, A., HALL, A. & ROBERTS, J. M. 2004. p27Kip1 modulates cell migration through the regulation of RhoA activation. *Genes Dev,* 18**,** 862-76.
BHATIA, N., THIYAGARAJAN, S., ELCHEVA, I., SALEEM, M., DLUGOSZ, A., MUKHTAR, H. & SPIEGELMAN, V. S. 2006. Gli2 is targeted for ubiquitination and degradation by beta-TrCP ubiquitin ligase. *Journal of Biological Chemistry,* 281**,** 19320-6.
BHATT, R. R. & FERRELL, J. E., JR. 1999. The protein kinase p90 rsk as an essential mediator of cytostatic factor activity. *Science,* 286**,** 1362-5.
BIGNONE, P. A., LEE, K. Y., LIU, Y., EMILION, G., FINCH, J., SOOSAY, A. E. R., CHARNOCK, F. M. L., BECK, S., DUNHAM, I., MUNGALL, A. J. & GANESAN, T. S. 2007. RPS6KA2, a putative tumour suppressor gene at 6q27 in sporadic epithelial ovarian cancer. *Oncogene,* 26**,** 683-700.
BIONDI, R. M., KIELOCH, A., CURRIE, R. A., DEAK, M. & ALESSI, D. R. 2001. The PIF-binding pocket in PDK1 is essential for activation of S6K and SGK, but not PKB. *Embo Journal,* 20**,** 4380-90.

BJORBAEK, C., ZHAO, Y. & MOLLER, D. E. 1995. Divergent Functional Roles for Pp90(Rsk) Kinase Domains. *Diabetes,* 44**,** A102-A102.
BLENIS, J., CHUNG, J. K., ERIKSON, E., ALCORTA, D. A. & ERIKSON, R. L. 1991. Distinct Mechanisms for the Activation of the Rsk Kinases Map2 Kinase Pp90rsk and Pp70-S6 Kinase Signaling Systems Are Indicated by Inhibition of Protein-Synthesis. *Cell Growth & Differentiation,* 2**,** 279-285.
BOHUSLAV, J., CHEN, L. F., KWON, H., MU, Y. J. & GREENE, W. C. 2004. p53 induces NF-kappa B activation by an I kappa B kinase-independent mechanism involving phosphorylation of p65 by ribosomal S6 kinase 1. *Journal of Biological Chemistry,* 279**,** 26115-26125.
BONNI, A., BRUNET, A., WEST, A. E., DATTA, S. R., TAKASU, M. A. & GREENBERG, M. E. 1999. Cell survival promoted by the Ras-MAPK signaling pathway by transcription-dependent and -independent mechanisms. *Science,* 286**,** 1358-62.
BORISOVA, S. A., GUPPI, S. R., KIM, H. J., WU, B., PENN, J. H., LIU, H. W. & O'DOHERTY, G. A. 2010. A de novo approach to the synthesis of glycosylated methymycin analogues with structural and stereochemical diversity. *Org Lett,* 12**,** 5150-3.
BOYER, S. J., BURKE, J., GUO, X., KIRRANE, T. M., SNOW, R. J., ZHANG, Y. L., SARKO, C., SOLEYMANZADEH, L., SWINAMER, A., WESTBROOK, J., DICAPUA, F., PADYANA, A., COGAN, D., GAO, A., XIONG, Z. M., MADWED, J. B., KASHEM, M., KUGLER, S. & O'NEILL, M. M. 2012. Indole RSK inhibitors. Part 1: Discovery and initial SAR. *Bioorganic & Medicinal Chemistry Letters,* 22**,** 733-737.
BRAND, M. D. & NICHOLLS, D. G. 2011. Assessing mitochondrial dysfunction in cells. *Biochemical Journal,* 435**,** 297-312.
BRANDT, R. B., LAUX, J. E. & YATES, S. W. 1987. Calculation of inhibitor Ki and inhibitor type from the concentration of inhibitor for 50% inhibition for Michaelis-Menten enzymes. *Biochem Med Metab Biol,* 37**,** 344-9.
BROZ, P. & MONACK, D. M. 2013. Newly described pattern recognition receptors team up against intracellular pathogens. *Nature Reviews Immunology,* 13**,** 551-565.
BRUNING, J. C., GILLETTE, J. A., ZHAO, Y., BJORBAECK, C., KOTZKA, J., KNEBEL, B., AVCI, H., HANSTEIN, B., LINGOHR, P., MOLLER, D. E., KRONE, W., KAHN, C. R. & MULLER-WIELAND, D. 2000. Ribosomal subunit kinase-2 is required for growth factor-stimulated transcription of the c-Fos gene. *Proceedings of the National Academy of Sciences of the United States of America,* 97**,** 2462-2467.
BUCHDUNGER, E., CIOFFI, C. L., LAW, N., STOVER, D., OHNO-JONES, S., DRUKER, B. J. & LYDON, N. B. 2000. Abl protein-tyrosine kinase inhibitor STI571 inhibits in vitro signal transduction mediated by c-kit and platelet-derived growth factor receptors. *Journal of Pharmacology and Experimental Therapeutics,* 295**,** 139-45.
BUCK, M., POLI, V., HUNTER, T. & CHOJKIER, M. 2001. C/EBP beta phosphorylation by RSK creates a functional XEXD caspase inhibitory box critical for cell survival. *Molecular Cell,* 8**,** 807-816.
BUCK, M., POLI, V., VAN DER GEER, P., CHOJKIER, M. & HUNTER, T. 1999. Phosphorylation of rat serine 105 or mouse threonine 217 in C/EBP beta is required for hepatocyte proliferation induced by TGF alpha. *Molecular Cell,* 4**,** 1087-92.
BUSIELLO, R. A., SAVARESE, S. & LOMBARDI, A. 2015. Mitochondrial uncoupling proteins and energy metabolism. *Front Physiol,* 6**,** 36.

BUTTGEREIT, F. & BRAND, M. D. 1995. A hierarchy of ATP-consuming processes in mammalian cells. *Biochemical Journal,* 312 (Pt 1)**,** 163-7.
CAI, J., MA, H., HUANG, F., ZHU, D., ZHAO, L., YANG, Y., BI, J. & ZHANG, T. 2014. Low expression of RSK4 predicts poor prognosis in patients with colorectal cancer. *Int J Clin Exp Pathol,* 7**,** 4959-70.
CAIRNS, R. A., HARRIS, I. S. & MAK, T. W. 2011. Regulation of cancer cell metabolism. *Nature Reviews Cancer,* 11**,** 85-95.
CALDERON-MONTANO, J. M., BURGOS-MORON, E., PEREZ-GUERRERO, C. & LOPEZ-LAZARO, M. 2011. A review on the dietary flavonoid kaempferol. *Mini Rev Med Chem,* 11**,** 298-344.
CARDINAUX, J. R., NOTIS, J. C., ZHANG, Q., VO, N., CRAIG, J. C., FASS, D. M., BRENNAN, R. G. & GOODMAN, R. H. 2000. Recruitment of CREB binding protein is sufficient for CREB-mediated gene activation. *Molecular and Cellular Biology,* 20**,** 1546-52.
CARRIERE, A., CARGNELLO, M., JULIEN, L. A., GAO, H., BONNEIL, E., THIBAULT, P. & ROUX, P. P. 2008a. Oncogenic MAPK signaling stimulates mTORC1 activity by promoting RSK-mediated Raptor phosphorylation. *Current Biology,* 18**,** 1269-1277.
CARRIERE, A., RAY, H., BLENIS, J. & ROUX, P. P. 2008b. The RSK factors of activating the Ras/MAPK signaling cascade. *Frontiers in Bioscience,* 13**,** 4258-75.
CHAFFER, C. L. & WEINBERG, R. A. 2011. A perspective on cancer cell metastasis. *Science,* 331**,** 1559-64.
CHAKRAVARTI, D., LAMORTE, V. J., NELSON, M. C., NAKAJIMA, T., SCHULMAN, I. G., JUGUILON, H., MONTMINY, M. & EVANS, R. M. 1996. Role of CBP/P300 in nuclear receptor signalling. *Nature,* 383**,** 99-103.
CHALKLEY, R. J., MEDZIHRADSZKY, K. F., LYNN, A. J., BAKER, P. R. & BURLINGAME, A. L. 2010. Statistical analysis of Peptide electron transfer dissociation fragmentation mass spectrometry. *Anal Chem,* 82**,** 579-84.
CHANDRAMOULI, A., HATSELL, S. J., PINDERHUGHES, A., KOETZ, L. & COWIN, P. 2013. Gli activity is critical at multiple stages of embryonic mammary and nipple development. *Plos One,* 8**,** e79845.
CHANDRASEKAR, B., MUMMIDI, S., CLAYCOMB, W. C., MESTRIL, R. & NEMER, M. 2005. Interleukin-18 is a pro-hypertrophic cytokine that acts through a phosphatidylinositol 3-kinase-phosphoinositide-dependent kinase-1-Akt-GATA4 signaling pathway in cardiomyocytes. *Journal of Biological Chemistry,* 280**,** 4553-67.
CHAPMAN, P. B., HAUSCHILD, A., ROBERT, C., HAANEN, J. B., ASCIERTO, P., LARKIN, J., DUMMER, R., GARBE, C., TESTORI, A., MAIO, M., HOGG, D., LORIGAN, P., LEBBE, C., JOUARY, T., SCHADENDORF, D., RIBAS, A., O'DAY, S. J., SOSMAN, J. A., KIRKWOOD, J. M., EGGERMONT, A. M., DRENO, B., NOLOP, K., LI, J., NELSON, B., HOU, J., LEE, R. J., FLAHERTY, K. T. & MCARTHUR, G. A. 2011. Improved survival with vemurafenib in melanoma with BRAF V600E mutation. *N Engl J Med,* 364**,** 2507-16.
CHEN, C., ZHANG, L., HUANG, N. J., HUANG, B. & KORNBLUTH, S. 2013. Suppression of DNA-damage checkpoint signaling by Rsk-mediated phosphorylation of Mre11. *Proc Natl Acad Sci U S A,* 110**,** 20605-10.
CHEN, R. H., ABATE, C. & BLENIS, J. 1993. Phosphorylation of the C-Fos Transrepression Domain by Mitogen-Activated Protein-Kinase and 90-Kda Ribosomal S6 Kinase. *Proceedings of the National Academy of Sciences of the United States of America,* 90**,** 10952-10956.

CHEN, R. H., JUO, P. C., CURRAN, T. & BLENIS, J. 1996. Phosphorylation of c-Fos at the C-terminus enhances its transforming activity. *Oncogene,* 12**,** 1493-502.
CHEN, R. H., SARNECKI, C. & BLENIS, J. 1992. Nuclear localization and regulation of erk- and rsk-encoded protein kinases. *Molecular and Cellular Biology,* 12**,** 915-27.
CHEN, S. & MACKINTOSH, C. 2009. Differential regulation of NHE1 phosphorylation and glucose uptake by inhibitors of the ERK pathway and p90RSK in 3T3-L1 adipocytes. *Cell Signal,* 21**,** 1984-93.
CHENG, Y. 2015. Single-Particle Cryo-EM at Crystallographic Resolution. *Cell,* 161**,** 450-457.
CHENG, Y. & PRUSOFF, W. H. 1973. Relationship between the inhibition constant (K1) and the concentration of inhibitor which causes 50 per cent inhibition (I50) of an enzymatic reaction. *Biochemical Pharmacology,* 22**,** 3099-108.
CHO, Y. Y., YAO, K., KIM, H. G., KANG, B. S., ZHENG, D., BODE, A. M. & DONG, Z. 2007. Ribosomal s6 kinase 2 is a key regulator in tumor promoter-induced cell transformation. *Cancer Research,* 67**,** 8104-8112.
CHOI, S. W., GERENCSER, A. A. & NICHOLLS, D. G. 2009. Bioenergetic analysis of isolated cerebrocortical nerve terminals on a microgram scale: spare respiratory capacity and stochastic mitochondrial failure. *J Neurochem,* 109**,** 1179-91.
CHRESTENSEN, C. A. & STURGILL, T. W. 2002. Characterization of the p90 ribosomal S6 kinase 2 carboxyl-terminal domain as a protein kinase. *Journal of Biological Chemistry,* 277**,** 27733-41.
CHRIVIA, J. C., KWOK, R. P., LAMB, N., HAGIWARA, M., MONTMINY, M. R. & GOODMAN, R. H. 1993. Phosphorylated CREB binds specifically to the nuclear protein CBP. *Nature,* 365**,** 855-9.
CHUNG, J., KUO, C. J., CRABTREE, G. R. & BLENIS, J. 1992. Rapamycin Fkbp Specifically Blocks Growth-Dependent Activation of and Signaling by the 70 Kd S6 Protein-Kinases. *Cell,* 69**,** 1227-1236.
CLARK, D. E., ERRINGTON, T. M., SMITH, J. A., FRIERSON, H. F., JR., WEBER, M. J. & LANNIGAN, D. A. 2005a. The serine/threonine protein kinase, p90 ribosomal S6 kinase, is an important regulator of prostate cancer cell proliferation. *Cancer Res,* 65**,** 3108-16.
CLARK, D. E., ERRINGTON, T. M., SMITH, J. A., FRIERSON, H. F., JR., WEBER, M. J. & LANNIGAN, D. A. 2005b. The serine/threonine protein kinase, p90 ribosomal S6 kinase, is an important regulator of prostate cancer cell proliferation. *Cancer Research,* 65**,** 3108-16.
CLARKL, D. E., POTEET-SMITH, C. E., SMITH, J. A. & LANNIGAN, D. A. 2001. Rsk2 allosterically activates estrogen receptor alpha by docking to the hormone-binding domain. *Embo Journal,* 20**,** 3484-3494.
COENE, E. D., SHAW, M. K. & VAUX, D. J. 2008. Anti-biotin antibodies offer superior organelle-specific labelling of mitochondria over avidin or streptavidin. *Methods Mol Biol,* 418**,** 157-70.
COHEN, M. S., HADJIVASSILIOU, H. & TAUNTON, J. 2007. A clickable inhibitor reveals context-dependent autoactivation of p90 RSK. *Nature Chemical Biology,* 3**,** 156-160.
COHEN, M. S., ZHANG, C., SHOKAT, K. M. & TAUNTON, J. 2005. Structural bioinformatics-based design of selective, irreversible kinase inhibitors. *Science,* 308**,** 1318-1321.
CONVERSO, A., HARTINGH, T., GARBACCIO, R. M., TASBER, E., RICKERT, K., FRALEY, M. E., YAN, Y. W., KREATSOULAS, C., STIRDIVANT, S., DRAKAS, B., WALSH, E. S., HAMILTON, K., BUSER, C. A., MAO, X. Z., ABRAMS, M. T., BECK, S. C., TAO, W. K., LOBELL, R., SEPP-LORENZINO, L., ZUGAY-MURPHY, J., SARDANA, V.,

MUNSHI, S. K., JEZEQUEL-SUR, S. M., ZUCK, P. D. & HARTMAN, G. D. 2009. Development of thioquinazolinones, allosteric Chk1 kinase inhibitors. *Bioorganic & Medicinal Chemistry Letters,* 19**,** 1240-1244.
CORNISH-BOWDEN, A. 1974. A simple graphical method for determining the inhibition constants of mixed, uncompetitive and non-competitive inhibitors. *Biochemical Journal,* 137**,** 143-4.
COSTALES, A., MATHUR, M., RAMURTHY, S., LAN, J., SUBRAMANIAN, S., JAIN, R., ATALLAH, G., SETTI, L., LINDVALL, M., APPLETON, B. A., ORNELAS, E., FEUCHT, P., WARNE, B., DOYLE, L., BASHAM, S. E., ARONCHIK, I., JEFFERSON, A. B. & SHAFER, C. M. 2014. 2-Amino-7-substituted benzoxazole analogs as potent RSK2 inhibitor. *Bioorganic & Medicinal Chemistry Letters,* 24**,** 1592-1596.
COWAN-JACOB, S. W., JAHNKE, W. & KNAPP, S. 2014. Novel approaches for targeting kinases: allosteric inhibition, allosteric activation and pseudokinases. *Future Medicinal Chemistry,* 6**,** 541-561.
CRIMAUDO, C., HORTSCH, M., GAUSEPOHL, H. & MEYER, D. I. 1987. Human ribophorins I and II: the primary structure and membrane topology of two highly conserved rough endoplasmic reticulum-specific glycoproteins. *Embo Journal,* 6**,** 75-82.
CROSS, D. A., ALESSI, D. R., COHEN, P., ANDJELKOVICH, M. & HEMMINGS, B. A. 1995. Inhibition of glycogen synthase kinase-3 by insulin mediated by protein kinase B. *Nature,* 378**,** 785-9.
CUELLO, F., SNABAITIS, A. K., COHEN, M. S., TAUNTON, J. & AVKIRAN, M. 2007. Evidence for direct regulation of myocardial Na+/H+ exchanger isoform 1 phosphorylation and activity by 90-kDa ribosomal S6 kinase (RSK): Effects of the novel and specific RSK inhibitor fmk on responses to alpha(1)-adrenergic stimulation. *Molecular Pharmacology,* 71**,** 799-806.
DALBY, K. N., MORRICE, N., CAUDWELL, F. B., AVRUCH, J. & COHEN, P. 1998. Identification of regulatory phosphorylation sites in mitogen-activated protein kinase (MAPK)-activated protein kinase-1a/p90rsk that are inducible by MAPK. *Journal of Biological Chemistry,* 273**,** 1496-505.
DANIAL, N. N. 2008. BAD: undertaker by night, candyman by day. *Oncogene,* 27 Suppl 1**,** S53-70.
DAS, F., GHOSH-CHOUDHURY, N., KASINATH, B. S. & CHOUDHURY, G. G. 2010. TGFbeta enforces activation of eukaryotic elongation factor-2 (eEF2) via inactivation of eEF2 kinase by p90 ribosomal S6 kinase (p90Rsk) to induce mesangial cell hypertrophy. *Febs Letters,* 584**,** 4268-72.
DAVID, J. P., MEHIC, D., BAKIRI, L., SCHILLING, A. F., MANDIC, V., PRIEMEL, M., IDARRAGA, M. H., RESCHKE, M. O., HOFFMANN, O., AMLING, M. & WAGNER, E. F. 2005. Essential role of RSK2 in c-Fos-dependent osteosarcoma development. *Journal of Clinical Investigation,* 115**,** 664-672.
DAVIES, S. P., REDDY, H., CAIVANO, M. & COHEN, P. 2000. Specificity and mechanism of action of some commonly used protein kinase inhibitors. *Biochemical Journal,* 351**,** 95-105.
DE CESARE, D., JACQUOT, S., HANAUER, A. & SASSONE-CORSI, P. 1998. Rsk-2 activity is necessary for epidermal growth factor-induced phosphorylation of CREB protein and transcription of c-fos gene. *Proc Natl Acad Sci U S A,* 95**,** 12202-7.
DE MESQUITA, D. D., ZHAN, Q., CROSSLEY, L. & BADWEY, J. A. 2001. p90-RSK and Akt may promote rapid phosphorylation/inactivation of glycogen synthase kinase 3 in chemoattractant-stimulated neutrophils. *Febs Letters,* 502**,** 84-8.

DEGEN, M., BARRON, P., NATARAJAN, E., WIDLUND, H. R. & RHEINWALD, J. G. 2013a. RSK activation of translation factor eIF4B drives abnormal increases of laminin gamma2 and MYC protein during neoplastic progression to squamous cell carcinoma. *Plos One,* 8**,** e78979.
DEGEN, M., BARRON, P., NATARAJAN, E., WIDLUND, H. R. & RHEINWALD, J. G. 2013b. RSK Activation of Translation Factor eIF4B Drives Abnormal Increases of Laminin gamma 2 and MYC Protein during Neoplastic Progression to Squamous Cell Carcinoma. *Plos One,* 8.
DEHAN, E., BASSERMANN, F., GUARDAVACCARO, D., VASILIVER-SHAMIS, G., COHEN, M., LOWES, K. N., DUSTIN, M., HUANG, D. C., TAUNTON, J. & PAGANO, M. 2009. betaTrCP- and Rsk1/2-mediated degradation of BimEL inhibits apoptosis. *Molecular Cell,* 33**,** 109-16.
DESAI, S. P., BHATIA, S. N., TONER, M. & IRIMIA, D. 2013. Mitochondrial localization and the persistent migration of epithelial cancer cells. *Biophysical Journal,* 104**,** 2077-88.
DESIDERI, E., VEGLIANTE, R. & CIRIOLO, M. R. 2015. Mitochondrial dysfunctions in cancer: Genetic defects and oncogenic signaling impinging on TCA cycle activity. *Cancer Letters,* 356**,** 217-223.
DIMROTH, P., KAIM, G. & MATTHEY, U. 2000. Crucial role of the membrane potential for ATP synthesis by F(1)F(o) ATP synthases. *J Exp Biol,* 203**,** 51-9.
DIMROTH, P., VON BALLMOOS, C., MEIER, T. & KAIM, G. 2003. Electrical power fuels rotary ATP synthase. *Structure,* 11**,** 1469-73.
DIXON, M. 1953. The determination of enzyme inhibitor constants. *Biochemical Journal,* 55**,** 170-1.
DOEHN, U., HAUGE, C., FRANK, S. R., JENSEN, C. J., DUDA, K., NIELSEN, J. V., COHEN, M. S., JOHANSEN, J. V., WINTHER, B. R., LUND, L. R., WINTHER, O., TAUNTON, J., HANSEN, S. H. & FRODIN, M. 2009. RSK Is a Principal Effector of the RAS-ERK Pathway for Eliciting a Coordinate Promotile/Invasive Gene Program and Phenotype in Epithelial Cells. *Molecular Cell,* 35**,** 511-522.
DROSE, S. & BRANDT, U. 2012. Molecular mechanisms of superoxide production by the mitochondrial respiratory chain. *Adv Exp Med Biol,* 748**,** 145-69.
DRUKER, B. J., GUILHOT, F., O'BRIEN, S. G., GATHMANN, I., KANTARJIAN, H., GATTERMANN, N., DEININGER, M. W. N., SILVER, R. T., GOLDMAN, J. M., STONE, R. M., CERVANTES, F., HOCHHAUS, A., POWELL, B. L., GABRILOVE, J. L., ROUSSELOT, P., REIFFERS, J., CORNELISSEN, J. J., HUGHES, T., AGIS, H., FISCHER, T., VERHOEF, G., SHEPHERD, J., SAGLIO, G., GRATWOHL, A., NIELSEN, J. L., RADICH, J. P., SIMONSSON, B., TAYLOR, K., BACCARANI, M., SO, C., LETVAK, L. & LARSON, R. A. 2006. Five-year follow-up of patients receiving imatinib for chronic myeloid leukemia. *New England Journal of Medicine,* 355**,** 2408-2417.
DUFRESNE, S. D., BJORBAEK, C., EL-HASCHIMI, K., ZHAO, Y., ASCHENBACH, W. G., MOLLER, D. E. & GOODYEAR, L. J. 2001. Altered extracellular signal-regulated kinase signaling and glycogen metabolism in skeletal muscle from p90 ribosomal S6 kinase 2 knockout mice. *Molecular and Cellular Biology,* 21**,** 81-7.
DUMMLER, B. A., HAUGE, C., SILBER, J., YNTEMA, H. G., KRUSE, L. S., KOFOED, B., HEMMINGS, B. A., ALESSI, D. R. & FRODIN, M. 2005. Functional characterization of human RSK4, a new 90-kDa ribosomal S6 kinase, reveals constitutive activation in most cell types. *Journal of Biological Chemistry,* 280**,** 13304-13314.

DUMONT, J., UMBHAUER, M., RASSINIER, P., HANAUER, A. & VERLHAC, M. H. 2005. p90Rsk is not involved in cytostatic factor arrest in mouse oocytes. *Journal of Cell Biology,* 169**,** 227-31.
DUVEL, K., YECIES, J. L., MENON, S., RAMAN, P., LIPOVSKY, A. I., SOUZA, A. L., TRIANTAFELLOW, E., MA, Q., GORSKI, R., CLEAVER, S., VANDER HEIDEN, M. G., MACKEIGAN, J. P., FINAN, P. M., CLISH, C. B., MURPHY, L. O. & MANNING, B. D. 2010. Activation of a metabolic gene regulatory network downstream of mTOR complex 1. *Molecular Cell,* 39**,** 171-83.
EDGAR, A. J., TROST, M., WATTS, C. & ZARU, R. 2014. A combination of SILAC and nucleotide acyl phosphate labelling reveals unexpected targets of the Rsk inhibitor BI-D1870. *Bioscience Reports,* 34**,** 28-42.
EISINGER-MATHASON, T. S., ANDRADE, J. & LANNIGAN, D. A. 2010a. RSK in tumorigenesis: connections to steroid signaling. *Steroids,* 75**,** 191-202.
EISINGER-MATHASON, T. S. K., ANDRADE, J., GROEHLER, A. L., CLARK, D. E., MURATORE-SCHROEDER, T. L., PASIC, L., SMITH, J. A., SHABANOWITZ, J., HUNT, D. F., MACARA, I. G. & LANNIGAN, D. A. 2008. Codependent functions of RSK2 and the apoptosis-promoting factor TIA-1 in stress granule assembly and cell survival. *Molecular Cell,* 31**,** 722-736.
EISINGER-MATHASON, T. S. K., ANDRADE, J. & LANNIGAN, D. A. 2010b. RSK in tumorigenesis: Connections to steroid signaling. *Steroids,* 75**,** 191-202.
EL-HASCHIMI, K., DUFRESNE, S. D., HIRSHMAN, M. F., FLIER, J. S., GOODYEAR, L. J. & BJORBAEK, C. 2003. Insulin resistance and lipodystrophy in mice lacking ribosomal S6 kinase 2. *Diabetes,* 52**,** 1340-6.
ELBAZ, H. A., STUECKLE, T. A., WANG, H. Y., O'DOHERTY, G. A., LOWRY, D. T., SARGENT, L. M., WANG, L., DINU, C. Z. & ROJANASAKUL, Y. 2012. Digitoxin and a synthetic monosaccharide analog inhibit cell viability in lung cancer cells. *Toxicol Appl Pharmacol,* 258**,** 51-60.
ELDAR-FINKELMAN, H., SEGER, R., VANDENHEEDE, J. R. & KREBS, E. G. 1995. Inactivation of glycogen synthase kinase-3 by epidermal growth factor is mediated by mitogen-activated protein kinase/p90 ribosomal protein S6 kinase signaling pathway in NIH/3T3 cells. *Journal of Biological Chemistry,* 270**,** 987-90.
ELF, S., BLEVINS, D., JIN, L., CHUNG, T. W., WILLIAMS, I. R., LEE, B. H., LIN, J. X., LEONARD, W. J., TAUNTON, J., KHOURY, H. J. & KANG, S. 2011. p90RSK2 is essential for FLT3-ITD- but dispensable for BCR-ABL-induced myeloid leukemia. *Blood,* 117**,** 6885-94.
ERIKSON, E. & MALLER, J. L. 1985. A Protein-Kinase from Xenopus Eggs Specific for Ribosomal-Protein S6. *Proceedings of the National Academy of Sciences of the United States of America,* 82**,** 742-746.
ERIKSON, E. & MALLER, J. L. 1986. Purification and characterization of a protein kinase from Xenopus eggs highly specific for ribosomal protein S6. *Journal of Biological Chemistry,* 261**,** 350-5.
FABBRO 2015. 25 years of small molecular weight kinase inhibitors: potentials and limitations. *Molecular Pharmacology,* 87**,** 766-775.
FANG, X., YU, S. X., LU, Y., BAST, R. C., JR., WOODGETT, J. R. & MILLS, G. B. 2000. Phosphorylation and inactivation of glycogen synthase kinase 3 by protein kinase A. *Proc Natl Acad Sci U S A,* 97**,** 11960-5.

FAURY, D., NANTEL, A., DUNN, S. E., GUIOT, M. C., HAQUE, T., HAUSER, P., GARAMI, M., BOGNAR, L., HANZELY, Z., LIBERSKI, P. P., LOPEZ-AGUILAR, E., VALERA, E. T., TONE, L. G., CARRET, A. S., DEL MAESTRO, R. F., GLEAVE, M., MONTES, J. L., PIETSCH, T., ALBRECHT, S. & JABADO, N. 2007. Molecular profiling identifies prognostic subgroups of pediatric glioblastoma and shows increased YB-1 expression in tumors. *Journal of Clinical Oncology,* 25**,** 1196-1208.
FEDORENKO, I. V., GIBNEY, G. T., SONDAK, V. K. & SMALLEY, K. S. 2015. Beyond BRAF: where next for melanoma therapy? *Br J Cancer,* 112**,** 217-26.
FERN, R. 2003. Variations in spare electron transport chain capacity: The answer to an old riddle? *J Neurosci Res,* 71**,** 759-62.
FERNIE, A. R., CARRARI, F. & SWEETLOVE, L. J. 2004. Respiratory metabolism: glycolysis, the TCA cycle and mitochondrial electron transport. *Curr Opin Plant Biol,* 7**,** 254-61.
FISHER, T. L. & BLENIS, J. 1996. Evidence for two catalytically active kinase domains in pp90rsk. *Molecular and Cellular Biology,* 16**,** 1212-9.
FOGARTY, S. & HARDIE, D. G. 2009. C-terminal Phosphorylation of LKB1 Is Not Required for Regulation of AMP-activated Protein Kinase, BRSK1, BRSK2, or Cell Cycle Arrest. *Journal of Biological Chemistry,* 284**,** 77-84.
FONSECA, B. D., ALAIN, T., FINESTONE, L. K., HUANG, B. P. H., ROLFE, M., JIANG, T., YAO, Z., HERNANDEZ, G., BENNETT, C. F. & PROUD, C. G. 2011. Pharmacological and Genetic Evaluation of Proposed Roles of Mitogen-activated Protein Kinase/Extracellular Signal-regulated Kinase Kinase (MEK), Extracellular Signal-regulated Kinase (ERK), and p90(RSK) in the Control of mTORC1 Protein Signaling by Phorbol Esters. *Journal of Biological Chemistry,* 286**,** 27111-27122.
FRODIN, M., ANTAL, T. L., DUMMLER, B. A., JENSEN, C. J., DEAK, M., GAMMELTOFT, S. & BIONDI, R. M. 2002. A phosphoserine/threonine-binding pocket in AGC kinases and PDK1 mediates activation by hydrophobic motif phosphorylation. *Embo Journal,* 21**,** 5396-5407.
FRODIN, M., JENSEN, C. J., MERIENNE, K. & GAMMELTOFT, S. 2000. A phosphoserine-regulated docking site in the protein kinase RSK2 that recruits and activates PDK1. *Embo Journal,* 19**,** 2924-2934.
FRY, D. W., BRIDGES, A. J., DENNY, W. A., DOHERTY, A., GREIS, K. D., HICKS, J. L., HOOK, K. E., KELLER, P. R., LEOPOLD, W. R., LOO, J. A., MCNAMARA, D. J., NELSON, J. M., SHERWOOD, V., SMAILL, J. B., TRUMPP-KALLMEYER, S. & DOBRUSIN, E. M. 1998. Specific, irreversible inactivation of the epidermal growth factor receptor and erbB2, by a new class of tyrosine kinase inhibitor. *Proc Natl Acad Sci U S A,* 95**,** 12022-7.
FRYER, R. M., MUTHUKUMARANA, A., CHEN, R. R., SMITH, J. D., MAZUREK, S. N., HARRINGTON, K. E., DINALLO, R. M., BURKE, J., DICAPUA, F. M., GUO, X., KIRRANE, T. M., SNOW, R. J., ZHANG, Y. L., SOLEYMANZADEH, F., MADWED, J. B., KASHEM, M. A., KUGLER, S. Z., O'NEILL, M. M., HARRISON, P. C., REINHART, G. A. & BOYER, S. J. 2012. Mitigation of Off-Target Adrenergic Binding and Effects on Cardiovascular Function in the Discovery of Novel Ribosomal S6 Kinase 2 Inhibitors. *Journal of Pharmacology and Experimental Therapeutics,* 340**,** 492-500.
FU, J. & KREIBICH, G. 2000. Retention of subunits of the oligosaccharyltransferase complex in the endoplasmic reticulum. *Journal of Biological Chemistry,* 275**,** 3984-90.

FUJITA, N., SATO, S. & TSURUO, T. 2003. Phosphorylation of p27(Kip1) at threonine 198 by p90 ribosomal protein S6 kinases promotes its binding to 14-3-3 and cytoplasmic localization. *Journal of Biological Chemistry,* 278**,** 49254-49260.
FUSTER, D. G. & ALEXANDER, R. T. 2014. Traditional and emerging roles for the SLC9 Na+/H+ exchangers. *Pflugers Archiv-European Journal of Physiology,* 466**,** 61-76.
GALAN, J. A., GERAGHTY, K. M., LAVOIE, G., KANSHIN, E., TCHERKEZIAN, J., CALABRESE, V., JESCHKE, G. R., TURK, B. E., BALLIF, B. A., BLENIS, J., THIBAULT, P. & ROUX, P. P. 2014. Phosphoproteomic analysis identifies the tumor suppressor PDCD4 as a RSK substrate negatively regulated by 14-3-3. *Proceedings of the National Academy of Sciences of the United States of America,* 111**,** E2918-E2927.
GARDINO, A. K. & YAFFE, M. B. 2011. 14-3-3 proteins as signaling integration points for cell cycle control and apoptosis. *Semin Cell Dev Biol,* 22**,** 688-95.
GEER, L. Y., MARKEY, S. P., KOWALAK, J. A., WAGNER, L., XU, M., MAYNARD, D. M., YANG, X., SHI, W. & BRYANT, S. H. 2004. Open mass spectrometry search algorithm. *J Proteome Res,* 3**,** 958-64.
GERAGHTY, K. M., CHEN, S., HARTHILL, J. E., IBRAHIM, A. F., TOTH, R., MORRICE, N. A., VANDERMOERE, F., MOORHEAD, G. B., HARDIE, D. G. & MACKINTOSH, C. 2007. Regulation of multisite phosphorylation and 14-3-3 binding of AS160 in response to IGF-1, EGF, PMA and AICAR. *Biochemical Journal,* 407**,** 231-241.
GHODA, L., LIN, X. & GREENE, W. C. 1997. The 90-kDa ribosomal S6 kinase (pp90(rsk)) phosphorylates the N-terminal regulatory domain of I kappa B alpha and stimulates its degradation in vitro. *Journal of Biological Chemistry,* 272**,** 21281-21288.
GIMENEZ-BONAFE, P., FEDORUK, M. N., WHITMORE, T. G., AKBARI, M., RALPH, J. L., ETTINGER, S., GLEAVE, M. E. & NELSON, C. C. 2004. YB-11s upregulated during prostate cancer tumor progression and increases P-glycoprotein activity. *Prostate,* 59**,** 337-349.
GIMENEZ-CASSINA, A. & DANIAL, N. N. 2015. Regulation of mitochondrial nutrient and energy metabolism by BCL-2 family proteins. *Trends Endocrinol Metab,* 26**,** 165-75.
GINTY, D. D., BONNI, A. & GREENBERG, M. E. 1994. Nerve Growth-Factor Activates a Ras-Dependent Protein-Kinase That Stimulates C-Fos Transcription Phosphorylation of Creb. *Cell,* 77**,** 713-725.
GOEL, A. & JANKNECHT, R. 2004. Concerted activation of ETS protein ER81 by p160 coactivators, the acetyltransferase p300 and the receptor tyrosine kinase HER2/Neu. *Journal of Biological Chemistry,* 279**,** 14909-16.
GOLDBERG, D. R., CHOI, Y., COGAN, D., CORSON, M., DELEON, R., GAO, A., GRUENBAUM, L., HAO, M. H., JOSEPH, D., KASHEM, M. A., MILLER, C., MOSS, N., NETHERTON, M. R., PARGELLIS, C. P., PELLETIER, J., SELLATI, R., SKOW, D., TORCELLINI, C., TSENG, Y. C., WANG, J., WASTI, R., WERNEBURG, B., WU, J. P. & XIONG, Z. 2008. Pyrazinoindolone inhibitors of MAPKAP-K2. *Bioorganic & Medicinal Chemistry Letters,* 18**,** 938-41.
GORGOULIS, V. G., VASSILIOU, L. V., KARAKAIDOS, P., ZACHARATOS, P., KOTSINAS, A., LILOGLOU, T., VENERE, M., DITULLIO, R. A., JR., KASTRINAKIS, N. G., LEVY, B., KLETSAS, D., YONETA, A., HERLYN, M., KITTAS, C. & HALAZONETIS, T. D. 2005. Activation of the DNA damage checkpoint and genomic instability in human precancerous lesions. *Nature,* 434**,** 907-13.
GRAY-SCHOPFER, V., WELLBROCK, C. & MARAIS, R. 2007. Melanoma biology and new targeted therapy. *Nature,* 445**,** 851-7.

GREEN, N. M. 1990. Avidin and streptavidin. *Methods Enzymol,* 184**,** 51-67.
GU, C. D., OYAMA, T., OSAKI, T., KOHNO, K. & YASUMOTO, K. 2001. Expression of Y box-binding protein-1 correlates with DNA topoisomerase II alpha and proliferating cell nuclear antigen expression in lung cancer. *Anticancer Research,* 21**,** 2357-2362.
GUO, H. & O'DOHERTY G, A. 2005. de novo asymmetric synthesis of daumone via a palladium-catalyzed glycosylation. *Org Lett,* 7**,** 3921-4.
GUO, H. & O'DOHERTY, G. A. 2006. De novo asymmetric synthesis of D- and L-swainsonine. *Org Lett,* 8**,** 1609-12.
GUO, H. & O'DOHERTY, G. A. 2007. De novo asymmetric synthesis of the anthrax tetrasaccharide by a palladium-catalyzed glycosylation reaction. *Angew Chem Int Ed Engl,* 46**,** 5206-8.
GUO, H. & O'DOHERTY, G. A. 2008. De novo asymmetric synthesis of anthrax tetrasaccharide and related tetrasaccharide. *J Org Chem,* 73**,** 5211-20.
GUPPI, S. R. & O'DOHERTY, G. A. 2007. Synthesis of aza-analogues of the glycosylated tyrosine portion of mannopeptimycin-E. *J Org Chem,* 72**,** 4966-9.
HANAHAN, D. & WEINBERG, R. A. 2011. Hallmarks of cancer: the next generation. *Cell,* 144**,** 646-74.
HANSTEIN, B., ECKNER, R., DIRENZO, J., HALACHMI, S., LIU, H., SEARCY, B., KUROKAWA, R. & BROWN, M. 1996. p300 is a component of an estrogen receptor coactivator complex. *Proc Natl Acad Sci U S A,* 93**,** 11540-5.
HARRIS, J. M., KERANEN, M. D., NGUYEN, H., YOUNG, V. G. & O'DOHERTY G, A. 2000a. Synthesis of four D- and L-hexoses via diastereoselective and enantioselective dihydroxylation reactions. *Carbohydrate Research,* 328**,** 17-36.
HARRIS, J. M., KERANEN, M. D., NGUYEN, H., YOUNG, V. G. & O'DOHERTY, G. A. 2000b. Syntheses of four D- and L-hexoses via diastereoselective and enantioselective dihydroxylation reactions. *Carbohydr Res,* 328**,** 17-36.
HARRIS, J. M., KERANEN, M. D. & O'DOHERTY, G. A. 1999. Syntheses of D- and L-Mannose, Gulose, and Talose via Diastereoselective and Enantioselective Dihydroxylation Reactions. *J Org Chem,* 64**,** 2982-2983.
HARRIS, M. A., CLARK, J., IRELAND, A., LOMAX, J., ASHBURNER, M., FOULGER, R., EILBECK, K., LEWIS, S., MARSHALL, B., MUNGALL, C., RICHTER, J., RUBIN, G. M., BLAKE, J. A., BULT, C., DOLAN, M., DRABKIN, H., EPPIG, J. T., HILL, D. P., NI, L., RINGWALD, M., BALAKRISHNAN, R., CHERRY, J. M., CHRISTIE, K. R., COSTANZO, M. C., DWIGHT, S. S., ENGEL, S., FISK, D. G., HIRSCHMAN, J. E., HONG, E. L., NASH, R. S., SETHURAMAN, A., THEESFELD, C. L., BOTSTEIN, D., DOLINSKI, K., FEIERBACH, B., BERARDINI, T., MUNDODI, S., RHEE, S. Y., APWEILER, R., BARRELL, D., CAMON, E., DIMMER, E., LEE, V., CHISHOLM, R., GAUDET, P., KIBBE, W., KISHORE, R., SCHWARZ, E. M., STERNBERG, P., GWINN, M., HANNICK, L., WORTMAN, J., BERRIMAN, M., WOOD, V., DE LA CRUZ, N., TONELLATO, P., JAISWAL, P., SEIGFRIED, T. & WHITE, R. 2004. The Gene Ontology (GO) database and informatics resource. *Nucleic Acids Research,* 32**,** D258-61.
HARRISON, W., COCHRANE, B., NEILL, G. & PHILPOTT, M. 2014. The oncogenic GLI transcription factors facilitate keratinocyte survival and transformation upon exposure to genotoxic agents. *Oncogene,* 33**,** 2432-40.
HAUGE, C., ANTAL, T. L., HIRSCHBERG, D., DOEHN, U., THORUP, K., IDRISSOVA, L., HANSEN, K., JENSEN, O. N., JORGENSEN, T. J., BIONDI, R. M. & FRODIN, M. 2007.

Mechanism for activation of the growth factor-activated AGC kinases by turn motif phosphorylation. *Embo Journal,* 26**,** 2251-2261.
HAUSCHILD, A., GROB, J. J., DEMIDOV, L. V., JOUARY, T., GUTZMER, R., MILLWARD, M., RUTKOWSKI, P., BLANK, C. U., MILLER, W. H., JR., KAEMPGEN, E., MARTIN-ALGARRA, S., KARASZEWSKA, B., MAUCH, C., CHIARION-SILENI, V., MARTIN, A. M., SWANN, S., HANEY, P., MIRAKHUR, B., GUCKERT, M. E., GOODMAN, V. & CHAPMAN, P. B. 2012. Dabrafenib in BRAF-mutated metastatic melanoma: a multicentre, open-label, phase 3 randomised controlled trial. *Lancet,* 380**,** 358-65.
HEFFRON, D. & MANDELL, J. W. 2005. Differential localization of MAPK-activated protein kinases RSK1 and MSK1 in mouse brain. *Brain Res Mol Brain Res,* 136**,** 134-41.
HEINRICH, T., GRADLER, U., BOTTCHER, H., BLAUKAT, A. & SHUTES, A. 2010. Allosteric IGF-1R Inhibitors. *ACS Med Chem Lett,* 1**,** 199-203.
HENNIG, J. & SATTLER, M. 2014. The dynamic duo: combining NMR and small angle scattering in structural biology. *Protein Science,* 23**,** 669-82.
HILINSKI, M. K., MROZOWSKI, R. M., CLARK, D. E. & LANNIGAN, D. A. 2012. Analogs of the RSK inhibitor SL0101: optimization of in vitro biological stability. *Bioorg Med Chem Lett,* 22**,** 3244-7.
HILL, Z. B., PERERA, B. G., ANDREWS, S. S. & MALY, D. J. 2012. Targeting diverse signaling interaction sites allows the rapid generation of bivalent kinase inhibitors. *ACS Chem Biol,* 7**,** 487-95.
HOFMAN, P. 2004. Molecular regulation of neutrophil apoptosis and potential targets for therapeutic strategy against the inflammatory process. *Curr Drug Targets Inflamm Allergy,* 3**,** 1-9.
HOMET, B. & RIBAS, A. 2014. New drug targets in metastatic melanoma. *Journal of Pathology,* 232**,** 134-41.
HOSHINO, R., CHATANI, Y., YAMORI, T., TSURUO, T., OKA, H., YOSHIDA, O., SHIMADA, Y., ARI-I, S., WADA, H., FUJIMOTO, J. & KOHNO, M. 1999. Constitutive activation of the 41-/43-kDa mitogen-activated protein kinase signaling pathway in human tumors. *Oncogene,* 18**,** 813-822.
HOUDE, V. P., RITORTO, M. S., GOURLAY, R., VARGHESE, J., DAVIES, P., SHPIRO, N., SAKAMOTO, K. & ALESSI, D. R. 2014. Investigation of LKB1 Ser(431) phosphorylation and Cys(433) farnesylation using mouse knockin analysis reveals an unexpected role of prenylation in regulating AMPK activity. *Biochemical Journal,* 458**,** 41-56.
HSU, P. P. & SABATINI, D. M. 2008. Cancer cell metabolism: Warburg and beyond. *Cell,* 134**,** 703-7.
HUANG, W. C., JU, T. K., HUNG, M. C. & CHEN, C. C. 2007. Phosphorylation of CBP by IKKalpha promotes cell growth by switching the binding preference of CBP from p53 to NF-kappaB. *Molecular Cell,* 26**,** 75-87.
HUNG, V., ZOU, P., RHEE, H. W., UDESHI, N. D., CRACAN, V., SVINKINA, T., CARR, S. A., MOOTHA, V. K. & TING, A. Y. 2014. Proteomic mapping of the human mitochondrial intermembrane space in live cells via ratiometric APEX tagging. *Molecular Cell,* 55**,** 332-41.
HUSE, M. & KURIYAN, J. 2002. The conformational plasticity of protein kinases. *Cell,* 109**,** 275-82.
IKUTA, M., KORNIENKO, M., BYRNE, N., REID, J. C., MIZUARAI, S., KOTANI, H. & MUNSHI, S. K. 2007. Crystal structures of the N-terminal kinase domain of human RSK1 bound

to three different ligands: Implications for the design of RSK1 specific inhibitors. *Protein Science,* 16**,** 2626-2635.
INOKI, K., LI, Y., XU, T. & GUAN, K. L. 2003. Rheb GTPase is a direct target of TSC2 GAP activity and regulates mTOR signaling. *Genes Dev,* 17**,** 1829-34.
IYER, A. K., ZHOU, M., AZAD, N., ELBAZ, H., WANG, L., ROGALSKY, D. K., ROJANASAKUL, Y., O'DOHERTY, G. A. & LANGENHAN, J. M. 2010. A Direct Comparison of the Anticancer Activities of Digitoxin MeON-Neoglycosides and O-Glycosides: Oligosaccharide Chain Length-Dependent Induction of Caspase-9-Mediated Apoptosis. *ACS Med Chem Lett,* 1**,** 326-330.
JACQUOT, S., MERIENNE, K., DE CESARE, D., PANNETIER, S., MANDEL, J. L., SASSONE-CORSI, P. & HANAUER, A. 1998. Mutation analysis of the RSK2 gene in Coffin-Lowry patients: Extensive allelic heterogeneity and a high rate of de novo mutations. *American Journal of Human Genetics,* 63**,** 1631-1640.
JASTROCH, M., DIVAKARUNI, A. S., MOOKERJEE, S., TREBERG, J. R. & BRAND, M. D. 2010. Mitochondrial proton and electron leaks. *Essays Biochem,* 47**,** 53-67.
JENSEN, C. J., BUCH, M. B., KRAG, T. O., HEMMINGS, B. A., GAMMELTOFT, S. & FRODIN, M. 1999. 90-kDa ribosomal S6 kinase is phosphorylated and activated by 3-phosphoinositide-dependent protein kinase-1. *Journal of Biological Chemistry,* 274**,** 27168-27176.
JEWELL, J. L. & GUAN, K. L. 2013. Nutrient signaling to mTOR and cell growth. *Trends in Biochemical Sciences,* 38**,** 233-42.
JEWELL, J. L., RUSSELL, R. C. & GUAN, K. L. 2013. Amino acid signalling upstream of mTOR. *Nat Rev Mol Cell Biol,* 14**,** 133-9.
JI, R. R. 2004. Mitogen-activated protein kinases as potential targets for pain killers. *Curr Opin Investig Drugs,* 5**,** 71-5.
JIA, J., ZHANG, L., ZHANG, Q., TONG, C., WANG, B., HOU, F., AMANAI, K. & JIANG, J. 2005. Phosphorylation by double-time/CKIepsilon and CKIalpha targets cubitus interruptus for Slimb/beta-TRCP-mediated proteolytic processing. *Dev Cell,* 9**,** 819-30.
JIANG, J., SARWAR, N., PESTON, D., KULINSKAYA, E., SHOUSHA, S., COOMBES, R. C. & ALI, S. 2007. Phosphorylation of estrogen receptor-alpha at Ser167 is indicative of longer disease-free and overall survival in breast cancer patients. *Clinical Cancer Research,* 13**,** 5769-76.
JIN, Y. & PENNING, T. M. 2007. Aldo-keto reductases and bioactivation/detoxication. *Annu Rev Pharmacol Toxicol,* 47**,** 263-92.
JOEL, P. B., SMITH, J., STURGILL, T. W., FISHER, T. L., BLENIS, J. & LANNIGAN, D. A. 1998. pp90(rsk1) regulates estrogen receptor-mediated transcription through phosphorylation of Ser-167. *Molecular and Cellular Biology,* 18**,** 1978-1984.
JOHNSON, D. A., AKAMINE, P., RADZIO-ANDZELM, E., MADHUSUDAN & TAYLOR, S. S. 2001. Dynamics of cAMP-dependent protein kinase. *Chemical Reviews,* 101**,** 2243-2270.
KANE, S., SANO, H., LIU, S. C. H., ASARA, J. M., LANE, W. S., GARNER, C. C. & LIENHARD, G. E. 2002. A method to identify serine kinase substrates - Akt phosphorylates a novel adipocyte protein with a Rab GTPase-activating protein (GAP) domain. *Journal of Biological Chemistry,* 277**,** 22115-22118.
KANG, S., DONG, S., GU, T., GUO, A., COHEN, M. S., LONIAL, S., BERGSAGEL, P. L., TAUNTON, J., POLAKIEWICZ, R. D. & CHEN, J. 2007a. P90RSK2 as a therapeutic target in treatment of FGFR3-expressing t(4;14) multiple myeloma. *Blood,* 110**,** 82A-82A.

KANG, S., ELF, S., DONG, S., HITOSUGI, T., LYTHGOE, K., GUO, A., RUAN, H., LONIAL, S., KHOURY, H. J., WILLIAMS, I. R., LEE, B. H., ROESEL, J. L., KARSENTY, G., HANAUER, A., TAUNTON, J., BOGGON, T. J., GU, T. L. & CHEN, J. 2009. Fibroblast growth factor receptor 3 associates with and tyrosine phosphorylates p90 RSK2, leading to RSK2 activation that mediates hematopoietic transformation. *Molecular and Cellular Biology,* 29**,** 2105-17.
KANG, S. M., DONG, S. Z., GU, T. L., GUO, A. L., COHEN, M. S., LONIAL, S., KHOURY, H. J., FABBRO, D., GILLILAND, D. G., BERGSAGEL, P. L., TAUNTON, J., POLAKIEWICZ, R. D. & CHEN, J. 2007b. FGFR3 activates RSK2 to mediate hematopoietic transformation through tyrosine phosphorylation of RSK2 and activation of the MEK/ERK pathway. *Cancer Cell,* 12**,** 201-214.
KANG, S. M., ELF, S., LYTHGOE, K., HITOSUGI, T., TAUNTON, J., ZHOU, W., XIONG, L., WANG, D. S., MULLER, S., FAN, S. Q., SUN, S. Y., MARCUS, A. I., GU, T. L., POLAKIEWICZ, R. D., CHEN, Z., KHURI, F. R., SHIN, D. M. & CHEN, J. 2010. p90 ribosomal S6 kinase 2 promotes invasion and metastasis of human head and neck squamous cell carcinoma cells. *Journal of Clinical Investigation,* 120**,** 1165-1177.
KARMAZYN, M. 1988. Amiloride Enhances Postischemic Ventricular Recovery - Possible Role of Na+-H+ Exchange. *American Journal of Physiology,* 255**,** H608-H615.
KAUFMAN, R. J. & MALHOTRA, J. D. 2014. Calcium trafficking integrates endoplasmic reticulum function with mitochondrial bioenergetics. *Biochim Biophys Acta,* 1843**,** 2233-9.
KAUL, G., PATTAN, G. & RAFEEQUI, T. 2011. Eukaryotic elongation factor-2 (eEF2): its regulation and peptide chain elongation. *Cell Biochem Funct,* 29**,** 227-34.
KEDERSHA, N., CHEN, S., GILKS, N., LI, W., MILLER, I. J., STAHL, J. & ANDERSON, P. 2002. Evidence that ternary complex (eIF2-GTP-tRNA(i)(Met))-deficient preinitiation complexes are core constituents of mammalian stress granules. *Molecular Biology of the Cell,* 13**,** 195-210.
KEDERSHA, N., CHO, M. R., LI, W., YACONO, P. W., CHEN, S., GILKS, N., GOLAN, D. E. & ANDERSON, P. 2000. Dynamic shuttling of TIA-1 accompanies the recruitment of mRNA to mammalian stress granules. *Journal of Cell Biology,* 151**,** 1257-1268.
KEDERSHA, N., STOECKLIN, G., AYODELE, M., YACONO, P., LYKKE-ANDERSEN, J., FITZLER, M. J., SCHEUNER, D., KAUFMAN, R. J., GOLAN, D. E. & ANDERSON, P. 2005. Stress granules and processing bodies are dynamically linked sites of mRNP remodeling. *Journal of Cell Biology,* 169**,** 871-884.
KEDERSHA, N. L., GUPTA, M., LI, W., MILLER, I. & ANDERSON, P. 1999. RNA-binding proteins TIA-1 and TIAR link the phosphorylation of eIF-2 alpha to the assembly of mammalian stress granules. *Journal of Cell Biology,* 147**,** 1431-1441.
KIM, J., PARRISH, A. B., KUROKAWA, M., MATSUURA, K., FREEL, C. D., ANDERSEN, J. L., JOHNSON, C. E. & KORNBLUTH, S. 2012. Rsk-mediated phosphorylation and 14-3-3varepsilon binding of Apaf-1 suppresses cytochrome c-induced apoptosis. *Embo Journal,* 31**,** 1279-92.
KING, F. W., SKEEN, J., HAY, N. & SHTIVELMAN, E. 2004. Inhibition of Chk1 by activated PKB/Akt. *Cell Cycle,* 3**,** 634-7.
KINTNER, D. B., SU, G., LENART, B., BALLARD, A. J., MEYER, J. W., NG, L. L., SHULL, G. E. & SUN, D. D. 2004. Increased tolerance to oxygen and glucose deprivation in astrocytes from Na+/H+ exchanger isoform 1 null mice. *American Journal of Physiology-Cell Physiology,* 287**,** C12-C21.

KIRRANE, T. M., BOYER, S. J., BURKE, J., GUO, X., SNOW, R. J., SOLEYMANZADEH, L., SWINAMER, A., ZHANG, Y. L., MADWED, J. B., KASHEM, M., KUGLER, S. & O'NEILL, M. M. 2012. Indole RSK inhibitors. Part 2: Optimization of cell potency and kinase selectivity. *Bioorganic & Medicinal Chemistry Letters,* 22**,** 738-742.
KNIGHT, Z. A. & SHOKAT, K. M. 2005. Features of selective kinase inhibitors. *Chemistry & Biology,* 12**,** 621-37.
KNOWLES, J. R. 1989. The mechanism of biotin-dependent enzymes. *Annu Rev Biochem,* 58**,** 195-221.
KOHN, M., HAMEISTER, H., VOGEL, M. & KEHRER-SAWATZKI, H. 2003. Expression pattern of the Rsk2, Rsk4 and Pdk1 genes during murine embryogenesis. *Gene Expr Patterns,* 3**,** 173-7.
KOLLURI, R. & KINNIBURGH, A. J. 1991. Full Length Cdna Sequence Encoding a Nuclease-Sensitive Element DNA-Binding Protein. *Nucleic Acids Research,* 19**,** 4771-4771.
KORNEV, A. P., HASTE, N. M., TAYLOR, S. S. & EYCK, L. F. 2006. Surface comparison of active and inactive protein kinases identifies a conserved activation mechanism. *Proc Natl Acad Sci U S A,* 103**,** 17783-8.
KOTENKO, S. V., GALLAGHER, G., BAURIN, V. V., LEWIS-ANTES, A., SHEN, M., SHAH, N. K., LANGER, J. A., SHEIKH, F., DICKENSHEETS, H. & DONNELLY, R. P. 2003. IFN-lambdas mediate antiviral protection through a distinct class II cytokine receptor complex. *Nature Immunology,* 4**,** 69-77.
KRAKER, A. J., HARTL, B. G., AMAR, A. M., BARVIAN, M. R., SHOWALTER, H. D. H. & MOORE, C. W. 2000. Biochemical and cellular effects of c-Src kinase-selective pyrido[2,3-d]pyrimidine tyrosine kinase inhibitors. *Biochemical Pharmacology,* 60**,** 885-898.
KROCZYNSKA, B., JOSHI, S., EKLUND, E. A., VERMA, A., KOTENKO, S. V., FISH, E. N. & PLATANIAS, L. C. 2011. Regulatory Effects of Ribosomal S6 Kinase 1 (RSK1) in IFN lambda Signaling. *Journal of Biological Chemistry,* 286**,** 1147-1156.
KROCZYNSKA, B., KAUR, S., KATSOULIDIS, E., MAJCHRZAK-KITA, B., SASSANO, A., KOZMA, S. C., FISH, E. N. & PLATANIAS, L. C. 2009. Interferon-dependent engagement of eukaryotic initiation factor 4B via S6 kinase (S6K)- and ribosomal protein S6K-mediated signals. *Molecular and Cellular Biology,* 29**,** 2865-75.
KROCZYNSKA, B., MEHROTRA, S., MAJCHRZAK-KITA, B., ARSLAN, A. D., ALTMAN, J. K., STEIN, B. L., MCMAHON, B., KOZLOWSKI, P., KAHLE, P. J., EKLUND, E. A., FISH, E. N. & PLATANIAS, L. C. 2014. Regulatory effects of SKAR in interferon alpha signaling and its role in the generation of type I IFN responses. *Proc Natl Acad Sci U S A,* 111**,** 11377-82.
KROCZYNSKA, B., SHARMA, B., EKLUND, E. A., FISH, E. N. & PLATANIAS, L. C. 2012. Regulatory effects of programmed cell death 4 (PDCD4) protein in interferon (IFN)-stimulated gene expression and generation of type I IFN responses. *Molecular and Cellular Biology,* 32**,** 2809-22.
KRUPA, A., PREETHI, G. & SRINIVASAN, N. 2004. Structural modes of stabilization of permissive phosphorylation sites in protein kinases: distinct strategies in Ser/Thr and Tyr kinases. *Journal of Molecular Biology,* 339**,** 1025-39.
KUANG, E., FU, B., LIANG, Q., MYOUNG, J. & ZHU, F. 2011. Phosphorylation of eukaryotic translation initiation factor 4B (EIF4B) by open reading frame 45/p90 ribosomal S6 kinase (ORF45/RSK) signaling axis facilitates protein translation during Kaposi sarcoma-associated herpesvirus (KSHV) lytic replication. *Journal of Biological Chemistry,* 286**,** 41171-82.

KUSTIKOVA, O., KRAMEROV, D., GRIGORIAN, M., BEREZIN, V., BOCK, E., LUKANIDIN, E. & TULCHINSKY, E. 1998. Fra-1 induces morphological transformation and increases in vitro invasiveness and motility of epithelioid adenocarcinoma cells. *Molecular and Cellular Biology,* 18**,** 7095-105.
KWOK, R. P., LUNDBLAD, J. R., CHRIVIA, J. C., RICHARDS, J. P., BACHINGER, H. P., BRENNAN, R. G., ROBERTS, S. G., GREEN, M. R. & GOODMAN, R. H. 1994. Nuclear protein CBP is a coactivator for the transcription factor CREB. *Nature,* 370**,** 223-6.
LAITINEN, O. H., HYTONEN, V. P., NORDLUND, H. R. & KULOMAA, M. S. 2006. Genetically engineered avidins and streptavidins. *Cell Mol Life Sci,* 63**,** 2992-3017.
LAM, S. S., MARTELL, J. D., KAMER, K. J., DEERINCK, T. J., ELLISMAN, M. H., MOOTHA, V. K. & TING, A. Y. 2015. Directed evolution of APEX2 for electron microscopy and proximity labeling. *Nat Methods,* 12**,** 51-4.
LANKAT-BUTTGEREIT, B. & GOKE, R. 2009. The tumour suppressor Pdcd4: recent advances in the elucidation of function and regulation. *Biology of the Cell,* 101**,** 309-317.
LARA, R., MAURI, F. A., TAYLOR, H., DERUA, R., SHIA, A., GRAY, C., NICOLS, A., SHINER, R. J., SCHOFIELD, E., BATES, P. A., WAELKENS, E., DALLMAN, M., LAMB, J., ZICHA, D., DOWNWARD, J., SECKL, M. J. & PARDO, O. E. 2011. An siRNA screen identifies RSK1 as a key modulator of lung cancer metastasis. *Oncogene,* 30**,** 3513-21.
LARA, R., SECKL, M. J. & PARDO, O. E. 2013. The p90 RSK Family Members: Common Functions and Isoform Specificity. *Cancer Research,* 73**,** 5301-5308.
LARREAA, M. D., HONG, F., WANDER, S. A., DA SILVA, T. G., HELFMAN, D., LANNIGAN, D., SMITH, J. A. & SLINGERLAND, J. M. 2009. RSK1 drives p27(Kip1) phosphorylation at T198 to promote RhoA inhibition and increase cell motility. *Proceedings of the National Academy of Sciences of the United States of America,* 106**,** 9268-9273.
LARSSON, O., LI, S., ISSAENKO, O. A., AVDULOV, S., PETERSON, M., SMITH, K., BITTERMAN, P. B. & POLUNOVSKY, V. A. 2007. Eukaryotic translation initiation factor 4E induced progression of primary human mammary epithelial cells along the cancer pathway is associated with targeted translational deregulation of oncogenic drivers and inhibitors. *Cancer Research,* 67**,** 6814-24.
LAUGEL-HAUSHALTER, V., PASCHAKI, M., MARANGONI, P., PILGRAM, C., LANGER, A., KUNTZ, T., DEMASSUE, J., MORKMUED, S., CHOQUET, P., CONSTANTINESCO, A., BORNERT, F., SCHMITTBUHL, M., PANNETIER, S., VIRIOT, L., HANAUER, A., DOLLE, P. & BLOCH-ZUPAN, A. 2014. RSK2 is a modulator of craniofacial development. *Plos One,* 9**,** e84343.
LE, N. T., TAKEI, Y., SHISHIDO, T., WOO, C. H., CHANG, E., HEO, K. S., LEE, H., LU, Y., MORRELL, C., OIKAWA, M., MCCLAIN, C., WANG, X., TOURNIER, C., MOLINA, C. A., TAUNTON, J., YAN, C., FUJIWARA, K., PATTERSON, C., YANG, J. & ABE, J. 2012. p90RSK Targets the ERK5-CHIP Ubiquitin E3 Ligase Activity in Diabetic Hearts and Promotes Cardiac Apoptosis and Dysfunction. *Circulation Research,* 110**,** 536-U84.
LEE, E. Y., JI, H., OUYANG, Z., ZHOU, B., MA, W., VOKES, S. A., MCMAHON, A. P., WONG, W. H. & SCOTT, M. P. 2010. Hedgehog pathway-regulated gene networks in cerebellum development and tumorigenesis. *Proc Natl Acad Sci U S A,* 107**,** 9736-41.
LEE, M. Y., SUN, L. & VELTMAAT, J. M. 2013. Hedgehog and Gli signaling in embryonic mammary gland development. *J Mammary Gland Biol Neoplasia,* 18**,** 133-8.
LEIGHTON, I. A., DALBY, K. N., CAUDWELL, F. B., COHEN, P. T. & COHEN, P. 1995. Comparison of the specificities of p70 S6 kinase and MAPKAP kinase-1 identifies a relatively

specific substrate for p70 S6 kinase: the N-terminal kinase domain of MAPKAP kinase-1 is essential for peptide phosphorylation. *Febs Letters,* 375**,** 289-93.
LENART, P., PETRONCZKI, M., STEEGMAIER, M., DI FIORE, B., LIPP, J. J., HOFFMANN, M., RETTIG, W. J., KRAUT, N. & PETERS, J. M. 2007. The small-molecule inhibitor BI 2536 reveals novel insights into mitotic roles of polo-like kinase 1. *Current Biology,* 17**,** 304-315.
LI, D., JIN, L. T., ALESI, G. N., KIM, Y. M., FAN, J., SEO, J. H., WANG, D. S., TUCKER, M., GU, T. L., LEE, B. H., TAUNTON, J., MAGLIOCCA, K. R., CHEN, Z. G., SHIN, D. M., KHURI, F. R. & KANG, S. M. 2013. The Prometastatic Ribosomal S6 Kinase 2-cAMP Response Element-binding Protein (RSK2-CREB) Signaling Pathway Up-regulates the Actin-binding Protein Fascin-1 to Promote Tumor Metastasis. *Journal of Biological Chemistry,* 288**,** 32528-32538.
LI, M., SCOTT, J. G. & O'DOHERTY G, A. 2004. Synthesis of 7-oxa-phomopsolide E and its C-4 epimer. *Tetrahedron Lett,* 45**,** 1005-1009.
LI, P., GOTO, H., KASAHARA, K., MATSUYAMA, M., WANG, Z., YATABE, Y., KIYONO, T. & INAGAKI, M. 2012a. P90 RSK arranges Chk1 in the nucleus for monitoring of genomic integrity during cell proliferation. *Molecular Biology of the Cell,* 23**,** 1582-92.
LI, T., LIU, Z., HU, X., MA, K. & ZHOU, C. 2012b. Involvement of ERK-RSK cascade in phenylephrine-induced phosphorylation of GATA4. *Biochim Biophys Acta,* 1823**,** 582-92.
LI, W. & WYSOCKI, V. H. 2012. ETD fragmentation features improve algorithm. *Expert Rev Proteomics,* 9**,** 241-3.
LIANG, Q., DE WINDT, L. J., WITT, S. A., KIMBALL, T. R., MARKHAM, B. E. & MOLKENTIN, J. D. 2001a. The transcription factors GATA4 and GATA6 regulate cardiomyocyte hypertrophy in vitro and in vivo. *Journal of Biological Chemistry,* 276**,** 30245-53.
LIANG, Q., WIESE, R. J., BUENO, O. F., DAI, Y. S., MARKHAM, B. E. & MOLKENTIN, J. D. 2001b. The transcription factor GATA4 is activated by extracellular signal-regulated kinase 1- and 2-mediated phosphorylation of serine 105 in cardiomyocytes. *Molecular and Cellular Biology,* 21**,** 7460-9.
LIM, H. C., XIE, L., ZHANG, W., LI, R., CHEN, Z. C., WU, G. Z., CUI, S. S., TAN, E. K. & ZENG, L. 2013a. Ribosomal S6 Kinase 2 (RSK2) maintains genomic stability by activating the Atm/p53-dependent DNA damage pathway. *Plos One,* 8**,** e74334.
LIM, S., SAW, T. Y., ZHANG, M., JANES, M. R., NACRO, K., HILL, J., LIM, A. Q., CHANG, C. T., FRUMAN, D. A., RIZZIERI, D. A., TAN, S. Y., FAN, H., CHUAH, C. T. & ONG, S. T. 2013b. Targeting of the MNK-eIF4E axis in blast crisis chronic myeloid leukemia inhibits leukemia stem cell function. *Proc Natl Acad Sci U S A,* 110**,** E2298-307.
LIN, C. H., NAI, P. L., BIEN, M. Y., YU, C. C. & CHEN, B. C. 2014. Thrombin-induced CCAAT/enhancer-binding protein beta activation and IL-8/CXCL8 expression via MEKK1, ERK, and p90 ribosomal S6 kinase 1 in lung epithelial cells. *J Immunol,* 192**,** 338-48.
LIN, J. X., SPOLSKI, R. & LEONARD, W. J. 2008. Critical role for Rsk2 in T-lymphocyte activation. *Blood,* 111**,** 525-33.
LITO, P., ROSEN, N. & SOLIT, D. B. 2013. Tumor adaptation and resistance to RAF inhibitors. *Nat Med,* 19**,** 1401-9.
LIU, Y., BISHOP, A., WITUCKI, L., KRAYBILL, B., SHIMIZU, E., TSIEN, J., UBERSAX, J., BLETHROW, J., MORGAN, D. O. & SHOKAT, K. M. 1999. Structural basis for selective inhibition of Src family kinases by PP1. *Chemistry & Biology,* 6**,** 671-8.

LIU, Z., LI, T., REINHOLD, M. I. & NASKI, M. C. 2014. MEK1-RSK2 contributes to Hedgehog signaling by stabilizing GLI2 transcription factor and inhibiting ubiquitination. *Oncogene,* 33**,** 65-73.
LOCHNER, A. & MOOLMAN, J. A. 2006. The many faces of H89: a review. *Cardiovasc Drug Rev,* 24**,** 261-74.
LONDON, N., MILLER, R. M., IRWIN, J. J., EIDAM, O., GIBOLD, L., BONNET, R., SHOICHET, B. K. & TAUNTON, J. 2014. Covalent Docking of Large Libraries for the Discovery of Chemical Probes. *Biophysical Journal,* 106**,** 263A-263A.
LOPEZ-VICENTE, L., ARMENGOL, G., PONS, B., COCH, L., ARGELAGUET, E., LLEONART, M., HERNANDEZ-LOSA, J., DE TORRES, I. & CAJAL, S. R. Y. 2009. Regulation of Replicative and Stress-Induced Senescence by RSK4, which is Down-regulated in Human Tumors. *Clinical Cancer Research,* 15**,** 4546-4553.
LUO, J., CHEN, H., KINTNER, D. B., SHULL, G. E. & SUN, D. 2005. Decreased neuronal death in Na+/H+ exchanger isoform 1-null mice after in vitro and in vivo ischemia. *Journal of Neuroscience,* 25**,** 11256-11268.
MAEKAWA, N., ABE, J., SHISHIDO, T., ITOH, S., DING, B., SHARMA, V. K., SHEU, S. S., BLAXALL, B. C. & BERK, B. C. 2006. Inhibiting p90 ribosomal S6 kinase prevents (Na+)-H+ exchanger-mediated cardiac ischemia-reperfusion injury. *Circulation,* 113**,** 2516-23.
MALAKHOVA, M., KURINOV, I., LIU, K., ZHENG, D., D'ANGELO, I., SHIM, J. H., STEINMAN, V., BODE, A. M. & DONG, Z. 2009. Structural diversity of the active N-terminal kinase domain of p90 ribosomal S6 kinase 2. *Plos One,* 4**,** e8044.
MALAKHOVA, M., TERESHKO, V., LEE, S. Y., YAO, K., CHO, Y. Y., BODE, A. & DONG, Z. 2008. Structural basis for activation of the autoinhibitory C-terminal kinase domain of p90 RSK2. *Nature Structural & Molecular Biology,* 15**,** 112-3.
MALLILANKARAMAN, K., CARDENAS, C., DOONAN, P. J., CHANDRAMOORTHY, H. C., IRRINKI, K. M., GOLENAR, T., CSORDAS, G., MADIREDDI, P., YANG, J., MULLER, M., MILLER, R., KOLESAR, J. E., MOLGO, J., KAUFMAN, B., HAJNOCZKY, G., FOSKETT, J. K. & MADESH, M. 2012a. MCUR1 is an essential component of mitochondrial Ca2+ uptake that regulates cellular metabolism. *Nature Cell Biology,* 14**,** 1336-43.
MALLILANKARAMAN, K., DOONAN, P., CARDENAS, C., CHANDRAMOORTHY, H. C., MULLER, M., MILLER, R., HOFFMAN, N. E., GANDHIRAJAN, R. K., MOLGO, J., BIRNBAUM, M. J., ROTHBERG, B. S., MAK, D. O., FOSKETT, J. K. & MADESH, M. 2012b. MICU1 is an essential gatekeeper for MCU-mediated mitochondrial Ca(2+) uptake that regulates cell survival. *Cell,* 151**,** 630-44.
MALONEY, D. J. & HECHT, S. M. 2005. Synthesis of a potent and selective inhibitor of p90 Rsk. *Org Lett,* 7**,** 1097-9.
MANHAS, N., SHI, Y., TAUNTON, J. & SUN, D. 2010. p90 activation contributes to cerebral ischemic damage via phosphorylation of Na+/H+ exchanger isoform 1. *J Neurochem,* 114**,** 1476-86.
MANNING, G., WHYTE, D. B., MARTINEZ, R., HUNTER, T. & SUDARSANAM, S. 2002. The protein kinase complement of the human genome. *Science,* 298**,** 1912-+.
MARTELL, J. D., DEERINCK, T. J., SANCAK, Y., POULOS, T. L., MOOTHA, V. K., SOSINSKY, G. E., ELLISMAN, M. H. & TING, A. Y. 2012. Engineered ascorbate peroxidase as a genetically encoded reporter for electron microscopy. *Nat Biotechnol,* 30**,** 1143-8.

MARTIN, S. E., SHABANOWITZ, J., HUNT, D. F. & MARTO, J. A. 2000. Subfemtomole MS and MS/MS peptide sequence analysis using nano-HPLC micro-ESI fourier transform ion cyclotron resonance mass spectrometry. *Anal Chem,* 72**,** 4266-74.
MAYER, C. & GRUMMT, I. 2006. Ribosome biogenesis and cell growth: mTOR coordinates transcription by all three classes of nuclear RNA polymerases. *Oncogene,* 25**,** 6384-6391.
MCCAFFREY, L. M. & MACARA, I. G. 2009. The Par3/aPKC interaction is essential for end bud remodeling and progenitor differentiation during mammary gland morphogenesis. *Genes Dev,* 23**,** 1450-60.
MCCUBREY, J. A., STEELMAN, L. S., BERTRAND, F. E., DAVIS, N. M., SOKOLOSKY, M., ABRAMS, S. L., MONTALTO, G., D'ASSORO, A. B., LIBRA, M., NICOLETTI, F., MAESTRO, R., BASECKE, J., RAKUS, D., GIZAK, A., DEMIDENKO, Z., COCCO, L., MARTELLI, A. M. & CERVELLO, M. 2014. GSK-3 as potential target for therapeutic irvention in cancer. *Oncotarget,* 5**,** 2881-2911.
MCMANUS, E. J., COLLINS, B. J., ASHBY, P. R., PRESCOTT, A. R., MURRAY-TAIT, V., ARMIT, L. J., ARTHUR, J. S. & ALESSI, D. R. 2004. The in vivo role of PtdIns(3,4,5)P3 binding to PDK1 PH domain defined by knockin mutation. *Embo Journal,* 23**,** 2071-82.
MELOCHE, S. & POUYSSEGUR, J. 2007. The ERK1/2 mitogen-activated protein kinase pathway as a master regulator of the G1- to S-phase transition. *Oncogene,* 26**,** 3227-39.
MERIC-BERNSTAM, F., CHEN, H., AKCAKANAT, A., DO, K. A., LLUCH, A., HENNESSY, B. T., HORTOBAGYI, G. N., MILLS, G. B. & GONZALEZ-ANGULO, A. 2012. Aberrations in translational regulation are associated with poor prognosis in hormone receptor-positive breast cancer. *Breast Cancer Research,* 14**,** R138.
MILLER, R. M., PAAVILAINEN, V. O., KRISHNAN, S., SERAFIMOVA, I. M. & TAUNTON, J. 2013. Electrophilic Fragment-Based Design of Reversible Covalent Kinase Inhibitors. *Journal of the American Chemical Society,* 135**,** 5298-5301.
MOHAMMADI, M., FROUM, S., HAMBY, J. M., SCHROEDER, M. C., PANEK, R. L., LU, G. H., ELISEENKOVA, A. V., GREEN, D., SCHLESSINGER, J. & HUBBARD, S. R. 1998. Crystal structure of an angiogenesis inhibitor bound to the FGF receptor tyrosine kinase domain. *Embo Journal,* 17**,** 5896-5904.
MOLKENTIN, J. D., LIN, Q., DUNCAN, S. A. & OLSON, E. N. 1997. Requirement of the transcription factor GATA4 for heart tube formation and ventral morphogenesis. *Genes Dev,* 11**,** 1061-72.
MOLKENTIN, J. D. & OLSON, E. N. 1997. GATA4: a novel transcriptional regulator of cardiac hypertrophy? *Circulation,* 96**,** 3833-5.
MOLLER, D. E., XIA, C. H., TANG, W., ZHU, A. X. & JAKUBOWSKI, M. 1994. Human rsk isoforms: cloning and characterization of tissue-specific expression. *American Journal of Physiology,* 266**,** C351-9.
MORISCO, C., SETA, K., HARDT, S. E., LEE, Y., VATNER, S. F. & SADOSHIMA, J. 2001. Glycogen synthase kinase 3beta regulates GATA4 in cardiac myocytes. *Journal of Biological Chemistry,* 276**,** 28586-97.
MORITZ, A., LI, Y., GUO, A., VILLEN, J., WANG, Y., MACNEILL, J., KORNHAUSER, J., SPROTT, K., ZHOU, J., POSSEMATO, A., REN, J. M., HORNBECK, P., CANTLEY, L. C., GYGI, S. P., RUSH, J. & COMB, M. J. 2010. Akt-RSK-S6 kinase signaling networks activated by oncogenic receptor tyrosine kinases. *Sci Signal,* 3**,** ra64.
MROZOWSKI, R. M., VEMULA, R., WU, B., ZHANG, Q., SCHROEDER, B. R., HILINSKI, M. K., CLARK, D. E., HECHT, S. M., O'DOHERTY, G. A. & LANNIGAN, D. A. 2012.

Improving the affinity of SL0101 for RSK using structure-based design. *ACS Med Chem Lett,* 4**,** 175-179.
NAKAJIMA, T., FUKAMIZU, A., TAKAHASHI, J., GAGE, F. H., FISHER, T., BLENIS, J. & MONTMINY, M. R. 1996. The signal-dependent coactivator CBP is a nuclear target for pp90(RSK). *Cell,* 86**,** 465-474.
NAON, D. & SCORRANO, L. 2014. At the right distance: ER-mitochondria juxtaposition in cell life and death. *Biochim Biophys Acta,* 1843**,** 2184-94.
NARAYANA, N., COX, S., XUONG, N. H., TENEYCK, L. F. & TAYLOR, S. S. 1997. A binary complex of the catalytic subunit of cAMP-dependent protein kinase and adenosine further defines conformational flexibility. *Structure,* 5**,** 921-935.
NESVIZHSKII, A. I., VITEK, O. & AEBERSOLD, R. 2007. Analysis and validation of proteomic data generated by tandem mass spectrometry. *Nat Methods,* 4**,** 787-97.
NGUYEN, T. L. 2008. Targeting RSK: An Overview of Small Molecule Inhibitors. *Anti-Cancer Agents in Medicinal Chemistry,* 8**,** 710-716.
NGUYEN, T. L., GUSSIO, R., SMITH, J. A., LANNIGAN, D. A., HECHT, S. M., SCUDIERO, D. A., SHOEMAKER, R. H. & ZAHAREVITZ, D. W. 2006. Homology model of RSK2 N-terminal kinase domain, structure-based identification of novel RSK2 inhibitors, and preliminary common pharmacophore. *Bioorg Med Chem,* 14**,** 6097-105.
NICKENS, K. P., WIKSTROM, J. D., SHIRIHAI, O. S., PATIERNO, S. R. & CERYAK, S. 2013. A bioenergetic profile of non-transformed fibroblasts uncovers a link between death-resistance and enhanced spare respiratory capacity. *Mitochondrion,* 13**,** 662-7.
NISHIYAMA, T., OHSUMI, K. & KISHIMOTO, T. 2007. Phosphorylation of Erp1 by p90rsk is required for cytostatic factor arrest in Xenopus laevis eggs. *Nature,* 446**,** 1096-1099.
O'BRIEN, S. G., GUILHOT, F., LARSON, R. A., GATHMANN, I., BACCARANI, M., CERVANTES, F., CORNELISSEN, J. J., FISCHER, T., HOCHHAUS, A., HUGHES, T., LECHNER, K., NIELSEN, J. L., ROUSSELOT, P., REIFFERS, J., SAGLIO, G., SHEPHERD, J., SIMONSSON, B., GRATWOHL, A., GOLDMAN, J. M., KANTARJIAN, H., TAYLOR, K., VERHOEF, G., BOLTON, A. E., CAPDEVILLE, R., DRUKER, B. J., DURRANT, S., SCHWARER, A., JOSKE, D., SEYMOUR, J., GRIGG, A., MA, D., ARTHUR, C., BRADSTOCK, K., JOSHUA, D., LOUWAGIE, A., MARTIAT, P., STRAETMANS, N., BOSLY, A., SHUSTIK, C., LIPTON, J., FORREST, D., WALKER, I., ROY, D. C., RUBINGER, M., BENCE-BRUCKLER, I., KOVACS, M., TURNER, A. R., BIRGENS, H., BJERRUM, O., FACON, T., HAROUSSEAU, J. L., TULLIEZ, M., GUERCI, A., BLAISE, D., MALOISEL, F., MICHALLET, M., HOSSFELD, D., MERTELSMANN, R., ANDREESEN, R., NERL, C., FREUND, M., GATTERMANN, N., HOEFFKEN, K., EHNINGER, G., DEININGER, M., OTTMANN, O., PESCHEL, C., FRUEHAUF, S., NEUBAUER, A., LE COUTRE, P., AULITZKY, W., FANIN, R., ROSTI, G., MANDELLI, F., MORRA, E., CARELLA, A., LAZZARINO, M., PETRINI, M., FERRINI, P. R., NOBILE, F., LISO, V., FERRARA, F., RIZZOLI, V., FIORITONI, G., MARTINELLI, G., OSSENKOPPELE, G., BROWETT, P., GEDDE-DAHL, T., TANGEN, J. M., DAHL, I., ODRIOZOLA, J., BOLUDA, J. C. H., STEEGMANN, J. L., CANIZO, C., SUREDA, A., DIAZ, J., GRANENA, A., FERNANDEZ, M. N., STENKE, L., PAUL, C., et al. 2003. Imatinib compared with interferon and low-dose cytarabine for newly diagnosed chronic-phase chronic myeloid leukemia. *New England Journal of Medicine,* 348**,** 994-1004.
ODA, Y., OHISHI, Y., SAITO, T., HINOSHITA, E., UCHIUMI, T., KINUKAWA, N., IWAMOTO, Y., KOHNO, K., KUWANO, M. & TSUNEYOSHI, M. 2003. Nuclear expression

of Y-box-binding protein-1 correlates with P-glycoprotein and topoisomerase II alpha expression, and with poor prognosis in synovial sarcoma. *Journal of Pathology,* 199**,** 251-258.
ODA, Y., SAKAMOTO, A., SHINOHARA, N., OHGA, T., UCHIUMI, T., KOHNO, K., TSUNEYOSHI, M., KUWANO, M. & IWAMOTO, Y. 1998. Nuclear expression of YB-1 protein correlates with P-glycoprotein expression in human osteosarcoma. *Clinical Cancer Research,* 4**,** 2273-2277.
OHREN, J. F., CHEN, H. F., PAVLOVSKY, A., WHITEHEAD, C., ZHANG, E. L., KUFFA, P., YAN, C. H., MCCONNELL, P., SPESSARD, C., BANOTAI, C., MUELLER, W. T., DELANEY, A., OMER, C., SEBOLT-LEOPOLD, J., DUDLEY, D. T., LEUNG, I. K., FLAMME, C., WARMUS, J., KAUFMAN, M., BARRETT, S., TECLE, H. & HASEMANN, C. A. 2004. Structures of human MAP kinase kinase 1 (MEK1) and MEK2 describe novel noncompetitive kinase inhibition. *Nature Structural & Molecular Biology,* 11**,** 1192-1197.
OLD, W. M., SHABB, J. B., HOUEL, S., WANG, H., COUTS, K. L., YEN, C. Y., LITMAN, E. S., CROY, C. H., MEYER-ARENDT, K., MIRANDA, J. G., BROWN, R. A., WITZE, E. S., SCHWEPPE, R. E., RESING, K. A. & AHN, N. G. 2009. Functional proteomics identifies targets of phosphorylation by B-Raf signaling in melanoma. *Molecular Cell,* 34**,** 115-31.
OVER, B., WETZEL, S., GRUTTER, C., NAKAI, Y., RENNER, S., RAUH, D. & WALDMANN, H. 2013. Natural-product-derived fragments for fragment-based ligand discovery. *Nature Chemistry,* 5**,** 21-28.
PALMER, A., GAVIN, A. C. & NEBREDA, A. R. 1998. A link between MAP kinase and p(34cdc2) cyclin B during oocyte maturation: p90(rsk) phosphorylates and inactivates the p34(cdc2) inhibitory kinase Myt1. *Embo Journal,* 17**,** 5037-5047.
PAN, Y., WANG, C. & WANG, B. 2009. Phosphorylation of Gli2 by protein kinase A is required for Gli2 processing and degradation and the Sonic Hedgehog-regulated mouse development. *Developmental Biology,* 326**,** 177-89.
PAPOUTSOPOULOU, S. & JANKNECHT, R. 2000. Phosphorylation of ETS transcription factor ER81 in a complex with its coactivators CREB-binding protein and p300. *Molecular and Cellular Biology,* 20**,** 7300-10.
PASIC, L., EISINGER-MATHASON, T. S., VELAYUDHAN, B. T., MOSKALUK, C. A., BRENIN, D. R., MACARA, I. G. & LANNIGAN, D. A. 2011a. Sustained activation of the HER1-ERK1/2-RSK signaling pathway controls myoepithelial cell fate in human mammary tissue. *Genes Dev,* 25**,** 1641-53.
PASIC, L., EISINGER-MATHASON, T. S. K., VELAYUDHAN, B. T., MOSKALUK, C. A., BRENIN, D. R., MACARA, I. G. & LANNIGAN, D. A. 2011b. Sustained activation of the HER1-ERK1/2-RSK signaling pathway controls myoepithelial cell fate in human mammary tissue. *Genes & Development,* 25**,** 1641-1653.
PATRICELLI, M. P., SZARDENINGS, A. K., LIYANAGE, M., NOMANBHOY, T. K., WU, M., WEISSIG, H., ABAN, A., CHUN, D., TANNER, S. & KOZARICH, J. W. 2007. Functional interrogation of the kinome using nucleotide acyl phosphates. *Biochemistry,* 46**,** 350-358.
PENDE, M., UM, S. H., MIEULET, V., STICKER, M., GOSS, V. L., MESTAN, J., MUELLER, M., FUMAGALLI, S., KOZMA, S. C. & THOMAS, G. 2004. S6K1(-/-)/S6K2(-/-) mice exhibit perinatal lethality and rapamycin-sensitive 5 '-terminal oligopyrimidine mRNA translation and reveal a mitogen-activated protein kinase-dependent S6 kinase pathway. *Molecular and Cellular Biology,* 24**,** 3112-3124.
PEREIRA, P. M., SCHNEIDER, A., PANNETIER, S., HERON, D. & HANAUER, A. 2010. Coffin-Lowry syndrome. *European Journal of Human Genetics,* 18**,** 627-633.

PEROCCHI, F., GOHIL, V. M., GIRGIS, H. S., BAO, X. R., MCCOMBS, J. E., PALMER, A. E. & MOOTHA, V. K. 2010. MICU1 encodes a mitochondrial EF hand protein required for Ca(2+) uptake. *Nature,* 467**,** 291-6.
PERVIN, S., TRAN, A. H., ZEKAVATI, S., FUKUTO, J. M., SINGH, R. & CHAUDHURI, G. 2008. Increased susceptibility of breast cancer cells to stress mediated inhibition of protein synthesis. *Cancer Research,* 68**,** 4862-74.
PIERRAT, B., CORREIA, J. S., MARY, J. L., TOMAS-ZUBER, M. & LESSLAUER, W. 1998. RSK-B, a novel ribosomal S6 kinase family member, is a CREB kinase under dominant control of p38alpha mitogen-activated protein kinase (p38alphaMAPK). *Journal of Biological Chemistry,* 273**,** 29661-71.
POTEET-SMITH, C. E., SMITH, J. A., LANNIGAN, D. A., FREED, T. A. & STURGILL, T. W. 1999. Generation of constitutively active p90 ribosomal S6 kinase in vivo. Implications for the mitogen-activated protein kinase-activated protein kinase family. *Journal of Biological Chemistry,* 274**,** 22135-8.
PUC, J., KENIRY, M., LI, H. S., PANDITA, T. K., CHOUDHURY, A. D., MEMEO, L., MANSUKHANI, M., MURTY, V. V., GACIONG, Z., MEEK, S. E., PIWNICA-WORMS, H., HIBSHOOSH, H. & PARSONS, R. 2005. Lack of PTEN sequesters CHK1 and initiates genetic instability. *Cancer Cell,* 7**,** 193-204.
QUINN, P. G. 1994. Inhibition by Insulin of Protein-Kinase a-Induced Transcription of the Phosphoenolpyruvate Carboxykinase Gene - Mediation by the Activation Domain of Camp Response Element-Binding Protein (Creb) and Factors Bound to the Tata Box. *Journal of Biological Chemistry,* 269**,** 14375-14378.
RAY-DAVID, H., ROMEO, Y., LAVOIE, G., DELERIS, P., TCHERKEZIAN, J., GALAN, J. A. & ROUX, P. P. 2013. RSK promotes G2 DNA damage checkpoint silencing and participates in melanoma chemoresistance. *Oncogene,* 32**,** 4480-9.
RHEE, H. W., ZOU, P., UDESHI, N. D., MARTELL, J. D., MOOTHA, V. K., CARR, S. A. & TING, A. Y. 2013. Proteomic mapping of mitochondria in living cells via spatially restricted enzymatic tagging. *Science,* 339**,** 1328-31.
RICHARDS, S. A., DREISBACH, V. C., MURPHY, L. O. & BLENIS, J. 2001. Characterization of regulatory events associated with membrane targeting of p90 ribosomal S6 kinase 1. *Molecular and Cellular Biology,* 21**,** 7470-7480.
RIVERA, V. M., MIRANTI, C. K., MISRA, R. P., GINTY, D. D., CHEN, R. H., BLENIS, J. & GREENBERG, M. E. 1993. A growth factor-induced kinase phosphorylates the serum response factor at a site that regulates its DNA-binding activity. *Molecular and Cellular Biology,* 13**,** 6260-73.
ROBERTS, N. A., HAWORTH, R. S. & AVKIRAN, M. 2005. Effects of bisindolylmaleimide PKC inhibitors on p90RSK activity in vitro and in adult ventricular myocytes. *Br J Pharmacol,* 145**,** 477-89.
ROFFE, M., LUPINACCI, F. C., SOARES, L. C., HAJJ, G. N. & MARTINS, V. R. 2015. Two widely used RSK inhibitors, BI-D1870 and SL0101, alter mTORC1 signaling in a RSK-independent manner. *Cell Signal,* 27**,** 1630-42.
ROLFE, D. F. & BROWN, G. C. 1997. Cellular energy utilization and molecular origin of standard metabolic rate in mammals. *Physiol Rev,* 77**,** 731-58.
ROMEO, Y., MOREAU, J., ZINDY, P. J., SABA-EL-LEIL, M., LAVOIE, G., DANDACHI, F., BAPTISSART, M., BORDEN, K. L. B., MELOCHE, S. & ROUX, P. P. 2013. RSK regulates

activated BRAF signalling to mTORC1 and promotes melanoma growth. *Oncogene,* 32**,** 2917-2926.
ROMEO, Y., ZHANG, X. & ROUX, P. P. 2012. Regulation and function of the RSK family of protein kinases. *Biochemical Journal,* 441**,** 553-69.
ROTTMANN, S. & LUSCHER, B. 2006. The Mad side of the Max network: antagonizing the function of Myc and more. *Curr Top Microbiol Immunol,* 302**,** 63-122.
ROUX, P. P., BALLIF, B. A., ANJUM, R., GYGI, S. P. & BLENIS, J. 2004. Tumor-promoting phorbol esters and activated Ras inactivate the tuberous sclerosis tumor suppressor complex via p90 ribosomal S6 kinase. *Proceedings of the National Academy of Sciences of the United States of America,* 101**,** 13489-13494.
ROUX, P. P., RICHARDS, S. A. & BLENIS, J. 2003. Phosphorylation of p90 ribosomal S6 kinase (RSK) regulates extracellular signal-regulated kinase docking and RSK activity. *Molecular and Cellular Biology,* 23**,** 4796-804.
ROUX, P. P., SHAHBAZIAN, D., VU, H., HOLZ, M. K., COHEN, M. S., TAUNTON, J., SONENBERG, N. & BLENIS, J. 2007. RAS/ERK signaling promotes site-specific ribosomal protein S6 phosphorylation via RSK and stimulates cap-dependent translation. *Journal of Biological Chemistry,* 282**,** 14056-14064.
RUIZ, F. X., PORTE, S., GALLEGO, O., MORO, A., ARDEVOL, A., DEL RIO-ESPINOLA, A., ROVIRA, C., FARRES, J. & PARES, X. 2011. Retinaldehyde is a substrate for human aldo-keto reductases of the 1C subfamily. *Biochemical Journal,* 440**,** 335-44.
RYAN, K. M., ERNST, M. K., RICE, N. R. & VOUSDEN, K. H. 2000. Role of NF-kappa B in p53-mediated programmed cell death. *Nature,* 404**,** 892-897.
SAKURA, H., MAEKAWA, T., IMAMOTO, F., YASUDA, K. & ISHII, S. 1988. 2 Human Genes Isolated by a Novel Method Encode DNA-Binding Proteins Containing a Common Region of Homology. *Gene,* 73**,** 499-507.
SAPKOTA, G. P., CUMMINGS, L., NEWELL, F. S., ARMSTRONG, C., BAIN, J., FRODIN, M., GRAUERT, M., HOFFMANN, M., SCHNAPP, G., STEEGMAIER, M., COHEN, P. & ALESSI, D. R. 2007. BI-D1870 is a specific inhibitor of the p90 RSK (ribosomal S6 kinase) isoforms in vitro and in vivo. *Biochemical Journal,* 401**,** 29-38.
SAPKOTA, G. P., KIELOCH, A., LIZCANO, J. M., LAIN, S., ARTHUR, J. S. C., WILLIAMS, M. R., MORRICE, N., DEAK, M. & ALESSI, D. R. 2001. Phosphorylation of the protein kinase mutated in Peutz-Jeghers cancer syndrome, LKB1/STK11, at Ser(431) by p90(RSK) and cAMP-dependent protein kinase, but not its farnesylation at Cys(433), is essential for LKB1 to suppress cell growth. *Journal of Biological Chemistry,* 276**,** 19469-19482.
SAYAN, A. E., STANFORD, R., VICKERY, R., GRIGORENKO, E., DIESCH, J., KULBICKI, K., EDWARDS, R., PAL, R., GREAVES, P., JARIEL-ENCONTRE, I., PIECHACZYK, M., KRIAJEVSKA, M., MELLON, J. K., DHILLON, A. S. & TULCHINSKY, E. 2012. Fra-1 controls motility of bladder cancer cells via transcriptional upregulation of the receptor tyrosine kinase AXL. *Oncogene,* 31**,** 1493-503.
SCHLAMOWITZ, M., SHAW, A. & JACKSON, W. T. 1969. Limitations of he Dixon plot for ascertaining naure of enzyme inhibition. *Tex Rep Biol Med,* 27**,** 483-8.
SCHMIDT, H., SIEMS, W., MULLER, M., DUMDEY, R. & RAPOPORT, S. M. 1991. ATP-producing and consuming processes of Ehrlich mouse ascites tumor cells in proliferating and resting phases. *Exp Cell Res,* 194**,** 122-7.
SCHMITT, A. & NEBREDA, A. R. 2002. Signalling pathways in oocyte meiotic maturation. *Journal of Cell Science,* 115**,** 2457-2459.

SCHNIDAR, H., EBERL, M., KLINGLER, S., MANGELBERGER, D., KASPER, M., HAUSER-KRONBERGER, C., REGL, G., KROISMAYR, R., MORIGGL, R., SIBILIA, M. & ABERGER, F. 2009. Epidermal growth factor receptor signaling synergizes with Hedgehog/GLI in oncogenic transformation via activation of the MEK/ERK/JUN pathway. *Cancer Research,* 69**,** 1284-92.
SCHOUTEN, G. J., VERTEGAAL, A. C. O., WHITESIDE, S. T., ISRAEL, A., TOEBES, M., DORSMAN, J. C., VANDEREB, A. J. & ZANTEMA, A. 1997. I kappa B alpha is a target for the mitogen-activated 90 kDa ribosomal S6 kinase. *Embo Journal,* 16**,** 3133-3144.
SCHROEDER, M. J., SHABANOWITZ, J., SCHWARTZ, J. C., HUNT, D. F. & COON, J. J. 2004. A neutral loss activation method for improved phosphopeptide sequence analysis by quadrupole ion trap mass spectrometry. *Anal Chem,* 76**,** 3590-8.
SCHWAB, M. S., ROBERTS, B. T., GROSS, S. D., TUNQUIST, B. J., TAIEB, F. E., LEWELLYN, A. L. & MALLER, J. L. 2001. Bub1 is activated by the protein kinase p90(Rsk) during Xenopus oocyte maturation. *Current Biology,* 11**,** 141-150.
SEBOLT-LEOPOLD, J. S. & HERRERA, R. 2004. Targeting the mitogen-activated protein kinase cascade to treat cancer. *Nature Reviews Cancer,* 4**,** 937-947.
SERAFIMOVA, I. M., PUFALL, M. A., KRISHNAN, S., DUDA, K., COHEN, M. S., MAGLATHLIN, R. L., MCFARLAND, J. M., MILLER, R. M., FRODIN, M. & TAUNTON, J. 2012. Reversible targeting of noncatalytic cysteines with chemically tuned electrophiles. *Nature Chemical Biology,* 8**,** 471-476.
SERRA, V., EICHHORN, P. J., GARCIA-GARCIA, C., IBRAHIM, Y. H., PRUDKIN, L., SANCHEZ, G., RODRIGUEZ, O., ANTON, P., PARRA, J. L., MARLOW, S., SCALTRITI, M., PEREZ-GARCIA, J., PRAT, A., ARRIBAS, J., HAHN, W. C., KIM, S. Y. & BASELGA, J. 2013. RSK3/4 mediate resistance to PI3K pathway inhibitors in breast cancer. *Journal of Clinical Investigation,* 123**,** 2551-63.
SETHI, N. & KANG, Y. 2011. Unravelling the complexity of metastasis - molecular understanding and targeted therapies. *Nature Reviews Cancer,* 11**,** 735-48.
SHACKELFORD, D. B. & SHAW, R. J. 2009. The LKB1-AMPK pathway: metabolism and growth control in tumour suppression. *Nature Reviews Cancer,* 9**,** 563-575.
SHAHBAZIAN, D., ROUX, P. P., MIEULET, V., COHEN, M. S., RAUGHT, B., TAUNTON, J., HERSHEY, J. W. B., BLENIS, J., PENDE, M. & SONENBERG, N. 2006. The mTOR/PI3K and MAPK pathways converge on eIF4B to control its phosphorylation and activity. *Embo Journal,* 25**,** 2781-2791.
SHAN, M. & O'DOHERTY, G. A. 2006. De novo asymmetric syntheses of SL0101 and its analogues via a palladium-catalyzed glycosylation. *Org Lett,* 8**,** 5149-52.
SHAN, M. & O'DOHERTY, G. A. 2008. Synthesis of carbasugar C-1 phosphates via Pd-catalyzed cyclopropanol ring opening. *Org Lett,* 10**,** 3381-4.
SHAN, M. & O'DOHERTY, G. A. 2010. Synthesis of SL0101 carbasugar analogues: carbasugars via Pd-catalyzed cyclitolization and post-cyclitolization transformations. *Org Lett,* 12**,** 2986-9.
SHAN, M., SHARIF, E. U. & O'DOHERTY, G. A. 2010. Total synthesis of jadomycin A and a carbasugar analogue of jadomycin B. *Angew Chem Int Ed Engl,* 49**,** 9492-5.
SHIBAHARA, K., SUGIO, K., OSAKI, T., UCHIUMI, T., MAEHARA, Y., KOHNO, K., YASUMOTO, K., SUGIMACHI, K. & KUWANO, M. 2001. Nuclear expression of the Y-box binding protein, YB-1, as a novel marker of disease progression in non-small cell lung cancer. *Clinical Cancer Research,* 7**,** 3151-3155.

SHIBAO, K., TAKANO, H., NAKAYAMA, Y., OKAZAKI, K., NAGATA, N., IZUMI, H., UCHIUMI, T., KUWANO, M., KOHNO, K. & ITOH, H. 1999. Enhanced coexpression of YB-1 and DNA topoisomerase II alpha genes in human colorectal carcinomas. *International Journal of Cancer,* 83**,** 732-737.
SHIMAMURA, A., BALLIF, B. A., RICHARDS, S. A. & BLENIS, J. 2000. Rsk1 mediates a MEK-MAP kinase cell survival signal. *Current Biology,* 10**,** 127-135.
SHIMURA, Y., KURODA, J., RI, M., NAGOSHI, H., YAMAMOTO-SUGITANI, M., KOBAYASHI, T., KIYOTA, M., NAKAYAMA, R., MIZUTANI, S., CHINEN, Y., SAKAMOTO, N., MATSUMOTO, Y., HORIIKE, S., SHIOTSU, Y., IIDA, S. & TANIWAKI, M. 2012. RSK2(Ser227) at N-terminal kinase domain is a potential therapeutic target for multiple myeloma. *Mol Cancer Ther,* 11**,** 2600-9.
SINGH, J., PETTER, R. C., BAILLIE, T. A. & WHITTY, A. 2011. The resurgence of covalent drugs. *Nat Rev Drug Discov,* 10**,** 307-17.
SMADJA-LAMERE, N., SHUM, M., DELERIS, P., ROUX, P. P., ABE, J. & MARETTE, A. 2013. Insulin activates RSK (p90 ribosomal S6 kinase) to trigger a new negative feedback loop that regulates insulin signaling for glucose metabolism. *Journal of Biological Chemistry,* 288**,** 31165-76.
SMAILI, S. S., HSU, Y. T., YOULE, R. J. & RUSSELL, J. T. 2000. Mitochondria in Ca2+ signaling and apoptosis. *J Bioenerg Biomembr,* 32**,** 35-46.
SMITH, J. A., MALONEY, D. J., CLARK, D. E., XU, Y., HECHT, S. M. & LANNIGAN, D. A. 2006. Influence of rhamnose substituents on the potency of SL0101, an inhibitor of the Ser/Thr kinase, RSK. *Bioorg Med Chem,* 14**,** 6034-42.
SMITH, J. A., MALONEY, D. J., HECHT, S. M. & LANNIGAN, D. A. 2007. Structural basis for the activity of the RSK-specific inhibitor, SL0101. *Bioorg Med Chem,* 15**,** 5018-34.
SMITH, J. A., POTEET-SMITH, C. E., MALARKEY, K. & STURGILL, T. W. 1999. Identification of an extracellular signal-regulated kinase (ERK) docking site in ribosomal S6 kinase, a sequence critical for activation by ERK in vivo. *Journal of Biological Chemistry,* 274**,** 2893-2898.
SMITH, J. A., POTEET-SMITH, C. E., XU, Y., ERRINGTON, T. M., HECHT, S. M. & LANNIGAN, D. A. 2005a. Identification of the first specific inhibitor of p90 ribosomal S6 kinase (RSK) reveals an unexpected role for RSK in cancer cell proliferation. *Cancer Research,* 65**,** 1027-34.
SMITH, J. A., POTEET-SMITH, C. E., XU, Y., ERRINGTON, T. M., HECHT, S. M. & LANNIGAN, D. A. 2005b. Identification of the first specific inhibitor of p90 ribosomal S6 kinase (RSK) reveals an unexpected role for RSK in cancer cell proliferation. *Cancer Res,* 65**,** 1027-34.
SMOLEN, G. A., ZHANG, J. M., ZUBROWSKI, M. J., EDELMAN, E. J., LUO, B. A., YU, M., NG, L. W., SCHERBER, C. M., SCHOTT, B. J., RAMASWAMY, S., IRIMIA, D., ROOT, D. E. & HABER, D. A. 2010. A genome-wide RNAi screen identifies multiple RSK-dependent regulators of cell migration. *Genes & Development,* 24**,** 2654-2665.
SONG, B., LAI, B., ZHENG, Z., ZHANG, Y., LUO, J., WANG, C., CHEN, Y., WOODGETT, J. R. & LI, M. 2010. Inhibitory phosphorylation of GSK-3 by CaMKII couples depolarization to neuronal survival. *Journal of Biological Chemistry,* 285**,** 41122-34.
SRISKANTHADEVAN, S., JEYARAJU, D. V., CHUNG, T. E., PRABHA, S., XU, W., SKRTIC, M., JHAS, B., HURREN, R., GRONDA, M., WANG, X., JITKOVA, Y., SUKHAI, M. A., LIN, F. H., MACLEAN, N., LAISTER, R., GOARD, C. A., MULLEN, P. J., XIE, S.,

PENN, L. Z., ROGERS, I. M., DICK, J. E., MINDEN, M. D. & SCHIMMER, A. D. 2015. AML cells have low spare reserve capacity in their respiratory chain that renders them susceptible to oxidative metabolic stress. *Blood,* 125**,** 2120-30.
STAMBOLIC, V. & WOODGETT, J. R. 1994. Mitogen inactivation of glycogen synthase kinase-3 beta in intact cells via serine 9 phosphorylation. *Biochemical Journal,* 303 (Pt 3)**,** 701-4.
STANTON, L. A., UNDERHILL, T. M. & BEIER, F. 2003. MAP kinases in chondrocyte differentiation. *Developmental Biology,* 263**,** 165-175.
STAYTON, P. S., FREITAG, S., KLUMB, L. A., CHILKOTI, A., CHU, V., PENZOTTI, J. E., TO, R., HYRE, D., LE TRONG, I., LYBRAND, T. P. & STENKAMP, R. E. 1999. Streptavidin-biotin binding energetics. *Biomol Eng,* 16**,** 39-44.
STEEG, P. S. 2006. Tumor metastasis: mechanistic insights and clinical challenges. *Nat Med,* 12**,** 895-904.
STEFANOVIC, S., BARNETT, P., VAN DUIJVENBODEN, K., WEBER, D., GESSLER, M. & CHRISTOFFELS, V. M. 2014. GATA-dependent regulatory switches establish atrioventricular canal specificity during heart development. *Nat Commun,* 5**,** 3680.
STEICHEN, J. M., KUCHINSKAS, M., KESHWANI, M. M., YANG, J., ADAMS, J. A. & TAYLOR, S. S. 2012. Structural basis for the regulation of protein kinase A by activation loop phosphorylation. *Journal of Biological Chemistry,* 287**,** 14672-80.
STOKOE, D., CAUDWELL, B., COHEN, P. T. & COHEN, P. 1993. The substrate specificity and structure of mitogen-activated protein (MAP) kinase-activated protein kinase-2. *Biochemical Journal,* 296 (Pt 3)**,** 843-9.
STOKOE, D., STEPHENS, L. R., COPELAND, T., GAFFNEY, P. R., REESE, C. B., PAINTER, G. F., HOLMES, A. B., MCCORMICK, F. & HAWKINS, P. T. 1997. Dual role of phosphatidylinositol-3,4,5-trisphosphate in the activation of protein kinase B. *Science,* 277**,** 567-70.
STRATFORD, A. L., FRY, C. J., DESILETS, C., DAVIES, A. H., CHO, Y. Y., LI, Y., DONG, Z. G., BERQUIN, I. M., ROUX, P. P. & DUNN, S. E. 2008. Y-box binding protein-1 serine 102 is a downstream target of p90 ribosomal S6 kinase in basal-like breast cancer cells. *Breast Cancer Research,* 10.
STRATFORD, A. L., HABIBI, G., ASTANEHE, A., JIANG, H., HU, K., PARK, E., SHADEO, A., BUYS, T. P., LAM, W., PUGH, T., MARRA, M., NIELSEN, T. O., KLINGE, U., MERTENS, P. R., APARICIO, S. & DUNN, S. E. 2007. Epidermal growth factor receptor (EGFR) is transcriptionally induced by the Y-box binding protein-1 (YB-1) and can be inhibited with Iressa in basal-like breast cancer, providing a potential target for therapy. *Breast Cancer Research,* 9.
STRATFORD, A. L., REIPAS, K., HU, K., FOTOVATI, A., BROUGH, R., FRANKUM, J., TAKHAR, M., WATSON, P., ASHWORTH, A., LORD, C. J., LASHAM, A., PRINT, C. G. & DUNN, S. E. 2012. Targeting p90 ribosomal S6 kinase eliminates tumor-initiating cells by inactivating Y-box binding protein-1 in triple-negative breast cancers. *Stem Cells,* 30**,** 1338-48.
SULZMAIER, F. J. & RAMOS, J. W. 2013. RSK Isoforms in Cancer Cell Invasion and Metastasis. *Cancer Research,* 73**,** 6099-6105.
SUN, Q., CHEN, X., MA, J., PENG, H., WANG, F., ZHA, X., WANG, Y., JING, Y., YANG, H., CHEN, R., CHANG, L., ZHANG, Y., GOTO, J., ONDA, H., CHEN, T., WANG, M. R., LU, Y., YOU, H., KWIATKOWSKI, D. & ZHANG, H. 2011. Mammalian target of rapamycin up-

regulation of pyruvate kinase isoenzyme type M2 is critical for aerobic glycolysis and tumor growth. *Proc Natl Acad Sci U S A,* 108**,** 4129-34.
SUN, Y., CAO, S., YANG, M., WU, S., WANG, Z., LIN, X., SONG, X. & LIAO, D. J. 2013. Basic anatomy and tumor biology of the RPS6KA6 gene that encodes the p90 ribosomal S6 kinase-4. *Oncogene,* 32**,** 1794-810.
SUTHERLAND, C., LEIGHTON, I. A. & COHEN, P. 1993. Inactivation of Glycogen-Synthase Kinase-3-Beta by Phosphorylation - New Kinase Connections in Insulin and Growth-Factor Signaling. *Biochemical Journal,* 296**,** 15-19.
SYKA, J. E., COON, J. J., SCHROEDER, M. J., SHABANOWITZ, J. & HUNT, D. F. 2004. Peptide and protein sequence analysis by electron transfer dissociation mass spectrometry. *Proc Natl Acad Sci U S A,* 101**,** 9528-33.
SZKLARCZYK, D., FRANCESCHINI, A., WYDER, S., FORSLUND, K., HELLER, D., HUERTA-CEPAS, J., SIMONOVIC, M., ROTH, A., SANTOS, A., TSAFOU, K. P., KUHN, M., BORK, P., JENSEN, L. J. & VON MERING, C. 2015. STRING v10: protein-protein interaction networks, integrated over the tree of life. *Nucleic Acids Research,* 43**,** D447-52.
TAKAHASHI, E., ABE, J., GALLIS, B., AEBERSOLD, R., SPRING, D. J., KREBS, E. G. & BERK, B. C. 1999. p90(RSK) is a serum-stimulated Na+/H+ exchanger isoform-1 kinase - Regulatory phosphorylation of serine 703 of Na+/H+ exchanger isoform-1. *Journal of Biological Chemistry,* 274**,** 20206-20214.
TAMAOKI, T., NOMOTO, H., TAKAHASHI, I., KATO, Y., MORIMOTO, M. & TOMITA, F. 1986. Staurosporine, a Potent Inhibitor of Phospholipid/Ca++Dependent Protein-Kinase. *Biochemical and Biophysical Research Communications,* 135**,** 397-402.
TANIMURA, S., HASHIZUME, J., KUROSAKI, Y., SEI, K., GOTOH, A., OHTAKE, R., KAWANO, M., WATANABE, K. & KOHNO, M. 2011. SH3P2 is a negative regulator of cell motility whose function is inhibited by ribosomal S6 kinase-mediated phosphorylation. *Genes to Cells,* 16**,** 514-526.
TAO, Z. F., WANG, L., STEWART, K. D., CHEN, Z., GU, W., BUI, M. H., MERTA, P., ZHANG, H., KOVAR, P., JOHNSON, E., PARK, C., JUDGE, R., ROSENBERG, S., SOWIN, T. & LIN, N. H. 2007. Structure-based design, synthesis, and biological evaluation of potent and selective macrocyclic checkpoint kinase 1 inhibitors. *Journal of Medicinal Chemistry,* 50**,** 1514-27.
TAYLOR, S. S., ILOUZ, R., ZHANG, P. & KORNEV, A. P. 2012. Assembly of allosteric macromolecular switches: lessons from PKA. *Nat Rev Mol Cell Biol,* 13**,** 646-58.
TAYLOR, S. S. & KORNEV, A. P. 2011. Protein kinases: evolution of dynamic regulatory proteins. *Trends in Biochemical Sciences,* 36**,** 65-77.
TAYLOR, S. S., ZHANG, P., STEICHEN, J. M., KESHWANI, M. M. & KORNEV, A. P. 2013. PKA: lessons learned after twenty years. *Biochim Biophys Acta,* 1834**,** 1271-8.
TEMTAMY, S. A., MILLER, J. D. & HUSSELSMAUMENEE, I. 1975. Coffin-Lowry Syndrome - Inherited Faciodigital Mental-Retardation Syndrome. *Journal of Pediatrics,* 86**,** 724-731.
TENNANT, D. A., DURAN, R. V. & GOTTLIEB, E. 2010. Targeting metabolic transformation for cancer therapy. *Nature Reviews Cancer,* 10**,** 267-77.
TERNETTE, N., YANG, M., LAROYIA, M., KITAGAWA, M., O'FLAHERTY, L., WOLHULTER, K., IGARASHI, K., SAITO, K., KATO, K., FISCHER, R., BERQUAND, A., KESSLER, B. M., LAPPIN, T., FRIZZELL, N., SOGA, T., ADAM, J. & POLLARD, P. J. 2013.

Inhibition of mitochondrial aconitase by succination in fumarate hydratase deficiency. *Cell Rep,* 3**,** 689-700.
THAKUR, A., SUN, Y., BOLLIG, A., WU, J., BILIRAN, H., BANERJEE, S., SARKAR, F. H. & LIAO, D. J. 2008. Anti-invasive and antimetastatic activities of ribosomal protein S6 kinase 4 in breast cancer cells. *Clinical Cancer Research,* 14**,** 4427-4436.
THIYAGARAJAN, S., BHATIA, N., REAGAN-SHAW, S., COZMA, D., THOMAS-TIKHONENKO, A., AHMAD, N. & SPIEGELMAN, V. S. 2007. Role of GLI2 transcription factor in growth and tumorigenicity of prostate cells. *Cancer Research,* 67**,** 10642-6.
THOMAS, G. M., RUMBAUGH, G. R., HARRAR, D. B. & HUGANIR, R. L. 2005. Ribosomal S6 kinase 2 interacts with and phosphorylates PDZ domain-containing proteins and regulates AMPA receptor transmission. *Proc Natl Acad Sci U S A,* 102**,** 15006-11.
TOMITA, N., HAYASHI, Y., SUZUKI, S., OOMORI, Y., ARAMAKI, Y., MATSUSHITA, Y., IWATANI, M., IWATA, H., OKABE, A., AWAZU, Y., ISONO, O., SKENE, R. J., HOSFIELD, D. J., MIKI, H., KAWAMOTO, T., HORI, A. & BABA, A. 2013. Structure-based discovery of cellular-active allosteric inhibitors of FAK. *Bioorganic & Medicinal Chemistry Letters,* 23**,** 1779-1785.
TORRES, M. A., ELDAR-FINKELMAN, H., KREBS, E. G. & MOON, R. T. 1999. Regulation of ribosomal S6 protein kinase-p90(rsk), glycogen synthase kinase 3, and beta-catenin in early Xenopus development. *Molecular and Cellular Biology,* 19**,** 1427-37.
TOURRIERE, H., CHEBLI, K., ZEKRI, L., COURSELAUD, B., BLANCHARD, J. M., BERTRAND, E. & TAZI, J. 2003. The RasGAP-associated endoribonuclease G3BP assembles stress granules. *Journal of Cell Biology,* 160**,** 823-831.
TROST, B. M. & CRAWLEY, M. L. 2003. Asymmetric transition-metal-catalyzed allylic alkylations: applications in total synthesis. *Chemical Reviews,* 103**,** 2921-44.
TROST, B. M., MACHACEK, M. R. & APONICK, A. 2006. Predicting the stereochemistry of diphenylphosphino benzoic acid (DPPBA)-based palladium-catalyzed asymmetric allylic alkylation reactions: a working model. *Acc Chem Res,* 39**,** 747-60.
TROST, B. M. & VAN VRANKEN, D. L. 1996. Asymmetric Transition Metal-Catalyzed Allylic Alkylations. *Chemical Reviews,* 96**,** 395-422.
UHLEN, M., FAGERBERG, L., HALLSTROM, B. M., LINDSKOG, C., OKSVOLD, P., MARDINOGLU, A., SIVERTSSON, A., KAMPF, C., SJOSTEDT, E., ASPLUND, A., OLSSON, I., EDLUND, K., LUNDBERG, E., NAVANI, S., SZIGYARTO, C. A., ODEBERG, J., DJUREINOVIC, D., TAKANEN, J. O., HOBER, S., ALM, T., EDQVIST, P. H., BERLING, H., TEGEL, H., MULDER, J., ROCKBERG, J., NILSSON, P., SCHWENK, J. M., HAMSTEN, M., VON FEILITZEN, K., FORSBERG, M., PERSSON, L., JOHANSSON, F., ZWAHLEN, M., VON HEIJNE, G., NIELSEN, J. & PONTEN, F. 2015. Proteomics. Tissue-based map of the human proteome. *Science,* 347**,** 1260419.
UTEPBERGENOV, D., DEREWENDA, U., OLEKHNOVICH, N., SZUKALSKA, G., BANERJEE, B., HILINSKI, M. K., LANNIGAN, D. A., STUKENBERG, P. T. & DEREWENDA, Z. S. 2012. Insights into the Inhibition of the p90 Ribosomal S6 Kinase (RSK) by the Flavonol Glycoside SL0101 from the 1.5 A Crystal Structure of the N-Terminal Domain of RSK2 with Bound Inhibitor. *Biochemistry,* 51**,** 6499-510.
VADLAMUDI, R. K., ADAM, L., NGUYEN, D., SANTOS, M. & KUMAR, R. 2002a. Differential regulation of components of the focal adhesion complex by heregulin: role of phosphatase SHP-2. *J Cell Physiol,* 190**,** 189-99.

VADLAMUDI, R. K., LI, F., ADAM, L., NGUYEN, D., OHTA, Y., STOSSEL, T. P. & KUMAR, R. 2002b. Filamin is essential in actin cytoskeletal assembly mediated by p21-activated kinase 1. *Nature Cell Biology,* 4**,** 681-90.
VESTERGAARD, B. & SAYERS, Z. 2014. Investigating increasingly complex macromolecular systems with small-angle X-ray scattering. *IUCrJ,* 1**,** 523-9.
VIETH, M., HIGGS, R. E., ROBERTSON, D. H., SHAPIRO, M., GRAGG, E. A. & HEMMERLE, H. 2004. Kinomics-structural biology and chemogenomics of kinase inhibitors and targets. *Biochimica Et Biophysica Acta-Proteins and Proteomics,* 1697**,** 243-257.
VIGNERON, S., BRIOUDES, E., BURGESS, A., LABBE, J. C., LORCA, T. & CASTRO, A. 2010. RSK2 is a kinetochore-associated protein that participates in the spindle assembly checkpoint. *Oncogene,* 29**,** 3566-3574.
VIK, T. A. & RYDER, J. W. 1997. Identification of serine 380 as the major site of autophosphorylation of Xenopus pp90rsk. *Biochem Biophys Res Commun,* 235**,** 398-402.
VOKES, S. A., JI, H., MCCUINE, S., TENZEN, T., GILES, S., ZHONG, S., LONGABAUGH, W. J., DAVIDSON, E. H., WONG, W. H. & MCMAHON, A. P. 2007. Genomic characterization of Gli-activator targets in sonic hedgehog-mediated neural patterning. *Development,* 134**,** 1977-89.
VOKES, S. A., JI, H., WONG, W. H. & MCMAHON, A. P. 2008. A genome-scale analysis of the cis-regulatory circuitry underlying sonic hedgehog-mediated patterning of the mammalian limb. *Genes Dev,* 22**,** 2651-63.
WANG, H. Y., QI, Z., WU, B., KANG, S. W., ROJANASAKUL, Y. & O'DOHERTY, G. A. 2011a. C5'-Alkyl Substitution Effects on Digitoxigenin alpha-l-Glycoside Cancer Cytotoxicity. *ACS Med Chem Lett,* 2**,** 259-263.
WANG, H. Y., ROJANASAKUL, Y. & O'DOHERTY, G. A. 2011b. Synthesis and Evaluation of the alpha-D-/alpha-L-Rhamnosyl and Amicetosyl Digitoxigenin Oligomers as Anti-tumor Agents. *ACS Med Chem Lett,* 2**,** 264-269.
WANG, H. Y., XIN, W., ZHOU, M., STUECKLE, T. A., ROJANASAKUL, Y. & O'DOHERTY, G. A. 2011c. Stereochemical survey of digitoxin monosaccharides: new anticancer analogues with enhanced apoptotic activity and growth inhibitory effect on human non-small cell lung cancer cell. *ACS Med Chem Lett,* 2**,** 73-78.
WANG, R. N., JUNG, S. Y., WU, C. F., QIN, J., KOBAYASHI, R., GALLICK, G. E. & KUANG, J. A. 2010. Direct roles of the signaling kinase RSK2 in Cdc25C activation during Xenopus oocyte maturation. *Proceedings of the National Academy of Sciences of the United States of America,* 107**,** 19885-19890.
WANG, X., BEUGNET, A., MURAKAMI, M., YAMANAKA, S. & PROUD, C. G. 2005. Distinct signaling events downstream of mTOR cooperate to mediate the effects of amino acids and insulin on initiation factor 4E-binding proteins. *Molecular and Cellular Biology,* 25**,** 2558-72.
WANG, X., LI, W., WILLIAMS, M., TERADA, N., ALESSI, D. R. & PROUD, C. G. 2001a. Regulation of elongation factor 2 kinase by p90(RSK1) and p70 S6 kinase. *Embo Journal,* 20**,** 4370-9.
WANG, X. M., JANMAAT, M., BEUGNET, A., PAULIN, F. E. M. & PROUD, C. G. 2002. Evidence that the dephosphorylation of Ser(535) in the epsilon-subunit of eukaryotic initiation factor (eIF) 2B is insufficient for the activation of eIF2B by insulin. *Biochemical Journal,* 367**,** 475-481.

WANG, X. M., LI, W., WILLIAMS, M., TERADA, N., ALESSI, D. R. & PROUD, C. G. 2001b. Regulation of elongation factor 2 kinase by p90(RSK1) and p70 S6 kinase. *Embo Journal,* 20**,** 4370-4379.
WANG, Z. Q., ZHANG, B. C., WANG, M. F. & CARR, B. I. 2003. Persistent ERK phosphorylation negatively regulates cAMP response element-binding protein (CREB) activity via recruitment of CREB-binding protein to pp90(RSK). *Journal of Biological Chemistry,* 278**,** 11138-11144.
WASHBURN, M. P., WOLTERS, D. & YATES, J. R., 3RD 2001. Large-scale analysis of the yeast proteome by multidimensional protein identification technology. *Nat Biotechnol,* 19**,** 242-7.
WAUGH, D. J. & WILSON, C. 2008. The interleukin-8 pathway in cancer. *Clinical Cancer Research,* 14**,** 6735-41.
WELLBROCK, J., LATUSKE, E., KOHLER, J., WAGNER, K., STAMM, H., VETTORAZZI, E., VOHWINKEL, G., KLOKOW, M., UIBELEISEN, R., EHM, P., RIECKEN, K., LOGES, S., THOL, F., SCHUBERT, C., AMLING, M., JUCKER, M., BOKEMEYER, C., HEUSER, M., KRAUTER, J. & FIEDLER, W. 2015. Expression of Hedgehog Pathway Mediator GLI Represents a Negative Prognostic Marker in Human Acute Myeloid Leukemia and Its Inhibition Exerts Antileukemic Effects. *Clinical Cancer Research,* 21**,** 2388-98.
WIESER, W. & KRUMSCHNABEL, G. 2001. Hierarchies of ATP-consuming processes: direct compared with indirect measurements, and comparative aspects. *Biochemical Journal,* 355**,** 389-95.
WIGGIN, G. R., SOLOAGA, A., FOSTER, J. M., MURRAY-TAIT, V., COHEN, P. & ARTHUR, J. S. C. 2002. MSK1 and MSK2 are required for the mitogen-and stress-induced phosphorylation of CREB and ATF1 in fibroblasts. *Molecular and Cellular Biology,* 22**,** 2871-2881.
WILLIAMS, G. S., BOYMAN, L., CHIKANDO, A. C., KHAIRALLAH, R. J. & LEDERER, W. J. 2013. Mitochondrial calcium uptake. *Proc Natl Acad Sci U S A,* 110**,** 10479-86.
WILLIAMSON, J. R. & COOPER, R. H. 1980. Regulation of the citric acid cycle in mammalian systems. *Febs Letters,* 117 Suppl**,** K73-85.
WIZNEROWICZ, M. & TRONO, D. 2005. Harnessing HIV for therapy, basic research and biotechnology. *Trends Biotechnol,* 23**,** 42-7.
WOO, M. S., OHTA, Y., RABINOVITZ, I., STOSSEL, T. P. & BLENIS, J. 2004. Ribosomal S6 kinase (RSK) regulates phosphorylation of filamin a on an important regulatory site. *Molecular and Cellular Biology,* 24**,** 3025-3035.
WOOD, E. R., TRUESDALE, A. T., MCDONALD, O. B., YUAN, D., HASSELL, A., DICKERSON, S. H., ELLIS, B., PENNISI, C., HORNE, E., LACKEY, K., ALLIGOOD, K. J., RUSNAK, D. W., GILMER, T. M. & SHEWCHUK, L. 2004. A unique structure for epidermal growth factor receptor bound to GW572016 (Lapatinib): relationships among protein conformation, inhibitor off-rate, and receptor activity in tumor cells. *Cancer Research,* 64**,** 6652-9.
WU, B., LI, M. & O'DOHERTY, G. A. 2010. Synthesis of several cleistrioside and cleistetroside natural products via a divergent de novo asymmetric approach. *Org Lett,* 12**,** 5466-9.
WU, C., OROZCO, C., BOYER, J., LEGLISE, M., GOODALE, J., BATALOV, S., HODGE, C. L., HAASE, J., JANES, J., HUSS, J. W., 3RD & SU, A. I. 2009. BioGPS: an extensible and customizable portal for querying and organizing gene annotation resources. *Genome Biol,* 10**,** R130.

WU, C. F., LIU, S., LEE, Y. C., WANG, R., SUN, S., YIN, F., BORNMANN, W. G., YU-LEE, L. Y., GALLICK, G. E., ZHANG, W., LIN, S. H. & KUANG, J. 2014. RSK promotes G2/M transition through activating phosphorylation of Cdc25A and Cdc25B. *Oncogene,* 33**,** 2385-94.
WU, J., JUN, H. & MCDERMOTT, J. R. 2015. Formation and activation of thermogenic fat. *Trends Genet,* 31**,** 232-238.
WU, J., LEE, C., YOKOM, D., JIANG, H., CHEANG, M. C. U., YORIDA, E., TURBIN, D., BERQUIN, I. M., MERTENS, P. R., IFTNER, T., GILKS, C. B. & DUNN, S. E. 2006. Disruption of the Y-box binding protein-1 results in suppression of the epidermal growth factor receptor and HER-2. *Cancer Research,* 66**,** 4872-4879.
XIAN, W., PAPPAS, L., PANDYA, D., SELFORS, L. M., DERKSEN, P. W., DE BRUIN, M., GRAY, N. S., JONKERS, J., ROSEN, J. M. & BRUGGE, J. S. 2009. Fibroblast Growth Factor Receptor 1-Transformed Mammary Epithelial Cells Are Dependent on RSK Activity for Growth and Survival. *Cancer Research,* 69**,** 2244-2251.
XING, J., GINTY, D. D. & GREENBERG, M. E. 1996. Coupling of the RAS-MAPK pathway to gene activation by RSK2, a growth factor-regulated CREB kinase. *Science,* 273**,** 959-63.
XU, S. Q., BAYAT, H., HOU, X. Y. & JIANG, B. B. 2006. Ribosomal S6 kinase-1 modulates interleukin-1 beta-induced persistent activation of NF-kappa B through phosphorylation of I kappa B beta. *American Journal of Physiology-Cell Physiology,* 291**,** C1336-C1345.
YAMAK, A., LATINKIC, B. V., DALI, R., TEMSAH, R. & NEMER, M. 2014. Cyclin D2 is a GATA4 cofactor in cardiogenesis. *Proc Natl Acad Sci U S A,* 111**,** 1415-20.
YAMNIK, R. L. & HOLZ, M. K. 2010. mTOR/S6K1 and MAPK/RSK signaling pathways coordinately regulate estrogen receptor a serine 167 phosphorylation. *Febs Letters,* 584**,** 124-128.
YANAZUME, T., HASEGAWA, K., WADA, H., MORIMOTO, T., ABE, M., KAWAMURA, T. & SASAYAMA, S. 2002. Rho/ROCK pathway contributes to the activation of extracellular signal-regulated kinase/GATA-4 during myocardial cell hypertrophy. *Journal of Biological Chemistry,* 277**,** 8618-25.
YANG, X. G., MATSUDA, K., BIALEK, P., JACQUOT, S., MASUOKA, H. C., SCHINKE, T., LI, L. Z., BRANCORSINI, S., SASSONE-CORSI, P., TOWNES, T. M., HANAUER, A. & KARSENTY, G. 2004. ATF4 is a substrate of RSK2 and an essential regulator of osteoblast biology: Implication for Coffin-Lowry syndrome. *Cell,* 117**,** 387-398.
YU, X., LI, M. & O'DOHERTY G, A. 2011. De novo asymmetric synthesis of the D-/L-disaccharide portion of Sch 47555. *Heterocycles,* 82**,** 1577-1584.
YU, X. & O'DOHERTY, G. A. 2008. De novo asymmetric synthesis and biological evaluation of the trisaccharide portion of PI-080 and vineomycin B2. *Org Lett,* 10**,** 4529-32.
ZARU, R., EDGAR, A. J., HANAUER, A. & WATTS, C. 2015. Structural and Functional Basis for p38-MK2-Activated Rsk Signaling in Toll-Like Receptor-Stimulated Dendritic Cells. *Molecular and Cellular Biology,* 35**,** 132-140.
ZARU, R., RONKINA, N., GAESTEL, M., ARTHUR, J. S. C. & WATTS, C. 2007. The MAPK-activated kinase Rsk controls an acute Toll-like receptor signaling response in dendritic cells and is activated through two distinct pathways. *Nature Immunology,* 8**,** 1227-1235.
ZENIOU, M., DING, T., TRIVIER, E. & HANAUER, A. 2002. Expression analysis of RSK gene family members: the RSK2 gene, mutated in Coffin-Lowry syndrome, is prominently expressed in brain structures essential for cognitive function and learning. *Hum Mol Genet,* 11**,** 2929-40.

ZHANG, J. M., YANG, P. L. & GRAY, N. S. 2009. Targeting cancer with small molecule kinase inhibitors. *Nature Reviews Cancer,* 9**,** 28-39.
ZHANG, L. P., CHENG, J. Z., MA, Y. W., THOMAS, W., ZHANG, J. Q. & DU, J. 2005. Dual pathways for nuclear factor kappa B activation by angiotensin II in vascular smooth muscle - Phosphorylation of p65 by I kappa B kinase and ribosomal kinase. *Circulation Research,* 97**,** 975-982.
ZHAO, H. & PIWNICA-WORMS, H. 2001. ATR-mediated checkpoint pathways regulate phosphorylation and activation of human Chk1. *Molecular and Cellular Biology,* 21**,** 4129-39.
ZHAO, J., YUAN, X. J., FRODIN, M. & GRUMMT, I. 2003. ERK-dependent phosphorylation of the transcription initiation factor TIF-IA is required for RNA polymerase I transcription and cell growth. *Molecular Cell,* 11**,** 405-413.
ZHAO, Y., BJORBAEK, C., WEREMOWICZ, S., MORTON, C. C. & MOLLER, D. E. 1995. RSK3 encodes a novel pp90rsk isoform with a unique N-terminal sequence: growth factor-stimulated kinase function and nuclear translocation. *Molecular and Cellular Biology,* 15**,** 4353-63.
ZHONG, Y., XUE, M., ZHAO, X., YUAN, J., LIU, X., HUANG, J., ZHAO, Z., LI, H. & XU, Y. 2013. Substituted indolin-2-ones as p90 ribosomal S6 protein kinase 2 (RSK2) inhibitors: Molecular docking simulation and structure-activity relationship analysis. *Bioorg Med Chem,* 21**,** 1724-34.
ZHOU, M. & O'DOHERTY, G. 2008a. The de novo synthesis of oligosaccharides: application to the medicinal chemistry SAR-study of digitoxin. *Curr Top Med Chem,* 8**,** 114-25.
ZHOU, M. & O'DOHERTY, G. A. 2006. A stereoselective synthesis of digitoxin and digitoxigen mono- and bisdigitoxoside from digitoxigenin via a palladium-catalyzed glycosylation. *Org Lett,* 8**,** 4339-42.
ZHOU, M. & O'DOHERTY, G. A. 2007. De novo approach to 2-deoxy-beta-glycosides: asymmetric syntheses of digoxose and digitoxin. *J Org Chem,* 72**,** 2485-93.
ZHOU, M. & O'DOHERTY, G. A. 2008b. De novo synthesis of the trisaccharide subunit of landomycins A and E. *Org Lett,* 10**,** 2283-6.
ZHU, J. D., BLENIS, J. & YUAN, J. Y. 2008. Activation of PI3K/Akt and MAPK pathways regulates Myc-mediated transcription by phosphorylating and promoting the degradation of Mad1. *Proceedings of the National Academy of Sciences of the United States of America,* 105**,** 6584-6589.
ZHU, J. H., GUSDON, A. M., CIMEN, H., VAN HOUTEN, B., KOC, E. & CHU, C. T. 2012. Impaired mitochondrial biogenesis contributes to depletion of functional mitochondria in chronic MPP+ toxicity: dual roles for ERK1/2. *Cell Death Dis,* 3**,** e312.